An Ecological Study of Hunting Creek

2020

FINAL REPORT

February 20, 2021

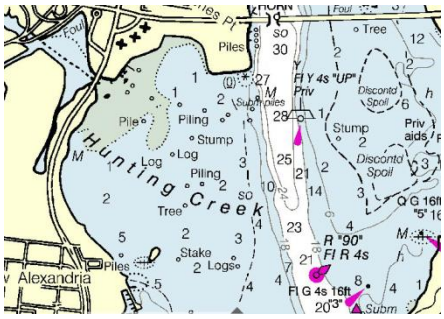

by

R. Christian Jones
Professor, Project Director

Kim de Mutsert
Assistant Professor, Co-Principal Investigator

Benoit Van Aken
Associate Professor, Co-Principal Investigator

Amy Fowler
Assistant Professor, Co-Principal Investigator

Potomac Environmental Research and Education Center
Department of Environmental Science and Policy
Department of Chemistry and Biochemistry
George Mason University

to

Alexandria Renew Enterprises
Alexandria, VA

This page intentionally blank.

Table of Contents

This page intentionally left blank.

An Ecological Study of Hunting Creek - 2020

Executive Summary

Hunting Creek is an embayment of the tidal Potomac River located just downstream of the City of Alexandria and the I-95/I-495 Woodrow Wilson bridge. This embayment receives treated wastewater from the Alexandria Renew Enterprises wastewater treatment plant and inflow from Cameron Run which drains most of the Cities of Alexandria and Falls Church and much of eastern Fairfax County. The Hunting Creek embayment is bordered on the north by the City of Alexandria and on the west and south by the George Washington Memorial Parkway and associated park land. Due to its tidal nature and shallowness, the embayment does not seasonally stratify vertically, and its water is flushed by rainstorms and may mix readily with the adjacent tidal Potomac River mainstem.

Beginning in 2013 the Potomac Environmental Research and Education (PEREC) in collaboration with Alexandria Renew Enterprises (AlexRenew) initiated a program to monitor water quality and biological communities in the Hunting Creek area including stations in the embayment itself, its tributaries, and the adjacent river mainstem. This document presents study findings from 2020 and compares them with that from the previous seven years. In addition, *Escherichia coli* levels in Hunting Creek and tributaries. And we completed a third year of benthic macroinvertebrate and water quality sampling on many tributaries of Cameron Run and Hunting Creek. Unfortunately, sampling of anadromous fish usage of Hunting Creek and Cameron Run was cancelled in 2020 due to COVID restrictions on GMU personnel in the spring of 2020.

The Chesapeake Bay, of which the tidal Potomac River is a major subestuary, is the largest and most productive coastal system in the United States. The use of the Bay as a fisheries and recreational resource has been threatened by overenrichment with nutrients which can cause nuisance algal blooms, hypoxia in stratified areas, loss of submersed aquatic vegetation, and declining fisheries. As a major discharger of treated wastewater into Hunting Creek, AlexRenew has been proactive in decreasing nutrient loading since the late 1970's. Also of concern are *E. coli* and nutrients derived from combined sewer overflows (CSO's) and nonpoint sources within the drainage basin as well as sediments derived from the watershed.

The ecological study reported here provides documentation of the current state of water quality and biological resources in Hunting Creek. In 2020 the COVID 19 pandemic outbreak resulted in a delayed start to the study. Sampling began at the beginning of July rather than the usual mid-April. Lab water quality measurements started in late July.

Water temperature followed a typical seasonal pattern at all stations with peak temperatures of about 30°C. Most of the embayment and river stations exhibited a peak in specific conductance and chloride in late July whereas stations nearer the shore increased steadily from July through September. Dissolved oxygen peaked in late July at values at or slightly above saturation at the time of a chlorophyll peak in the embayment and river stations. Field and lab pH did not increase in late July remaining fairly constant at about 7.0-8.0. Total alkalinity was generally 80-90 mg/L as $CaCO_3$ at most embayment and river stations, but was lower at near shore stations such as AR1, AR24, and AR25.

Secchi disk transparency was generally 0.5-0.7 m and there was little change through the sampling period. Light attenuation was in the -2 to -3 m^{-1} range through the study period. The values of both Secchi and light attenuation indicate water clarity continues to be a problem for SAV recolonization in Hunting Creek.

Ammonia nitrogen showed a general increase from July through September at most stations and all values were quite low (<0.2 mg/L). Nitrate nitrogen was very low in late July at the time of the phytoplankton bloom as the algae drew down the levels and then increased through September. Nitrite was very low at all stations and did not show consistent seasonal patterns. Organic nitrogen was mostly in the range 0.2-1.0 mg/L and showed little seasonal pattern. Total phosphorus was generally between 0.5 and 1.0 mg/L but was somewhat higher on occasion at nearshore Hunting Creek stations. N/P ratio remained above 7.2, consistently pointing to P limitation of primary producers. BOD was generally below 4 mg/L. Total suspended solids was typically in the 10-30 mg/L range with some higher spikes at the near shore Hunting Creek stations. VSS values hovered around 5 mg/L in the river mainstem with higher values at the nearshore Hunting Creek embayment stations in late July and early August. It is of note that several of the nearshore stations were classified as CSO impact stations and higher levels of certain water quality variables there may reflect CSO impacts.

In the tributaries, water temperature also generally followed air temperature although somewhat cooler than the tidal stations. Specific conductance at the tributary stations showed a general rise from 100-200 µS/cm in early July to 300-500 µS/cm in late September. Dissolved oxygen was generally 80-100 percent saturation except at AR34 in Hooffs Run which showed one value of less than 4 mg/L in late July. pH values were consistently 7.0 to 7.8 range. YSI turbidity was generally low (<30 NTU) except in early July during a period of substantial precipitation and runoff. Total alkalinity was fairly uniform in all of the tributaries exhibited a gradual increase over the period. Total phosphorus and ortho-phosphorus were variable with no clear pattern. Organic nitrogen showed a general decline except at AR23 and AR34 which remained high in September. Ammonia nitrogen was uniformly low (<0.15 mg/L) at all stream stations except AR34. Nitrate nitrogen was consistently elevated at AR33, followed by AR13. Other stations were consistently below 1 mg/L. Nitrite nitrogen was consistently below 0.04 mg/L except for an unexplained spike at AR12 in early September. TSS and was generally less than 20 mg/L except at AR30 and AR23 which were sometimes higher.

Phytoplankton biomass as indicated by chlorophyll *a* exhibited a distinct maximum (of over 40 µg/L) at the Hunting Creek embayment stations in late July. This maximum is one of the highest values observed during the eight years of study and was also reflected in high values of total phytoplankton density and biovolume. This was followed by a steady decline for the remainder of the year. Cell density at the late July maximum was dominated by cyanobacteria and green algae with diatoms also contributing at both stations. At this time *Oscillatoria* was the most abundant cyanobacterium with *Anabaena* also contributing at both stations. *Dictyosphaerium* was the most numerous green alga. When biovolume was considered diatoms were dominant during this July peak and *Melosira* was the dominant at both stations with Pennate 50x15 being subdominant at AR2.

Rotifers were very abundant in early July reaching over 3000/L at both AR2 and AR4. These values were similar to those found in 2019 and among the highest observed to date in the study. Rotifers declined somewhat in late July and then were much reduced in August and September at both stations. *Brachionus* was the strong dominant on every sampling date.

Since spring sampling was missed in 2020 due to COVID 19 and spring is the time when most zooplankton reach their maxima, observed levels of zooplankton were generally quite low in 2020. *Bosmina, Diaphanosoma, Daphnia, Sida, Leptodora,* Chydoridae and *Ceriodaphnia* all showed highest values in July and then declined. Copepods also exhibited this pattern.

With its above average rainfall and resulting stream flows, many water quality parameters continued to be impacted in 2020. Specific conductance values in 2020 were depressed similar to 2018. Light transparency (as measured by Secchi disk depth and light attenuation coefficient) continued to show depressed values as in 2018 and 2019 especially at AR2 and AR3. TSS and VSS which impacts light transparency also continued to be elevated in 2020. As in 2019, water column chlorophyll *a* levels in 2020 were among the highest observed in the eight years of the study. This reflects nutrients brought in by stream flows and the lack of SAV as competitors to the phytoplankton. Rotifers, particularly *Brachionus*, were also unusually high in 2020 as in 2019. Copepod nauplii continued their recovery to pre-2018 values, but were similar to recent years. Many other zooplankton showed below average ranges because sampling was not done during spring when their abundances tend to be higher.

The ichthyoplankton data show a much lower density of fish larvae than previous years, likely due to the much lower number of sampling events and the fact that the peak spawning time occurred before sampling could commence in early July. Looking at relative abundance, the same species as previous years were abundant in the samples, but some are missing (e.g. Hickory Shad) likely as a result of not sampling at a time when they are present, and the low encounter rate due to having two sampling events. Species found in relative higher densities than previous years were sunfishes such as Bluegill and Green Sunfish. The trend of relative high densities of river herring (Alewife and Blueback Herring) continued in 2020.

Trawl sampling, conducted between July 17 and September 17 gathered a total of 2076 fishes comprising 13 species. This abundance is very high, especially for such a truncated collection season, but diversity is low (low number of species with high dominance of one species). These results are not directly comparable to previous years since diversity is highly related to the number of samples taken. Collections were dominated by White Perch (88.36%). The second most abundant species was Spottail Shiner (3.72%). Other relatively abundant species were Blue Catfish (2.95%), Alewife (1.91%) and Gizzard Shad (1.02%). An interesting finding was the collection of three native catfishes (Channel Catfish, White Bullhead and Brown Bullhead) after finding four last year. Native catfishes have seen declining abundances since the invasion of Blue Catfish. A concerning find is the Flathead Catfish, which is an invasive species like Blue Catfish. We are not the first to report this species here, but we had not seen it before in

our samples.

Seine sampling was conducted between July 17 and September 17 and total of 10 seine samples were taken (5 per station), comprising 1447 fishes of at least 14 species (Table 8). This is less than last year, but we took only half the samples of last year. Like last year, Banded Killifish was not the most dominant species in seine catches (10.16%), in contrast to most previous years. Instead, very high abundances were found of White Perch (74.98%). This year the reason could simply be that the part of the season where Banded Killifish is dominant was not sampled. Other species with relatively high abundance were Alewife (5.04%), Gizzard Shad (3.46%), Threadfin Shad (1.66%), and Spottail Shiner (1.31%).

As in 2019, SAV was virtually absent in 2020 as verified by surveys that were made by GMU personnel and aerial imagery from VIMS This is most certainly attributable to the very turbid water in 2018 and continued turbidity at critical periods in 2019 and 2020 which obstructed light penetration.

Benthic invertebrate data from the tidal stations in 2020 indicated that the river station AR4 had the highest diversity and most samples from that station were distinctly different from the other two stations when compared by multivariate analysis. Annual aggregate taxa richness was more similar in 2020 than in recent years with 9 taxa found at AR4, 7 at AR2, and 9 at AR3. Oligochaetes, amphipods, and midges were the most abundant organisms at the tidal benthic stations. Total abundance in 2020 was higher in lower than normal at AR2, but near normal at AR3 and AR4.

In 2016 a benthic macroinvertebrate sampling program was implemented for the flowing tributary streams starting with six stations. In 2018 two more stations were added with sampling continuing annually in November. Twenty-three taxa were identified across all sites in 2020. In general, the top four most abundant taxa observed across all sites stayed the same as in previous years with the exception of an increase in the Insecta family Chironomidae across all sites. In 2020, Holmes Run 2 had the highest abundance of all macroinvertebrates and the four dominant taxa, mostly composed of the Insecta family Hydropsychidae. Similar to previous years, Hydropsychidae larvae (caddisflies) were the dominant group at the majority of the sites. Taxa richness across all sites ranged from 8 to 16 taxa, with lowest richness at Indian Run and Timber Branch and highest richness at Holmes Run 2. Using 10 measures of biological health, we calculated a summary statistic of relative overall health of these streams. Using the criteria for each metric laid out above, four streams were categorized as “good”, two were categorized as “fair”, and two were categorized as “poor”.

E. coli sampling was expanded to a total of 17 stations in 2020, to better characterize especially the CSO outfall areas. Due to COVID restrictions sampling could not be initiated until July and a total of 5 dates were included from July through September. The data continue to support a conclusion that the entire area sampled, including the mainstem of the Potomac River (AR-4), is impaired for the bacteriological water quality criterion (*E. coli*) content under Section 9VAC25-260-170 of the Virginia Water Quality Standards that applies to primary contact recreational use surface waters. Although our data showed an increase of the *E. coli* abundance and percent exceedance of the 235 per

100 mL criterion from 2014 to 2016, these numbers seemed to have peaked in 2016 – 2017 and even showed a slight decrease in 2018 and 2019. The increased counts recorded in 2020 seems to be partially caused by high counts occurring during high-flow conditions in July 2020.

Sampling additional sites in Hooff Run/Cameron Run as was done in 2020 indicates that Hooff Run is a significant contributor of the Hunting Creek contamination by *E. coli*. Similarly, sampling additional sites on the Potomac River by the Royal St. CSO indicate a contribution of this CSO to *E. coli* contamination of the receiving water.

We recommend that:

1. The basic ecosystem monitoring should continue. A range of climatic conditions is needed to effectively establish baseline conditions in Hunting Creek. Interannual, seasonal and spatial patterns are starting to appear, but need validation with future years's data. With record rainfall and runoff, 2018 provided a glimpse of the vulnerability of the system to flushing and sediment related effects. Continued monitoring will allow us to assess the resiliency of the ecosystem; i.e., how quickly will it recovery from a very wet year. The system did not recover completely in 2019.
2. Water quality mapping should be continued. This provides much needed spatial resolution of water quality patterns as well as allowing mapping of SAV distributions.
3. Fyke nets have proven to be a useful new gear to enhance fish collections and should be continued.
4. Anadromous fish sampling is an important part of this monitoring program and has gained interest now that the stock of river herring has collapsed generally, and a moratorium on these taxa has been established in 2012. The discovery and continue presence of river herring spawning in Cameron Run increases the importance of continuing studies of anadromous fish in the study area.
5. We recommend continuing the more intensive *E. coli* sampling plan which seems to be giving better insight into the dynamics of *E. coli* in the study area.
6. We recommend continuing macroinvertebrate studies the tributaries of Hunting Creek to further ascertain overall aquatic biota health and that tidal benthos sampling should continue and the data should be more thoroughly examined.

List of Abbreviations

BOD	Biochemical oxygen demand
cfs	cubic feet per second
DO	Dissolved oxygen
ha	hectare
l	liter
LOWESS	locally weighted sum of squares trend line
m	meter
mg	milligram
MGD	Million gallons per day
NS	not statistically significant
NTU	Nephelometric turbidity units
SAV	Submersed aquatic vegetation
SRP	Soluble reactive phosphorus
TP	Total phosphorus
TSS	Total suspended solids
um	micrometer
VSS	Volatile suspended solids
#	number

This page intentionally left blank.

The Aquatic Monitoring Program for the Hunting Creek Area of the Tidal Freshwater Potomac River 2020

FINAL REPORT
February 20, 2021

by

R. Christian Jones
Professor, Department of Environmental Science and Policy
Director, Potomac Environmental Research and Education Center
George Mason University
Project Director

Kim de Mutsert
Assistant Professor, Department of Environmental Science and Policy
George Mason University
Co-Principal Investigator

Amy Fowler
Assistant Professor, Department of Environmental Science and Policy
George Mason University
Co-Principal Investigator

to

Alexandria Renew Enterprises
Alexandria, VA

ACKNOWLEDGEMENTS

The authors wish to thank the numerous individuals and organizations whose cooperation, hard work, and encouragement have made this project successful. We wish to thank the Alexandria Renew Enterprises especially CEO Karen Pallansch for her vision in initiating the study and to Blake Hamilton, Aster Tekle, and Ashley Tatge of Alex Renew for their advice and assistance during the study.

Without a dedicated group of field and laboratory workers this project would not have been possible. Thanks go to Laura Birsa for managing water quality/plankton/benthos field trips and to field/lab workers Chelsea Gray, Tabitha King, Alex Mott, David Tolentino, Sam Mohney, and Jackie Davis. Benthic samples were analyzed with the help of Bryce Bossuot, James Burmeister, Haley Haasch, Keith Keel and Eran O'Keefe. E. coli samples were collected and processed with the assistance of Aaron Newborn, Fanella Zamcho, Ayesah Karamat, Alison Gomeiz, and Steven Chan. Others that have helped in the field and in the laboratory to collect and process fish samples include Beverly Bachman, Rachel Kelmartin, and Sammie Alexander. Dr. Saiful Islam conducted all phytoplankton counts. Claire Buchanan served as a voluntary consultant on plankton identification.

INTRODUCTION

This section reports the results of the eighth year of an aquatic monitoring program conducted for Alexandria Renew Enterprises by the Potomac Environmental Research and Education Center (PEREC) in the College of Science at George Mason University. This year there as only one other section: the survey of *Escherichia coli* levels in the Hunting Creek area of the tidal Potomac River. The Anadromous fish survey was terminated before any fish were collected due to COVID 19 restrictions. The rest of the sampling was initiated in early July rather than mid-April, again due to the COVID 19 pandemic.

This work was in response to a request from Karen Pallansch, Chief Executive Officer of Alexandria Renew Enterprises (Alex Renew), operator of the wastewater reclamation and reuse facility (WRRF) which serves about 350,000 people in the City of Alexandria and the County of Fairfax in northern Virginia. The study is patterned on the long-running Gunston Cove Study which PEREC has been conducting in partnership with the Fairfax County Department of Public Works and Environmental Services since 1984. The goal of these projects is to provide baseline data and on-going trend analysis of the ecosystems receiving reclaimed water from wastewater treatment facilities with the objective of adaptive management of these valuable freshwater resources. This will facilitate the formulation of well-grounded management strategies for maintenance and improvement of water quality and biotic resources in the tidal Potomac. A secondary but important educational goal is to provide training for Mason graduate and undergraduate students in water quality and biological monitoring and assessment.

Setting of Hunting Creek

Hunting Creek is an embayment of the tidal Potomac River located just downstream of the City of Alexandria and the Woodrow Wilson Bridge. Waters are shallow with the entire embayment having a depth of 2 m or less at mean tide. According to the "Environmental Atlas of the Potomac Estuary" (Lippson et al. 1981), the mean depth of Hunting Creek is 1.0 m, the surface area is 2.26 km^2, and the volume of 2.1 x 10^6 m^3.

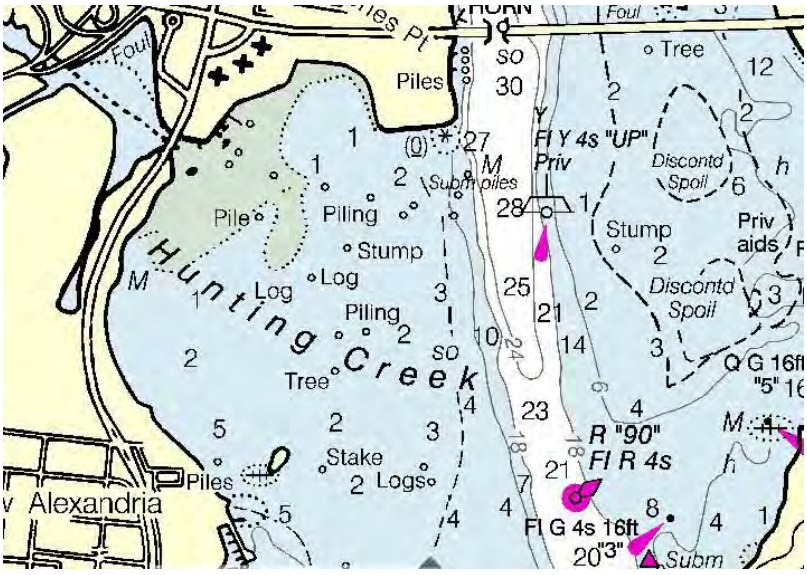

On the left is the Hunting Creek embayment. The Woodrow Wilson Bridge spans the tidal Potomac River at the top of the map. The Potomac River main channel is the whitish area running from north to south through the middle of the map. Soundings (numbers on the map) are in feet at mean low water. For the purposes of this report "Hunting Creek" will extend to the head of tide, roughly to Telegraph Rd.

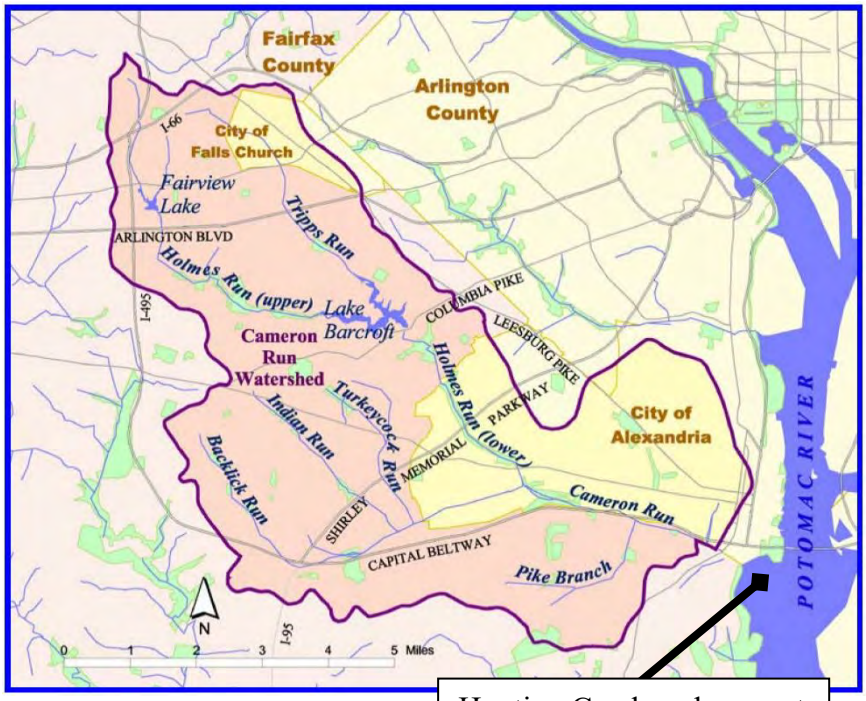

Hunting Creek embayment

On the left is a map of the Hunting Creek watershed. Cameron Run is the freshwater stream which drains the vast majority of the watershed of Hunting Creek. The watershed is predominantly suburban in nature with areas of higher density commercial and residential development. The watershed has an area of 44 square miles and drains most of the Cities of Alexandria and Falls Church and much of east central Fairfax County. A major aquatic feature of the watershed is Lake Barcroft. The suburban land uses in the watershed are a source of nonpoint pollution to Hunting Creek.

The Alex Renew WRRF serves an area similar in extent to the Cameron Run watershed with the addition of some areas along the Potomac shoreline from Four Mile Run to Dyke Marsh. The effluent of the Alexandria Renew Enterprises plant enters the upper tidal reach of Hunting Creek under the Rt 1/I-95 interchange.

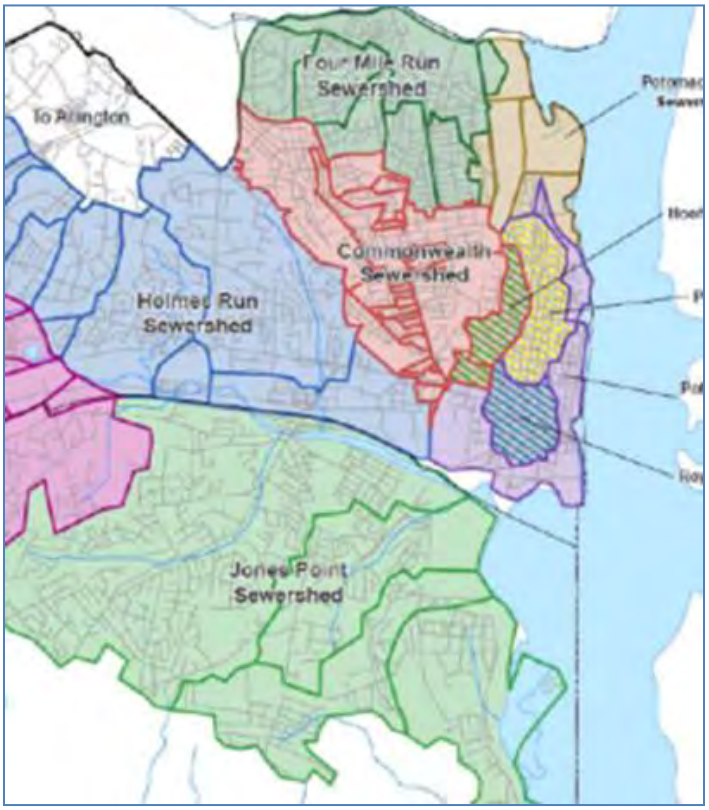

The map at the left shows the sewersheds which contribute to the AlexRenew WRRF. Of particular note are the shaded areas within the City of Alexandria. These sewersheds (Hooffs Run, Pendleton, and Royal St.) all contain combined sewers meaning that domestic wastewater is co-mingled with street runoff. Under most conditions, all of this water is directed to the AlexRenew WRRF for treatment. But in extreme runoff conditions (like torrential rains), some may be diverted directly into the tidal Potomac via a Combined Sewer outfall (CSO).

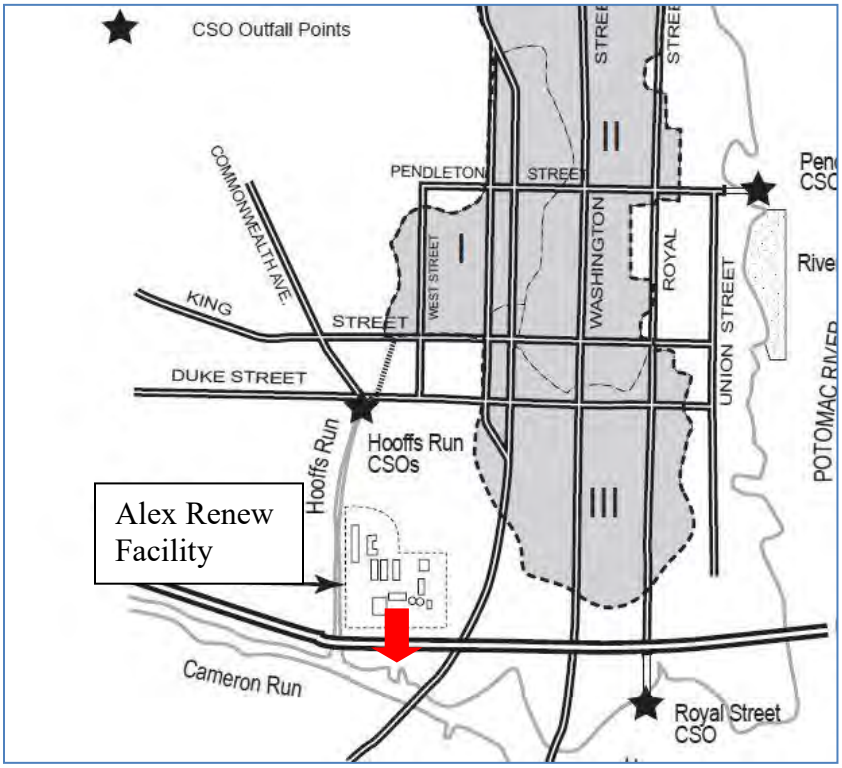

The map at the left is an enlargement of the area where the Alex Renew WRRF is found and where the discharge sites of the CSO's are located. Note the close proximity of two of the CSO's to the Alex Renew WRRF discharge (shown as red arrow).

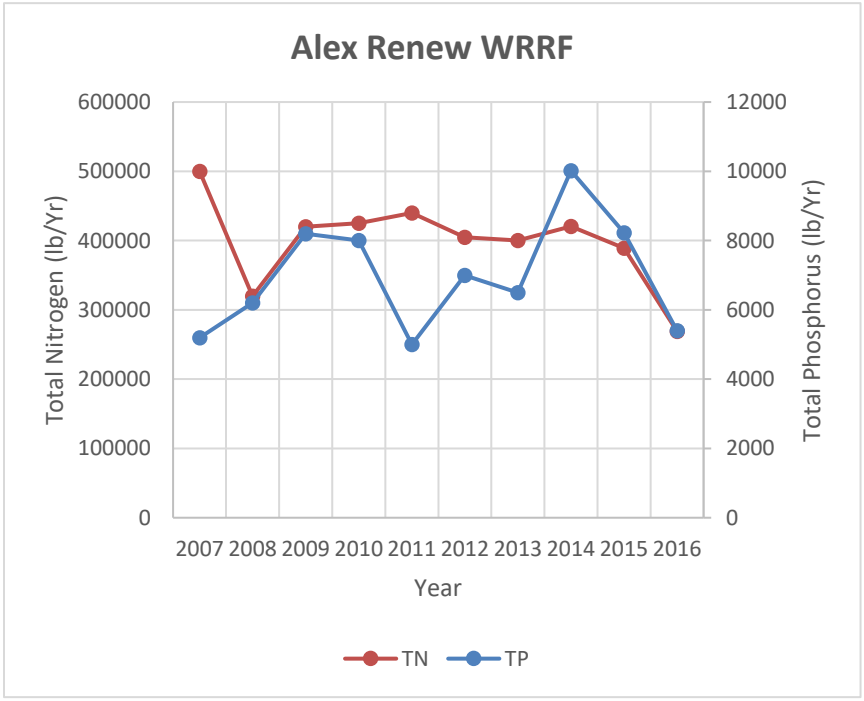

The graph at the left shows the loading of nitrogen and phosphorus from the Alexandria Renew WRRF for the last seven years. Loadings of both nutrient elements were among the lowest in the last decade in 2016: 269,000 lb/yr for nitrogen and 5,400 lb/yr for phosphorus.

Ecology of the Freshwater Tidal Potomac

The tidal Potomac River is an integral part of the Chesapeake Bay tidal system and at its mouth the Potomac is contiguous to the bay proper. The tidal Potomac is often called a subestuary of the Chesapeake Bay and as such it is the largest subestuary of the bay in terms of size and amount of freshwater input. The mixing of freshwater with saltwater is the hallmark of an estuary. While the water elevation in an estuary is "sea level", the water contained in an estuary is not pure sea water such as found in the open ocean. Pure ocean sea water has a salt concentration of about 35 parts per thousand by weight (ppt). Water in Chesapeake Bay ranges from about 30 ppt near its mouth to 0 ppt in the upper reaches where there is substantial freshwater inflow such as in the upper tidal Potomac River. Salinity at a given location is determined by the balance between freshwater input and salt water mixing in from the ocean. It generally varies with season being lower in spring when freshwater inflows are greater and higher in summer when there is less freshwater inflow. In the Hunting Creek study area, the salinity is essentially 0 yearround.

Figure 2. The tidal Potomac River and Estuary.

(map courtesy USGS)

The tidal Potomac is generally divided into three salinity zones as indicated by the map to the left:
-Estuarine or Mesohaline zone (6-14 ppt)
-Transition or Oligohaline zone (0.5-6 ppt)
-Tidal River or Tidal Fresh zone (<0.5 ppt)
Hunting Creek is in the upper part of the Tidal River/Tidal Fresh zone and as such it never experiences detectable salinity

Within the tidal freshwater zone, the flora and fauna are generally characterized by the same species that would occur in a freshwater lake in this area and the food web is similar. Primary producers are freshwater species of submersed aquatic vegetation (SAV) such as native taxa *Vallisneria americana* (water celery), *Potomogeton* spp, (pondweeds), and *Ceratophyllum* (coontail) as well as introduced species such as *Hydrilla verticallata* (hydrilla) and *Myriophyllum spicatum* (water milfoil). Historical accounts indicate that most of the shallow areas of the tidal freshwater Potomac were colonized by SAV when observations were made around 1900 (Carter et al. 1985).

The other group of important primary producers are phytoplankton, a mixed assemblage

of algae and cyanobacteria which may turn over rapidly on a seasonal basis. The dominant groups of phytoplankton in the tidal freshwater Potomac are diatoms (considered a good food source for aquatic consumers) and cyanobacteria (considered a less desirable food source for aquatic consumers). For the latter part of the 20th century, the high nutrient loadings into the river favored cyanobacteria over both diatoms and SAV resulting in large production of undesirable food for consumers. In the last decade or so, as nutrient reductions have become manifest, cyanobacteria have decreased and diatoms and SAV have increased.

The biomass contained in the cells of phytoplankton nourishes the growth of zooplankton and benthic macroinvertebrates which provide an essential food supply for the juvenile and smaller fish. These in turn provide food for the larger fish like striped bass and largemouth bass. The species of zooplankton and benthos found in the tidal fresh zone are similar to those found in lakes in the area, but the fish fauna is augmented by species that migrate in and out from the open interface with the estuary.

Resident fish species include typical lake species such as sunfish (*Lepomis* spp.), bass (*Micropterus* spp.), and crappie (*Pomoxis* spp.) as well as estuarine species such as white perch (*Morone americana*) and killifish (*Fundulus* spp.). Species which spend part of their year in the area include striped bass (*Morone saxitilis*) and river herrings and shad (*Alosa* spp.). Non-native fish species have also become established in the tidal freshwater Potomac such as northern snakehead (*Channa argus*) and blue catfish (*Ictalurus furcatus*).

Larval fishes are transitional stages in the development of juvenile fishes. They range in development from newly hatched, embryonic fish to juvenile fish with morphological features similar to those of an adult. Many fishes such as clupeids (herring family), white perch, striped bass, and yellow perch disperse their eggs and sperm into the open water. The larvae of these species are carried with the current and termed “ichthyoplankton”. Other fish species such as sunfish and bass lay their eggs in “nests” on the bottom and their larvae are rare in the plankton.

After hatching from the egg, the larva draws nutrition from a yolk sack for a few days. When the yolk sack diminishes to nothing, the fish begins a life of feeding on other organisms. This post yolk sack larva feeds on small planktonic organisms (mostly small zooplankton) for a period of several days. It continues to be a fragile, almost transparent larva and suffers high mortality to predatory zooplankton and juvenile and adult fishes of many species, including its own. When it has fed enough, it changes into an opaque juvenile, with greatly enhanced swimming ability. It can no longer be caught with a slow-moving plankton net, but is soon susceptible to capture with the seine or trawl net.

METHODS

A. Profiles and Plankton: Sampling Day

Tidal Stations

Sampling was conducted on a semimonthly basis at stations representing both the Hunting Creek embayment and the Potomac mainstem (Figure 1a). Two stations (AR 2 & 3) were located in the Hunting Creek embayment proper. A fourth station (AR 4) was located in the river channel about 100 m upstream from Buoy 90. Dates for sampling as well as weather conditions on sampling dates and immediately preceding days are shown in Table 1. Note that certain dates had significant rainfall in days preceding sampling which may have impacted conditions in Hunting Creek due to it shallow nature and relatively large watershed contributing runoff.

Figure 1a. Hunting Creek area of the Tidal Potomac River showing water quality, plankton, and benthos sampling stations. AR2, AR3, and AR4 are embayment stations. AR11 and AR31 have been retired. Stations shown in red are new for 2020. Stations in green are macroinvertebrate bioassessment stations. AR1, AR2, AR3, AR4, AR10, AR23, AR31, AR32, AR33, and AR34 represent water quality stations, AR2 and AR4 are the phytoplankton and zooplankton stations and AR2, AR3, and AR4 are tidal benthos stations.

Table 1. Water quality monitoring stations.

Station ID	Access Type	Sample Type	Other Sampling	Location Description	Latitude	Longitude
AR1	Shore	Surface Grab	None	Hunting Cr at the GW Parkway Bridge	38.78992	-77.05126
AR2	Boat	Surface Bottom	Plankton Benthos	Northern portion of Hunting Cr.	38.78509	-77.04951
AR3	Boat	Surface Bottom	Benthos	Southern portion of Hunting Cr.	38.78181	-77.04890
AR4	Boat	Surface Bottom	Plankton Benthos	Potomac River Mainstem off Hunting Cr.	38.78124	-77.03529
AR10	Boat	Surface Grab	None	Potomac River North of Wilson Bridge	38.79816	-77.03907
AR12	Shore	Surface Grab	None	Last Riffle of Cameron Run near Beltway crossing	38.80218	-77.08467
AR13	Shore	Surface Grab	None	Hoff's Run upstream of CSO 003 and 004 outfalls	38.80278	-77.05848
AR21	Shore	Surface Grab	None	South side of Cameron Run downstream from Lake Cook drain	38.80318	-77.09565
AR23	Shore	Surface Grab	None	South side of upper Hunting Creek across from AlexRenew outfall	38.79372	-77.05966
AR24	Shore	Surface Grab	None	Hunting Creek north shore W. of Royal Street CSO outfall	38.79156	-77.04680
AR25	Shore	Surface Grab	None	Hunting Creek north shore E. of Royal Street CSO outfall	38.79205	-77.04538
AR30	Shore	Surface Grab	None	Cameron Run upstream near metro rail bridge	38.80545	-77.10745
AR32	Boat	Surface Grab	None	Potomac River Mainstem just S of Orinoco Bay CSO outfall	38.80940	-77.03727
AR33	Shore	Surface Grab	None	Hooffs Run at Linden St.	38.81103	-77.05993
AR34	Shore	Surface Grab	None	Hooffs Run at Alex Renew	38.79918	-77.05997
AR35	Shore	Surface Grab	None	Timber Branch at Ivy Hill Cemetery	38.8175	-77.07065
AR38	Boat	Surface Grab	None	Potomac River Mainstem near Daingerfield Island	38.82348	-77.03802

Table 2
Hunting Creek Study: Sampling Dates and Weather Data for 2020

	Type of Sampling						Avg Daily Temp (°C)		Precipitation (cm)	
Date	WP	B	D	T	S	F*	1-Day	3-Day	1-Day	3-Day
July 7	X	B					28.9	29.4	5.18	6.29
July 17				X	X		27.8	27.8	0	0
July 21	X						31.7	31.7	1.32	1.70
July 31				X	X		28.9	29.4	0.18	0.56
August 14				X	X		27.8	27.6	0.15	2.31
August 19	X	B					25.0	24.8	0.23	0.58
August 21			D				25.0	24.8	T	0.24
August 27				X	X		28.9	28.0	0	0.03
Sept 2	X	B					27.2	24.6	0.03	1.32
Sept 16	X						17..8	19.1	0	T
Sept 17				X	X		21.1	18.7	0.99	0.99

Type of Sampling: WP: Water quality (samples to AlexRenew Lab), profiles and plankton, B: benthos, D: dataflow (water quality mapping), T: fish collected by trawling, S: fish collected by seining. F: fish collected by fyke net. T under Precipitation equals "trace". X indicates full station suite on that date. *fyke nets were not set in 2020 due to reduced crew and lack of SAV.

Sampling was initiated about 9:00 am. Four types of measurements or samples were obtained depending on the station. At stations AR2, AR3, and AR4, (1) depth profiles of temperature, conductivity, dissolved oxygen, pH, and irradiance (photosynthetically active radiation, PAR) measured directly in the field; (2) water samples for GMU lab determination of chlorophyll *a* and phytoplankton species composition and abundance (phytoplankton at AR2 and AR4 only); (3) water samples for determination of N and P forms, BOD, COD, alkalinity, hardness, suspended solids, chloride, and pH by the Alexandria Renew Enterprises lab; (4) net sampling of zooplankton and ichthyoplankton (AR2 and AR4 only).

Profiles of temperature, conductivity, and dissolved oxygen were conducted at each station using a YSI 6600 datasonde with temperature, conductivity, dissolved oxygen and pH probes. Measurements were taken at 0.3 m increments from surface to bottom at the embayment stations. In the river measurements were made with the sonde at depths of 0.3 m and 2.0 m increments to the bottom. Meters were checked for calibration before and after sampling. Profiles of irradiance (photosynthetically active radiation, PAR) were collected with a LI-COR underwater flat scalar PAR probe. PAR measurements were taken at 10 cm intervals to a depth of 1.0 m. Simultaneous measurements were made with a terrestrial probe in air during each profile to correct for changes in ambient light if needed. Secchi depth was also determined. The

readings of at least two crew members were averaged due to variability in eye sensitivity among individuals. If the Secchi disk was still visible at the bottom or if its path was block by SAV while still visible, a proper reading could not be obtained.

A 1-liter depth-composited sample for GMU lab work was constructed from equal volumes of water collected at each of three depths (0.3 m below the surface, middepth, and 0.3 m off of the bottom) using a submersible bilge pump. A 100-mL aliquot of this sample was preserved immediately with acid Lugol's iodine for later identification and enumeration of phytoplankton at stations AR2 and AR4. The remainder of the sample was placed in an insulated cooler with ice. A separate 1-liter surface sample was collected from 0.3 m using the submersible bilge pump and placed in the insulated cooler with ice for lab analysis of surface chlorophyll *a*.

At selected embayment and river mainstream sampling stations (AR2, AR3, and AR4), 2-liter samples were collected monthly at each station from just below the surface (0.3 m) and near the bottom (0.3 m off bottom) at each station using the submersible pump. At other tidal stations sampled by boat (AR10, AR32, AR38), 2-liter samples were collected by hand from just below the surface. This water was promptly delivered to the nearby Alexandria Renew Laboratory for determination of nitrogen, phosphorus, BOD, TSS, VSS, pH, total alkalinity, and chloride. Surface water grab samples were collected at all of these stations for *E. coli* determination (see *E. coli* chapter).

At stations AR2 and AR4, microzooplankton was collected by pumping 32 liters from each of three depths (0.3 m, middepth, and 0.3 m off the bottom) through a 44 µm mesh sieve. The sieve consisted of a 12-inch long cylinder of 6-inch diameter PVC pipe with a piece of 44 µm nitex net glued to one end. The 44 µm cloth was backed by a larger mesh cloth to protect it. The pumped water was passed through this sieve from each depth and then the collected microzooplankton was backflushed into the sample bottle. The resulting sample was treated with about 50 mL of club soda and then preserved with formalin containing a small amount of rose bengal to a concentration of 5-10%.

At stations AR2 and AR4, macrozooplankton was collected by towing a 202 µm net (0.3 m opening, 2 m long) for 1 minute at each of three depths (near surface, middepth, and near bottom). Ichthyoplankton (larval fish) was sampled by towing a 333 µm net (0.5 m opening, 2 m long) for 2 minutes at each of the same depths at Stations AR2 and AR4. In the embayment, the boat traveled from AR2 toward AR3 during the tow while in the river the net was towed in a linear fashion along the channel. Macrozooplankton tows were about 300 m and ichthyoplankton tows about 600 m. Actual distance depended on specific wind conditions and tidal current intensity and direction, but an attempt was made to maintain a constant slow forward speed (approximately 2 miles per hour) through the water during the tow. The net was not towed directly in the wake of the engine. A General Oceanics flowmeter, fitted into the mouth of each net, was used to establish the exact towing distance. During towing the three depths were attained by playing out rope equivalent to about 1.5-2 times the desired depth. Samples which had obviously scraped bottom were discarded and the tow was repeated. Flowmeter readings taken before and after towing allowed precise determination of the distance towed and when multiplied by the area of the opening produced the total volume of water filtered.

Macrozooplankton were preserved immediately with rose bengal formalin with club soda pretreatment. Ichthyoplankton was preserved in 70% ethanol. Macrozooplankton was collected on each sampling trip; ichthyoplankton collections ended after July because larval fish were normally not found after this time.

Benthic macroinvertebrate samples were collected monthly at stations AR2, AR3, and AR4. Three samples were collected at each station using a petite ponar grab. The bottom material was sieved through a 0.5 mm stainless steel sieve and resulting organisms were preserved in rose bengal formalin for lab analysis.

Samples for water quality determination were maintained on ice and delivered to the Alexandria Renew Enterprises (AlexRenew) Laboratory by 2 pm on sampling day and returned to GMU by 3 pm. At GMU 10-15 mL aliquots of both depth-integrated and surface samples were filtered through 0.45 µm membrane filters (Gelman GN-6 and Millipore MF HAWP) at a vacuum of less than 10 lbs/in^2 for chlorophyll a and pheopigment determination. During the final phases of filtration, 0.1 mL of $MgCO_3$ suspension (1 g/100 mL water) was added to the filter to prevent premature acidification. Filters were stored in 20 mL plastic scintillation vials in the lab freezer for later analysis. Seston dry weight and seston organic weight were measured by filtering 200-400 mL of depth-integrated sample through a pretared glass fiber filter (Whatman 984AH).

Tributary Stations

At tributary stations (Figure 1a: AR1, AR11, AR12, AR13, AR21, AR22, AR23, and AR30), 2-liter samples were collected by hand from just below the surface. This water was promptly delivered to the nearby Alexandria Renew Laboratory for determination of nitrogen, phosphorus, BOD, TSS, VSS, pH, total alkalinity, and chloride. While at the site, water temperature, specific conductance, dissolved oxygen, pH, and turbidity were taken at 0.1 m depth with a YSI ProDDS minisonde. Surface water grab samples were collected at all of these stations for *E. coli* determination (see *E. coli* chapter).

Sampling day activities were normally completed by 5:30 pm.

B. Profiles and Plankton: Follow-up Analyses

Chlorophyll *a* samples were extracted in a ground glass tissue grinder to which 4 mL of dimethyl sulfoxide (DMSO) was added. The filter disintegrated in the DMSO and was ground for about 1 minute by rotating the grinder under moderate hand pressure. The ground suspension was transferred back to its scintillation vial by rinsing with 90% acetone. Ground samples were stored in the refrigerator overnight. Samples were removed from the refrigerator and centrifuged for 5 minutes to remove residual particulates.

Chlorophyll *a* concentration in the extracts was determined fluorometrically using a Turner Designs Model 10 field fluorometer configured for chlorophyll analysis as specified by the manufacturer. The instrument was calibrated using standards obtained from Turner Designs.

Fluorescence was determined before and after acidification with 2 drops of 10% HCl. Chlorophyll *a* was calculated from the following equation which corrects for pheophytin interference:

$$\text{Chlorophyll } a \text{ } (\mu g/L) = F_s R_s (R_b - R_a)/(R_s - 1)$$

where F_s=concentration per unit fluorescence for pure chlorophyll *a*
R_s=fluorescence before acid/fluorescence after acid for pure chlorophyll *a*
R_b=fluorescence of sample before acid
R_a=fluorescence of sample after acid

All chlorophyll analyses were completed within one month of sample collection.

Phytoplankton species composition and abundance was determined using the inverted microscope-settling chamber technique (Lund et al. 1958). Ten milliters of well-mixed algal sample were added to a settling chamber and allowed to stand for several hours. The chamber was then placed on an inverted microscope and random fields were enumerated. At least two hundred cells were identified to species and enumerated on each slide. Counts were converted to number per mL by dividing number counted by the volume counted. Biovolume of individual cells of each species was determined by measuring dimensions microscopically and applying volume formulae for appropriate solid shapes.

Microzooplankton and macrozooplankton samples were rinsed by sieving a well-mixed subsample of known volume and resuspending it in tap water. This allowed subsample volume to be adjusted to obtain an appropriate number of organisms for counting and for formalin preservative to be purged to avoid fume inhalation during counting. One mL subsamples were placed in a Sedgewick-Rafter counting cell and whole slides were analyzed until at least 200 animals had been identified and enumerated. A minimum of two slides was examined for each sample. References for identification were: Ward and Whipple (1959), Pennak (1978), and Rutner-Kolisko (1974). Zooplankton counts were converted to number per liter (microzooplankton) or per cubic meter (macrozooplankton) with the following formula:

$$\text{Zooplankton } (\#/L \text{ or } \#/m^3) = NV_s/(V_c V_f)$$

where N = number of individuals counted
V_s = volume of reconstituted sample, (mL)
V_c = volume of reconstituted sample counted, (mL)
V_f = volume of water sieved, (L or m^3)

Larval fish were picked from the ethanol-preserved ichthyoplankton samples with the aid of a stereo dissecting microscope. Identification of ichthyoplankton was made to family and further to genus and species where possible. If the number of animals in the sample exceeded several hundred, then the sample was split with a plankton splitter and the resulting counts were multiplied by the subsampling factor. The works Hogue et al. (1976), Jones et al. (1978), Lippson and Moran (1974), and Mansueti and Hardy (1967) were used for identification. The number of ichthyoplankton in each sample was expressed as number per 10 m^3 using the following formula:

Ichthyoplankton (#/10m^3) = 10N/V
where N = number ichthyoplankton in the sample
V = volume of water filtered, (m^3)

C. Adult and Juvenile Fish

Fishes were sampled by trawling at stations AR3 and AR4, and seining at stations AR5 and AR6 (Figure 1b). For trawling, a try-net bottom trawl with a 15-foot horizontal opening, a ¾ inch square body mesh and a ¼ inch square cod end mesh was used. The otter boards were 12 inches by 24 inches. Towing speed was 2-3 miles per hour and tow length was 5 minutes. The trawls were towed upriver parallel to the channel at AR4, and following the curve away from the channel at AR3. The direction of tow should not be crucial. Dates of sampling and weather conditions are found in Table 1.

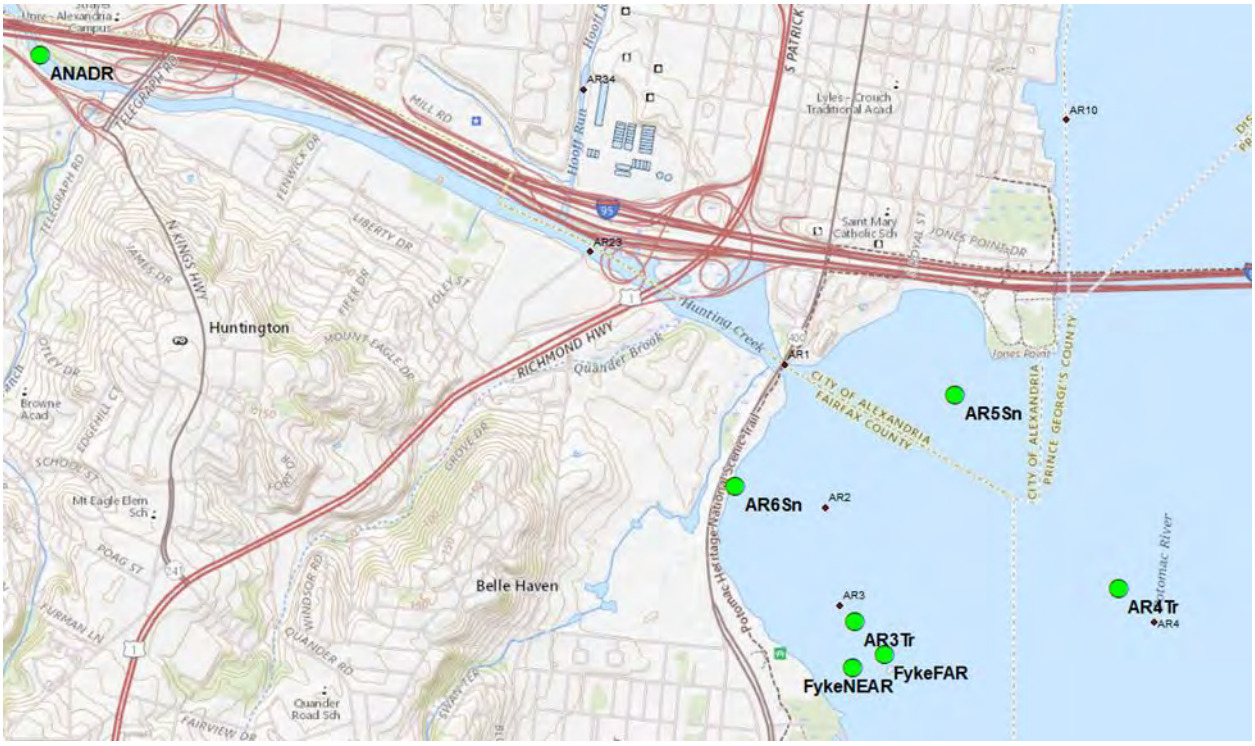

Figure 1b. Hunting Creek area of the Tidal Potomac River showing fish monitoring stations – Large Green circles. Stations with Tr in name are trawl stations; those with Sn in name are seine stations and those with Fyke in name are fyke stations. ANADR is the anadromous station. Water quality stations shown as small symbols and lettering for comparison.

Seining was performed with a bag seine that was 50 feet long, 3 feet high, and made of knotted nylon with a ¼ inch square mesh. The bag is located in the middle of the net and measures 3 ft^3. The seining procedure was standardized as much as possible. The net was stretched out perpendicular to the shore with the shore end right at the water line. The net was then pulled parallel to the shore for a distance of 100 feet by a worker at each end moving at a slow walk. Actual distance was recorded if in any circumstance it was lower than 100 feet. At

the end of the prescribed distance, the offshore end of the net was swung in an arc to the shore and the net pulled up on the beach to trap the fish. Dates for seine sampling were the same as those for trawl sampling (Table 1). An additional seine sample was collected on June 25.

Due to extensive submerged aquatic vegetation (SAV) cover in Hunting Creek, we adjusted our sampling regime in years of high SAV growth to include fyke netting. The fyke netting procedure is described below, but we did not use the fyke nets in 2020 due to continued absence of SAV. The trawl at AR3 has been impeded more frequently each year due to this vegetation, and two fyke nets were set in the area close to AR3 (Figure 1). The fyke net sampling stations are called 'fyke near' and 'fyke far' in reference to their distance from shore. These fyke nets were set within the SAV to sample the fish community that uses the SAV cover as habitat. Fyke nets were set for 4 hours to passively collect fish. The fyke nets have 5 hoops, a 1/4 inch mesh size, 16 feet wings and a 32 feet lead. Fish enter the net by actively swimming and/or due to tidal motion of the water. The lead increases catch by capturing the fish swimming parallel to the wings. Fyke nets were not set in 2020 due to crew limitations under COVID. Due to lower densities of SAV in 2020, trawling in this location (AR3) continued throughout the year (Table 1).

After the catch from each of these three gear types was hauled in, the fishes were measured for standard length and total length to the nearest mm. Standard length is the distance from the front tip of the snout to the end of the vertebral column and base of the caudal fin. This is evident in a crease perpendicular to the axis of the body when the caudal fin is pulled to the side. Total length is the distance from the tip of the snout to the tip of the longer lobe of the caudal fin, measured by straightening the longer lobe toward the midline.

If the identification of the fish was not certain in the field, a specimen was preserved in 70% ethanol and identified later in the lab. Fishes kept for chemical analysis were kept on ice wrapped in aluminum foil until frozen in the lab. All fishes retained for laboratory analysis or identification were first euthanized by submerging them in an ice sludge conforming to the AICUC protocol. Identification was based on characteristics in dichotomous keys found in several books and articles, including Jenkins and Burkhead (1983), Hildebrand and Schroeder (1928), Loos et al (1972), Dahlberg (1975), Scott and Crossman (1973), Bigelow and Schroeder (1953), Eddy and Underhill (1978), Page and Burr (1998), and Douglass (1999).

D. Submersed Aquatic Vegetation

Data on coverage and composition of submersed aquatic vegetation (SAV) are generally obtained from the SAV webpage of the Virginia Institute of Marine Science (http://www.vims.edu/bio/sav). Information on this web site is obtained from aerial photographs near the time of peak SAV abundance as well as ground surveys which are used to determine species composition. We also recorded SAV relative abundance on a 0-3 scale at 4 minute intervals using visual observations and rake tow during data mapping cruises.

E. Benthic Macroinvertebrates

Benthic macroinvertebrates were sampled monthly using a petite ponar sampler at

embayment stations AR2, AR3, and AR4. Triplicate samples were collected at each station monthly. Bottom samples were sieved on-site through a 0.5 mm stainless steel sieve and preserved with rose bengal formalin. In the laboratory benthic samples were rinsed with tap water through a 0.5 mm sieve to remove formalin preservative and resuspended in tap water. All organisms were picked, sorted, identified and enumerated.

In 2020 benthic invertebrates were also sampled at selected flowing tributary stations which possessed natural riffle-run areas. At each site one-minute kick samples were collected at one riffle and one run and composited in a single bottle. The sample was preserved with formalin to a concentration of 5%. In the lab the sample was sieved through a 0.5 mm mesh (same as the kick net) and thoroughly washed with tap water before picking and sorting. Following sorting animals were enumerated by taxon and held in ethanol-glycerin. Sampling sites for tributary macroinvertebrate sampling are shown in Figure 1c.

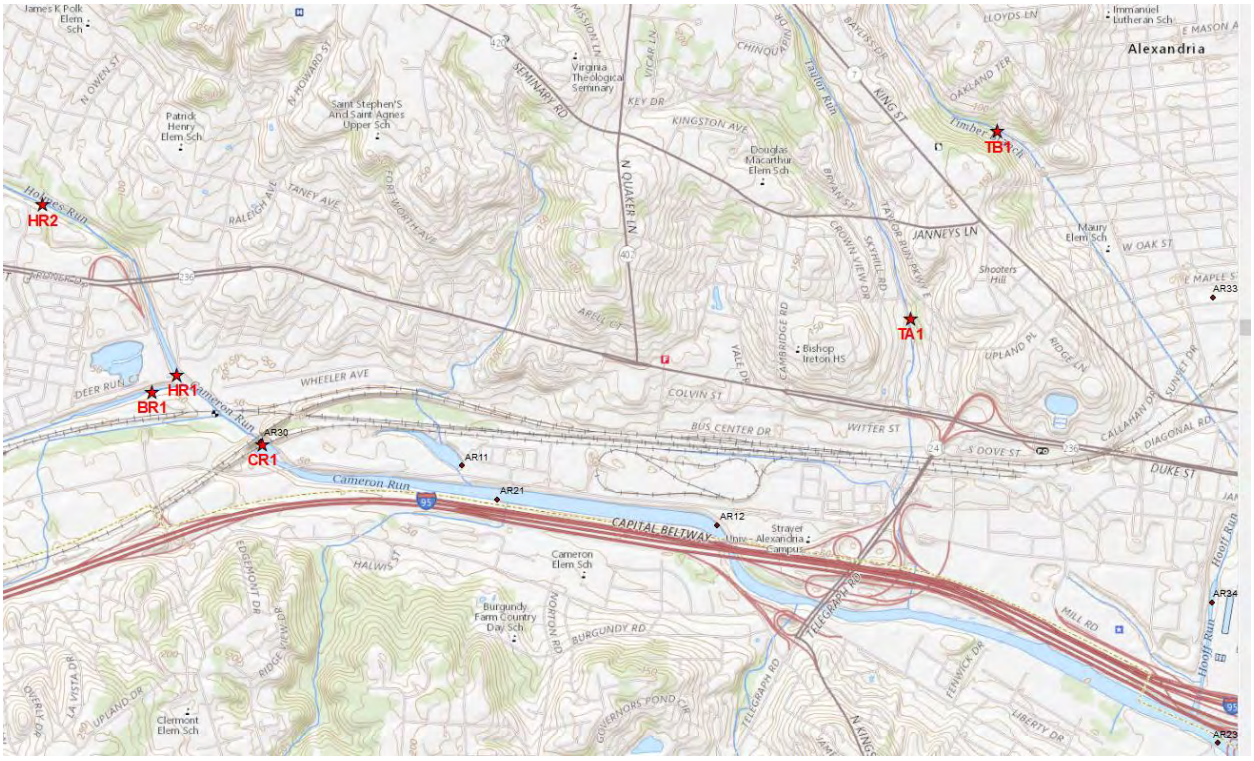

Figure 1c. Benthic sampling stations on flowing tributaries of Cameron Run. CR1: Cameron Run: HR1, HR2: Holmes Run; BR: Backlick Run; IR: Indian Run; TR: Turkeycock Run.

F. Water Quality Mapping (Dataflow)

On one additional date in 2020 (August 21) *in situ* water quality mapping was conducted by slowly transiting through much of the Hunting Creek study area as water was pumped through a chamber containing a YSI 6600 sonde equipped with temperature, specific conductance, dissolved oxygen, pH, turbidity, and chlorophyll probes. Readings were recorded at 15 second intervals along with simultaneous GPS position readings. Every 2 minutes SAV relative abundance by species was recorded and every 4 minutes water samples were collected

for extracted chlorophyll and TSS determination. Some areas of the Hunting Creek embayment could not be surveyed due to shallow water or heavy SAV growth. These surveys allowed a much better understanding of spatial patterns in water quality within the Hunting Creek area which facilitated interpretation of data from the fixed stations. This approach is in wide use in the Chesapeake Bay region by both Virginia and Maryland under the name “dataflow”.

G. Data Analysis

Data for each parameter were entered into spreadsheets (Excel or SigmaPlot) for graphing of temporal and spatial patterns. SYSTAT was used for statistical calculations and to create illustrations of the water quality mapping cruises. JMP v8.0.1was used for fish graphs. Other data analysis approaches are explained in the text.

RESULTS

A. Climatic and Hydrologic Factors - 2020

In 2020 temperature was below normal in April and May, but well above normal from June through August (Table 3). There were 38 days with maximum temperature above 32.2ºC (90ºF) in 2020 which is well above the median number over the past decade. Precipitation closer to normal in 2020 than in the extremely wet year 2018. However, it was again well above normal in 2020. April, July, and August were about double their normal precipitation in 2020.

Table 3. Meteorological Data for 2020. National Airport. Monthly Summary.

	Air Temp (ºC)		Precipitation (cm)	
MONTH				
March	11.9	(8.1)	5.9	(9.1)
April	12.9	(13.4)	16.0	(7.0)
May	17.7	(18.7)	6.3	(9.7)
June	24.9	(23.6)	8.9	(8.0)
July	29.1	(26.2)	16.5	(9.3)
August	26.8	(25.2)	22.2	(8.7)
September	21.5	(21.4)	14.0	(9.6)
October	17.2	(14.9)	11.6	(8.2)

Note: 2020 monthly averages or totals are shown accompanied by long-term monthly averages (1971-2000). Source: Local Climatological Data. National Climatic Data Center, National Oceanic and Atmospheric Administration.

River and stream flow in 2020 were closer to average for all months in the Potomac mainstem, but in Cameron Run were well above average in April, July, and August (Table 4).

Table 4. Monthly mean discharge at USGS Stations representing freshwater flow into the study area. (+) 2020 month > 2x Long Term Avg. (-) 2020 month < ½ Long Term Avg.

	Potomac River at Little Falls (cfs)		**Cameron Run at Wheeler Ave (cfs)**	
	2020	**Long Term Average**	**2020**	**Long Term Average**
March	9137 (-)	23600	34.2	55
April	16424	20400	96.0 (+)	42
May	20824	15000	47.5	41
June	9747	9030	43.3	38
July	3453	4820	79.1 (+)	31
August	6109	4550	102.0 (+)	28
September	4558	5040	52.5	38
October	3198	5930	62.1	33

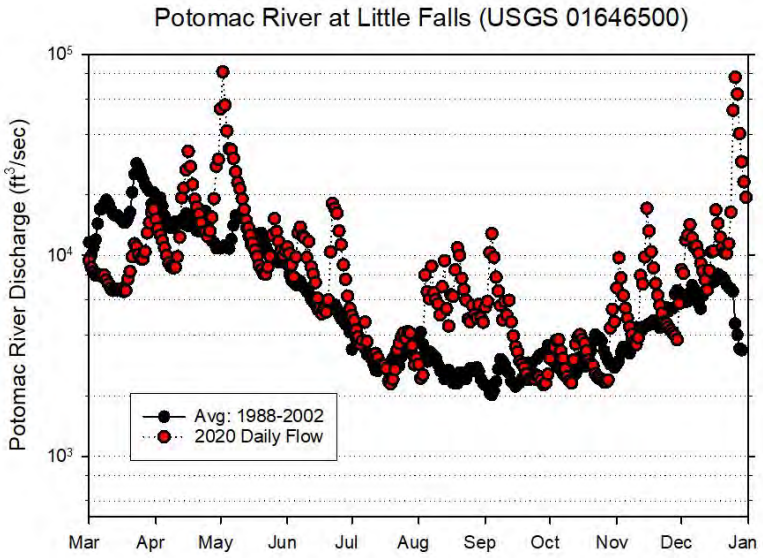

In a tidal freshwater system like the Potomac River, river flow entering from upstream is important in maintaining freshwater conditions and also serves to bring in dissolved and particulate substances from the watershed. High freshwater flows may also flush planktonic organisms downstream and bring in suspended sediments that decrease water clarity. The volume of river flow per unit time is referred to as "river discharge" by hydrologists. Note the general long term seasonal pattern of higher discharges in winter and spring and lower discharges in summer and fall.

Figure 2. Mean Daily Discharge: Potomac River at Little Falls (USGS Data). Month tick is at the beginning of the month.

These same patterns were seen in the graphs of daily river flow when compared to long-term averages (Figure 2). The long-term average shows a steadily decreasing trend from April through September. In 2020 this general seasonal pattern was observed except for the notable surges in May, June, and August which have the potential to strongly impact the ongoing growth of SAV and plankton in the river. Discharge in Cameron Run showed many short-lived pulses during July and August. (Figure 3).

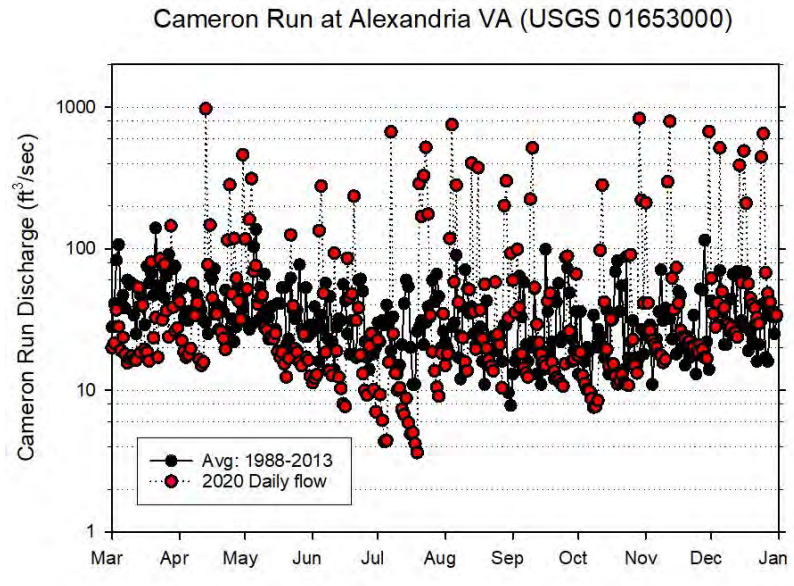

In the Hunting Creek region of the tidal Potomac, freshwater discharge is occurring from both the major Potomac River watershed upstream (measured at Little Falls) and from immediate tributaries, principally Cameron Run which empties directly into Hunting Creek. The gauge on Cameron Run at Wheeler Avenue is located just above the head of tide and covers most area which contributes runoff directly to the Hunting Creek embayment from the watershed. The contributing area to the Wheeler Ave gauge is 33.9 sq mi. (USGS)

.

Figure 3. Mean Daily Discharge: Cameron Run at Alexandria (Wheeler Ave) (USGS Data).

B. Physico-chemical Parameters: Embayment and River Stations – 2020

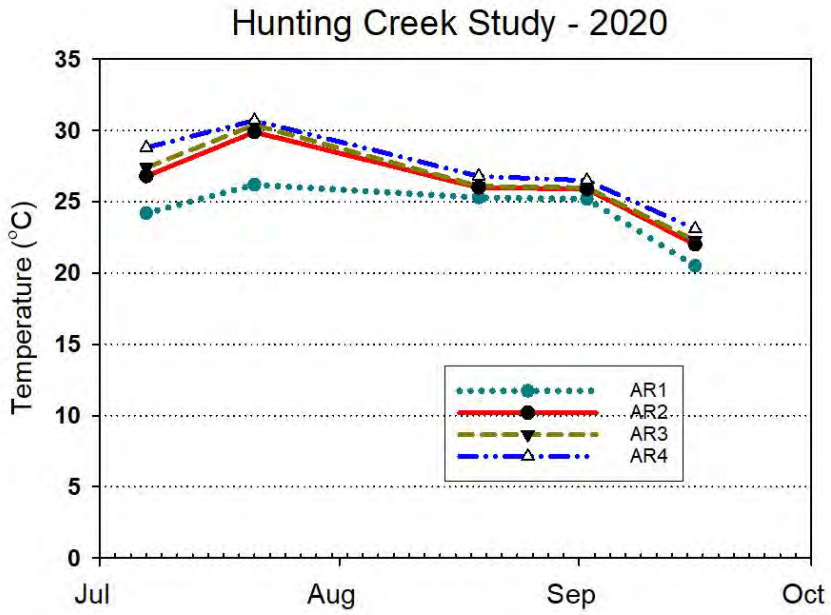

Water temperature is an important factor affecting both water quality and aquatic life. In a well-mixed system like the tidal Potomac, water temperatures are generally fairly uniform with depth. In a shallow mixed system such as the tidal Potomac, water temperature often closely tracks daily changes in air temperature.

Figure 4. Water Temperature (ºC). Tidal Main Stations. Month tick is at first day of month.

Due to COVID restrictions field sampling started in early July, yielding approximately ½ year of data. Water temperature followed the typical seasonal pattern at Tidal Main Stations (Figure 4). Temperatures in mid-July approached 30°C. A fairly steady decline was observed through August and September. Similar patterns were observed at the Tidal CSO Impact Stations with the exception that AR24 and AR25 were consistently 2-5 degrees cooler (Figure 5).

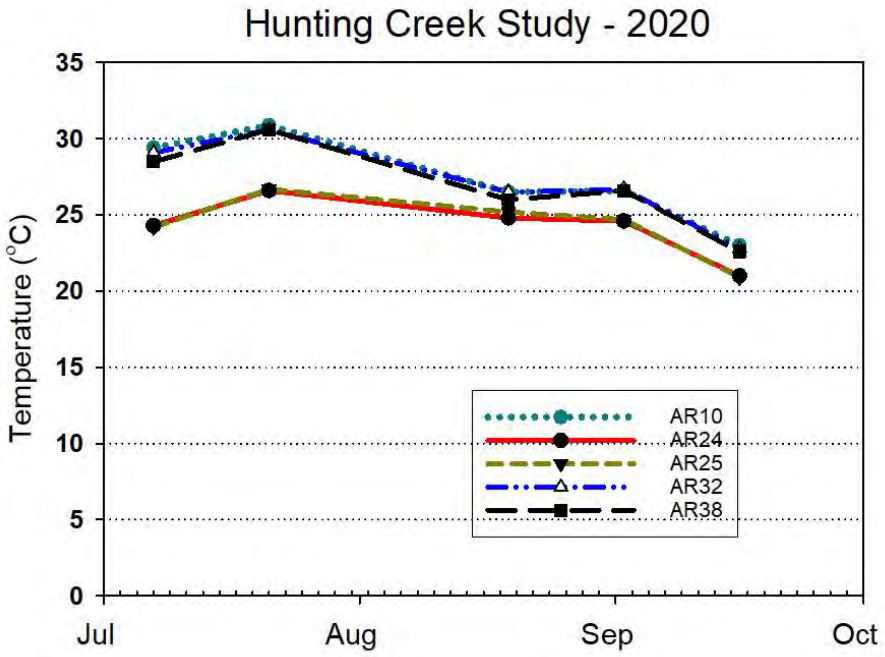

In this section of the report, we have placed the stations into two groups: Tidal Main Stations which were sited to get general conditions in the tidal open water in Hunting Creek and the Potomac mainstem. The second group was Tidal CSO Impact Stations that were situated above and below CSO outfalls to examine their effects on tidal water quality.

Figure 5. Water Temperature (ºC). Tidal CSO Impact Stations.

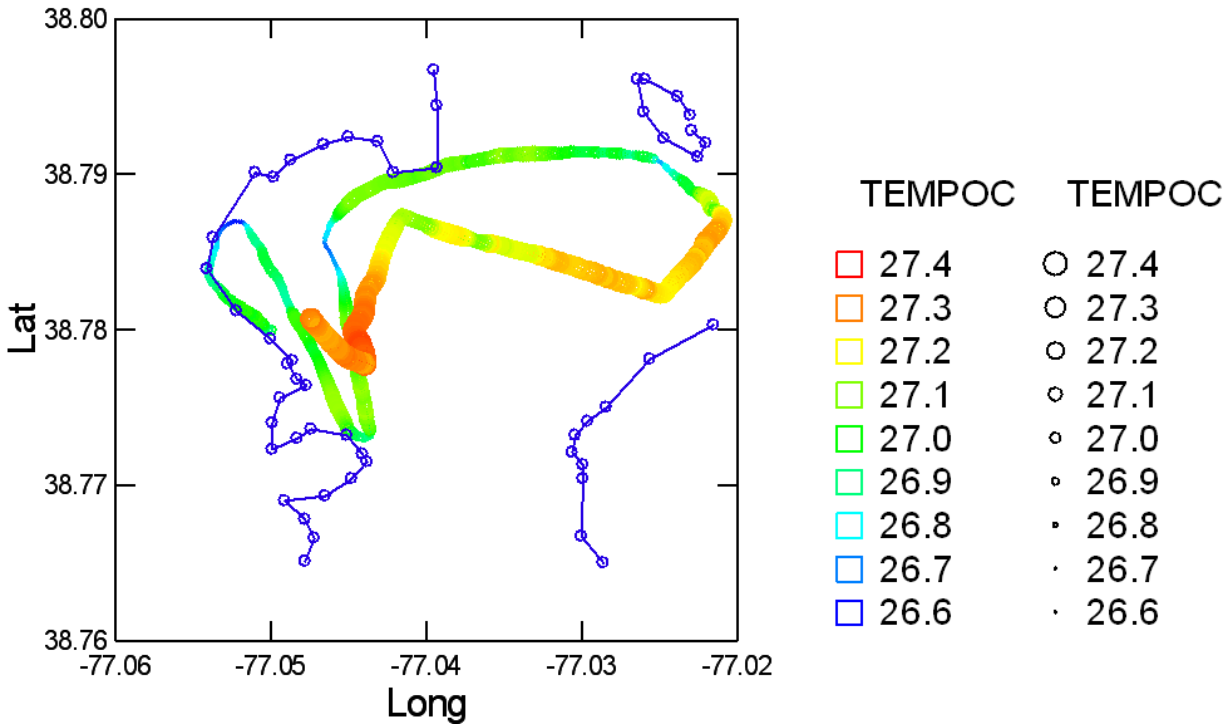

Figure 6. Water Quality Mapping. August 21, 2020. Temperature (°C).

Mapping of water temperature was conducted on August 21, 2020 (Figure 6). Water temperature ranged from 26.6 to 27.4°C. There was little difference in water temperature spatially. It appeared that the main driver was warming of water as the day progressed. The lower temperatures were found at the beginning of the transect (about 9 am) and higher temperatures at the end (about noon).

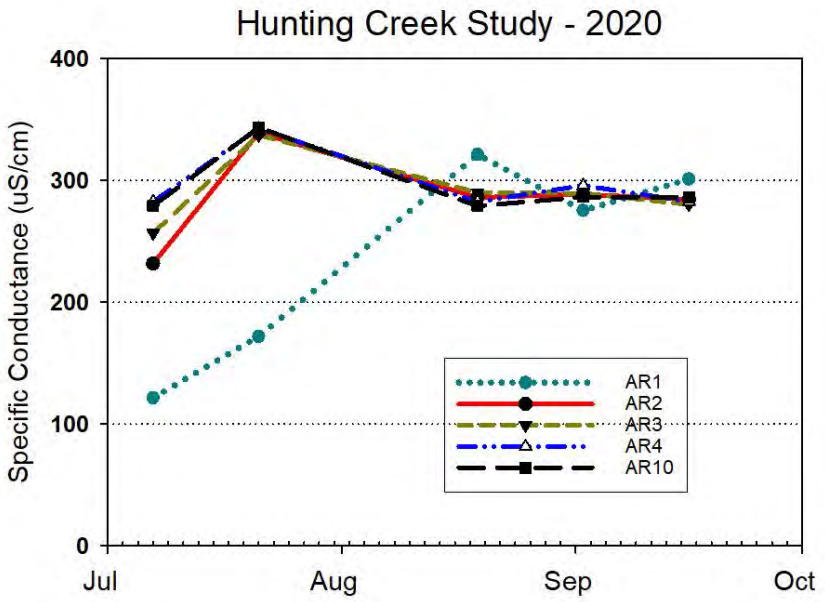

Specific conductance measures the capacity of the water to conduct electricity standardized to 25°C. This is a measure of the concentration of dissolved ions in the water. In freshwater, conductivity is relatively low. Ion concentration generally increases slowly during periods of low freshwater inflow and decreases during periods of high freshwater inflow. Sewage treatment facilities can be a source of elevated conductivity. In winter road salts can be a major source of conductivity in urban streams.

Figure 7. Specific Conductance (µS/cm). Tidal Main Stations. Month tick is at first day of month.

Specific conductance was generally lower at AR1 than at the other stations reflecting its location at the mouth of Cameron Run (Figure 7). This was particularly true in July when storm runoff was high. Values at other stations were quite similar. AR10, AR32, and AR38 exhibited similar and fairly steady values around 300 for the July – September period that were similar to most of the Tidal Main Stations. AR24 and AR25 on the north shore of Hunting Creek were different with low values in July increasing for the rest of the study period similar to AR1.

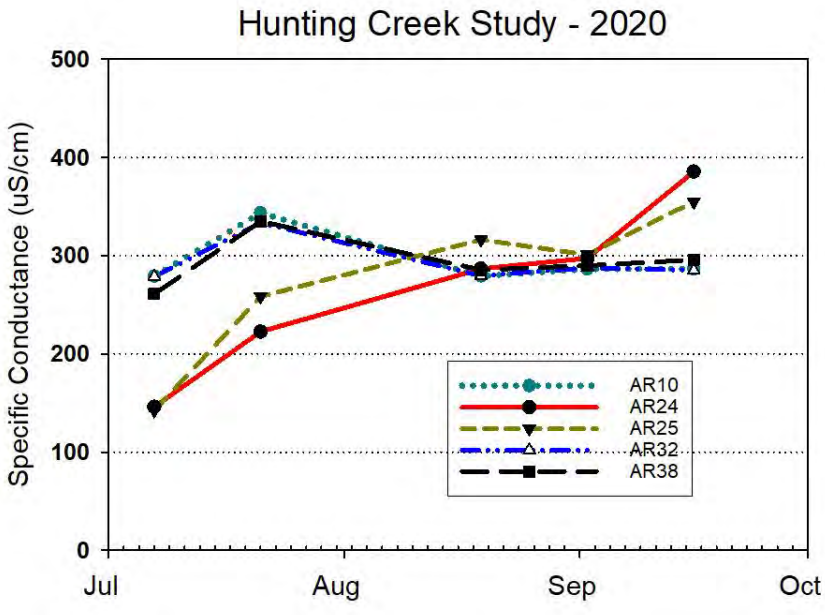

Figure 8. Specific Conductance (µS/cm). CSO Impact River Stations.

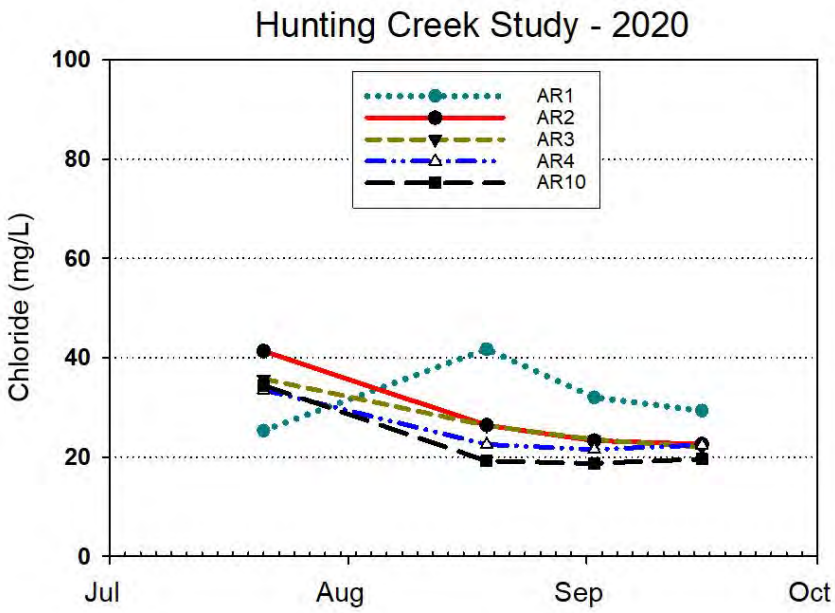

Chloride ion (Cl-) is a principal contributor to conductance. Major sources of chloride in the study area are sewage treatment plant discharges, road salt, and brackish water from the downriver portion of the tidal Potomac. Chloride concentrations observed in the Hunting Creek area are very low relative to those observed in brackish, estuarine, and coastal areas of the Mid-Atlantic region. Chloride may increased slightly in late summer or fall when brackish water from down estuary may reach the area as freshwater discharge declines.

Figure 9. Chloride (mg/L). Tidal Main Stations. Month tick is at first day of month.

Chloride was 20-40 mg/L at all of the Tidal Main Stations.The pattern at most of theses stations was higher values in July and a decline through August and September. AR1 showed an opposite pattern. AR10, AR32, and AR38, located on the mainstem of the Potomac, followed a seasonal pattern similar to most of the Tidal Main Stations whereas AR24 and AR25 were more similar to AR1.

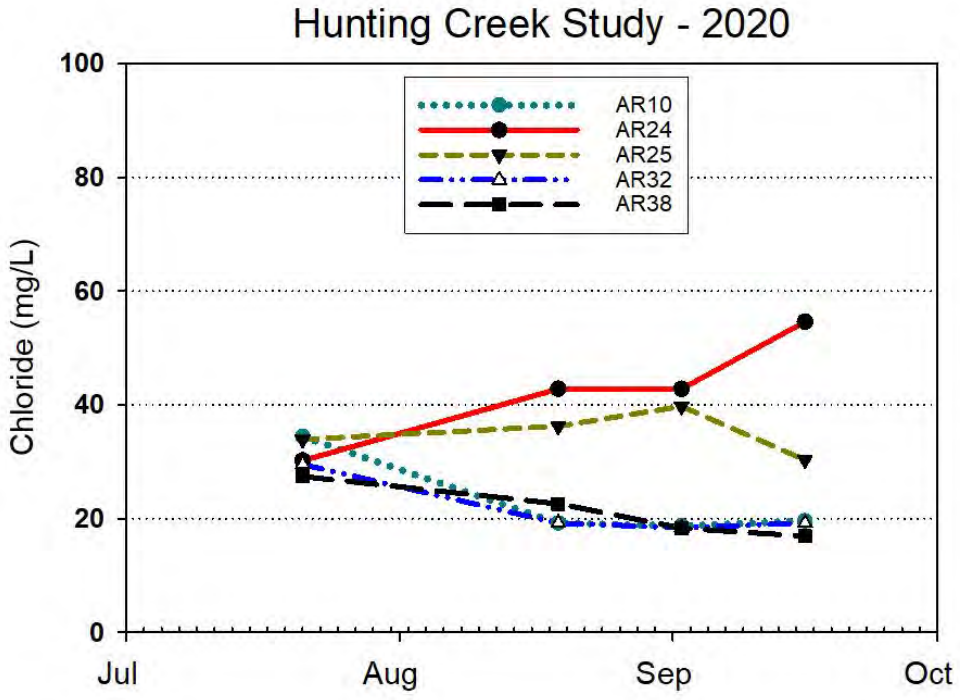

Figure 10. Chloride (mg/L). Tidal CSO Impact Stations

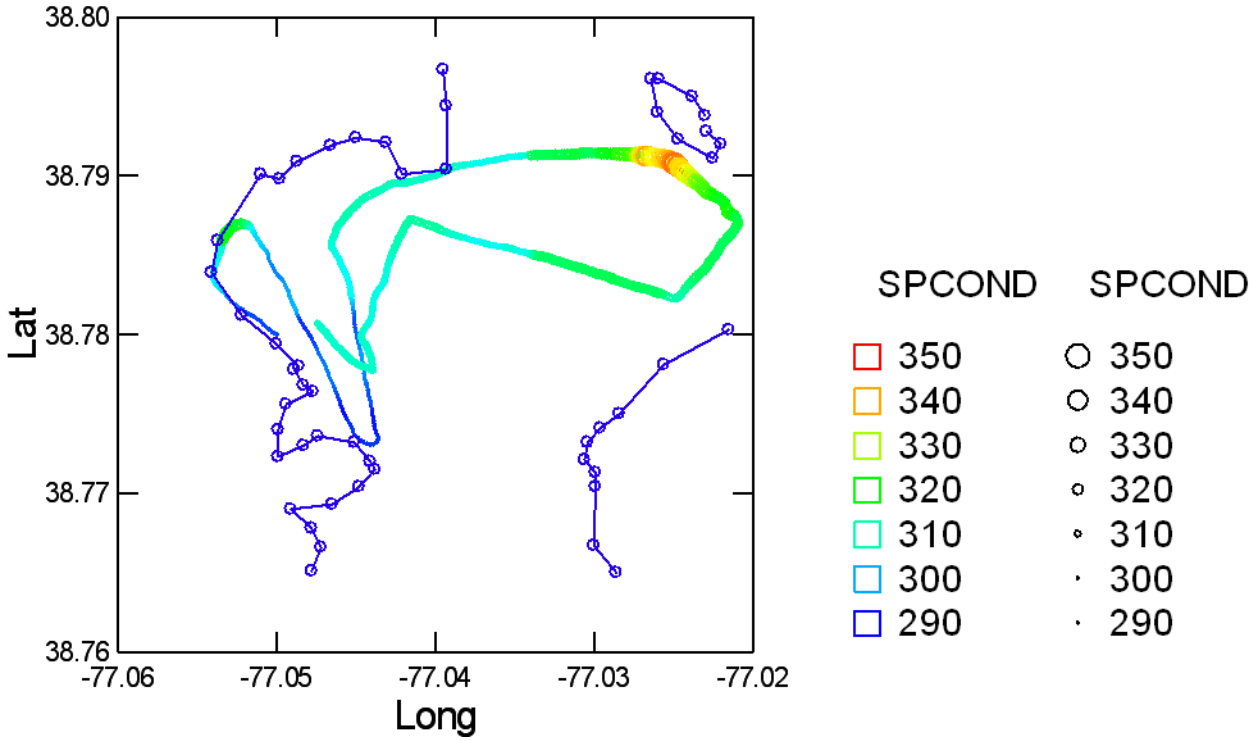

Figure 11. Water Quality Mapping. August 21, 2020. Specific conductance (µS).

Mapping of specific conductance on August 21, 2020 showed that lower values (290-310 uS/cm) were found in the Hunting Creek embayment (on the left in the map) and somewhat higher values (320-350 uS/cm) were found in the Potomac mainstem and Maryland side of the river. The higher values in the latter area may be due to proximity to Blue Plains.

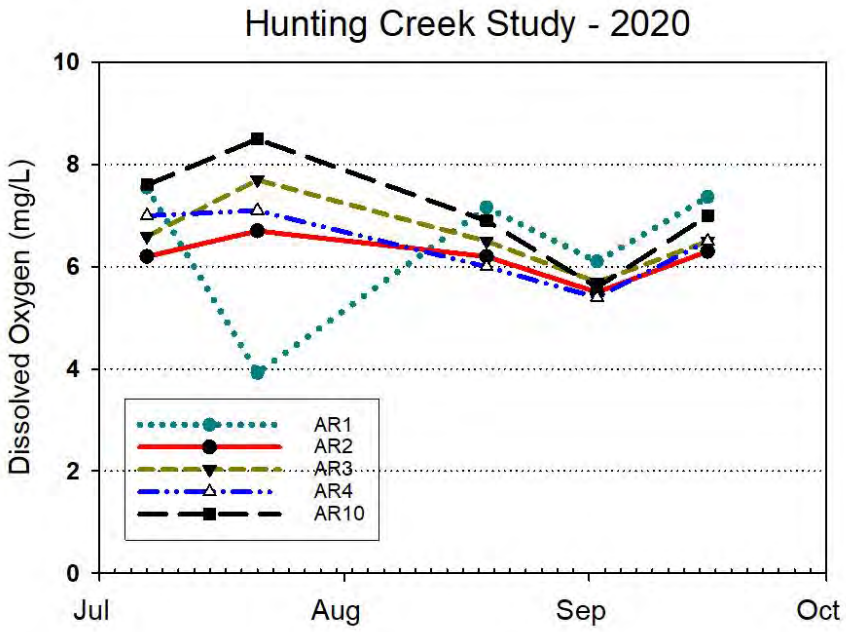

Oxygen dissolved in the water is required by freshwater animals for survival. The standard for dissolved oxygen (DO) in most surface waters is 5 mg/L. Oxygen concentrations in freshwater are in balance with oxygen in the atmosphere, but oxygen is only weakly soluble in water so water contains much less oxygen than air. This solubility is determined by temperature with oxygen more soluble at low temperatures.

Figure 12. Dissolved Oxygen (mg/L). Tidal Main Stations. Month tick is at first day of month.

The general pattern for dissolved oxygen (mg/L) at Tidal Main Stations was an increased to a maximum in late July, a decline through August and early September followed by another increase in late September (Figure 12). AR1 was similar except for a pronounced decline in late July. Looking at DO as percent saturation (Figure 11), the basic seasonal pattern similar with the peak in late July somewhat higher and again a decline at AR1. DO was generally highest at AR10 and lowest at AR2. DO rarely exceeded 100% and was only slightly below 80% indicating that photosynthesis and respiration were not major factors.

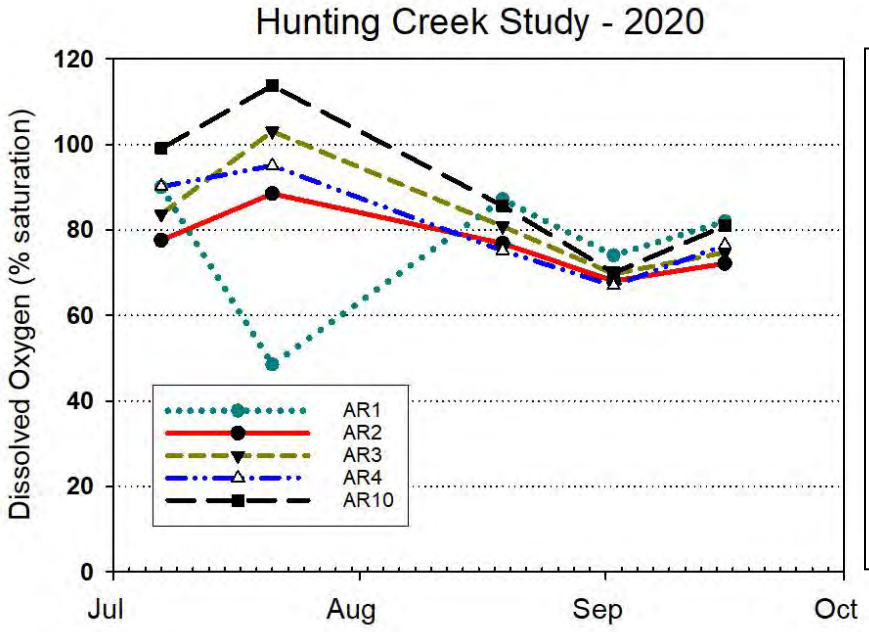

The temperature effect on oxygen concentration can be removed by calculating DO as percent saturation. This allows examination of the balance between photosynthesis and respiration both of which also impact DO. Photosynthesis adds oxygen to the water while respiration removes it. Values above 120% saturation are indicative of intense photosynthesis while values below 80% reflect a preponderance of respiration or decomposition.

Figure 13. Dissolved Oxygen (% saturation). Tidal Main Stations. Month tick is at first day.

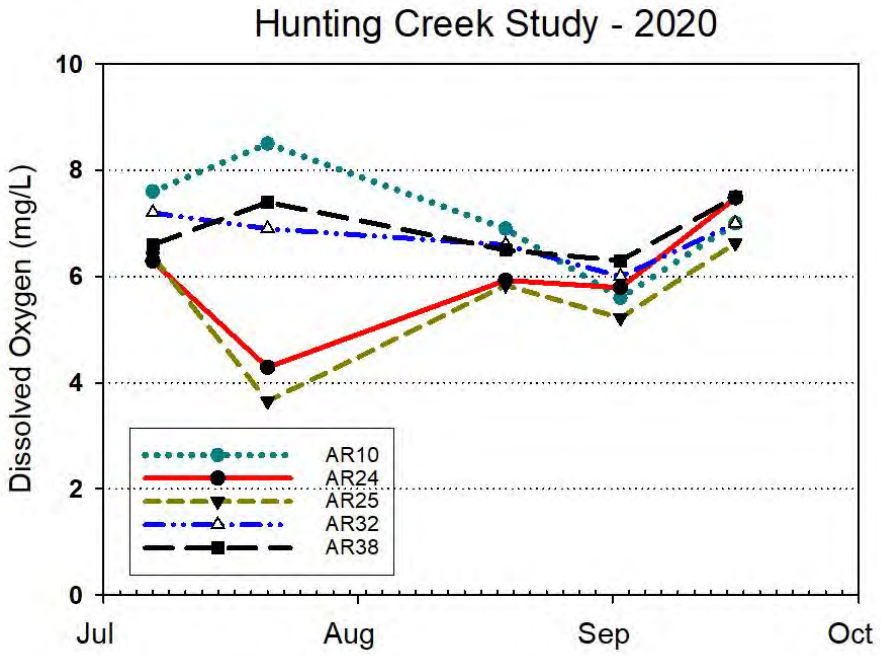

Figure 14. Disssolved oxygen (mg/L). Tidal CSO Impact Stations.

At the Tidal CSO Impact Stations there was general agreement among all site except in late July when the two stations in northern Hunting Creek (AR24 and AR25) exhibited much lower values than the other stations (Figure 14). DO as percent saturation (Figure 15) showed similar trends. The levels at AR24 and AR25 in late July were below 50% indicated strong action by respiration.

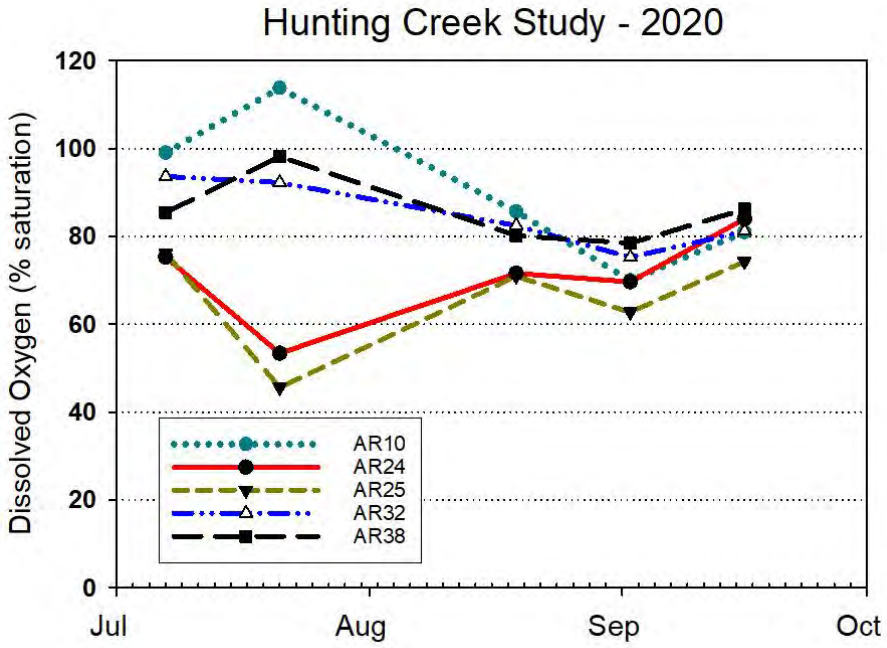

Figure 15. Dissolved oxygen (% saturation). Tidal CSO Impact Stations.

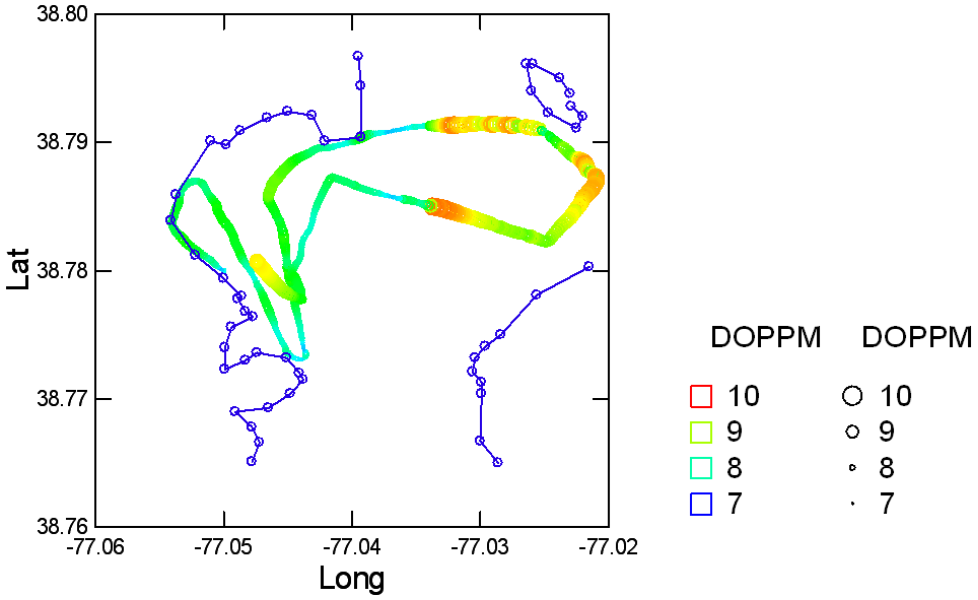

Figure 16a. Water Quality Mapping. August 21, 2020. Dissolved oxygen (mg/L).

Water quality mapping of dissolved oxygen on August 21, 2020 revealed lower values of 7-8 mg/L in the Hunting Creek embayment while the Potomac mainstem showed values as high as 9-10 mg/L (Figure 16a). This spatial pattern was also found in percent saturation values of DO (Figure 16b) which were generally around saturation (100%) in Hunting Creek and somewhat above saturation in the Potomac mainstem (110-120%).

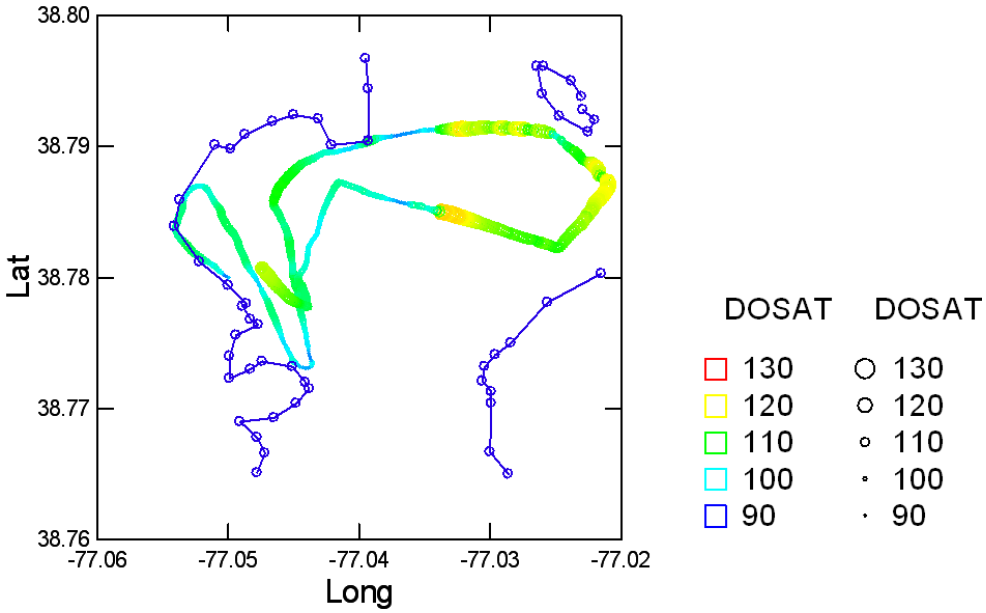

Figure 16b. Water Quality Mapping. August 21, 2020. Dissolved oxygen (percent saturation)

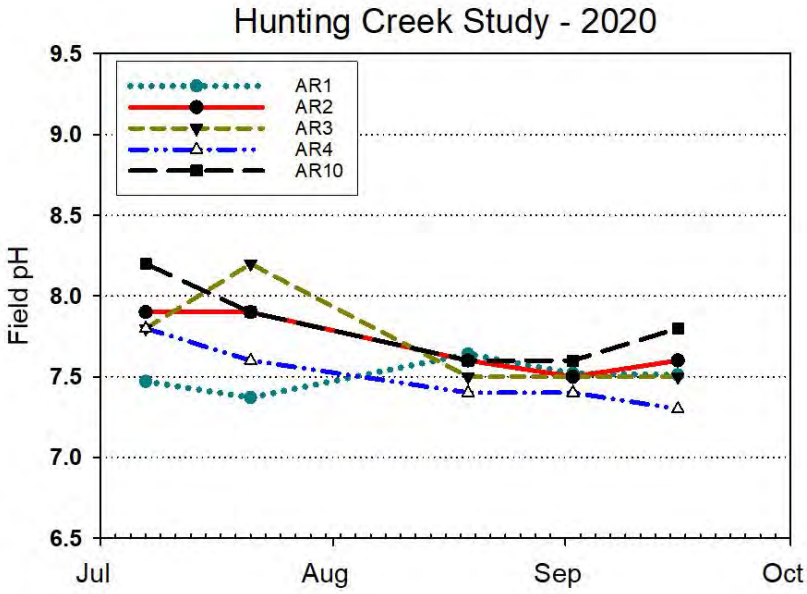

pH is a measure of the concentration of hydrogen ions (H+) in the water. Neutral pH in water is 7. Values between 6 and 8 are often called circumneutral, values below 6 are acidic and values above 8 are termed alkaline. Like DO, pH is affected by photosynthesis and respiration. In the tidal Potomac, pH above 8 indicates active photosynthesis and values above 9 indicate intense photosynthesis. A decrease in pH following a rainfall event may be due to acids in the rain or in the watershed.

Figure 17. Field pH. Tidal Main Stations. Month tick is at first day of month.

In 2020 pH values remained in a fairly narrow range (7.2-8.0) with little seasonal pattern at most sample stations (Figures 17&18). pH was consistently lower at AR1, AR24, and AR25, but the values at the other stations were very similar.

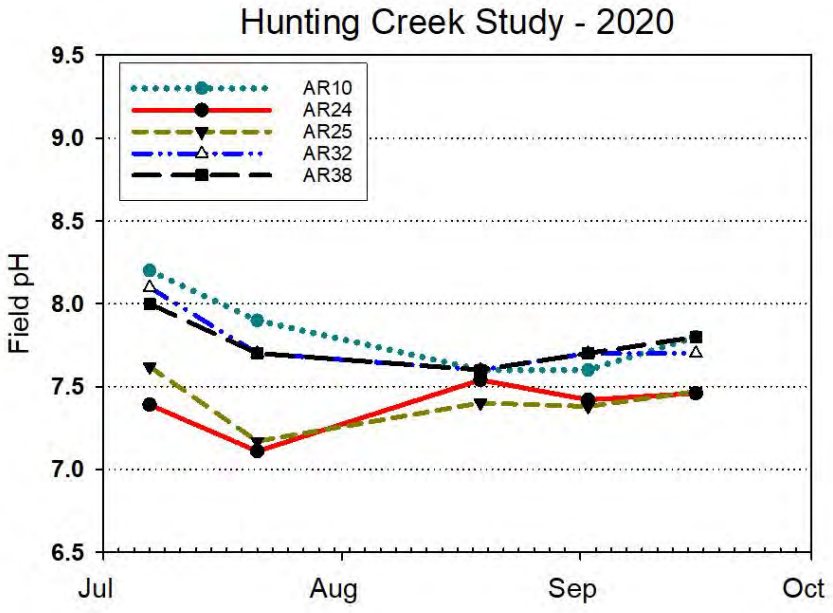

pH may be measured in the field or in the lab. Field pH is more reflective of in situ conditions while lab pH is done under more stable and controlled laboratory conditions and is less subject to error. Newer technologies such as the Hydrolab and YSI sondes used in GMU field data collection are more reliable than previous field pH meters and should give results that are most representative of values actually observed in the river.

Figure 18. pH. AlexRenew Lab Data. Month tick is at first day of month.

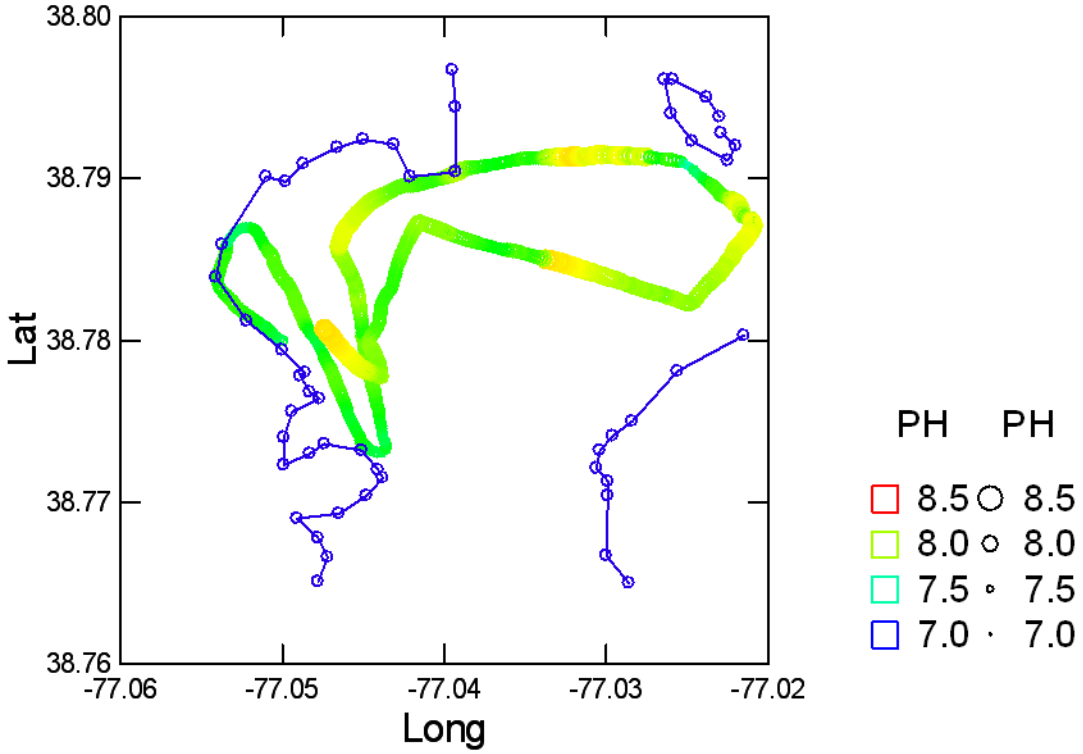

Figure 19. Water Quality Mapping. August 21, 2020. pH.

Water quality mapping of pH did not show a consistent seasonal pattern (Figure 19). Values were generally in the 7.5 to 8.0 range throughout the study area.

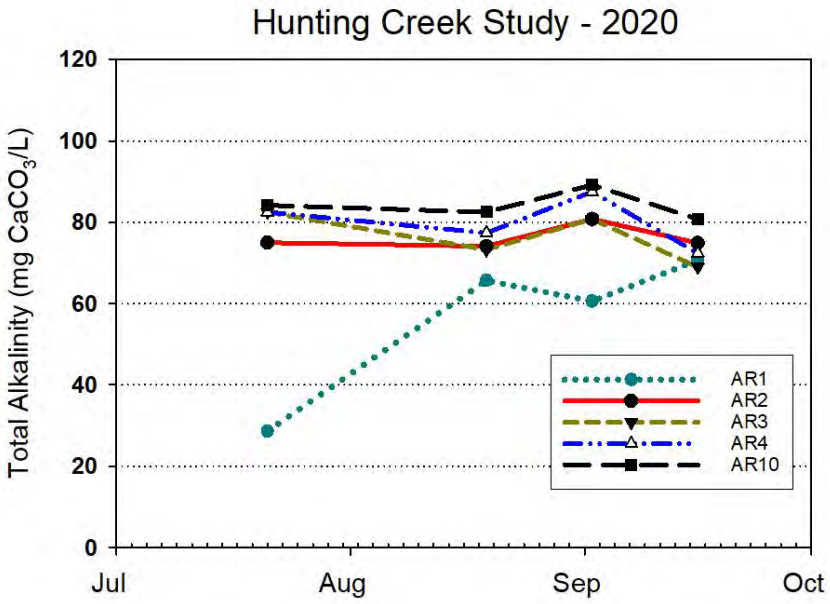

Total alkalinity measures the amount of bicarbonate and carbonate dissolved in the water. In freshwater this corresponds to the ability of the water to absorb hydrogen ions (acid) and still maintain a near neutral pH. Alkalinity in the tidal freshwater Potomac generally falls into the moderate range allowing adequate buffering without carbonate precipitation.

Figure 20. Total Alkalinity (mg/L as $CaCO_3$). Tidal Main Stations. Month tick is at first day.

Total alkalinity was fairly constant at most stations (Figures 20&21). The Tidal Main stations and other river mainstem stations (AR2, AR3, AR4, AR10, AR32, and AR38) were in a fairly narrow range between 70 and 90. AR1, AR24, and AR25 tended to be lower.

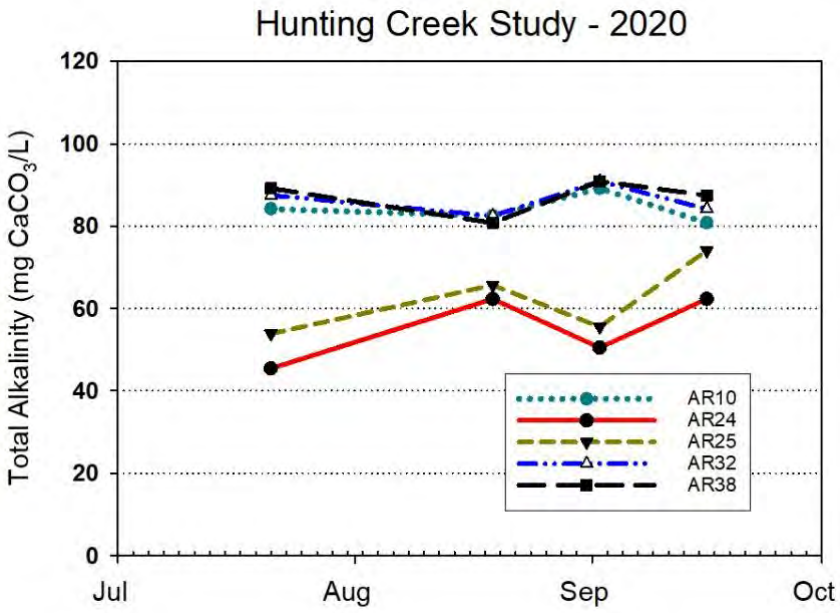

Figure 21. Total Alkalinity (mg/L as CaCO3). Tidal CSO Impact Stations.

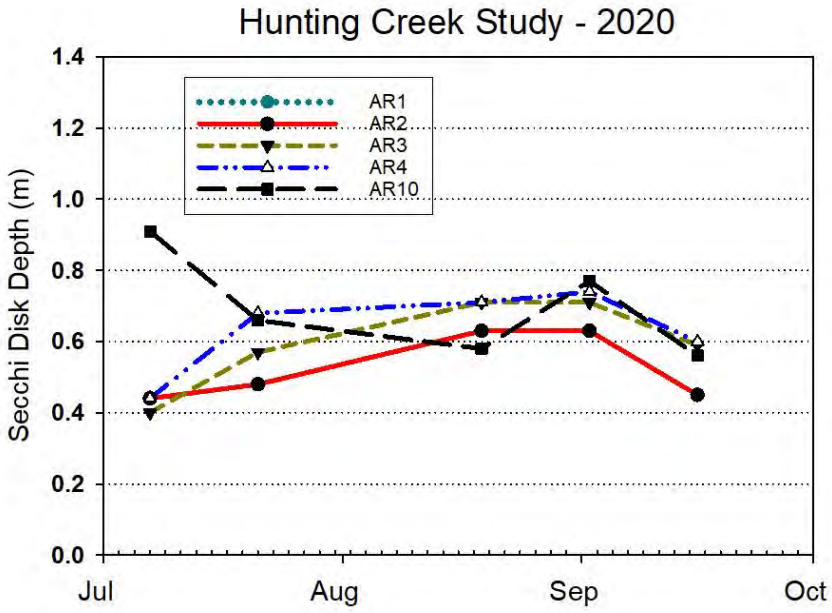

Secchi Depth is a measure of the transparency of the water. The Secchi disk is a flat circle of thick sheet metal or plywood about 6 inches in diameter which is painted into alternate black and white quadrants. It is lowered on a calibrated rope or rod to a depth at which the disk disappears. This depth is termed the Secchi Depth. This is a quick method for determining how far light is penetrating into the water column. Light is necessary for photosynthesis and thereby for growth of aquatic plants and algae.

Figure 22. Secchi Disk Depth (m). Tidal Main Stations. Month tick is at first day of month.

Water clarity as reflected by Secchi disk did not show strong seasonal patterns, but was generally in the 0.4 to 0.6 m range (Figure 22&23). Somewhat higher values were observed at AR10.

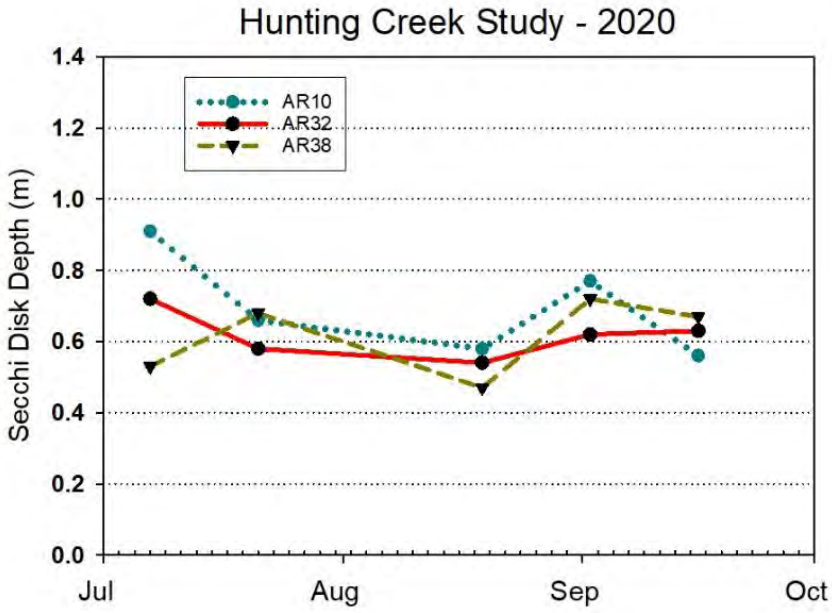

Figure 23. Secchi Disk Depth (m). Tidal CSO Impact Stations.

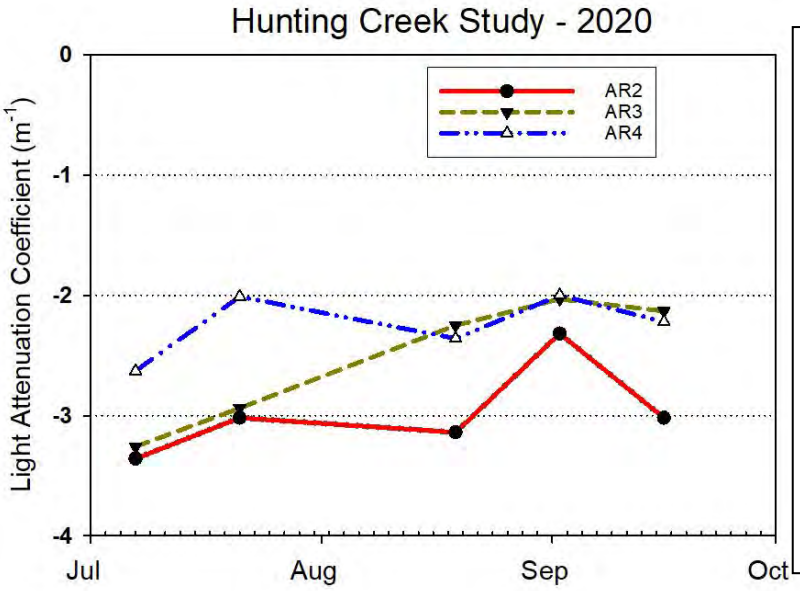

Light Attenuation is another approach to measuring light penetration. This is determined by measuring light levels at a series of depths starting near the surface. The resulting relationship between depth and light is fit to a semi-logarithmic curve and the resulting slope is called the light attenuation coefficient. This relationship is called Beer's Law. It is analogous to absorbance on a spectrophotometer. The greater the light attenuation, the faster light is absorbed with depth. More negative values indicate greater attenuation. Greater attenuation is due to particulate and dissolved material which absorbs and deflects light.

Figure 24. Light Attenuation Coefficient (m^{-1}). Tidal Main Stations. Month tick is at first day of month.

Light attenuation coefficient was fairly constant over the period (Figure 24). Values at AR4 indicated consistently clearer water than at AR2. AR3 was more like AR2 in July and more like AR3 in August and September. These values indicate that light penetration is not conducive for SAV recolonization.

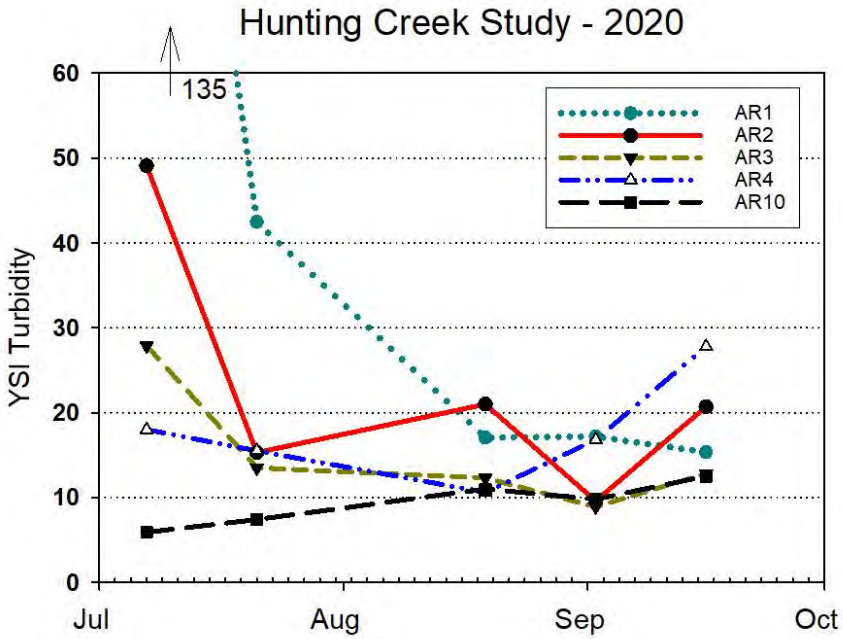

Turbidity is yet a third way of measuring light penetration. Turbidity is a measure of the amount of light scattering by the water column. Light scattering is a function of the concentration and size of particles in the water. Small particles scatter more light than large ones (per unit mass) and more particles result in more light scattering than fewer particles.

Figure 25. Turbidity (NTU). Tidal Main Stations. Month tick is at first day of month.

Turbidity exhibited some very high values in early July at AR1 and AR2 (Figure 25). These high values were also observed at AR24 and AR25 (Figure 26), all of these stations being located in the northern part of Hunting Creek. Otherwise turbidity was generally substantially lower in the 5-20 range.

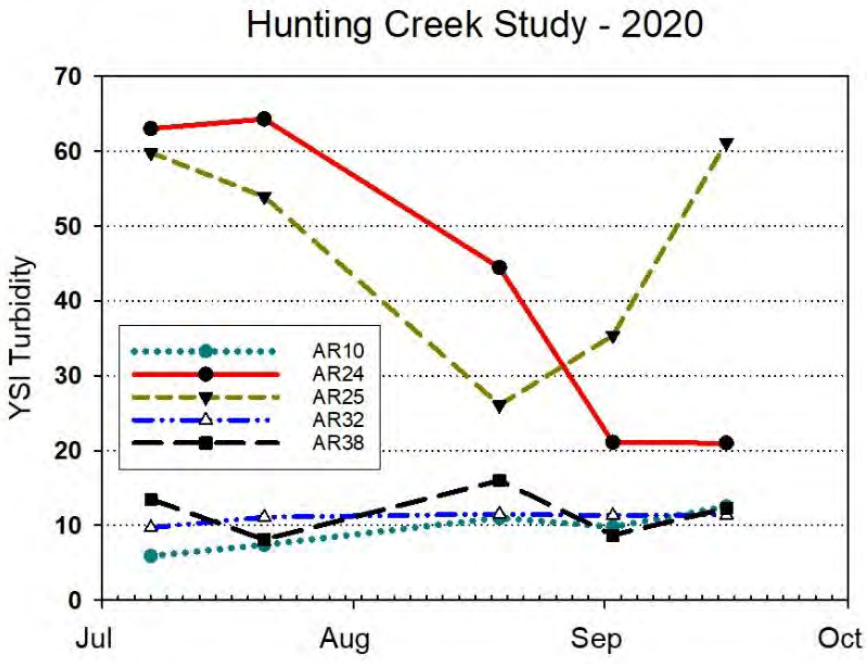

Figure 26. Turbidity (NTU). Tidal CSO Impact Stations.

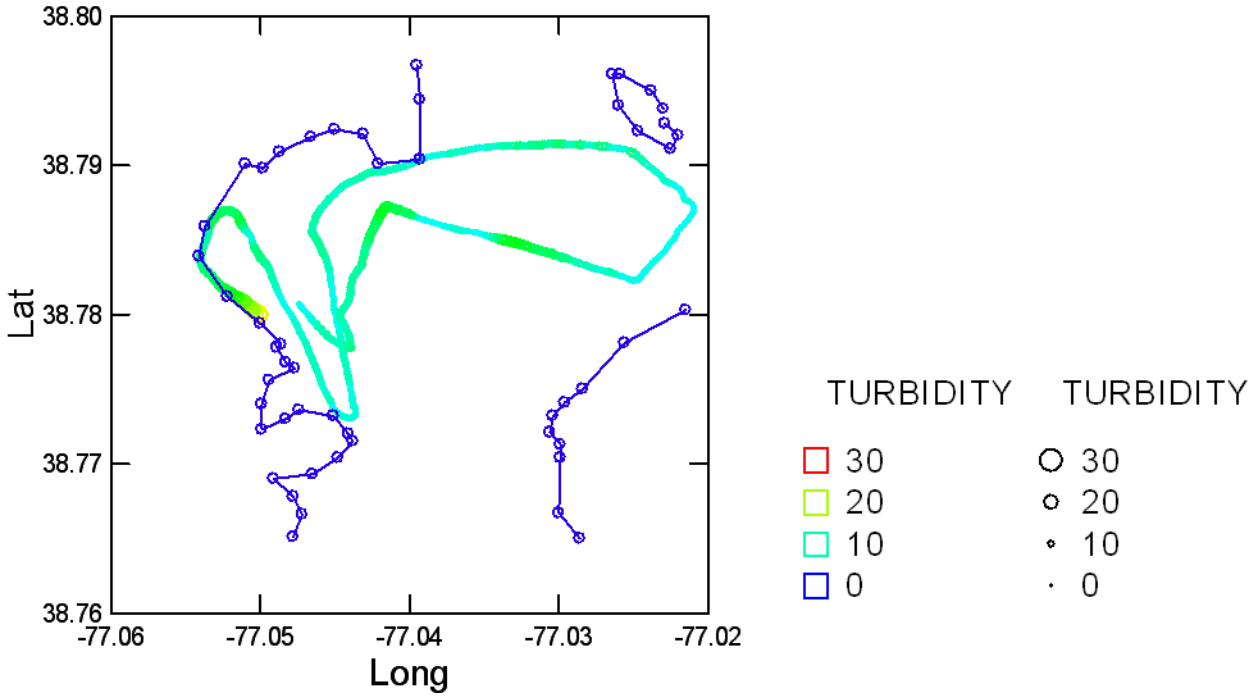

Figure 27. Water Quality Mapping. August 21, 2020. Turbidity YSI.

Turbidity was generally quite low throughout the study area with values typically 10-20 NTU throughout the study area on August 21, 2020 (Figure 27).

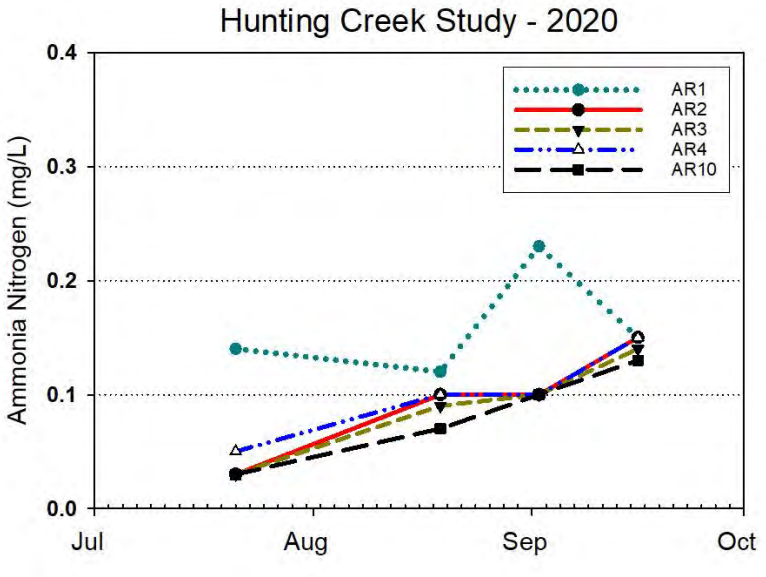

Ammonia nitrogen measures the amount of ammonium ion (NH_4^+) and ammonia gas (NH_3) dissolved in the water. Ammonia nitrogen is readily available to algae and aquatic plants and acts to stimulate their growth. While phosphorus is normally the most limiting nutrient in freshwater, nitrogen is a close second. Ammonia nitrogen is rapidly oxidized to nitrate nitrogen when oxygen is present in the water so high ammonia levels suggest proximity to a source.

Figure 28. Ammonia Nitrogen (mg/L). Tidal Main Stations. Month tick is at first day of month.

Ammonia nitrogen was consistently low (<0.15 mg/L) for the entire study period (Figure 28&29). Slightly higher values were seen on some dates at AR24 and AR25 and there was a general pattern of increase at all stations. Many of the values for ammonia nitrogen were reported as below detection limits at which time values equal to ½ of the detection limit were used in graphing.

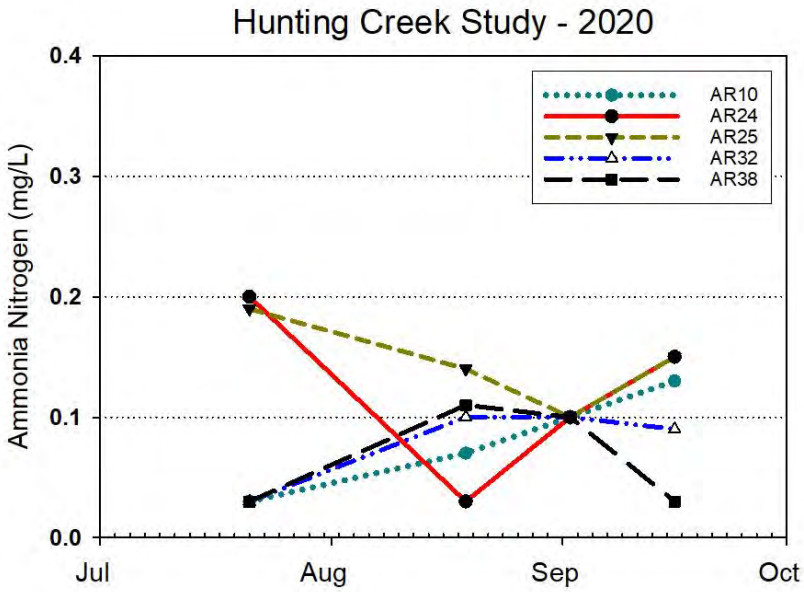

Figure 29. Ammonia Nitrogen (mg/L). Tidal SCO Impact Stations.

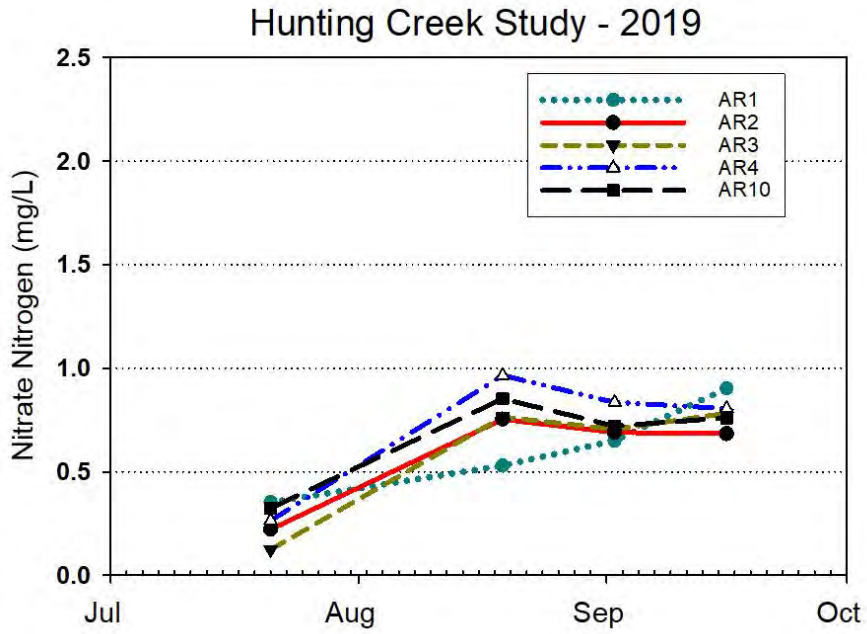

Nitrate Nitrogen refers to the amount of N that is in the form of nitrate ion (NO_3^-). Nitrate ion is the most common form of nitrogen in most well oxidized freshwater systems. Nitrate concentrations are increased by input of wastewater, nonpoint sources, and oxidation of ammonia in the water. Nitrate concentrations decrease when algae and plants are actively growing and removing nitrogen as part of their growth.

Figure 30. Nitrate Nitrogen (mg/L). Tidal Main Stations. Month tick is at first day of month.

Nitrate nitrogen levels showed a general pattern of increase from late July to mid-August and then a leveling through the rest of the year between 0.5 and 1.0 mg/L (Figure 30 & 31). AR24 and AR25 behaved somewhat differently and on the last sampling date AR24 was at 1.5 mg/L.

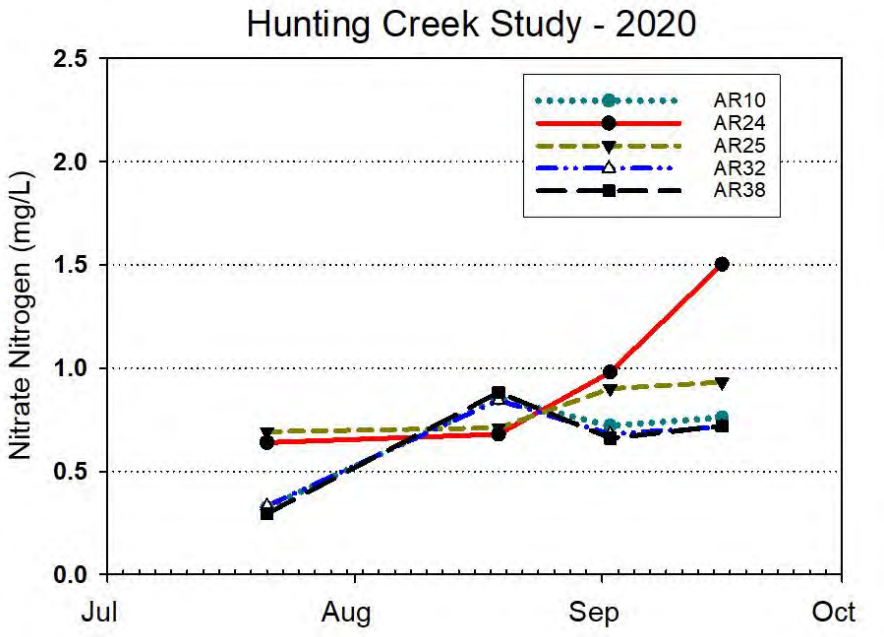

Figure 31. Nitrate Nitrogen (mg/L). Tidal CSO Impact Stations.

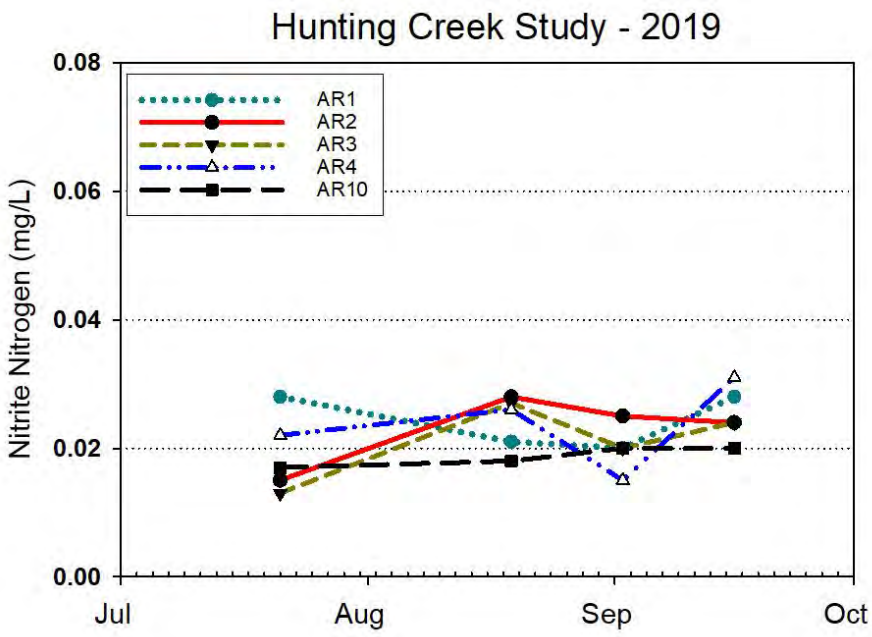

Nitrite nitrogen consists of nitrogen in the form of nitrite ion (NO_2^-). Nitrite is an intermediate in the oxidation of ammonia to nitrate, a process called nitrification. Nitrite is usually in very low concentrations unless there is active nitrification.

Figure 32. Nitrite Nitrogen (mg/L). Tidal Main Stations. Month tick is at first day of month.

Nitrite nitrogen was generally low (<0.03 mg/L) at all stations throughout the year (Figures 32&33). Slightly higher values were observed at AR1, AR24, and AR25 in late July.

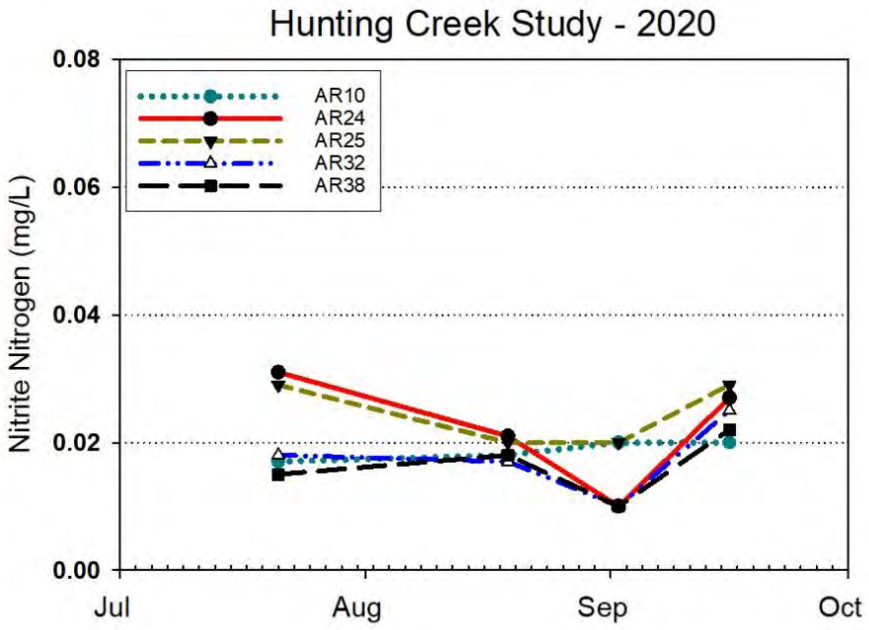

Figure 33. Nitrite Nitrogen (mg/L). Tidal CSO Impact Stations.

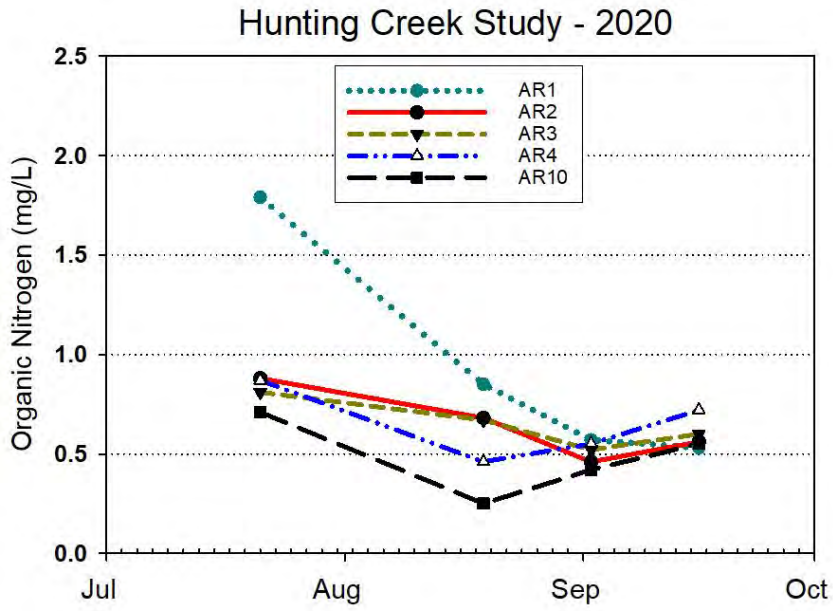

Organic nitrogen measures the nitrogen in dissolved and particulate organic compounds in the water. Organic nitrogen comprises algal and bacterial cells, detritus (particles of decaying plant, microbial, and animal matter), amino acids, urea, and small proteins. When broken down in the environment, organic nitrogen results in ammonia nitrogen. Organic nitrogen is determined as the difference between total Kjeldahl nitrogen and ammonia nitrogen.

Figure 34. Organic Nitrogen (mg/L). Tidal Main Stations. Month tick is at first day of month.

Organic nitrogen values were generally in the range of 0.2-1.0 mg/L at most stations throughout the year (Figures 34&35). AR1, AR24, and AR25 were consistently higher.

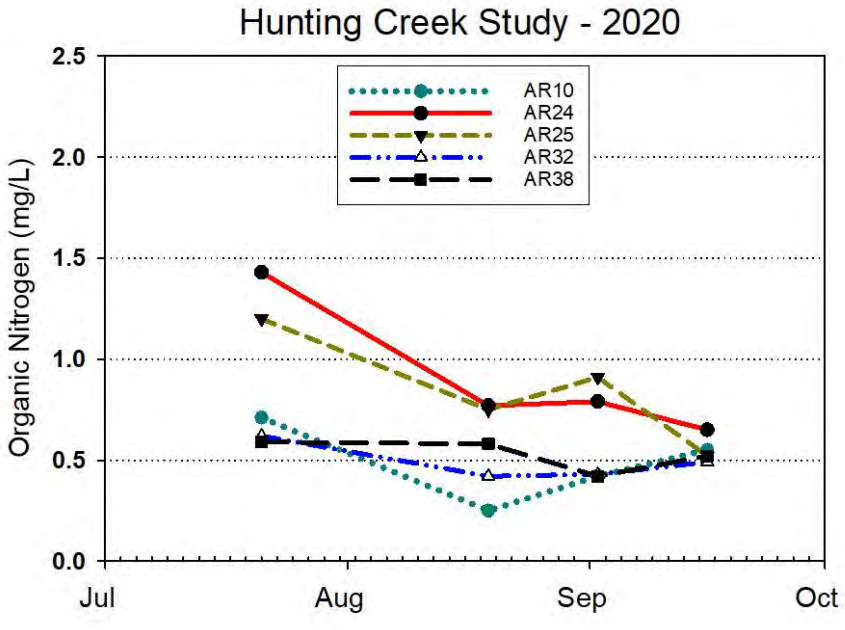

Figure 35. Organic Nitrogen (mg/L). Tidal CSO Impact Stations.

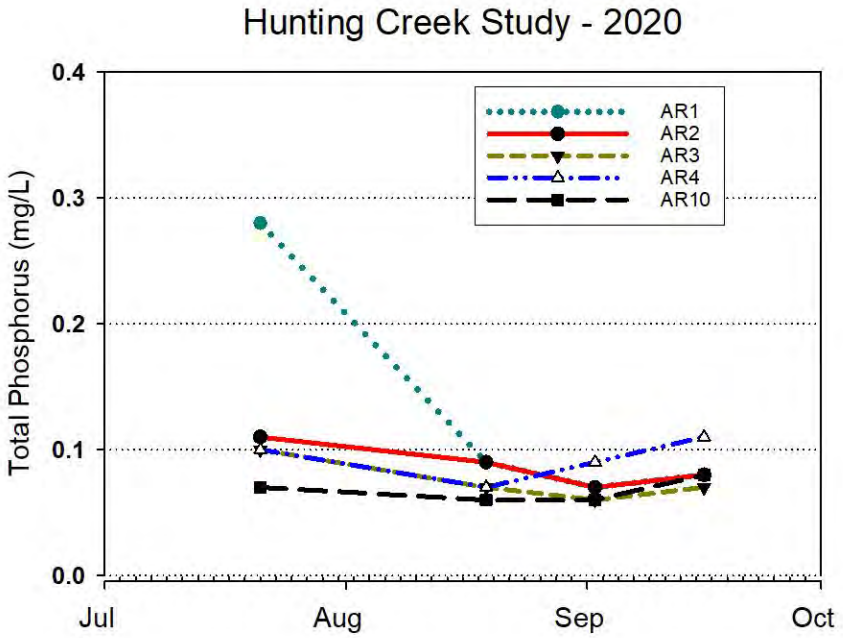

Phosphorus (P) is often the limiting nutrient in freshwater ecosystems. As such the concentration of P can set the upper limit for algal growth. Total phosphorus is the best measure of P availability in freshwater since much of the P is tied up in biological tissue such as algal cells. Total P includes phosphate ion (PO_4^{-3}) as well as phosphate inside cells and phosphate bound to inorganic particles such as clays.

Figure 36. Total Phosphorus (mg/L). Tidal Main Stations. Month tick is at first day of month.

Total phosphorus did not vary much through the year at most stations remaining in the 0.05 to 0.10 range (Figures 36&37). Again, somewhat higher values were observed at AR1, AR24, and AR25 along the northern shore of Hunting Creek.

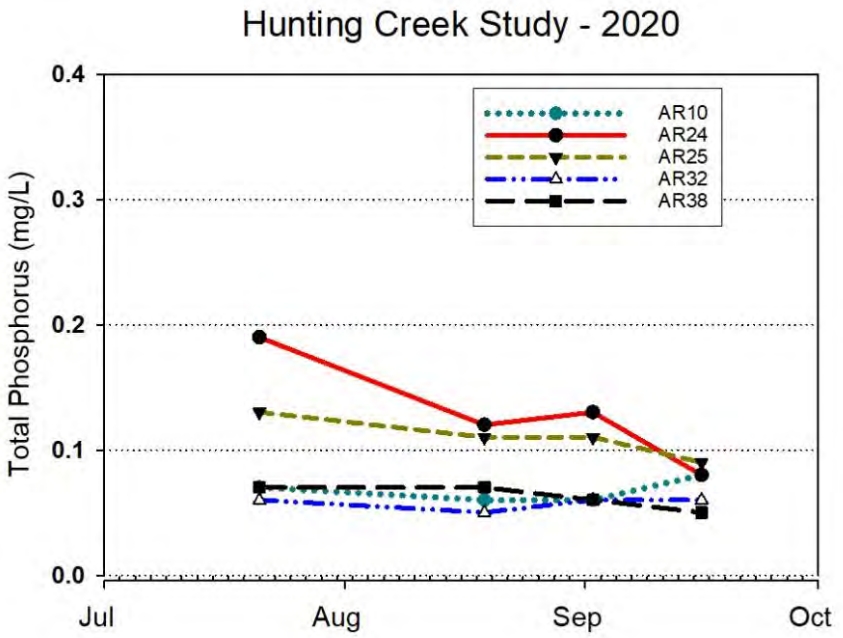

Figure 37. Total Phosphorus (mg/L). Tidal CSO Impact Stations.

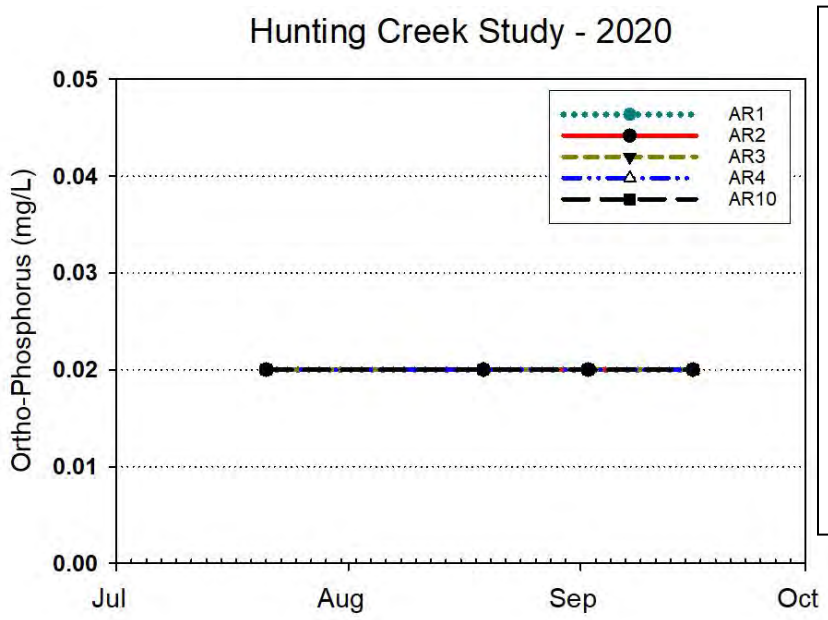

Soluble reactive phosphorus (SRP) is a measure of phosphate ion (PO_4^{-3}). Phosphate ion is the form in which P is most available to primary producers such as algae and aquatic plants in freshwater. However, SRP is often inversely related to the activity of primary producers because they tend to take it up so rapidly. So, higher levels of SRP indicate either a local source of SRP to the waterbody or limitation by a factor other than P.

Figure 38. Soluble Reactive Phosphorus (mg/L). Tidal Main Stations. Month tick is at first day of month.

Ortho-phosphorus values were all below the detection limit of 0.04 mg/L and thus were represented as half the detection limit (Figures 38&39). Little can be said other than that.

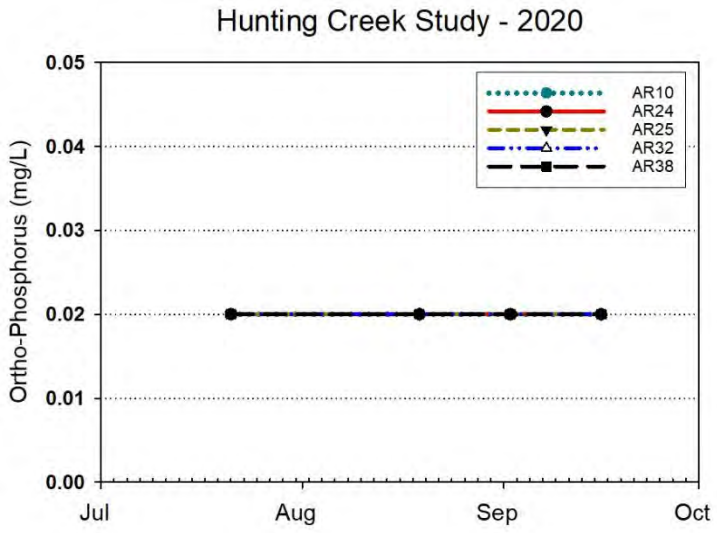

Figure 39. Soluble Reactive Phosphorus (mg/L). Tidal CSO Impact Stations.

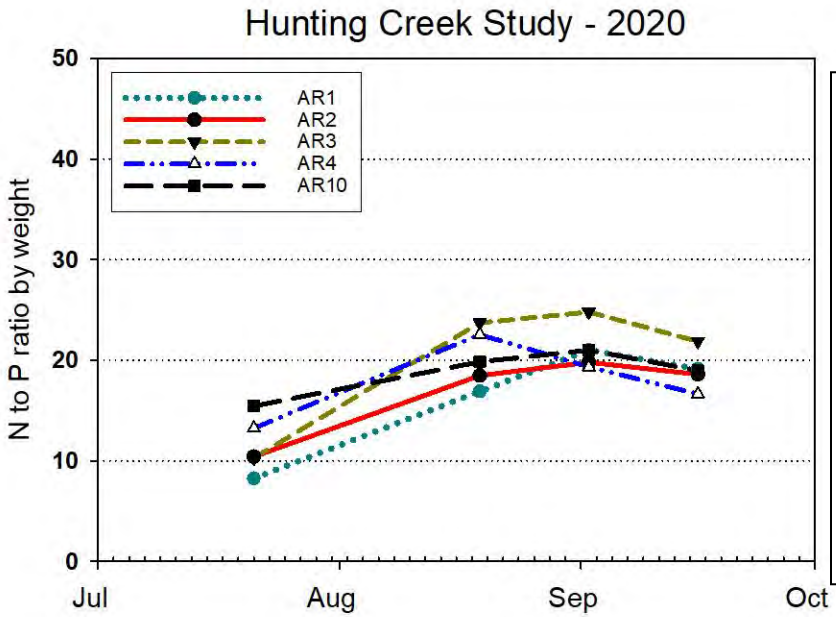

N:P ratio is determined by summing all of the components of N (ammonia, nitrate, nitrite, and organic nitrogen) and dividing by total P. This ratio gives an indication of whether N or P is more likely to be limiting primary production in a given freshwater system. Generally, values above 7.2 are considered indicative of P limitation while values below 7.2 suggest N limitation. N limitation could lead to dominance by cyanobacteria who can fix their own N from the atmosphere.

Figure 40. N/P Ratio (by mass). Tidal Main Stations. Month tick is at first day of month.

N/P ratio consistently pointed to P limitation, being greater than 7.2 in all samples (Figure 28). Values were generally in the 10 to 30 range. Biochemical oxygen demand (BOD) was often below the detection limit of 2 mg/L, but was somewhat higher on several dates (Figure 29).

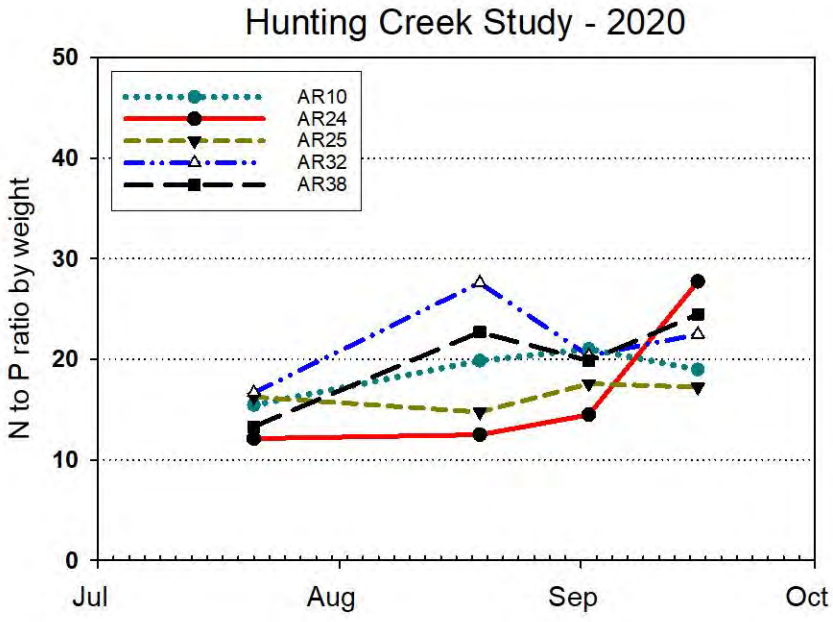

Figure 41. N/P Ratio (by mass). Tidal CSO Impact Stations.

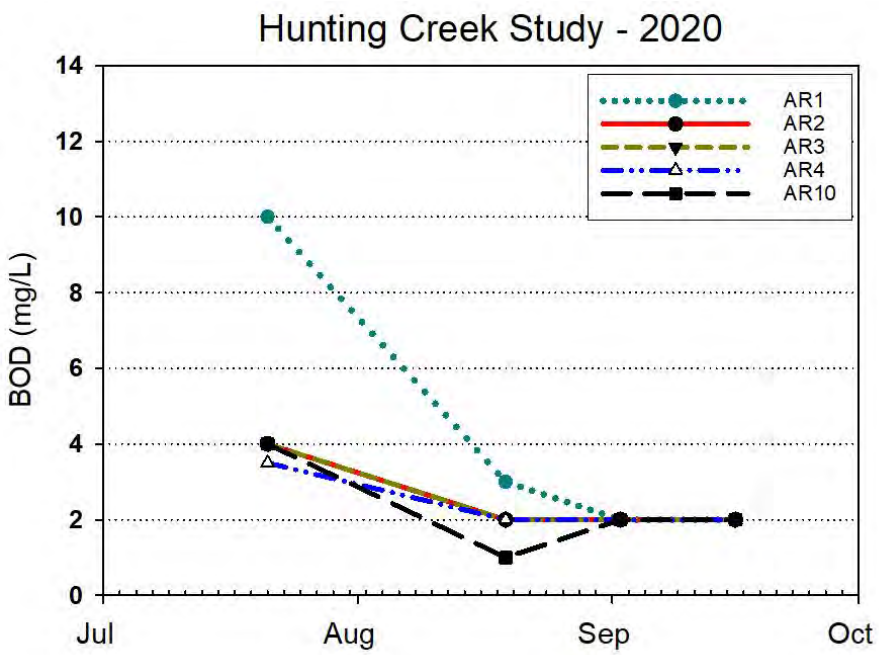

Biochemical oxygen demand (BOD) measures the amount of decomposable organic matter in the water as a function of how much oxygen it consumes as it breaks down over a given number of days. Most commonly the number of days used is 5. BOD is a good indicator of the potential for oxygen depletion in water. BOD is composed both dissolved organic compounds in the water as well as microbes such as bacteria and algae which will respire and consume oxygen during the period of measurement.

Figure 42. Biochemical Oxygen Demand (mg/L). Tidal Main Stations. Month tick is at first day of month.

BOD was consistently less than 4 mg/L as all stations (Figures 42&43). There were a few higher values at AR1 and AR25 on the north shore of Hunting Creek.

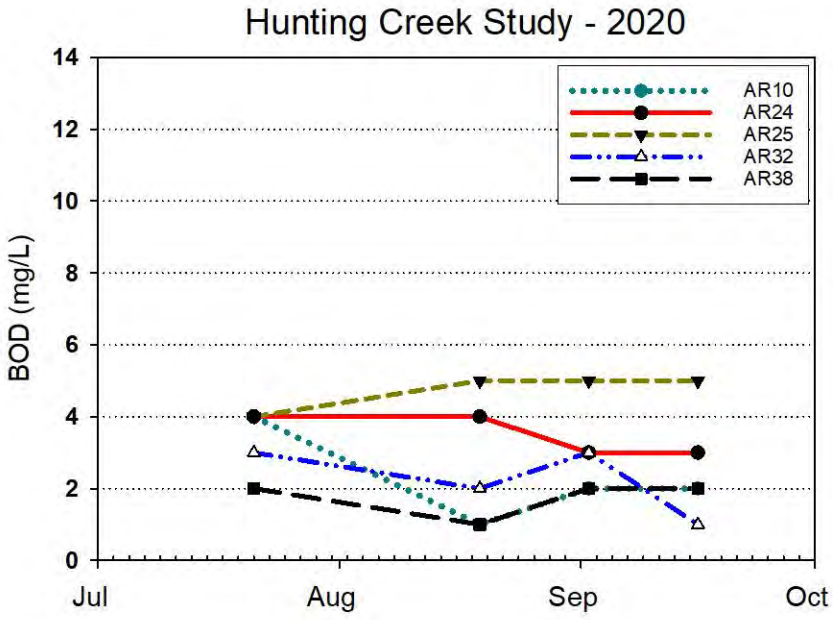

Figure 43. Biochemical Oxygen Demand (mg/L). Tidal SCO Impact Stations.

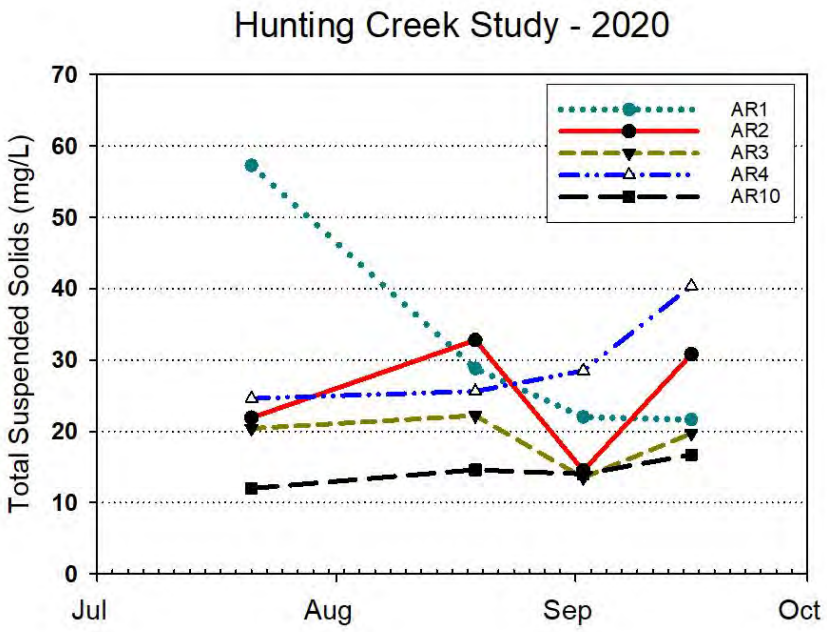

Total suspended solids (TSS) is measured by filtering a known amount of water through a fine filter which retains all or virtually all particles in the water. This filter is then dried and the weight of particles on the filter determined by difference. TSS consists of both organic and inorganic particles. During periods of low river and tributary inflow, organic particles such as algae may dominate. During storm flow periods or heavy winds causing resuspension, inorganic particles may dominate.

Figure 44. Total Suspended Solids (mg/L). Tidal Main Stations. Month tick is at first day of month.

Total suspended solids was generally in the range 15-30 mg/L at the Tidal Main Stations and at AR10, AR32, and AR38 (Figures 44&45). Again, higher values were observed at AR1, AR24, and AR25.

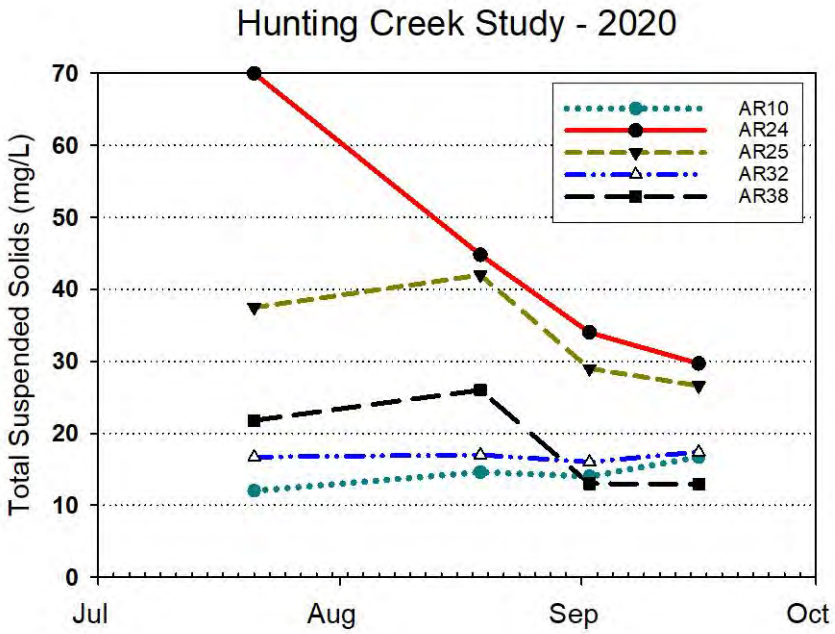

Figure 45. Total Suspended Solids. Tidal CSO Impact Stations.

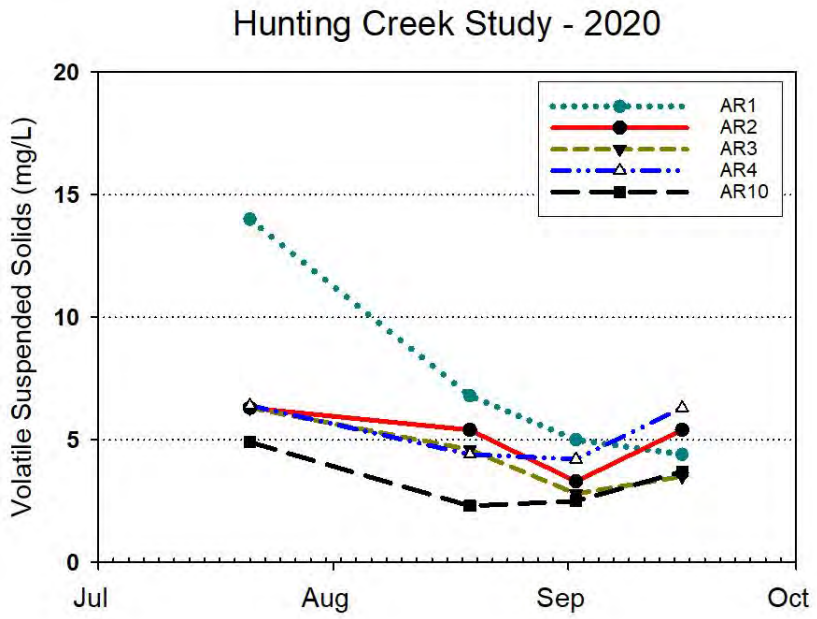

Volatile suspended solids (VSS) is determined by taking the filters used for TSS and then ashing them to combust (volatilize) the organic matter. The organic component is then determined by difference. VSS is a measure of organic solids in a water sample. These organic solids could be bacteria, algae, or detritus. Origins include sewage effluent, algae growth in the water column, or detritus produced within the waterbody or from tributaries. In summer in Gunston Cove a chief source is algal (phytoplankton) growth.

Figure 46. Volatile Suspended Solids (mg/L). Tidal Main Stations. Month tick is at first day of month.

VSS values followed similar patterns. At the Tidal Main Stations and AR32 and AR38 values remained in the 2-6 mg/L range with a slight decline seasonally (Figures 46&47). Higher values were observed at AR1, AR24, and AR25.

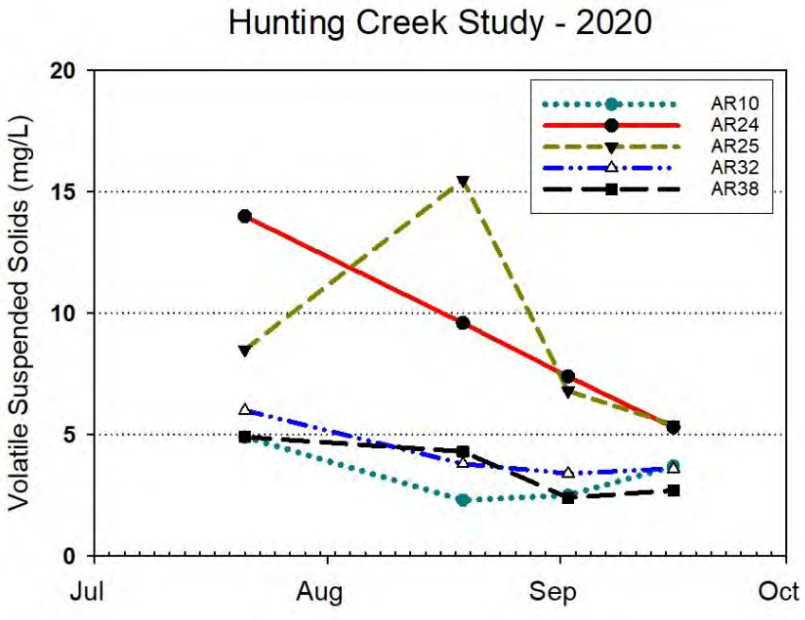

Figure 47. Volatile Suspended Solids (mg/L). Tidal CSO Impact Stations.

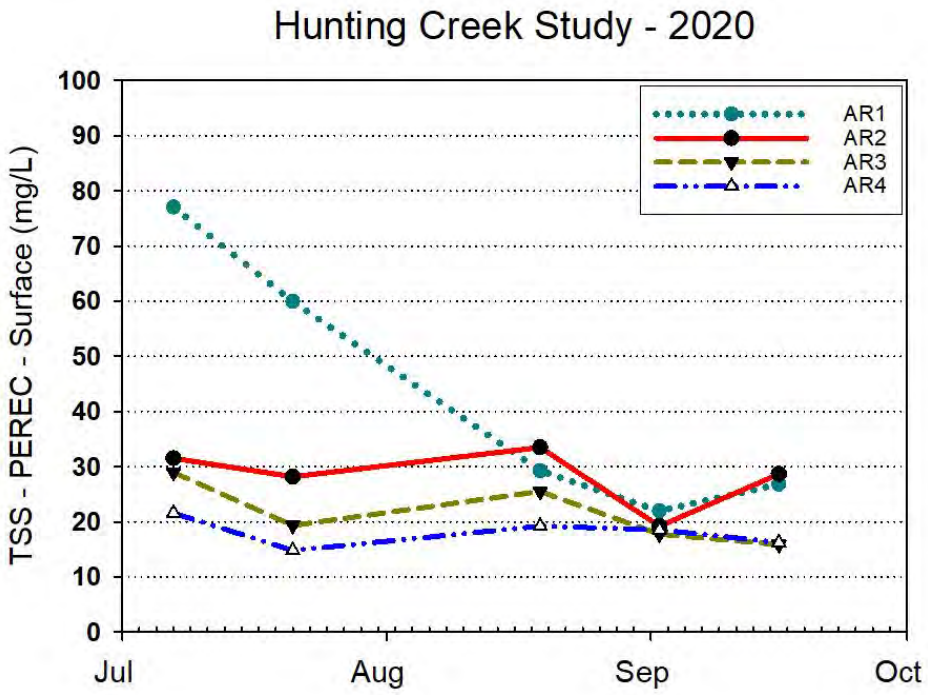

Figure 48. Total Suspended Solids. PEREC. Tidal Main Stations.

PEREC staff conducted TSS and VSS at the Tidal Main Stations. Again, AR2, AR3, and AR4 were in the 15-30 mg/L range for TSS while AR1 was higher in July (Figure 48). AR2, AR3, and AR4 were less than 10 mg/L for VSS and showed a seasonal decline (Figure 49).

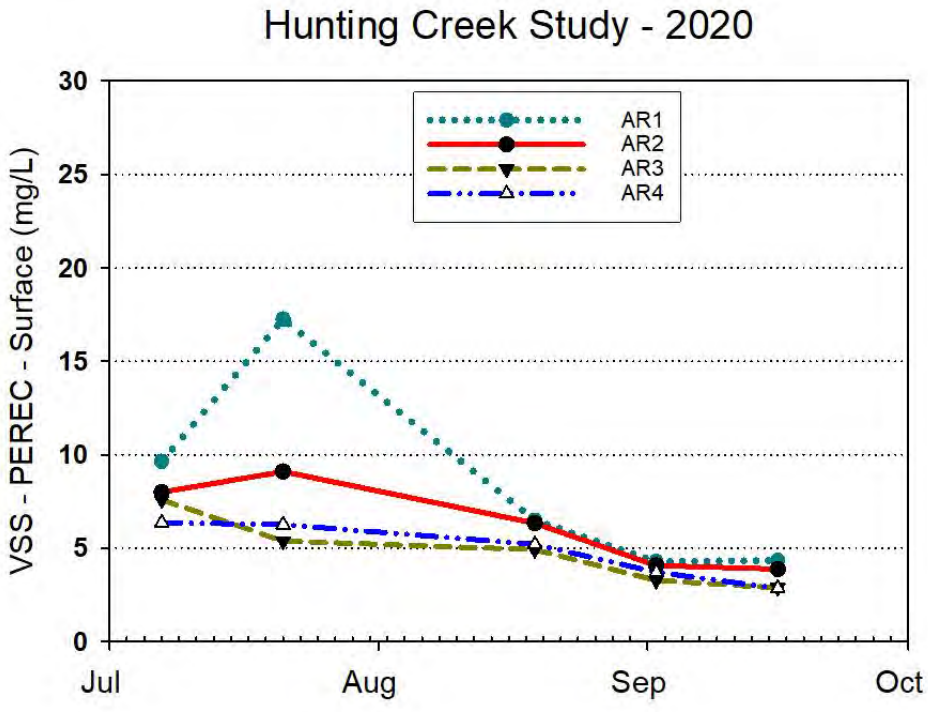

Figure 49. Volatile Suspended Solids. PEREC. Tidal CSO Impact Stations.

C. Physico-chemical Parameters: Tributary Stations – 2020

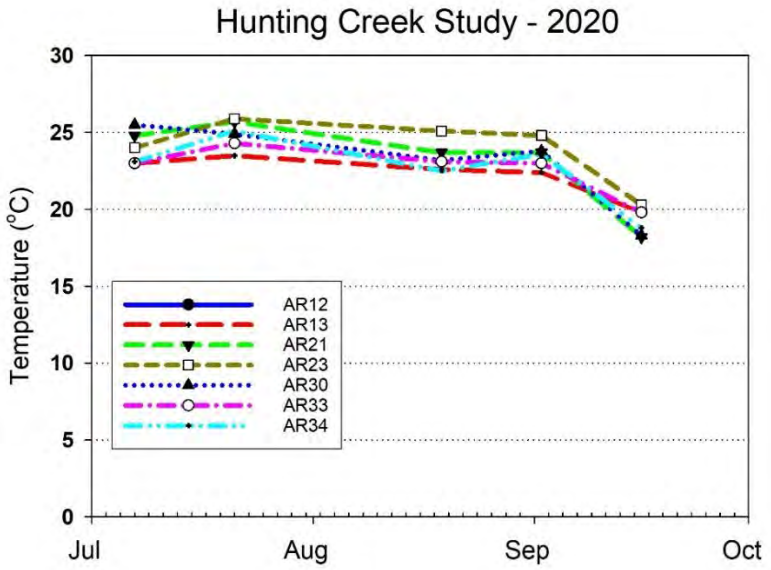

Figure 50. Water Temperature (°C). GMU Field Data. Month tick is at first day of month.

Water quality data for the tributary stations was combined into a series of graphs by parameter. Temperatures at almost all stations closely followed air temperatures (Figure 50). The most obvious exception was AR13 which exhibited lower temperatures during most of the year. The water at AR13 is just emerging from underground storm sewers and is buffered from the higher air temperatures. Specific conductance was generally in the 200-600 uS/cm range and showed a clear increase seasonally at all stations (Figure 51). Values were generally lower than in previous years due to the wet conditions. AR13 was consistently somewhat higher than the other stations.

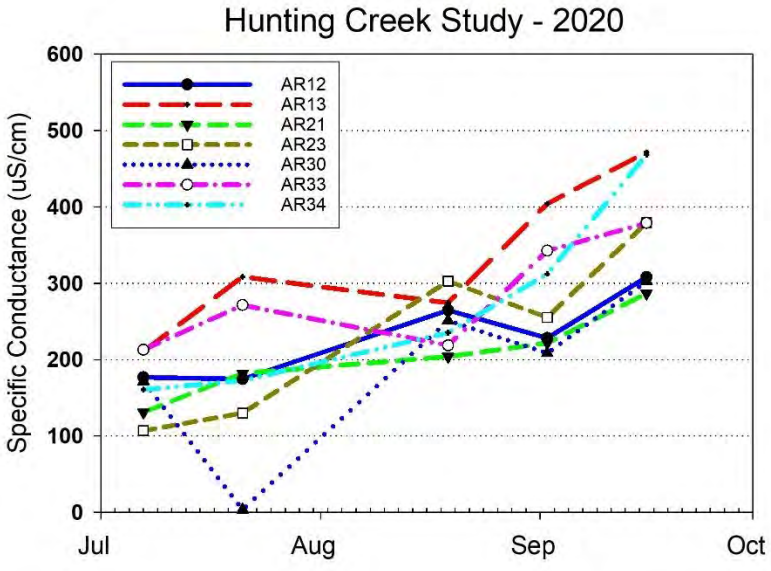

Figure 51. Specific Conductance (uS/cm). GMU Field Data. Month tick is at first day of month.

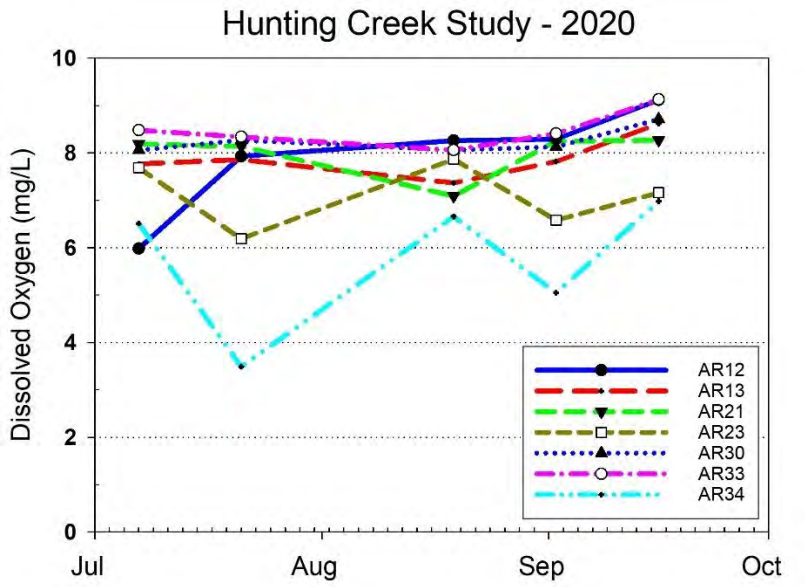

Figure 52. Dissolved Oxygen (mg/L) GMU Field Data. Month tick is at first day of month.

Dissolved oxygen (mg/L) at several of the tributary stations including AR12, AR13, AR21, AR30, and AR33 was quite constant seasonally (Figure 52). AR34 showed the most variability with one value below 4 mg/L. AR23 was also variable. The same group of 5 stations exhibited steady DO as percent saturation with values generally in the 80-100% range (Figure 53). And again, AR34 showed lower and variable values.

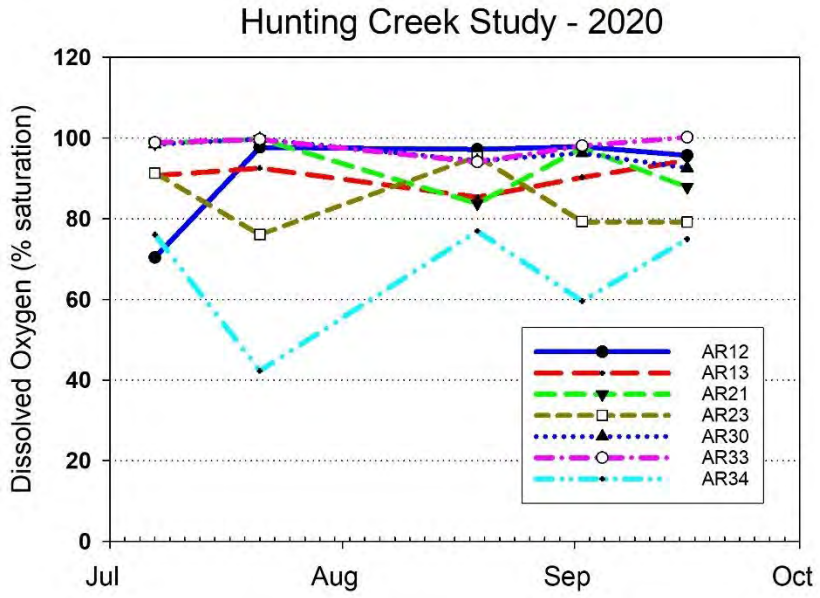

Figure 53. Dissolved Oxygen (% saturation) GMU Field Data. Month tick is at first day of month.

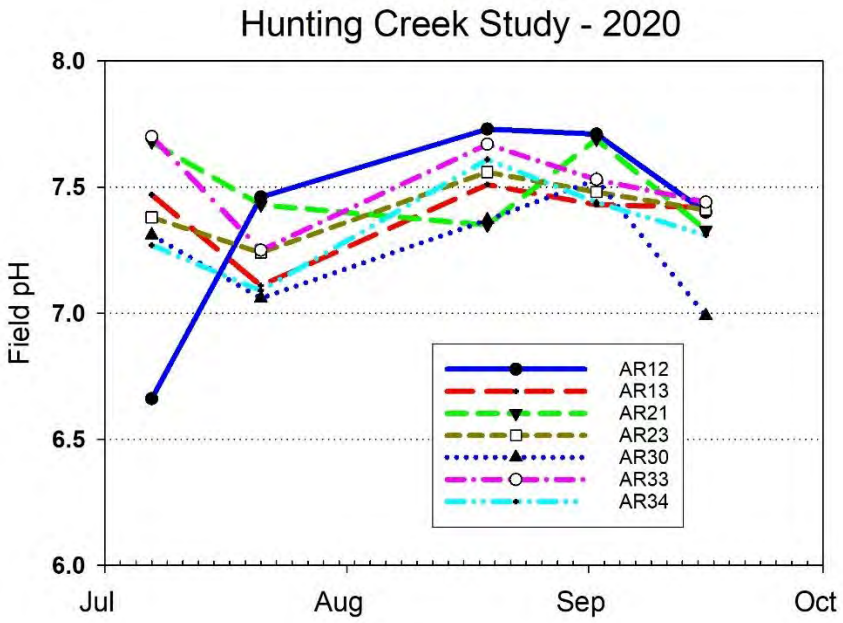

Figure 54. Field pH. GMU Field Data. Month tick is at first day of month.

Other than one low reading in early July at AR12, Field pH followed a very similar seasonal pattern at all stations with most values centered around 7.5 (Figure 54). AR12, AR21, or AR33 were generally among the higher values while AR30 was typically on the low end. Lab pH values were more tightly grouped but again were generally in the range 7 to 7.5 (Figure 55).

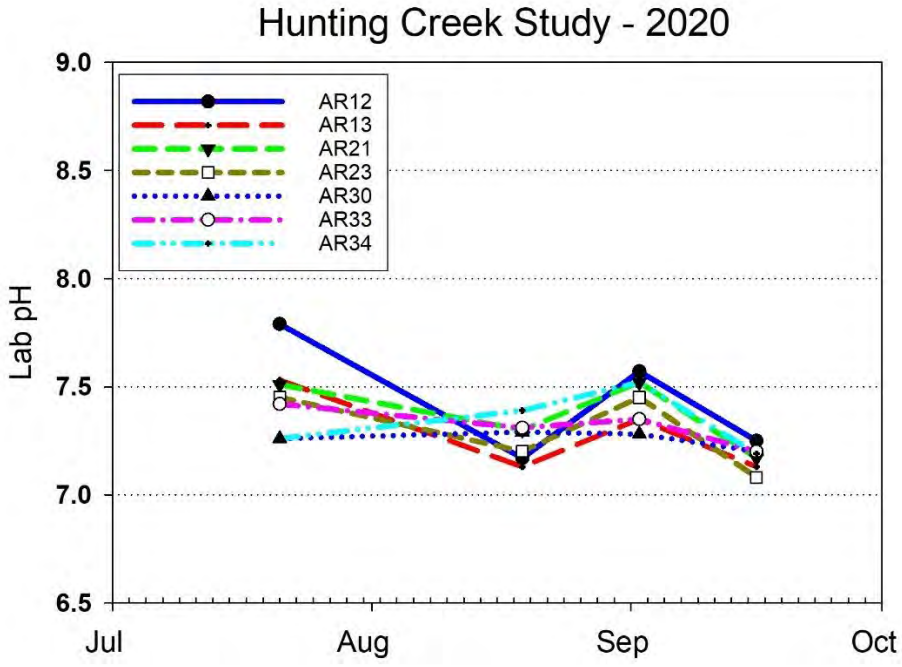

Figure 55. Lab pH. Alex Renew Lab Data. Month tick is at first day of month.

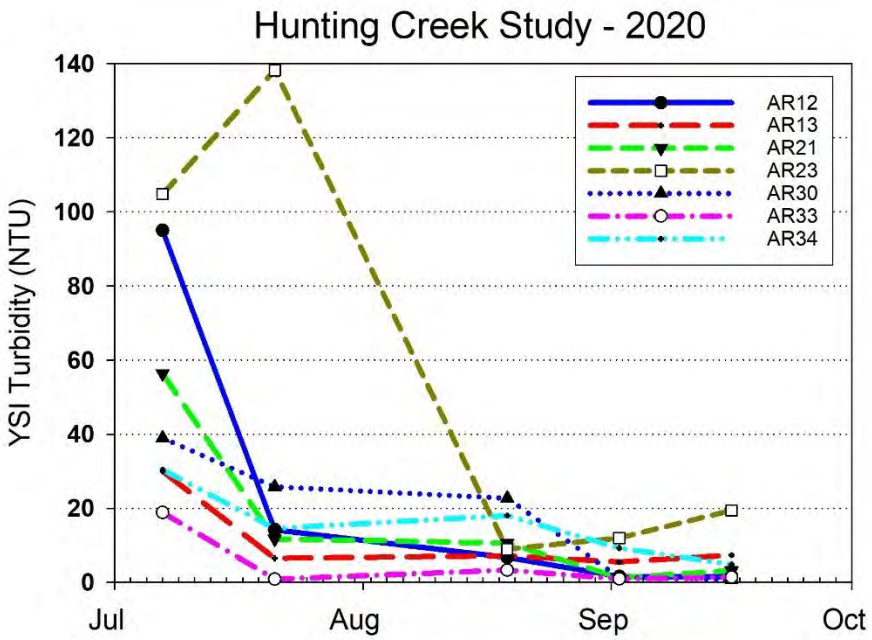

Figure 56. YSI Turbidity. GMU Field Data. Month tick is at first day of month.

YSI Turbidity was elevated at several stations in early July, but declined to below 20 NTU for the rest of the year (Figure 56). At AR23 values were over 100 for both July samples, but then declined.

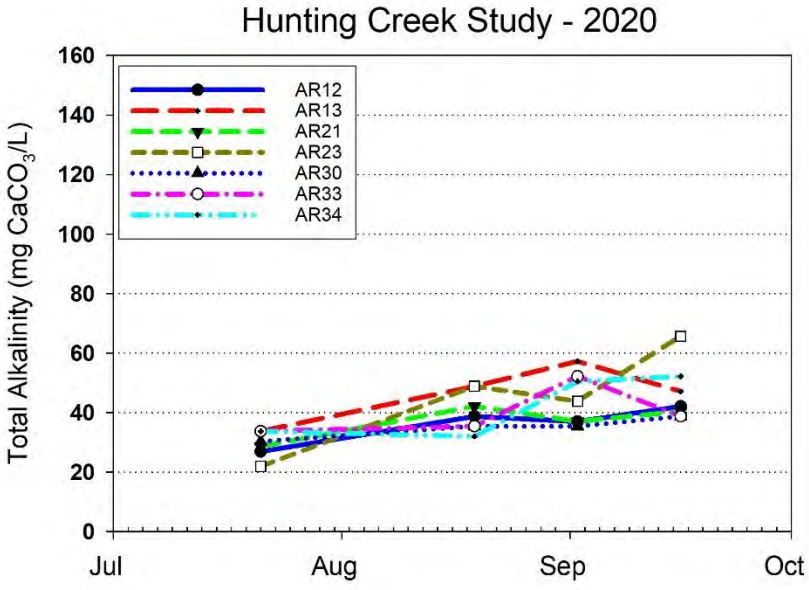

Figure 57. Total Alkalinity (mg/L as $CaCO_3$) AlexRenew Lab Data. Month tick is at first day of month.

Total alkalinity was generally in the 20-60 mg/L range with a clear and steady increase over the study period (Figure 57). Chloride levels showed a general pattern of increase from late July to mid September, but this pattern was not totally consistent at all stations (Figure 58). Chloride levels were generally highest at AR13 and lowest at AR21.

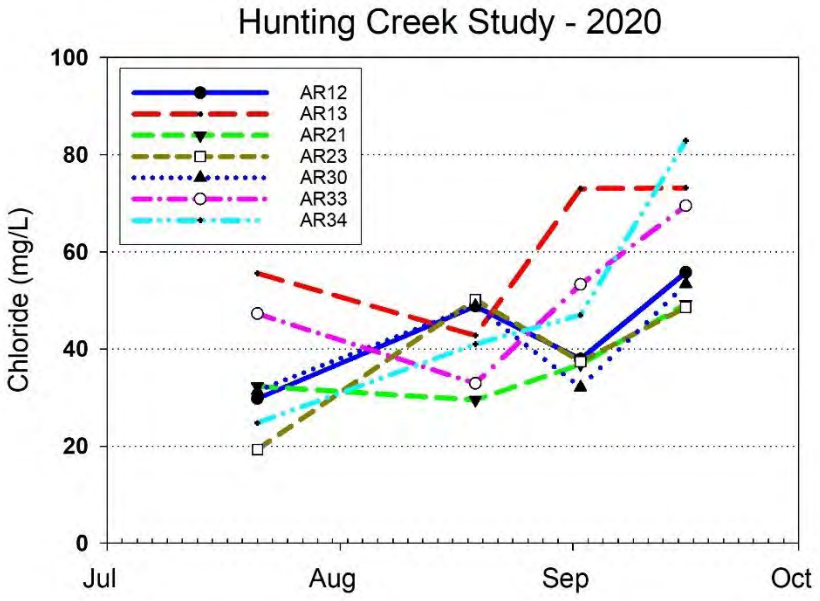

Figure 58. Chloride (mg/L) AlexRenew Lab Data. Month tick is at first day of month.

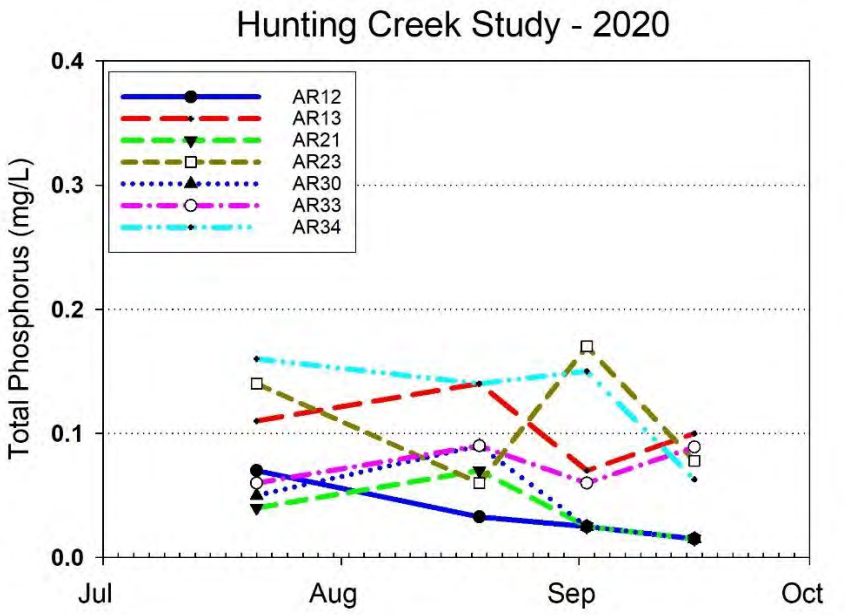

Figure 59. Total Phosphorus (mg/L) AlexRenew Lab Data. Month tick is at first day of month.

Total phosphorus levels were generally relatively low at most tributary stations (<0.2 mg/L) and did not vary much seasonally (Figure 59). Highest values were observed sporadically at AR13, AR23, and AR34. Lowest values were generally at AR12 and AR21. Ortho phosphorus levels were consistently less than 0.02 mg/L (Figure 60). Some higher readings were observed on two occasions at AR13, AR33, and AR34, all Hooffs Run. AR12 and AR21 were lowest.

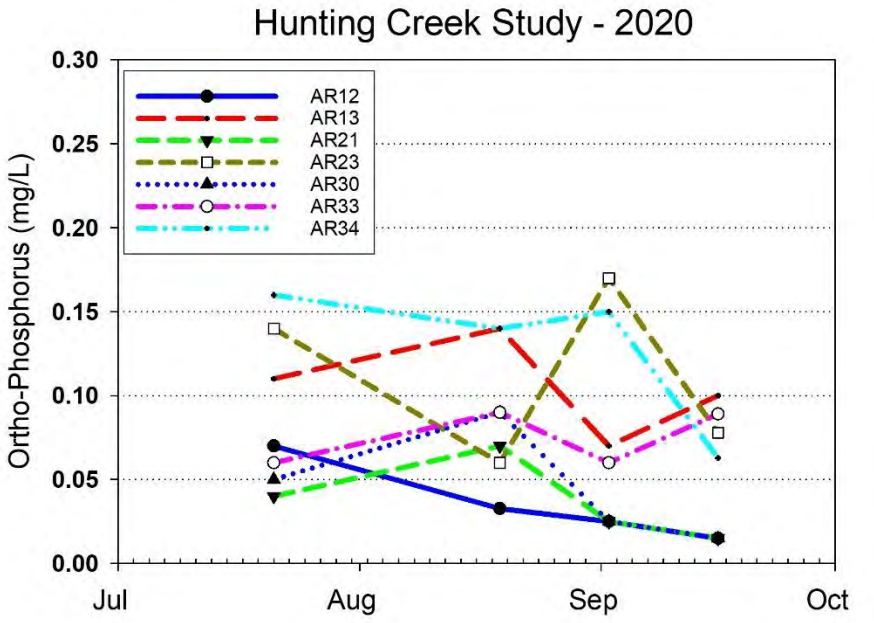

Figure 60. Ortho-Phosphorus (mg/L) AlexRenew Lab Data. Month tick is at first day of month.

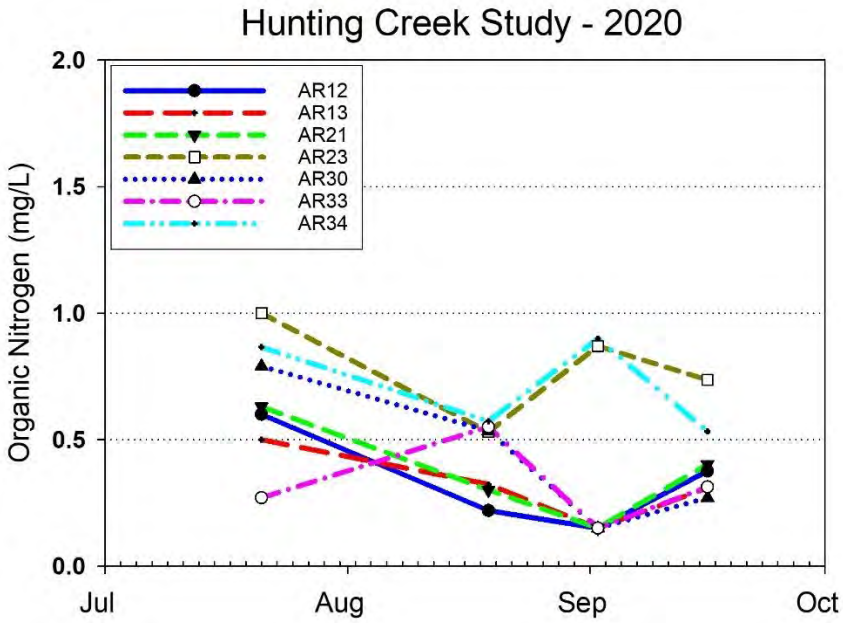

Figure 61. Organic Nitrogen (mg/L) AlexRenew Lab Data. Month tick is at first day of month.

Tributary levels of organic nitrogen are depicted in Figure 61. Values were generally below 1.0 mg/L with little obvious pattern. Ammonia nitrogen values were below 0.2 mg/L at most sites, but otherwise there was little seasonal pattern (Figure 62).

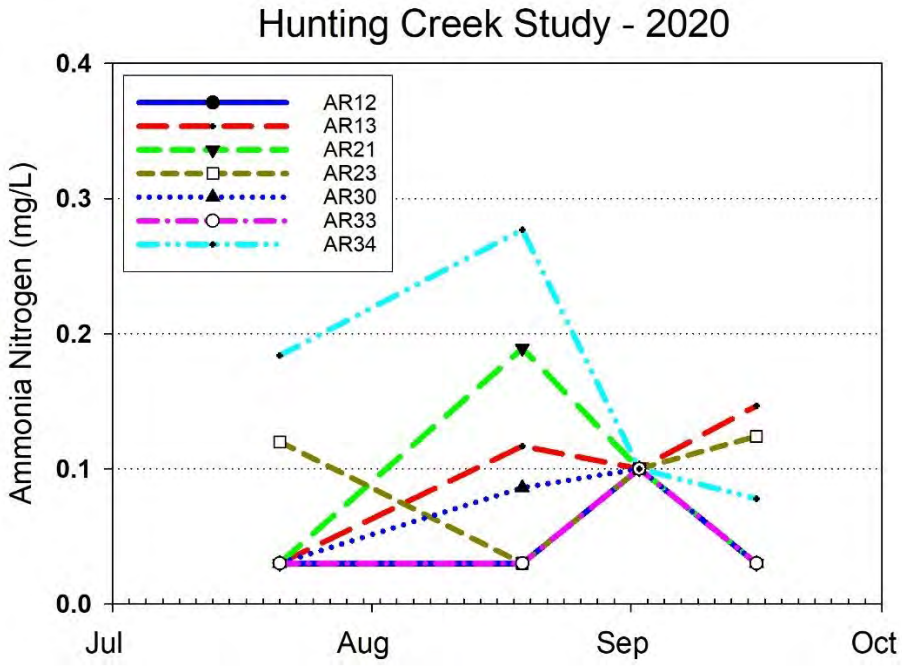

Figure 62. Ammonia Nitrogen (mg/L) AlexRenew Lab Data. Month tick is at first day of month.

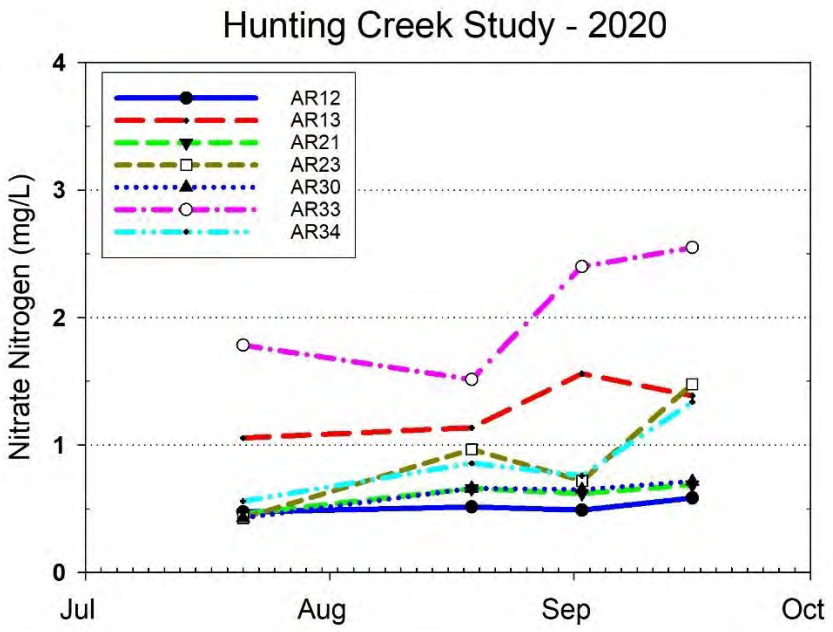

Figure 63. Nitrate Nitrogen (mg/L) AlexRenew Lab Data. Month tick is at first day of month.

Nitrate nitrogen values was generally below 1.0 mg/L (Figure 63). AR33 had values near 2.0 mg/L and AR13 was consistently above 1.0 mg/L. Nitrite nitrogen was generally quite low (<0.04) at all stations (Figure 64). The exception was exceptionally high values at AR12 in early September.

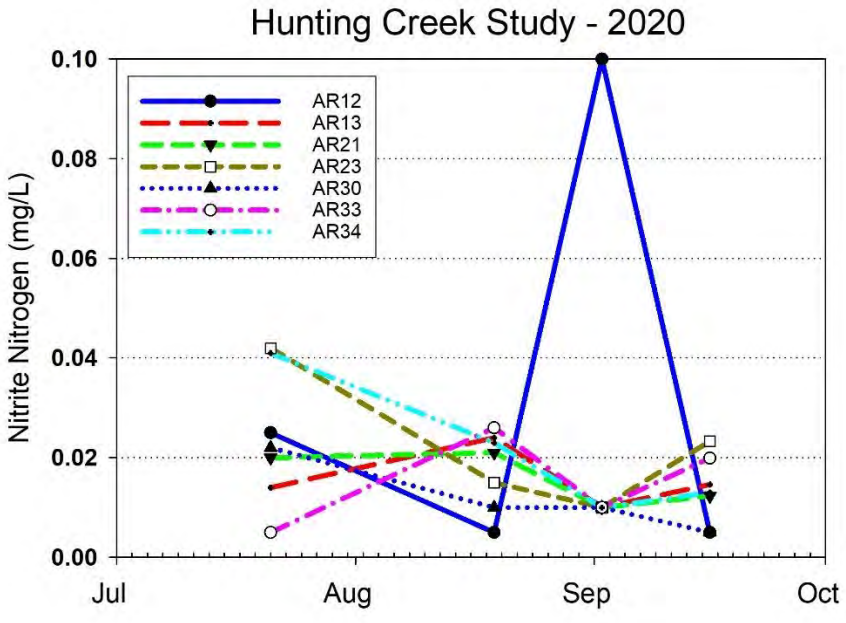

Figure 64. Nitrite Nitrogen (mg/L) AlexRenew Lab Data. Month tick is at first day of month.

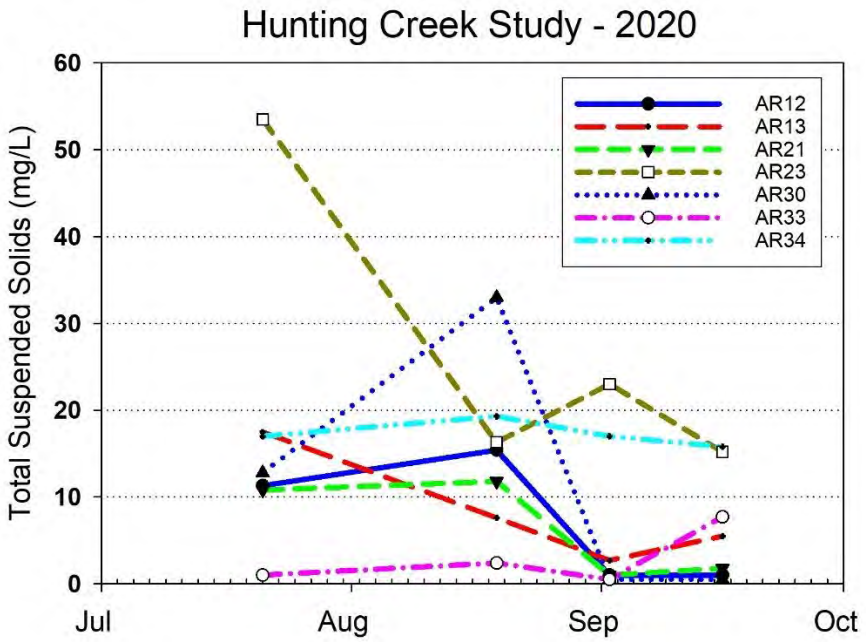

Figure 65. Total Suspended Solids (mg/L) AlexRenew Lab Data. Month tick is at first day of month.

Total suspended solids concentrations at tributary stations are shown in Figure 65. TSS was quite low (<20 mg/L) at most stations for most of the year. The exceptions were AR23 and AR30 which had higher values on occasion. VSS was generally half of TSS with highest values at AR34 (Figure 66). VSS values were below 5 mg/L on the last sampling date.

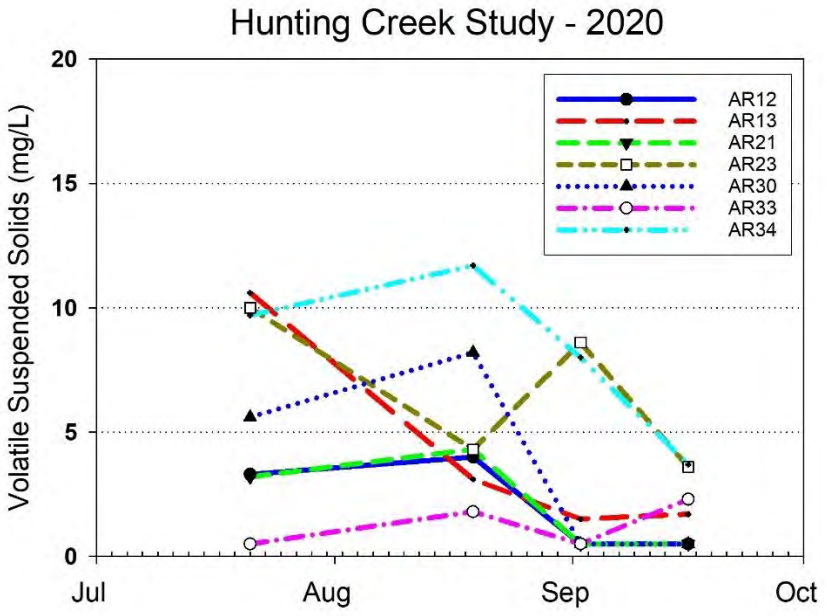

Figure 66. Volatile Suspended Solids (mg/L) AlexRenew Lab Data. Month tick is at first day of month.

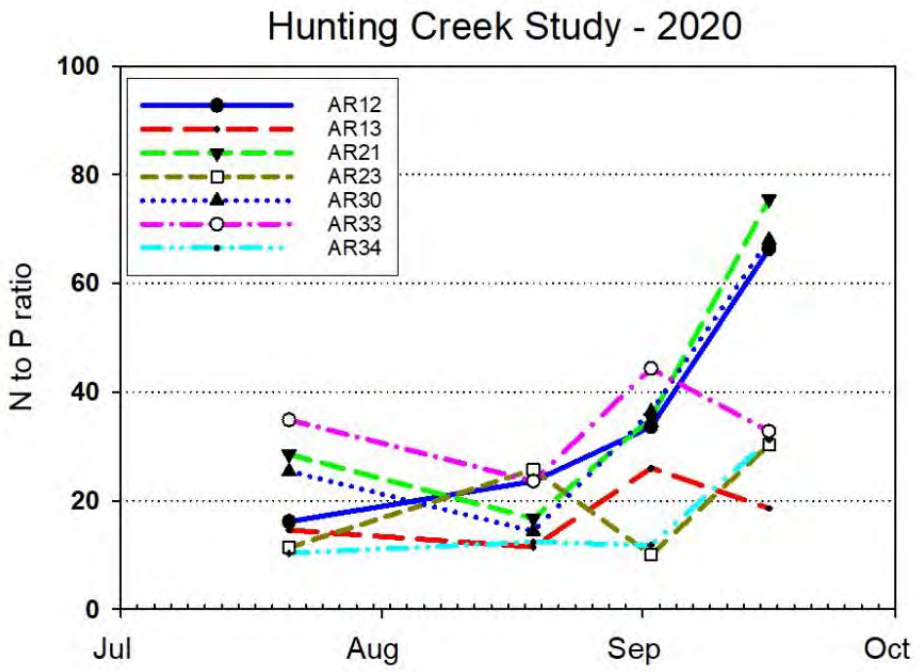

Figure 67. N to P ratio (by weight).

N to P ratios were uniformly in the range of 10-40 in July and August (Figure 67). Higher values were observed in September at AR33, AR30, AR12, and AR21. All values were above 7.2 indicating that inputs from the tributaries are consistent with P limitation of phytoplankton growth.

D. Phytoplankton - 2020

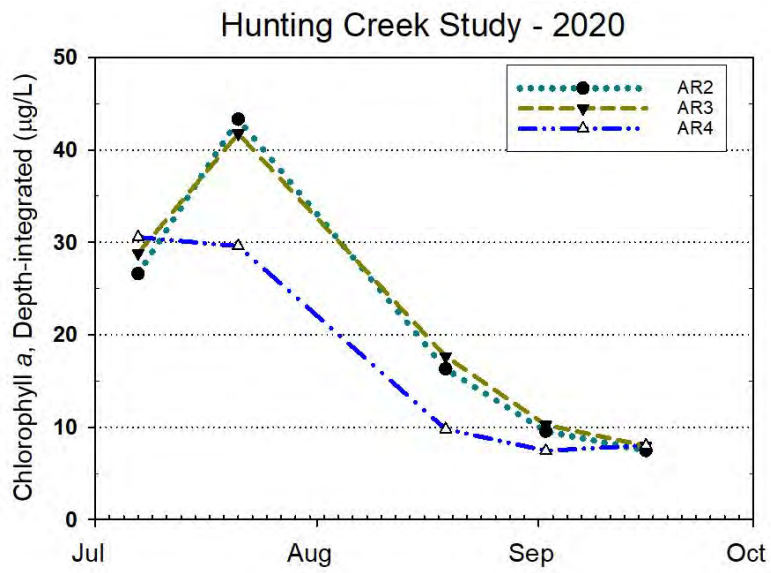

Chlorophyll *a* is a measure of the amount of algae growing in the water column. These suspended algae are called phytoplankton, meaning "plant wanderers". In addition to the true algae (greens, diatoms, cryptophytes, etc.) the term phytoplankton includes cyanobacteria (sometimes known as "blue-green" algae). Both depth-integrated and surface chlorophyll values are measured due to the capacity of phytoplankton to aggregate near the surface under certain conditions.

Figure 68. Chlorophyll *a* (µg/L). Depth-integrated. GMU Lab Data. Month tick is at the first day of month.

Chlorophyll *a* was similar at all stations at all embayment and river mainstem stations (AR2, AR3, AR4) in early July at about 30 µg/L (Figure 68 & 69). At AR2 and AR3 in the Hunting Creek embayment chlorophyll *a* increased substantially in late July to about 40 µg/L and then steadily declined through the remainder of the year to about 10 µg/L. At the river mainstem station (AR4) chlorophyll remained steady in late July and then declined through the remainder of the year. At AR1 (located at the GW Parkway bridge), chlorophyll a started quite low in early July and spiked in late July at about 70 µg/L. It then steadily declined through August and September.

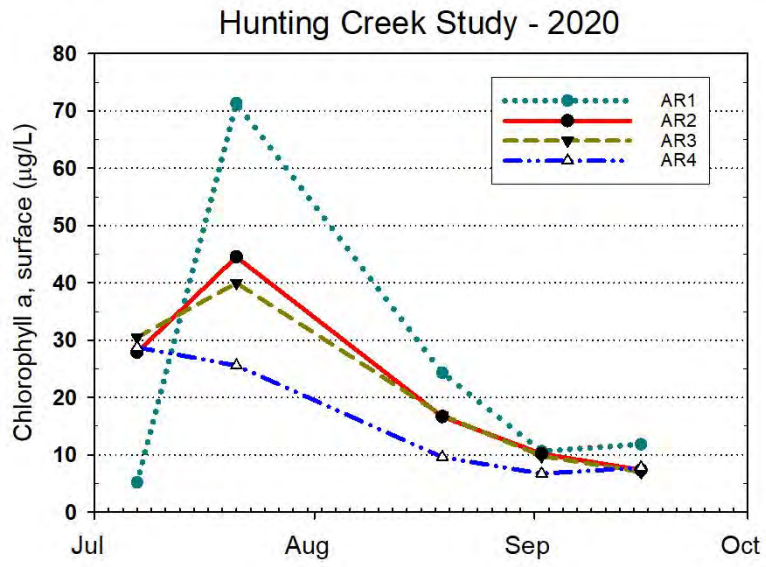

In the tidal freshwater Potomac generally, there is very little difference in surface and depth-integrated chlorophyll levels because tidal action keeps the water well-mixed which overcomes any potential surface aggregation by the phytoplankton. Summer chlorophyll concentrations above 30 ug/L are generally considered characteristic or eutrophic conditions.

Figure 69. Chlorophyll *a* (µg/L). Surface. GMU Lab Data. Month tick is at first day of month.

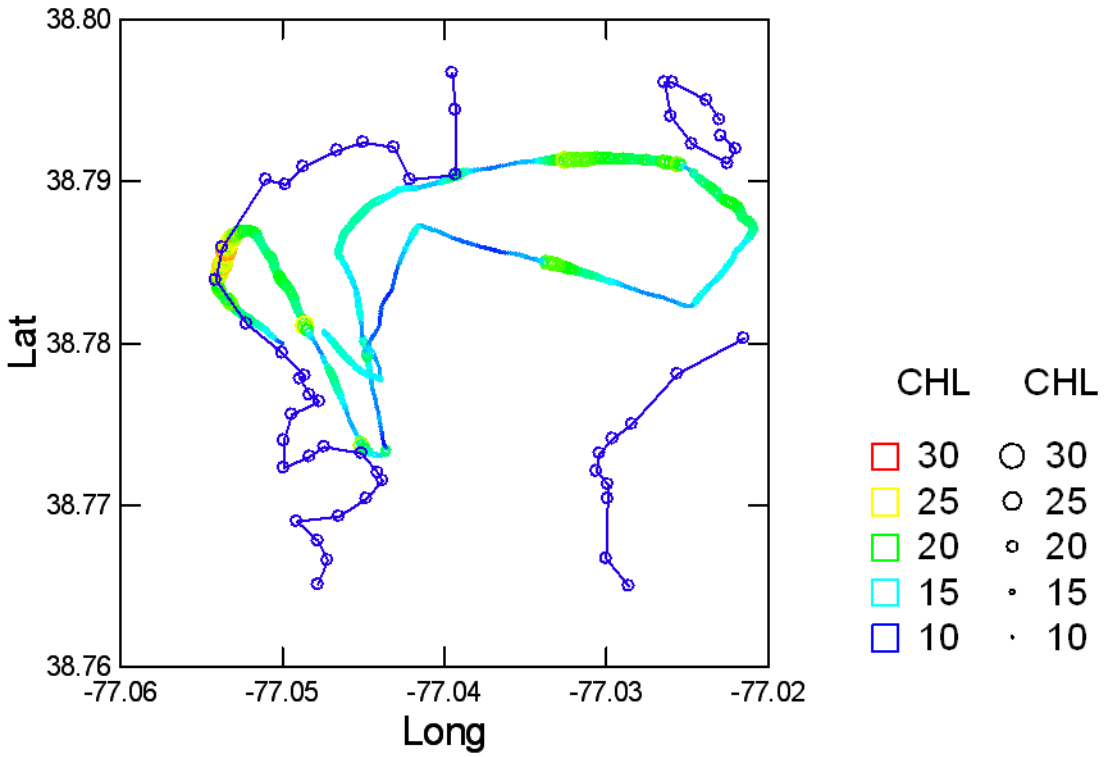

Figure 70. Water Quality Mapping. August 21, 2020. Chlorophyll YSI (µg/L).

On August 21, water quality mapping showed that chlorophyll a did not vary greatly or consistently through the study area with values generally 10-15 µg/L.

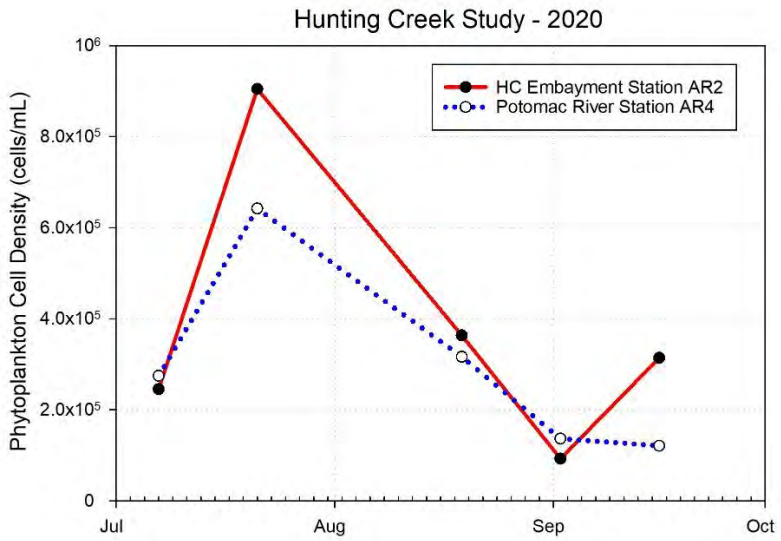

Phytoplankton cell density provides a measure of the number of algal cells per unit volume. This is a rough measure of the abundance of phytoplankton, but does not discriminate between large and small cells. Therefore, a large number of small cells may actually represent less biomass (weight of living tissue) than a smaller number of large cells. However, small cells are typically more active than larger ones so cell density is probably a better indicator of activity than of biomass. The smaller cells are mostly cyanobacteria.

Figure 71. Phytoplankton Cell Density (cells/mL).

Phytoplankton cell density exhibited a strong peak at both stations in late July (Figure 71). As with chlorophyll *a* the peak was slightly higher at AR2 than at AR4. AR2 showed a secondary peak in mid-September that was not observed in the chlorophyll *a* data. Total biovolume also exhibited a peak at both stations in late July (Figure 54). However, the peak was higher at AR4 than AR2. There was a secondary peak at AR4 in early September that was not seen at AR2.

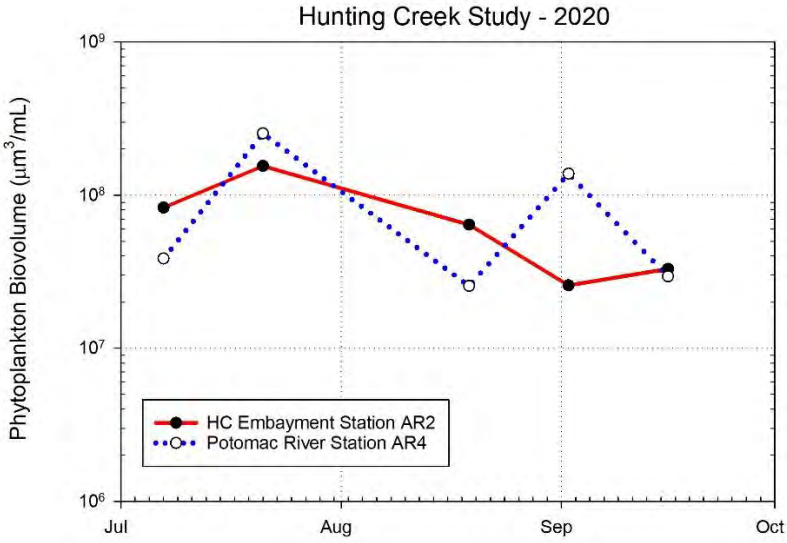

The volume of individual cells of each species is determined by approximating the cells of each species to an appropriate geometric shape (e.g. sphere, cylinder, cone, cube, etc.) and then making the measurements of the appropriate dimensions under the microscope. Total phytoplankton biovolume (shown here) is determined by multiplying the cell density of each species by the biovolume of each cell of that species. Biovolume accounts for the differing size of various phytoplankton cells and is probably a better measure of biomass. However, it does not account for the varying amount of water and other nonliving constituents in cells.

Figure 72. Phytoplankton Biovolume (um^3/mL).

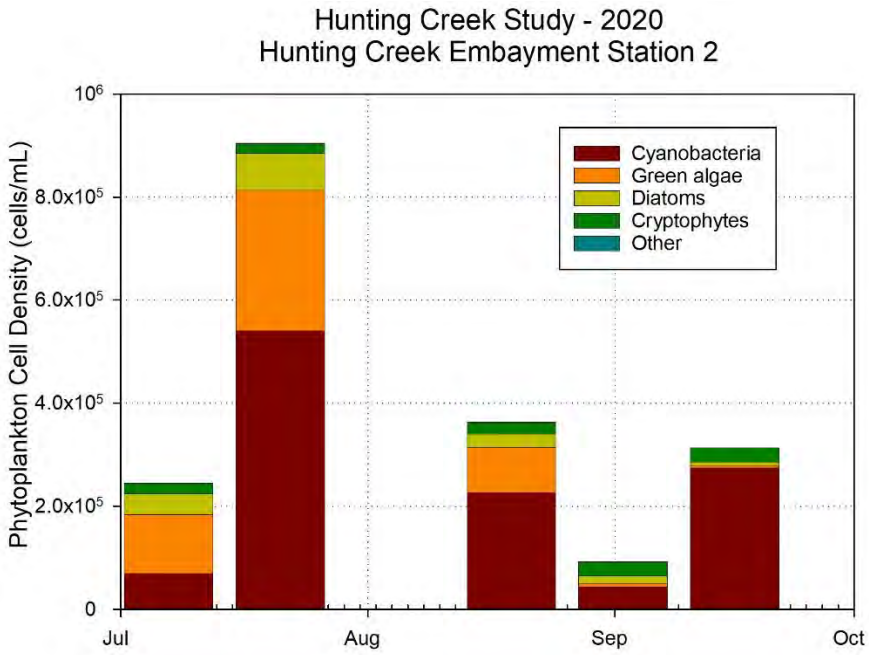

Total phytoplankton cell density can be broken down by major group. **Cyanobacteria** are sometimes called "blue-green algae". **Other** includes euglenoids and dinoflagellates. Due to their small size cyanobacteria typically dominate cell density numbers. Their numbers are typically highest in the late summer reflecting an accumulation of cells during favorable summer growing conditions.

Figure 73. Phytoplankton Density by Major Group (cells/mL). Hunting Creek.

Phytoplankton cell density at AR2 was generally dominated by cyanobacteria including the large peak in early July (Figure 73). Green algae were also important in July and August. In the river mainstem (AR4), cyanobacteria were again dominant on most dates, especially at the late July peak sample (Figure 74). Green algae were actually more numerous than cyanobacteria in early July and late August. Overall values were slightly lower at AR4 than AR2.

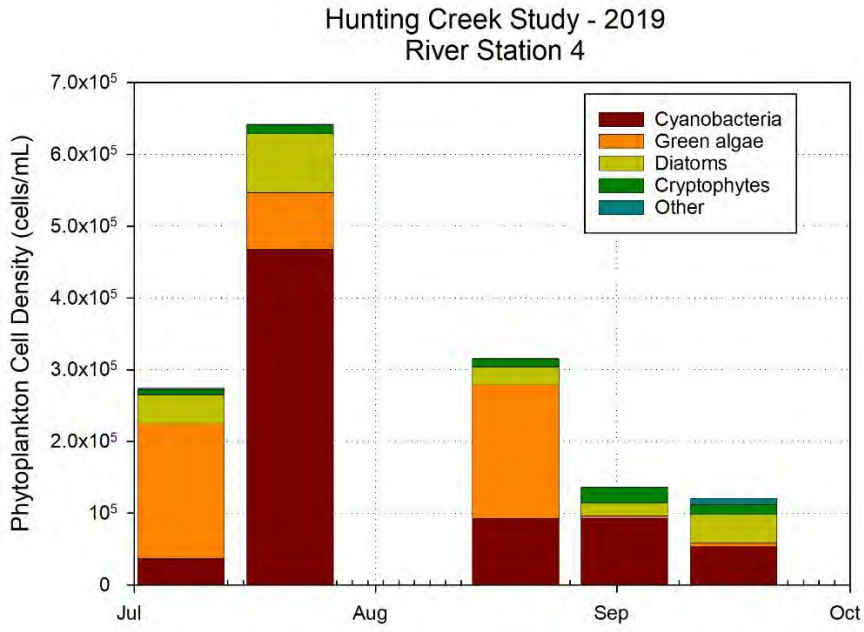

In the river cyanobacteria normally follow similar patterns as in the embayments, but may attain lower abundances. This is probably due to the deeper water column which leads to lower effective light levels and greater mixing. Other groups such as diatoms and green algae tend to be more important on a relative basis than in the embayments.

Figure 74. Phytoplankton Density by Major Group (cells/mL). River.

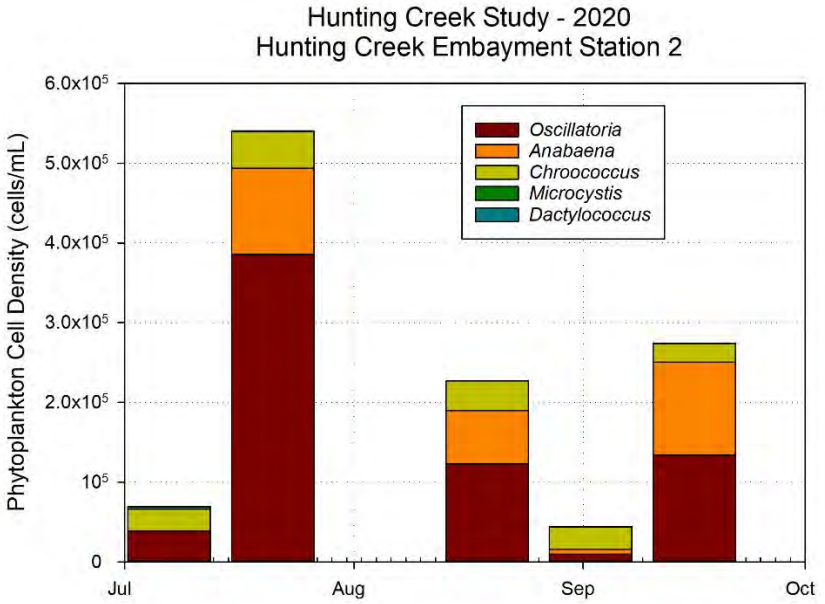

The dominant cyanobacteria on a numerical basis were:
- *Oscillatoria* – a filament with disc-like cells
- *Anabaena* – a filament with bead-like cells & heterocysts
- *Chroococcus* – individual spherical cells
- Unknown cyanobacterium About 2 um

Figure 75. Phytoplankton Density by Dominant Cyanobacteria (cells/mL). Hunting Creek.

Oscillatoria, *Anabaena*, and *Chroococcus*,were the most important cyanobacteria in cell density at the embayment station (AR2) (Figure 75). The major peak in late July was strongly dominated by *Oscillatoria*. In the river mainstem *Oscillatoria* was even more dominant (Figure 76). *Chroococcus* and *Anabaena* were subdominant.

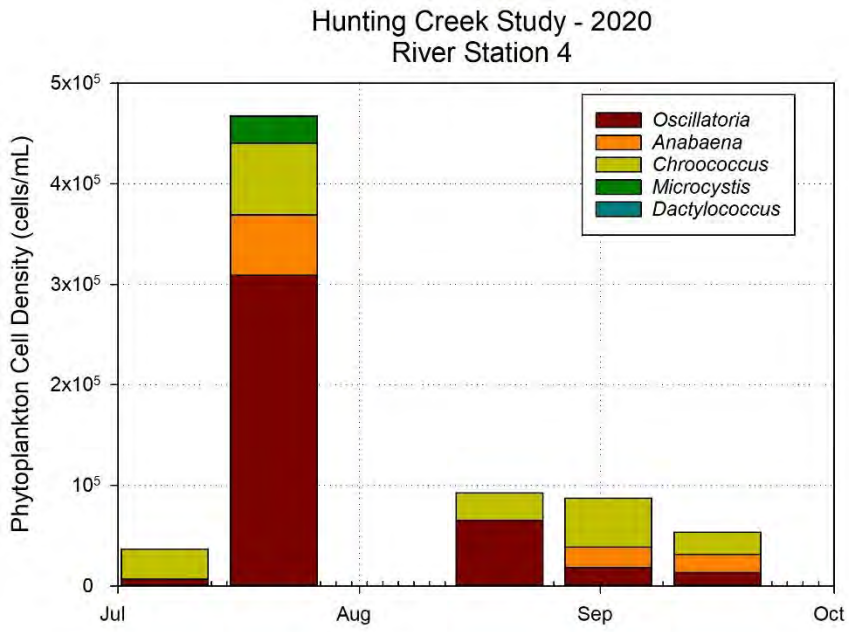

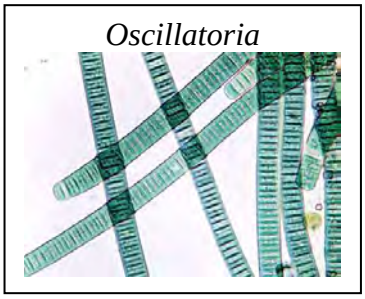

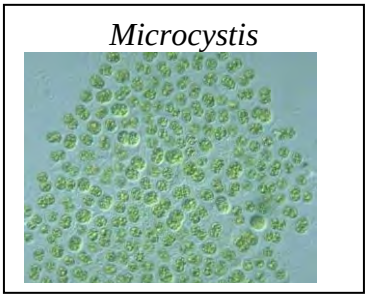

Figure 76. Phytoplankton Density by Dominant Cyanobacteria (cells/mL). River.

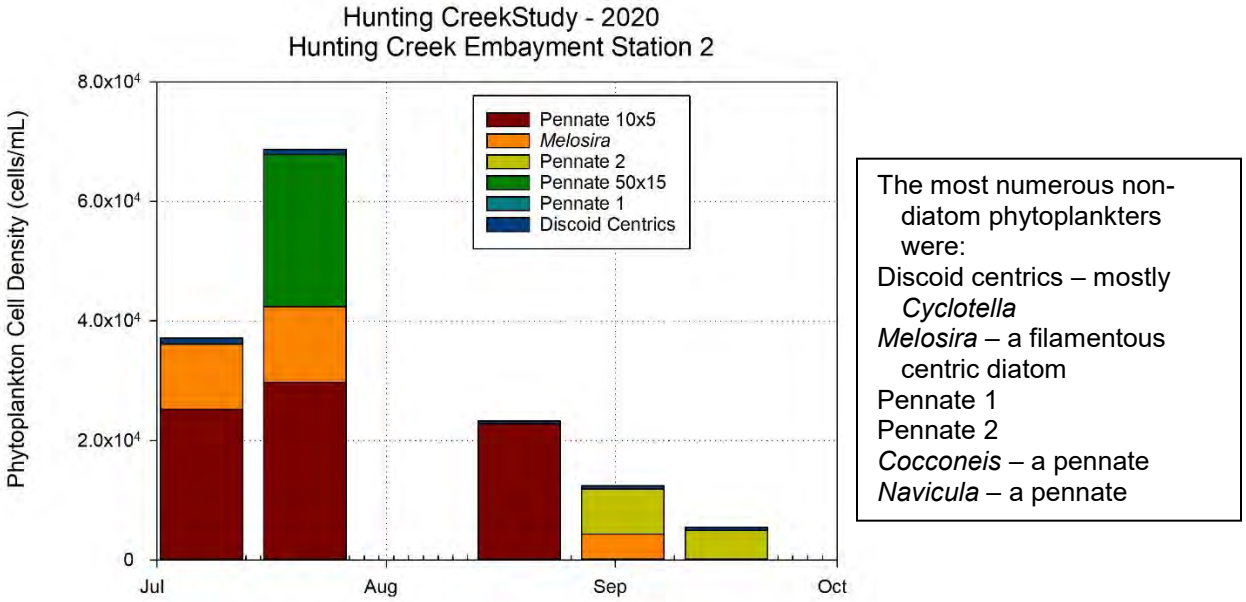

Figure 77. Phytoplankton Density (#/mL) by Dominant Diatom Taxa. Hunting Creek.

Diatom cell density dominance was variable. In July at August at AR2, Pennate 10x5 was the most dominant (Figure 77). *Melosira* was important at AR2 in July and Pennate 50x15 was co-dominant in late July. At AR4 *Melosira* and Pennate 2 were dominant in July (Figure 78). Pennate 50x15 was dominant in mid-September.

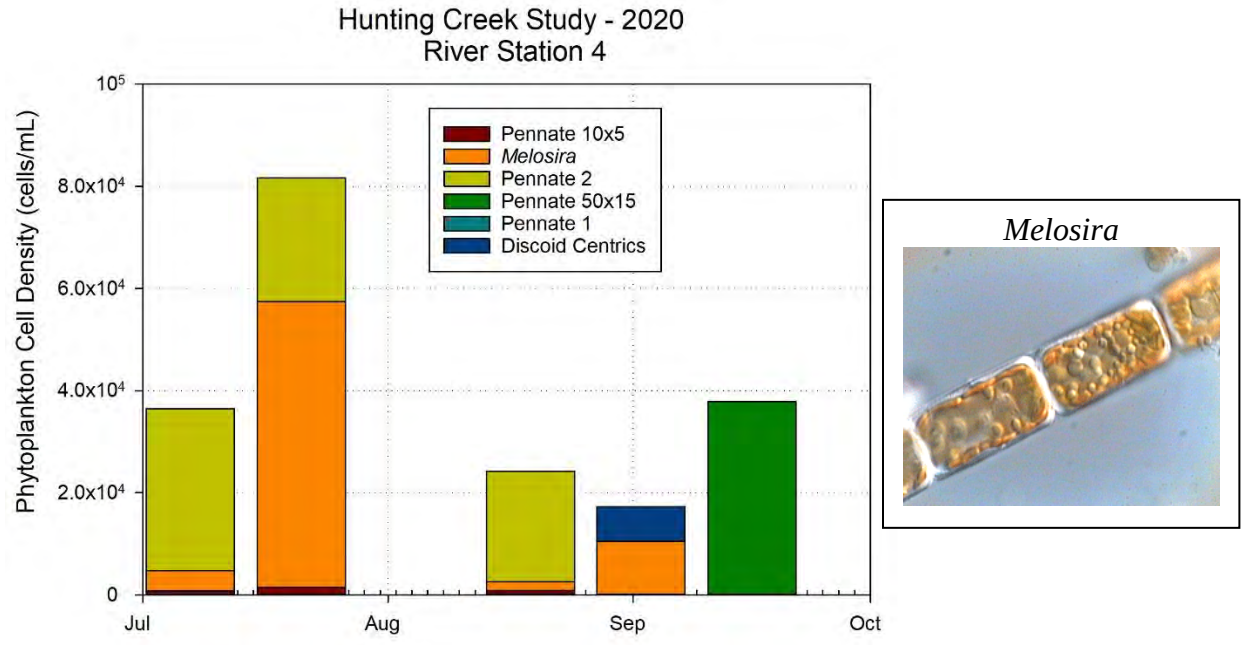

Figure 78. Phytoplankton Density (#/mL) by Dominant Diatom Taxa. River.

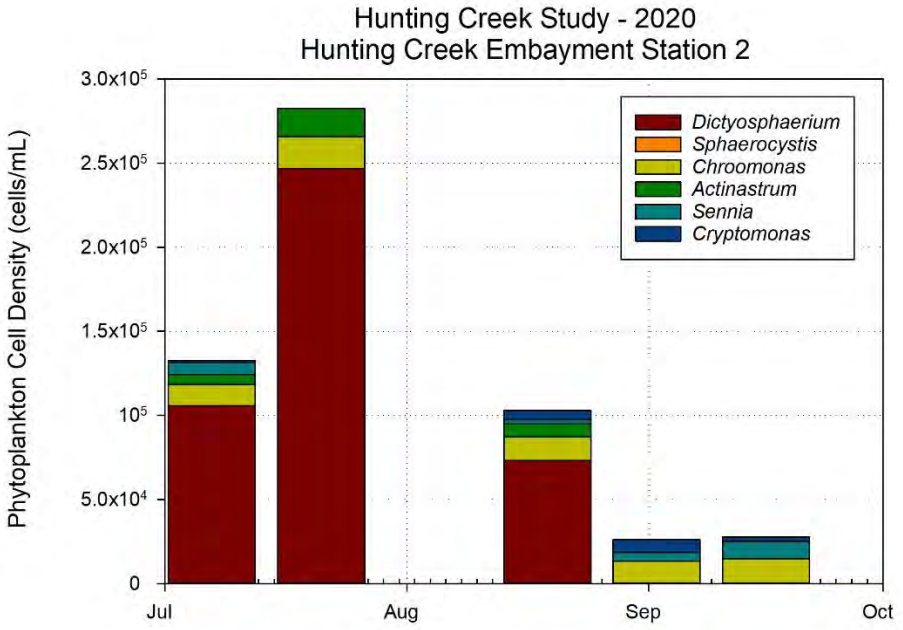

The most numerous other phytoplankton were:

- *Chromulina* – a flagellated chrysophyte
- *Chroomonas* – a flagellated cryptomonad unicell
- Kirchneriella – a colonial green alga
- *Cryptomonas* – a flagellated cryptomonad unicell
- Chlamydomonas – a biflagellate green unicell
- *Spermatozoopsis* – flagellated green unicell

Figure 79. Phytoplankton Density (#/mL) by Dominant Other Taxa. Hunting Creek.

Phytoplankton species that were neither cyanobacteria nor diatoms were grouped together as "other" for these graphs; these included most numerous taxa of green algae, cryptophytes, euglenoids, and dinoflagellates. The green alga *Dictyosphaerium* was clearly dominant in cell density in July and August at AR2 (Figure 79). At AR4 *Chroomonas* was dominant in July while Sennia was dominant in August (Figure 80).

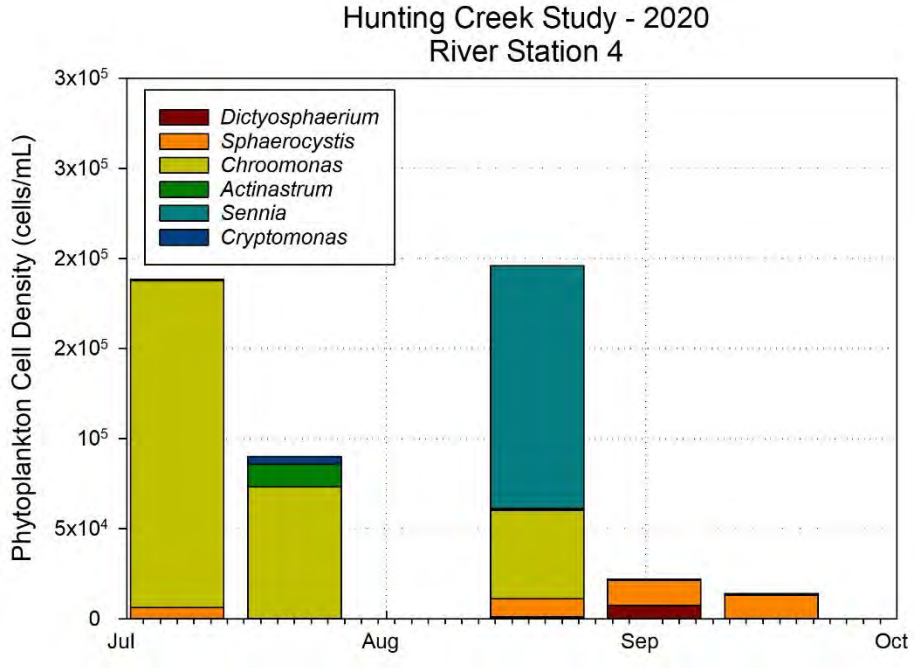

Figure 80. Phytoplankton Density (#/mL) by Dominant Other Taxa. River.

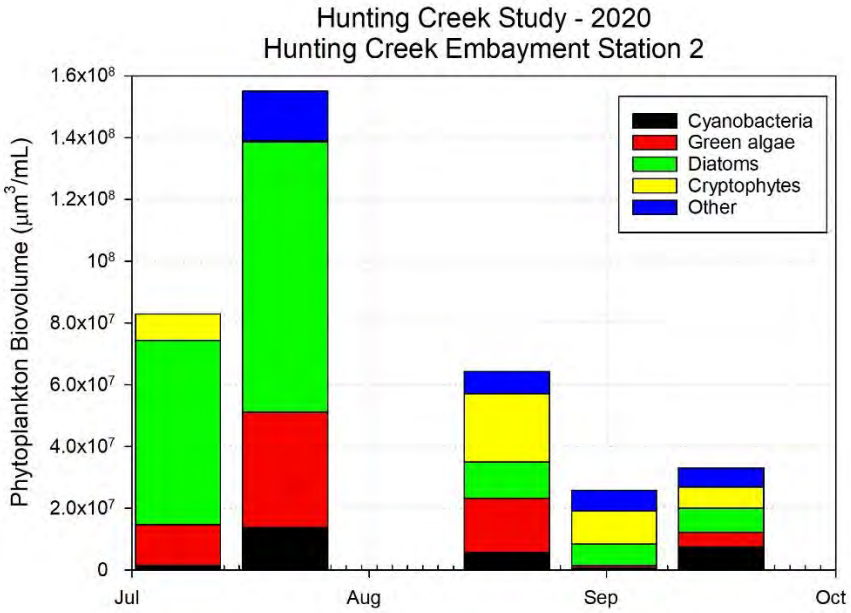

Total phytoplankton biovolume can be broken down into groups:

Cyano – cyanobacteria ("blue-green" algae)
Greens – green algae
Diatoms – includes both centric and pinnate
Cryptos – cryptophytes
Other – includes euglenoids, chrysophytes, and dinoflagellates

Figure 81. Phytoplankton Biovolume (um³/mL) by Major Groups. Hunting Creek.

At AR2 in Hunting Creek diatoms were dominant in biovolume in July (Figure 81). Several groups were co-dominant in August and September at AR2. At AR4 in the river, diatoms were dominant on all dates with cryptophytes making a strong contribution in late July (Figure 82).

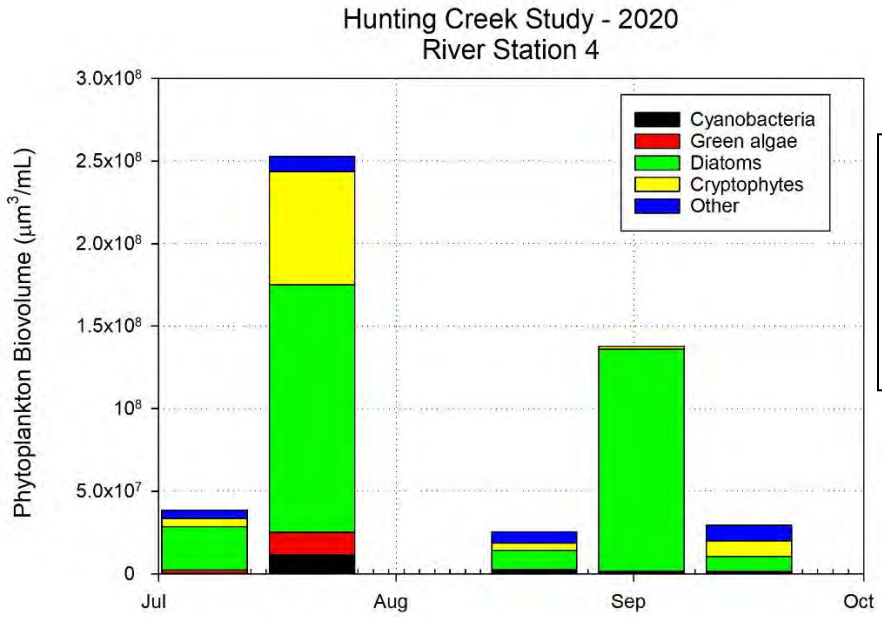

While dominating cell density, cyanobacteria typically make up a much smaller portion of phytoplankton biovolume. Diatoms generally are dominant.

Figure 82. Phytoplankton Biovolume (um³/mL) by Major Groups. River.

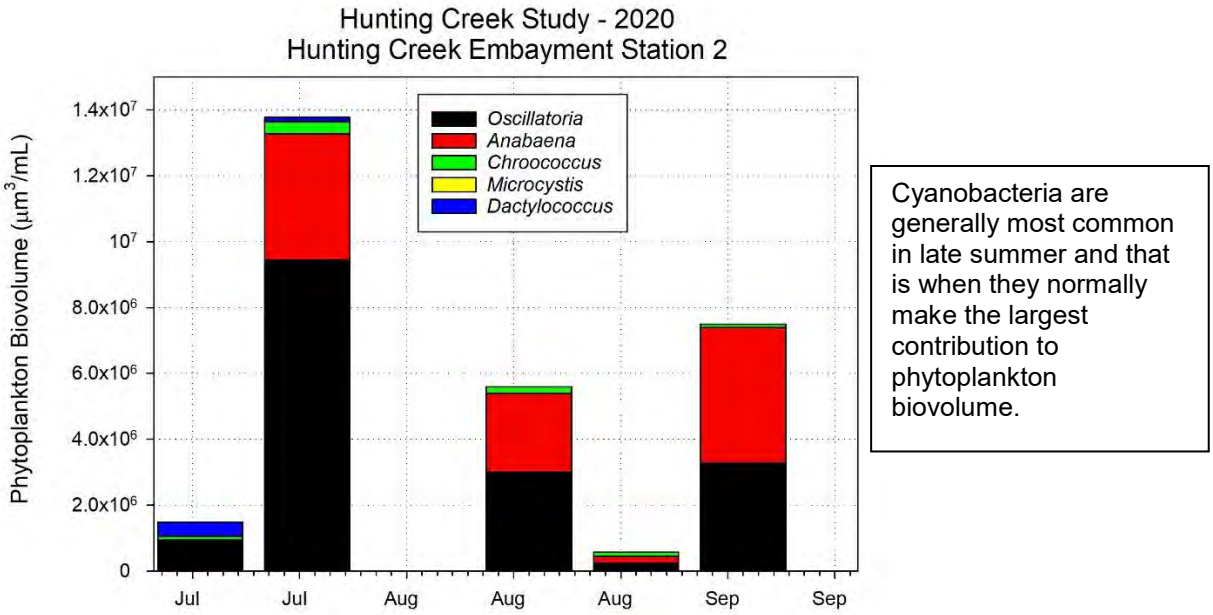

Figure 83. Phytoplankton Biovolume (um³/mL) by Cyanobacteria Taxa. Hunting Creek.

Among the cyanobacteria *Oscillatoria* was dominant on most dates at both stations (Figures 83&84). However, in certain samples at both stations *Anabaena* was co-dominant.

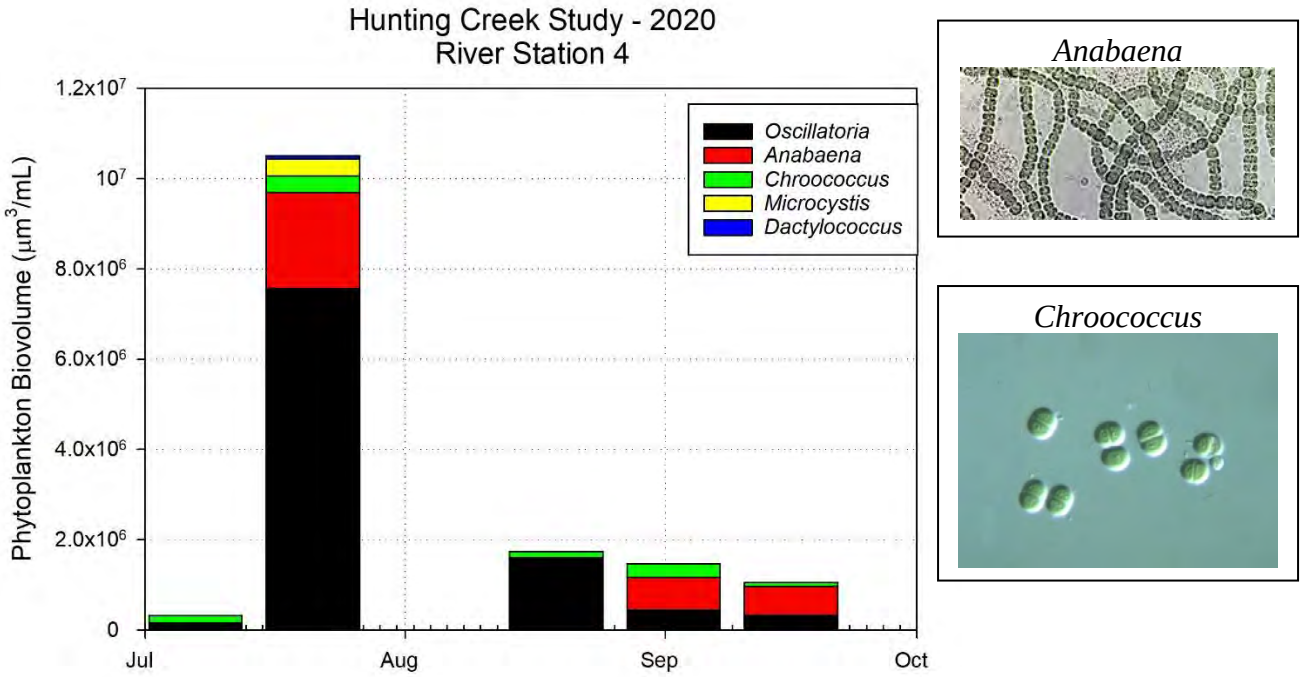

Figure 84. Phytoplankton Biovolume (um³/mL) by Cyanobacterial Taxa. River.

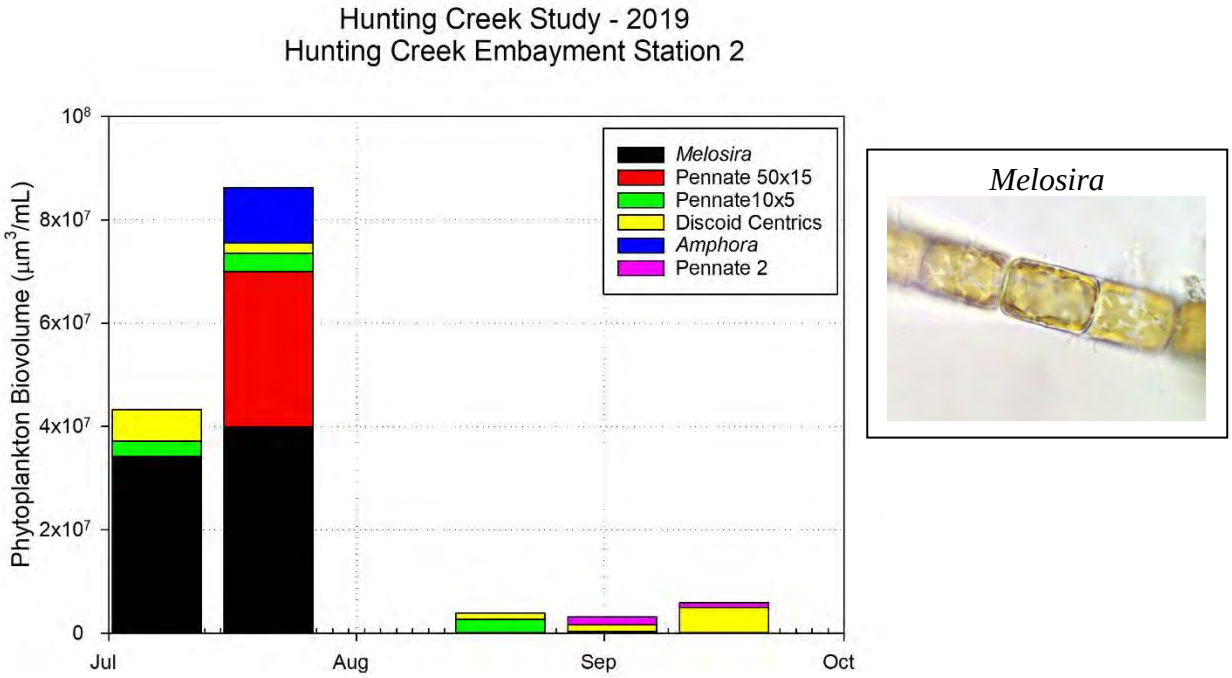

Figure 85. Phytoplankton Biovolume (um³/mL) by Dominant Diatom Taxa. Hunting Creek.

At both stations, *Melosira* was the dominant on most dates (Figures 85&86). Pennate 50x15 was co-dominant at AR2 in late July.

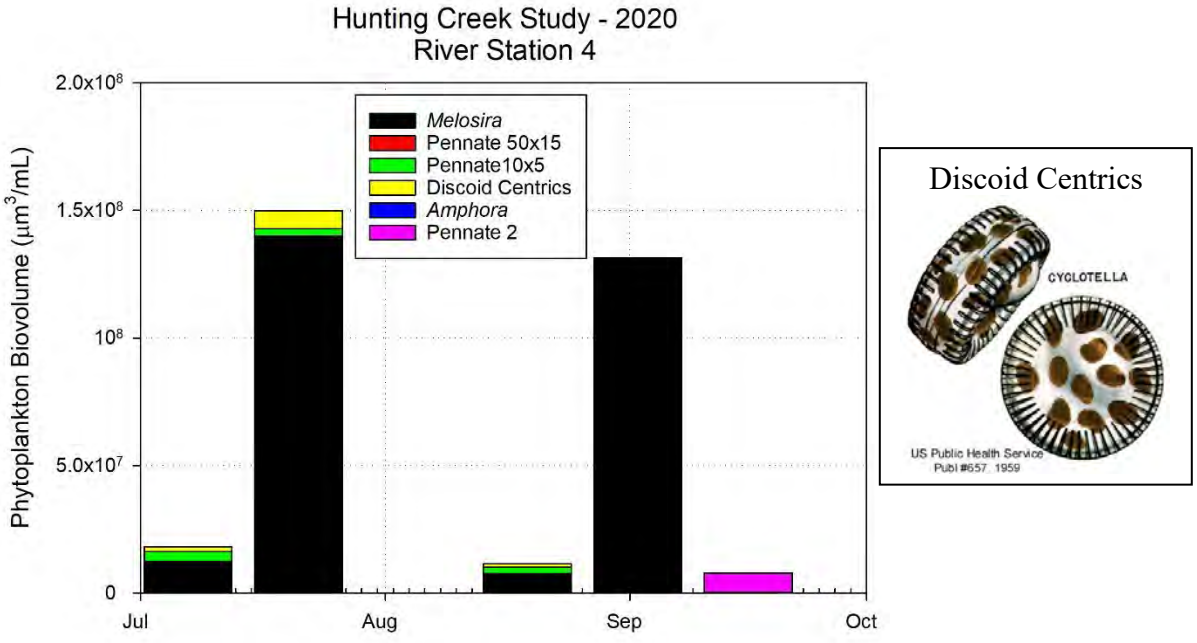

Figure 86. Phytoplankton Biovolume (um³/mL) by Dominant Diatom Taxon. River.

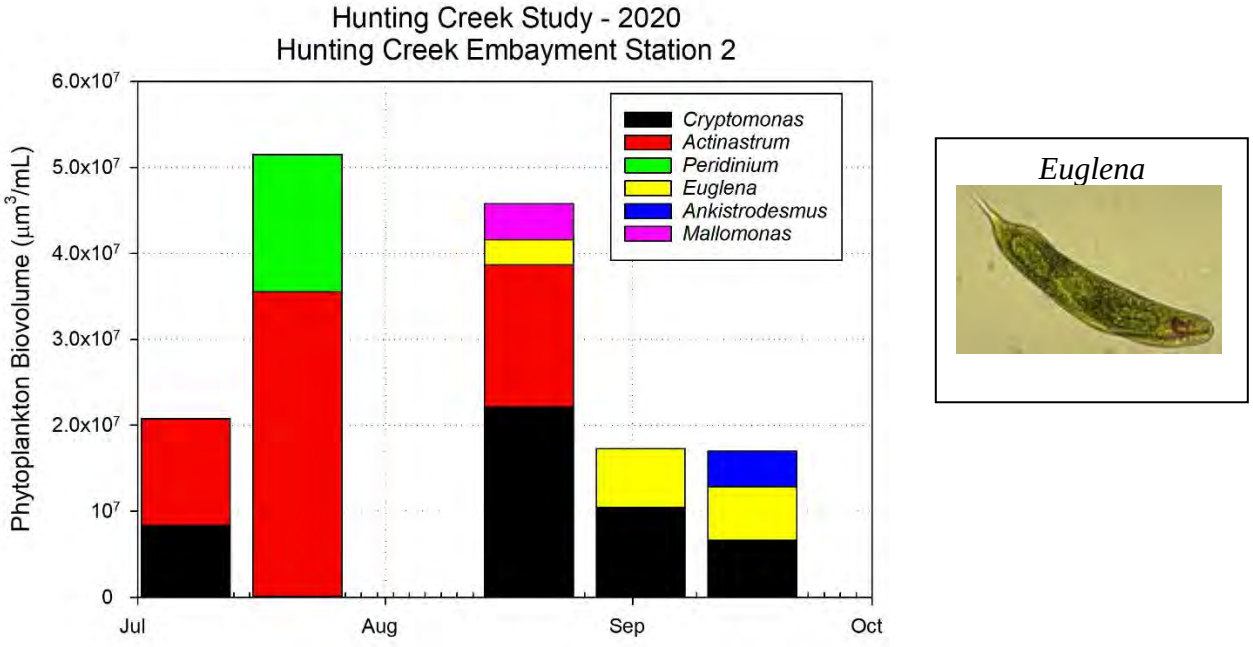

Figure 87. Phytoplankton Biovolume (um³/mL) by Dominant Other Taxa. Hunting Creek.

The green alga *Actinastrum* and the cryptophyte *Cryptomonas* dominated biovolume in most samples at AR2 (Figure 87). The dinoflagellate *Peridinium* was important in late July. *Cryptomonas* dominant in most river samples at AR4 (Figure 88). The euglenoid *Euglena* made substantial contributions in some samples.

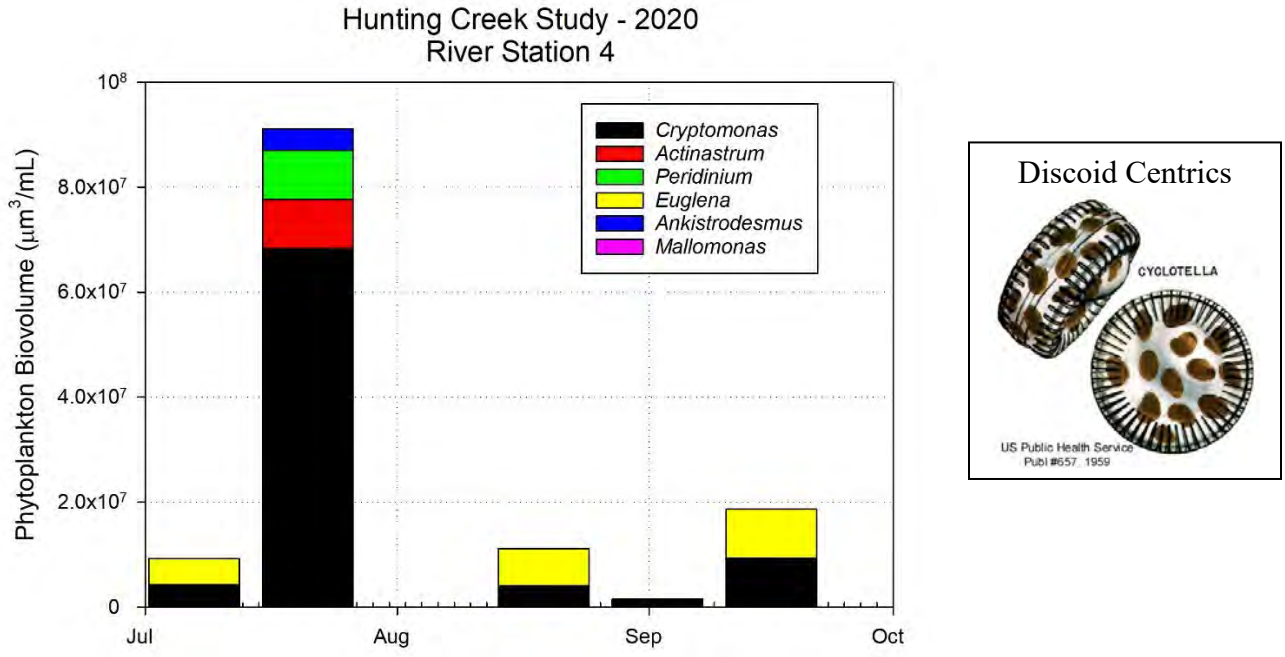

Figure 88. Phytoplankton Biovolume (um³/mL) by Dominant Other Taxon. River.

E. Zooplankton – 2020

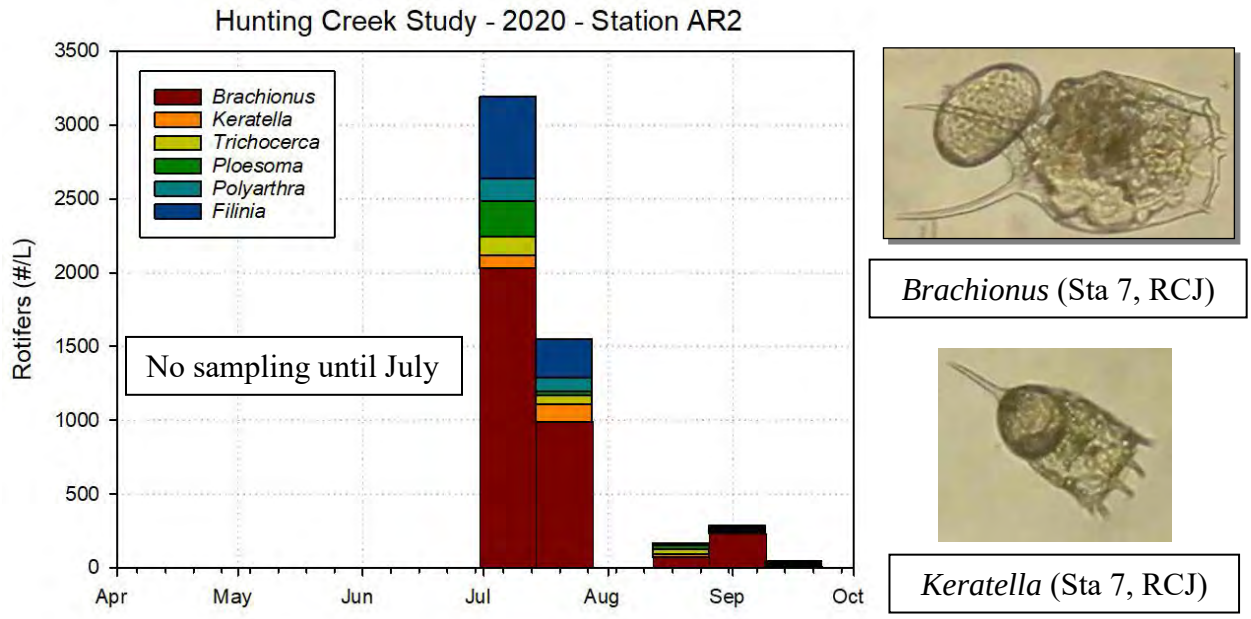

Figure 89. Rotifer Density by Dominant Taxa (#/L). Hunting Creek.

At the embayment station AR2, rotifer populations quite high in July and decreased markedly in August and September (Figure 89). *Brachionus* was dominant at all times with *Filinia* assuming a subdominant position. In the river at AR4, rotifer populations followed a similar pattern and were even slightly higher than those at AR2 in July (Figure 90). *Brachionus* was dominant in almost all samples with *Keratella* and *Filinia* being important at some times.

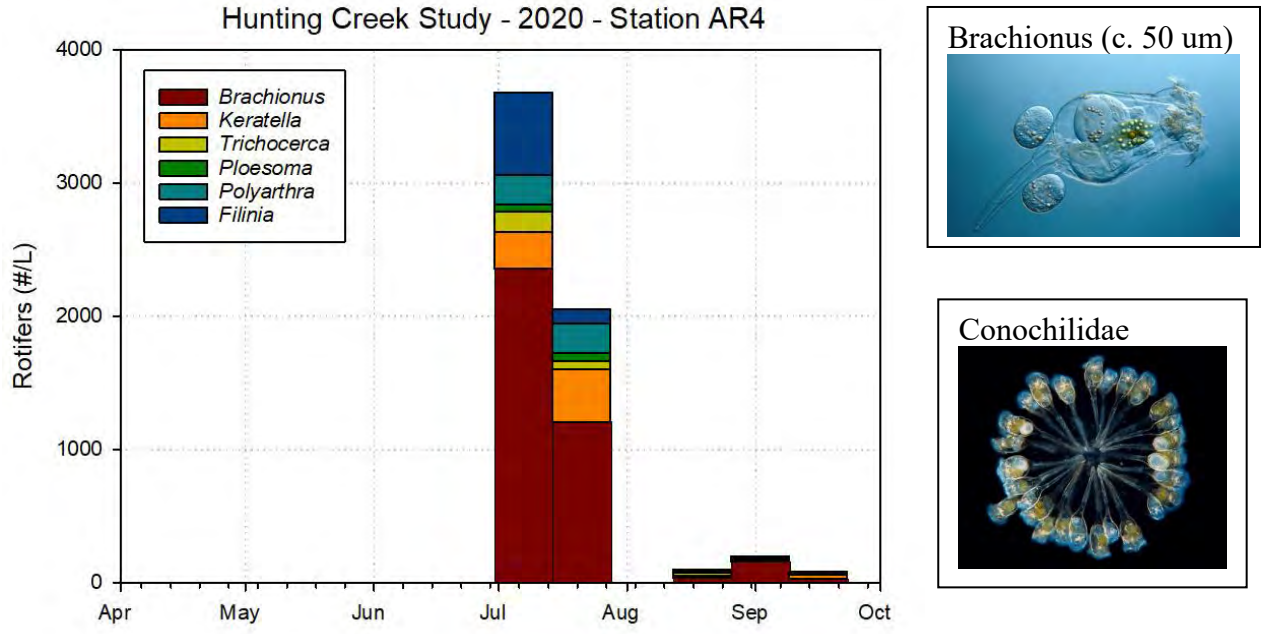

Figure 90. Rotifer Density by Dominant Taxa (#/L). River.

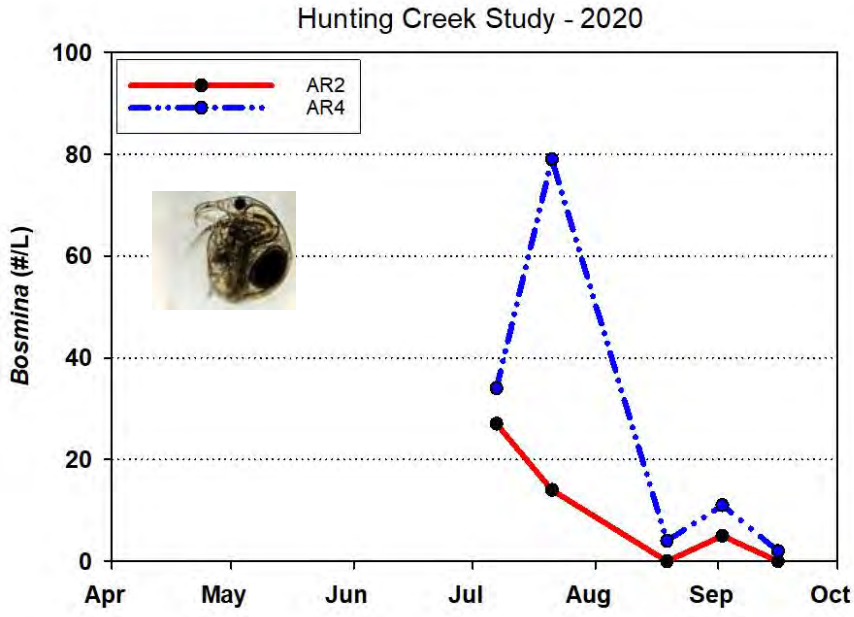

Bosmina is a small-bodied cladoceran, or "waterflea", which is common in lakes and freshwater tidal areas. It is typically the most abundant cladoceran with maximum numbers generally about 100-1000 animals per liter. Due to its small size and relatively high abundances, it is enumerated in the micro-zooplankton samples. *Bosmina* can graze on smaller phytoplankton cells, but can also utilize some cells from colonies by knocking them loose.

Figure 91. *Bosmina* Density by Station (#/L).

At the embayment station AR2 the small cladoceran *Bosmina* was generally quite low from July through September (Figure 91). In the river *Bosmina* exhibited a distinct peak of 80/L in late July before dropping off. *Diaphanosoma*, typically the most abundant larger cladoceran in the tidal Potomac, was moderately abundant in early July (about 250/L) at both AR2 and AR4 (Figure 92). Remained high at AR4 in late July, but dropped off strongly at AR2 in late July. Abundances dropped off strongly at AR2, but showed a moderate rebound in early September at AR4.

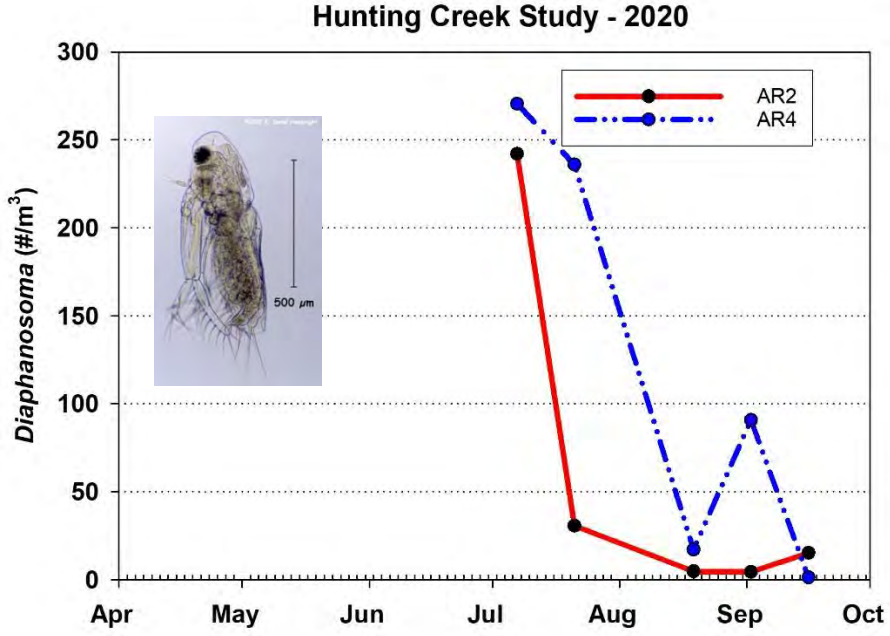

Diaphanosoma is the most abundant larger cladoceran found in the tidal Potomac River. It generally reaches numbers of 1,000-10,000 per m^3 (which would be 1-10 per liter). Due to their larger size and lower abundances, *Diaphanosoma* and the other cladocera are enumerated in the macrozooplankton samples. *Diaphanosoma* prefers warmer temperatures than some cladocera and is often common in the summer.

Figure 92. *Diaphanosoma* Density by Station (#/m^3).

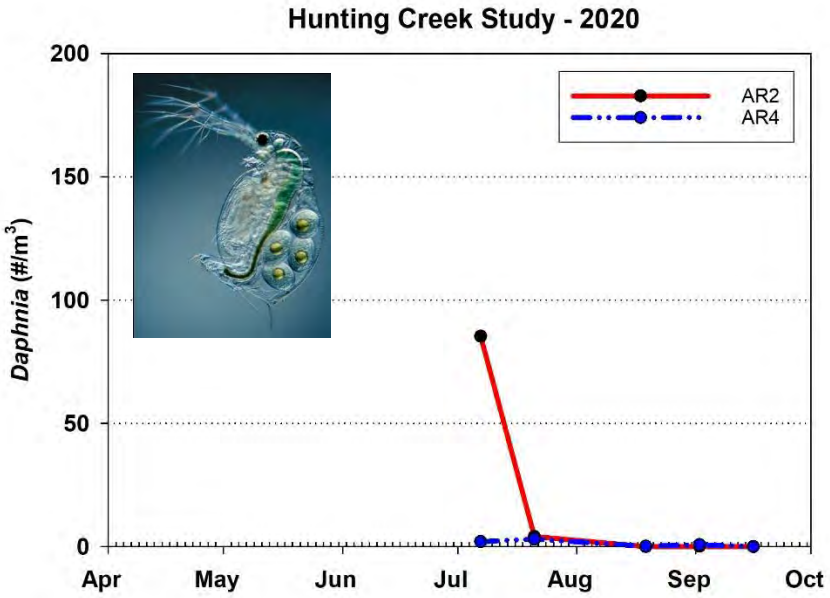

Daphnia, the common waterflea, is one of the most efficient grazers of phytoplankton in freshwater ecosystems. In the tidal Potomac River it is present, but has not generally been as abundant as *Diaphanosoma*. It is typically most common in spring.

Figure 93. *Daphnia* Density by Station (#/m^3).

Daphnia was only moderately abundant in one sample in 2020, that in early July at AR2 (Figure 93). *Ceriodaphnia* showed a very similar temporal pattern with slightly higher abundance (Figure 94).

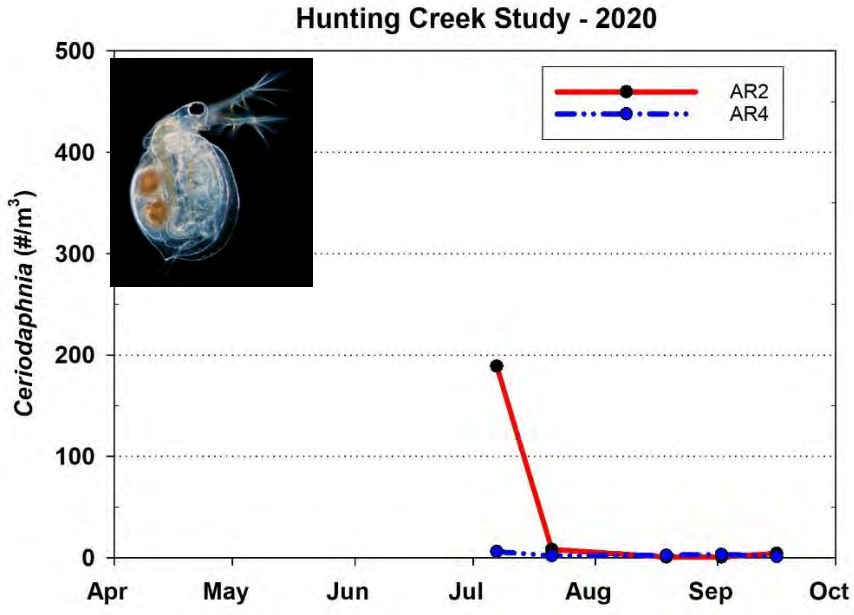

Ceriodaphnia, another common large-bodied cladoceran, is usually present in numbers similar to *Daphnia*. Like all waterfleas, the juveniles look like miniature adults and grow through a series of molts to a larger size and finally reach reproductive maturity. Most reproduction is asexual except during stressful environmental conditions.

Figure 94. *Ceriodaphnia* Density by Station (#/m^3).

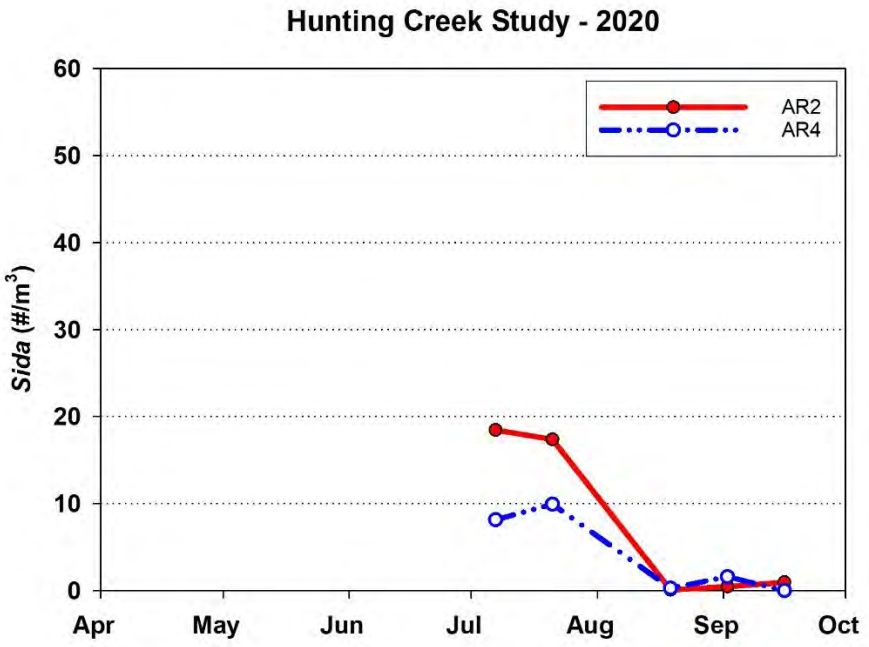

Sida is another waterflea that is often observed in the tidal Potomac River. Like the other cladocera mentioned so far, *Sida* grazes on phytoplankton to obtain its food supply.

Figure 95. *Sida* Density by Station (#/m^3).

Sida was found low levels at both stations in July, but disappeared in August and September (Figure 95). *Leptodora*, the large cladoceran predator, was found at moderately high levels in early July but declined sharply in late July and disappeared in August and September at both stations (Figure 96).

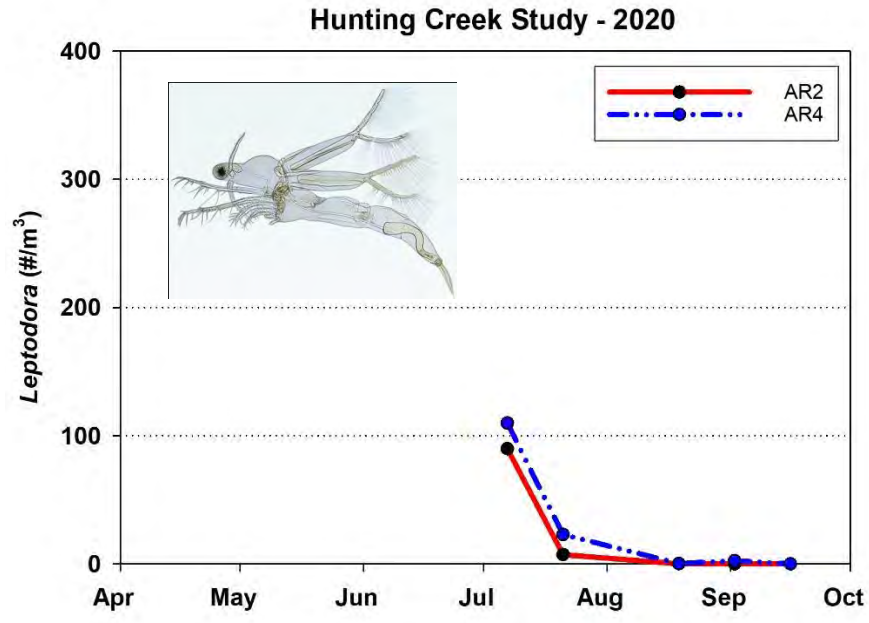

Leptodora is substantially larger than the other cladocera mentioned. Also different is its mode of feeding – it is a predator on other zooplankton. It normally occurs for brief periods in the late spring or early summer.

Figure 96. *Leptodora* Density by Station (#/m^3).

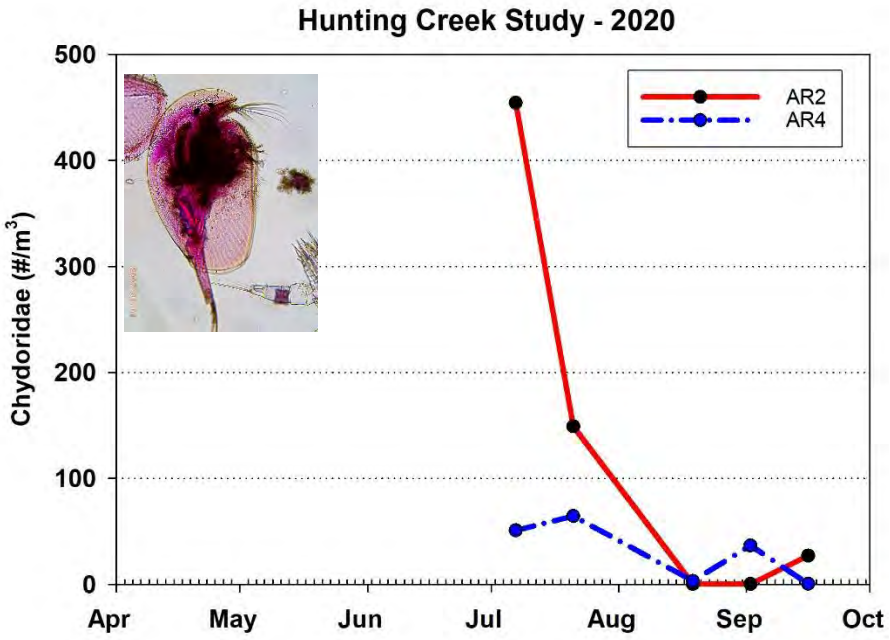

Figure 97. Chydoridae Density by Station (#/m^3). (photo: L. Birsa from HC samples)

Chydoridae is a cladoceran family whose members are associated with shallow water and SAV (Figure 97). In 2020, levels were quite low except at AR2 in early July. Macrothricids, another group associated with SAV, were of very minor importance in 2020 (Figure 98).

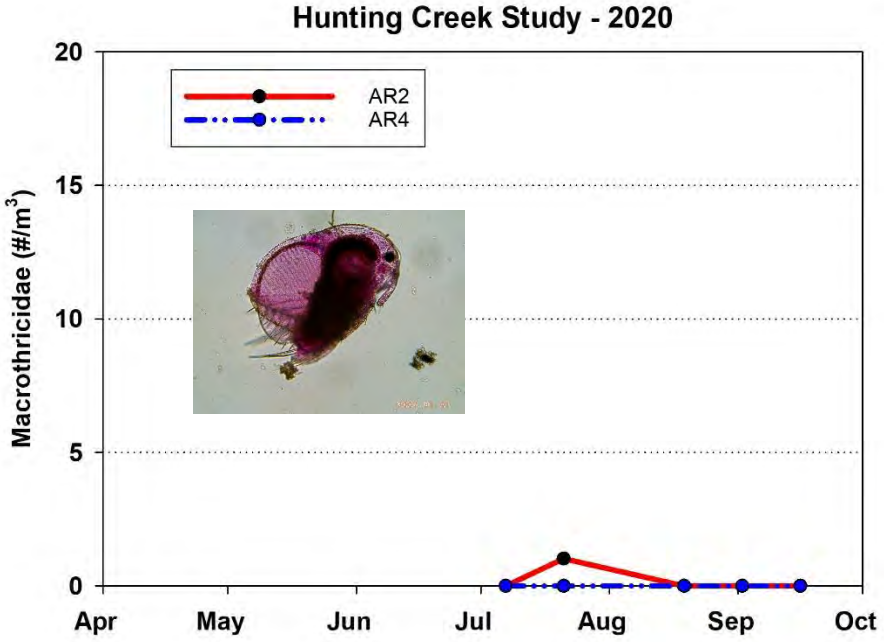

Figure 98. Macrothricid Density by Station (#/m^3). (photo: L. Birsa from HC samples)

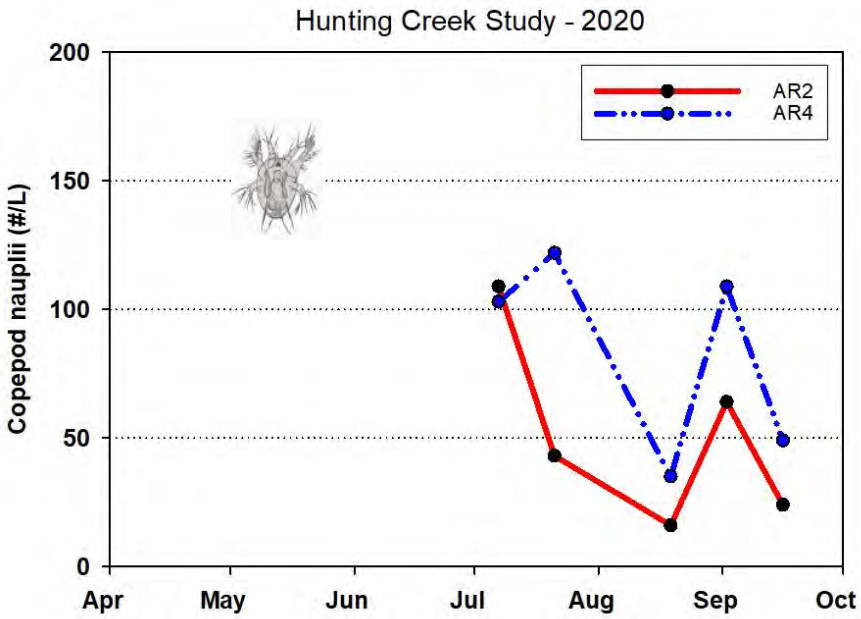

Copepod eggs hatch to form an immature stage called a nauplius. The nauplius is a larval stage that does not closely resemble the adult and the nauplii of different species of copepods are not easily distinguished so they are lumped in this study. Copepods go through 5 naupliar molts before reaching the copepodid stage which is morphologically very similar to the adult. Because of their small size and high abundance, copepod nauplii are enumerated in the micro-zooplankton samples.

Figure 99. Copepod Nauplii Density by Station (#/L).

Copepod nauplii, the larval stage of copepods, were the most numerous group of crustacean zooplankton. They were present at levels of about 100/L at both stations in early July (Figure 99). In late July values at AR2 declined, but at AR4 they remained about the same. Values declined at both station in late August, but showed another peak in early September. In the river *Eurytemora*, a large calanoid copepod, was present at relatively high values at both station in early July, but declined rapidly thereafter (Figure 100).

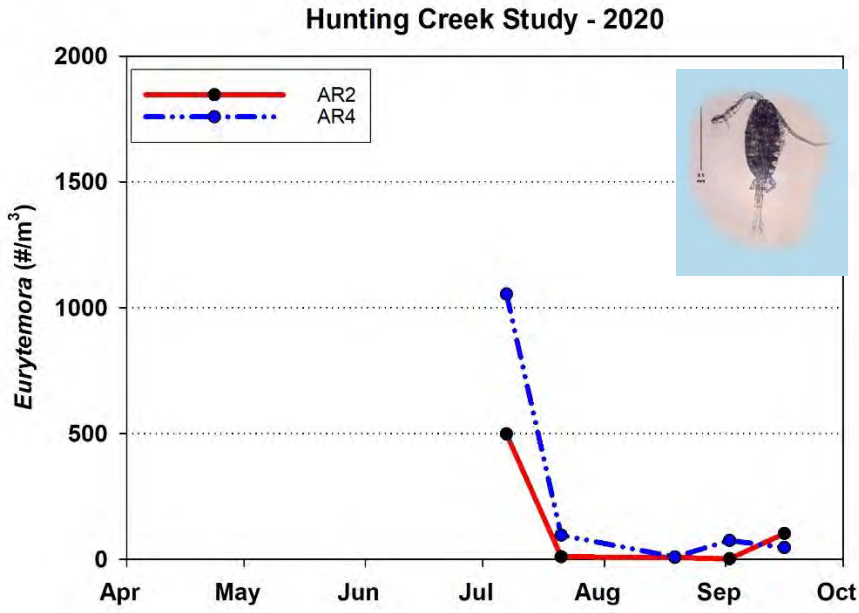

Eurytemora affinis is a large calanoid copepod characteristic of the freshwater and brackish areas of the Chesapeake Bay. *Eurytemora* is a cool water copepod which often reaches maximum abundance in the late winter or early spring. Included in this graph are adults and those copepodids that are recognizable as *Eurytemora*.

Figure 100. *Eurytemora* Density by Station (#/m^3).

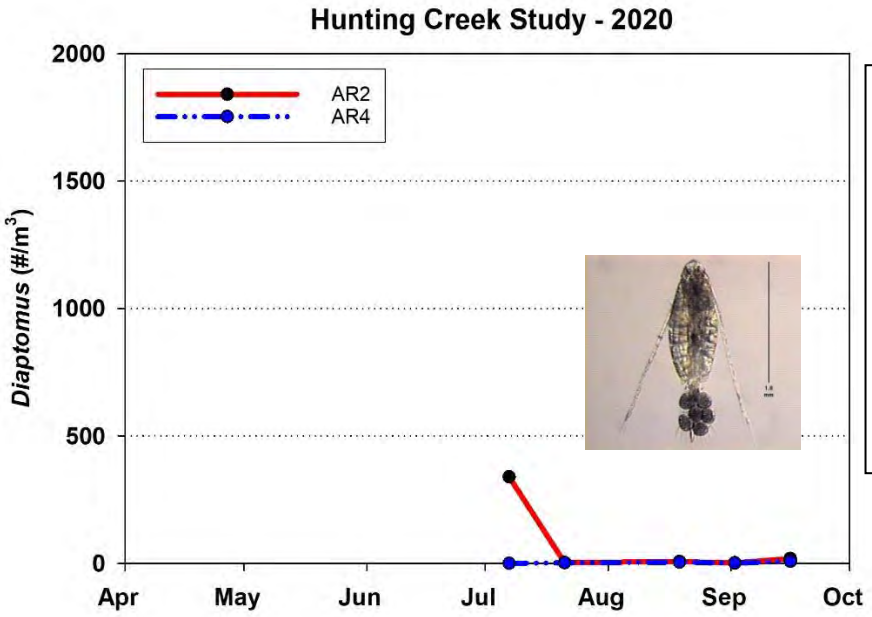

Diaptomus pallidus is a calanoid copepod often found in moderate densities in the Gunston Cove area. *Diaptomus* is an efficient grazer of algae, bacteria, and detrital particles in freshwater ecosystems Included in this graph are adults and those copepodids that are recognizable as *Diaptomus*.

Figure 101. *Diaptomus* Density by Station (#/m^3).

Diaptomus was present in only one sample in 2020, early July at AR2 (Figure 101). Cyclopoid copepods were present at moderate levels at both stations in early July, but declined for the rest of the year (Figure 102).

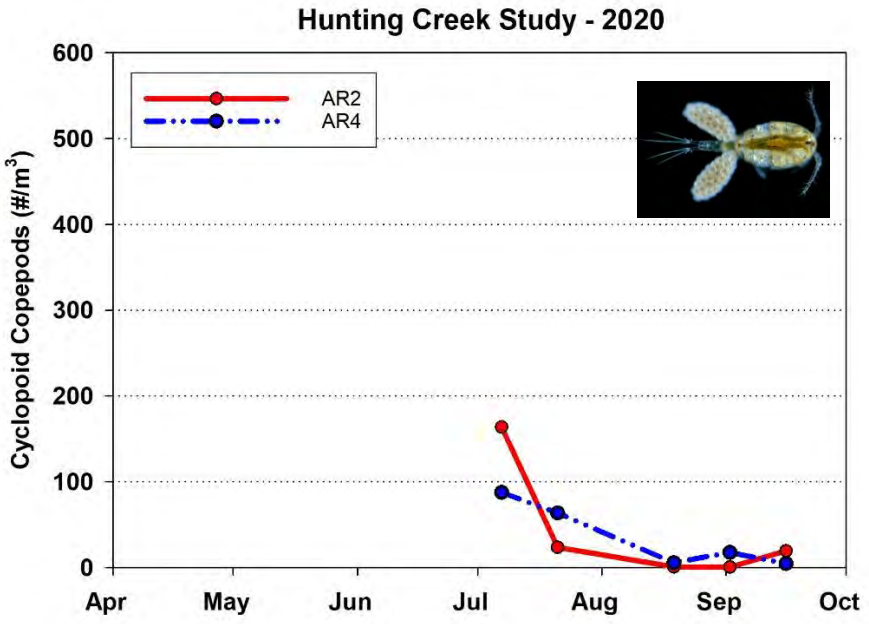

Cyclopoids are the other major group of planktonic copepods. Cyclopoids feed on individual particles suspended in the water including small zooplankton as well as phytoplankton. In this study we have lumped all copepodid and adult cyclopoids together.

Figure 102. Cyclopoid Copepods by Station (#/m^3).

F. Ichthyoplankton – 2020

We collected 4 samples (2 at Station 2 and 2 at Station 4) during the month of July and found an average total larval density of 10.54 larvae of at least 7 species per 10 m^3 (Table 5a). This is based on 159 larvae collected over two dates, and is not representative of what is present during a normal sampling season (Table 5b). This should be kept in mind, as 2020 is thereby not comparable to the other collection years. The dominant family was Clupeidae, of which Blueback herring (*Alosa aestivalis*) had the highest density with an average larval density of 2.44 larvae per $10m^3$. Alewife (*Alosa pseudoharengus*) had the second highest density with an average of 1.82 larvae per $10m^3$. Another clupeid present that could positively be identified to the species level is Gizzard Shad (*Dorosoma cepedianum*) at an average of 0.49 larvae per $10m^3$. The taxon Clupeidae, which is comprised of clupeids (*Alosa* or *Dorosoma* sp.) that could not be identified to a lower taxonomic level had an average density of 2.78 larvae per $10m^3$. A different taxon with relatively high representation is Bluegill (*Lepomis macrochirus* with an average of 1.19 larvae per $10m^3$. Inland silverside (*Menidia beryllina*) was relatively abundant as well, with an average of 0.89 larvae per $10m^3$. With only two sampling dates in the same month, we were unable to create graphs representing the larval density of different species per month and cannot report on the seasonal pattern of larval density.

Table 5a. The average larval density (#/$10m^3$) in Hunting Creek (AR 2) and the Potomac River (AR 4) in 2020.

Scientific Name	Common Name	AR2	AR4	Average
Alosa aestivalis	Blueback Herring	1.51	3.38	2.44
Alosa pseudoharengus	Alewife	1.85	1.80	1.82
Clupeidae	unk. clupeid species	4.85	0.70	2.78
Dorosoma cepedianum	Gizzard Shad	0.48	0.50	0.49
Eggs	eggs	0.00	0.00	0.00
Lepomis cyanellus	Green Sunfish	0.00	0.37	0.19
Lepomis macrochirus	Bluegill	2.38	0.00	1.19
Lepomis sp.	unk. sunfish	0.31	0.00	0.16
Menidia beryllina	Inland Silverside	1.68	0.10	0.89
Morone americana	White Perch	0.14	0.00	0.07
Unidentified	unidentified	1.03	0.00	0.51
Total		14.24	6.85	10.54

Table 5b. Abundance of larvae collected by date. Hunting Creek - 2020.

Scientific Name	Common Name	07/07	07/21	Total
Alosa aestivalis	Blueback Herring	39	4	43
Alosa pseudoharengus	Alewife	25	5	30
Clupeidae	unk. clupeid species	41	0	41
Dorosoma cepedianum	Gizzard Shad	6	2	8
Eggs	eggs	0	0	0
Lepomis cyanellus	Green Sunfish	0	2	2
Lepomis macrochirus	Bluegill	0	14	14
Lepomis sp.	unk. sunfish	1	1	2
Menidia beryllina	Inland Silverside	2	9	11
Morone americana	White Perch	1	0	1
Unidentified	unidentified	6	1	7
Total		121	38	159

G. Adult and juvenile fishes – 2020

Trawls

Trawl sampling was conducted between July 17 and September 17 at station 3 and 4. A total of 2076 fishes comprising 13 species were collected with trawls (Table 6). This abundance is very high, especially for such a truncated collection season, but diversity is low (low number of species with high dominance of one species). These results are not comparable to previous years since diversity is highly related to the number of samples taken. Collections were dominated by White Perch (88.36%). The second most abundant species was Spottail Shiner (3.72%). Other relatively abundant species were Blue Catfish (2.95%), Alewife (1.91%) and Gizzard Shad (1.02%) (Tables 6 and 7). An interesting find was the collection of three native catfishes (Channel Catfish, White Bullhead and Brown Bullhead) after finding four last year. Native catfishes have seen declining abundances since the invasion of Blue Catfish. A concerning find is the Flathead Catfish, which is an invasive species like Blue Catfish. We are not the first to report this species here, but we had not seen it before in our samples.

Table 6. Adult and juvenile fish collected by trawling. Hunting Creek - 2020.

Scientific Name	Common Name	Abundance	Percent
Morone americana	White Perch	1835	88.36
Notropis hudsonius	Spottail Shiner	77	3.72

Ictalurus furcatus	Blue Catfish	61	2.95
Alosa pseudoharengus	Alewife	40	1.91
Dorosoma cepedianum	Gizzard Shad	21	1.02
Etheostoma olmstedi	Tessellated Darter	8	0.40
Alosa sp.	unk. Alosa species	8	0.37
Anchoa mitchilli	Bay anchovy	8	0.36
Lepomis gibbosus	Pumpkinseed	6	0.26
Alosa mediocris	Hickory Shad	4	0.19
Ameiurus catus	White Bullhead	4	0.19
Ictalurus punctatus	Channel Catfish	3	0.14
Pylodictis olivaris	Flathead Catfish	1	0.06
Ameiurus nebulosus	Brown Bullhead	1	0.05
Total		2076	100.00

Table 7. Adult and juvenile fish collected by trawling. Hunting Creek study - 2020.

Scientific Name	Common Name	07/17	07/31	08/14	08/27	09/17	Total
Alosa mediocris	Hickory Shad	0	0	0	0	4	4
Alosa pseudoharengus	Alewife	0	2	15	9	14	40
Alosa sp.	unk. Alosa species	2	2	0	4	0	8
Ameiurus catus	White Bullhead	0	0	1	1	2	4
Ameiurus nebulosus	Brown Bullhead	1	0	0	0	0	1
Anchoa mitchilli	Bay anchovy	0	0	1	2	4	8
Dorosoma cepedianum	Gizzard Shad	12	3	2	1	3	21
Etheostoma olmstedi	Tessellated Darter	2	1	2	1	2	8
Ictalurus furcatus	Blue Catfish	29	1	2	21	8	61
Ictalurus punctatus	Channel Catfish	0	0	1	1	1	3
Lepomis gibbosus	Pumpkinseed	1	1	1	2	0	6

Morone americana	White Perch	185	233	315	356	746	1835
Notropis hudsonius	Spottail Shiner	34	16	5	3	19	77
Pylodictis olivaris	Flathead Catfish	0	0	0	1	0	1
Total		**266**	**259**	**345**	**404**	**803**	**2076**

The highest catch occurred on September 17, which was due to the high abundance of White Perch in that trawl sample (Table 7). Most catches occurred at station 4 (Table 8). At both stations, catches of White Perch were mostly responsible for the total catch. The catch at station 4 was more than twice that of last year with 1133 individuals, and more diverse with 9 species. At Station 3, 944 specimens were collected of 13 species, as compared to 499 specimens of 20 species in 2019. White Perch was the dominant species as in previous years. Looking at species by dominance (Figure 103A and B) White Perch was the dominant species both at station 3 and 4 in 2020. The species distribution is not even at all both in station 3 than station 4, with almost all abundance on one species.

Table 8. Adult and juvenile fish collected by trawling. Hunting Creek study - 2020.

Scientific Name	Common Name	AR3	AR4
Alosa mediocris	Hickory Shad	3	1
Alosa pseudoharengus	Alewife	38	2
Alosa sp.	unk. Alosa species	8	0
Ameiurus catus	White Bullhead	1	3
Ameiurus nebulosus	Brown Bullhead	1	0
Anchoa mitchilli	Bay anchovy	4	4
Dorosoma cepedianum	Gizzard Shad	21	0
Etheostoma olmstedi	Tessellated Darter	7	1
Ictalurus furcatus	Blue Catfish	3	58
Ictalurus punctatus	Channel Catfish	0	3
Lepomis gibbosus	Pumpkinseed	6	0
Morone americana	White Perch	795	1040
Notropis hudsonius	Spottail Shiner	56	21
Pylodictis olivaris	Flathead Catfish	1	0
Total		944	1133

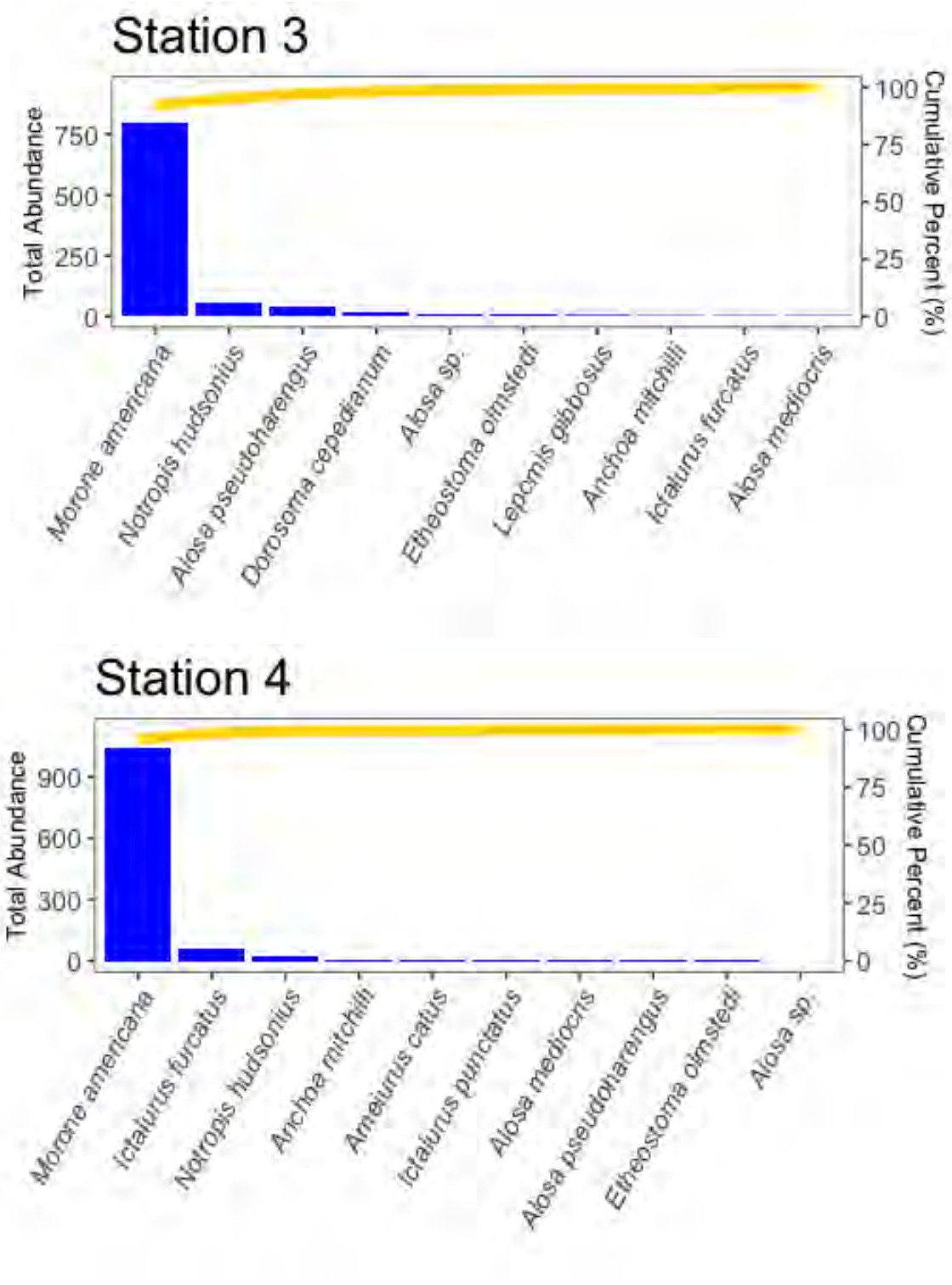

Figure 103A and B. Pareto chart of adult and juvenile fishes collected by trawling in 2020. Dominant species by station in total abundance and cumulative percentage of total for Station 3 (top) and Station 4 (bottom).

White Perch is a dominant species in all months sampled (Figure 104 A&B). Other species present in all months sampled, but in low numbers, were Alewife (*Alosa pseudoharengus*), Gizzard Shad (*Dorosoma cepedianum*), Tessellated Darter (*Etheostema olmstedi*), Blue Catfish (Ictalurus furcatus), and Spottail Shiner (*Notropis hudsonius*).

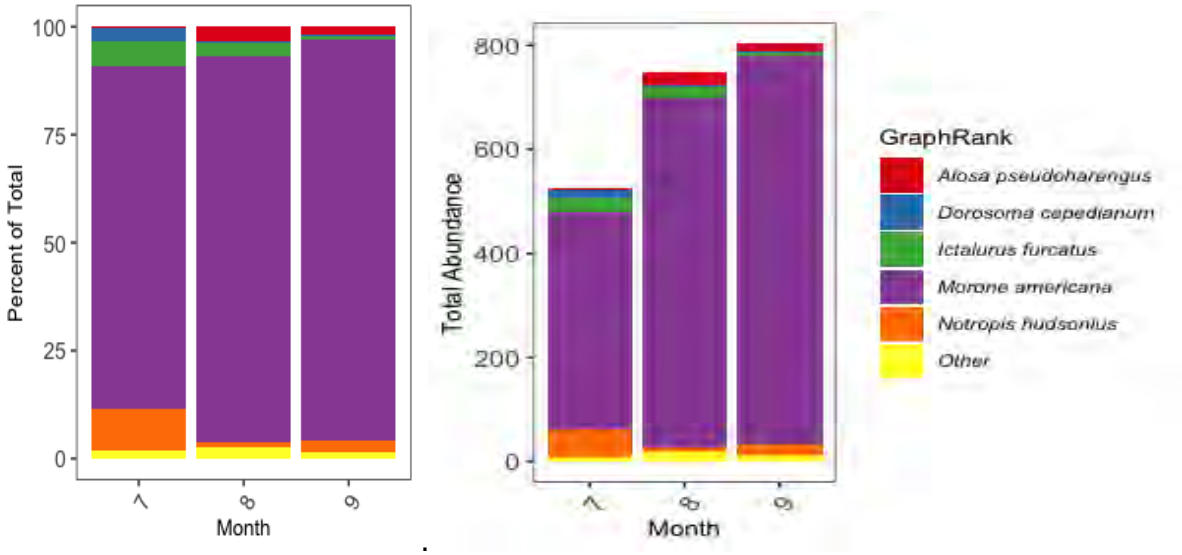

Figure 104A&B. Adult and juvenile fishes collected by trawling in 2020. Dominant species by month in percentage of total (A) and total abundance (B).

Seines

Seine sampling was conducted between July 17 and September 17 at station 5 and 6. Two sampling trips per month were performed until (and including) August, and one sampling trip in September. These two seines stations were selected as sites with shallow sloping shorelines that would enable us to tow a beach seine. The net was towed up onto the beach unless high water completely submerged the beach. In those cases, the net was towed into the boat.
A total of 10 seine samples were taken (5 per station), comprising 1447 fishes of at least 14 species (Table 8). This is less than last year, but we took only half the samples of last year. Like last year, Banded Killifish was not the most dominant species in seine catches (10.16%), while this was the case in most previous years. Instead, very high abundances were found of White Perch (74.98%). This year the reason could simply be that the part of the season where Banded Killifish is dominant was not sampled. Other species with relatively high abundance were Alewife (5.04%), Gizzard Shad (3.46%), Threadfin Shad (1.66%), and Spottail Shiner (1.31%). Other species occurred at low abundances (Table 9).

White Perch and Banded Killifish were collected during each trip throughout the sampling period of July to September, both with highest abundances mid-August (Table 10). The total number of specimens at station 6 was higher than station 5, which was due to the fact that almost

all White perch were collected at station 6 (Table 11). Evenness distribution of abundance over multiple species was higher at station 5 than station 6, due to the very high abundance of White Perch in station 6 (Figure 105A&B). Banded killifish was the most dominant species in station 5, with total abundance of fishes much lower than station 6 (Table 11, Figure 106A&B)
The abundance by month of dominant species shows White Perch is dominant each month except for September, when Alewife was dominant (Figure 106A&B). Banded Killifish is an important representative of the fish assemblage and shows highest abundance in August. While the highest abundance of fishes was collected on a mid-August sampling trip (Table 10), the fact that both sampling trips in July had consistent high catches of especially White Perch made July the month with the highest total abundance (Figure 106B). Other species that were abundant but not ubiquitous or dominant in seine collections throughout the sampling season were Gizzard Shad (*Dorosoma cepedianum*), Threadfin Shad (*Dorosoma petenense*), and Spottail Shiner (*Notropis hudsonius*) (Figures 106A&B). Threadfin Shad was an interesting find that we saw in relatively high abundance, while it was previously assumed that the low salinity would prevent this species from occurring in our sampling area.

Table 9. Adult and juvenile fish collected by seining. Hunting Creek- 2020.

Scientific Name	Common Name	Abundance	Percent
Alosa pseudoharengus	Alewife	73	5.04
Alosa sp.	unk. Alosa species	10	0.69
Carpiodes cyprinus	Quillback	13	0.90
Dorosoma cepedianum	Gizzard Shad	50	3.46
Dorosoma petenense	Threadfin Shad	24	1.66
Etheostoma olmstedi	Tessellated Darter	3	0.21
Fundulus diaphanus	Banded Killifish	147	10.16
Fundulus heteroclitus	Mummichog	4	0.28
Gambusia holbrooki	Mosquitofish	6	0.41
Lepomis gibbosus	Pumpkinseed	1	0.07
Lepomis macrochirus	Bluegill	1	0.07
Lepomis sp.	unk. sunfish	1	0.07
Menidia beryllina	Inland Silverside	4	0.28
Micropterus dolomieu	Smallmouth Bass	6	0.41
Morone americana	White Perch	1085	74.98
Notropis hudsonius	Spottail Shiner	19	1.31
Total		1447	100.00

Table 10. Adult and juvenile fish collected by seining. Hunting Creek study - 2020.

Scientific Name	Common Name	07/17	07/31	08/14	08/27	09/17	Total
Alosa pseudoharengus	Alewife	1	3	7	0	62	73
Alosa sp.	unk. Alosa species	8	2	0	0	0	10
Carpiodes cyprinus	Quillback	11	2	0	0	0	13
Dorosoma cepedianum	Gizzard Shad	34	11	5	0	0	50
Dorosoma petenense	Threadfin Shad	0	23	1	0	0	24
Etheostoma olmstedi	Tessellated Darter	1	0	1	1	0	3
Fundulus diaphanus	Banded Killifish	6	32	104	3	2	147
Fundulus heteroclitus	Mummichog	1	1	1	1	0	4
Gambusia holbrooki	Mosquitofish	0	1	5	0	0	6
Lepomis gibbosus	Pumpkinseed	0	0	1	0	0	1
Lepomis macrochirus	Bluegill	0	0	0	1	0	1
Lepomis sp.	unk. sunfish	0	0	1	0	0	1
Menidia beryllina	Inland Silverside	4	0	0	0	0	4
Micropterus dolomieu	Smallmouth Bass	1	4	1	0	0	6
Morone americana	White Perch	360	189	513	11	12	1085
Notropis hudsonius	Spottail Shiner	6	3	9	0	1	19
Total		**433**	**271**	**649**	**17**	**77**	**1447**

Table 11. Adult and juvenile fish collected by seining. Hunting Creek study – 2020.

Scientific Name	Common Name	5	6
Alosa pseudoharengus	Alewife	5	68
Alosa sp.	unk. Alosa species	6	4
Carpiodes cyprinus	Quillback	4	9
Dorosoma cepedianum	Gizzard Shad	3	47
Dorosoma petenense	Threadfin Shad	0	24
Etheostoma olmstedi	Tessellated Darter	1	2
Fundulus diaphanus	Banded Killifish	85	62
Fundulus heteroclitus	Mummichog	4	0
Gambusia holbrooki	Mosquitofish	6	0
Lepomis gibbosus	Pumpkinseed	0	1
Lepomis macrochirus	Bluegill	1	0
Lepomis sp.	unk. sunfish	1	0
Menidia beryllina	Inland Silverside	3	1
Micropterus dolomieu	Smallmouth Bass	2	4
Morone americana	White Perch	19	1066
Notropis hudsonius	Spottail Shiner	0	19
Total		140	1307

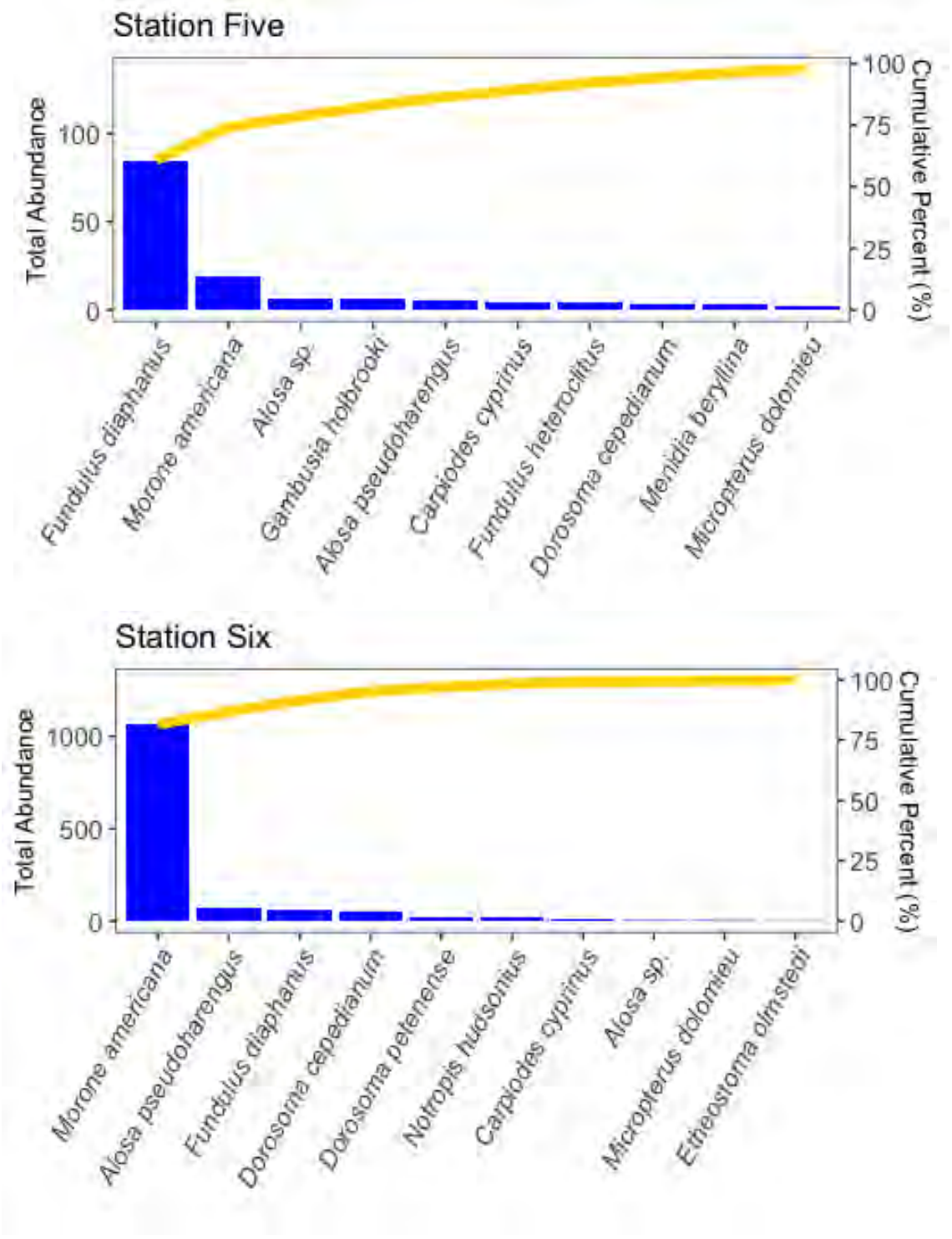

Figure 105A and B. Pareto chart of adult and juvenile fishes collected by seining in 2020. Dominant species by station in total abundance and cumulative percentage of total for Station 5 (top) and Station 6 (bottom).

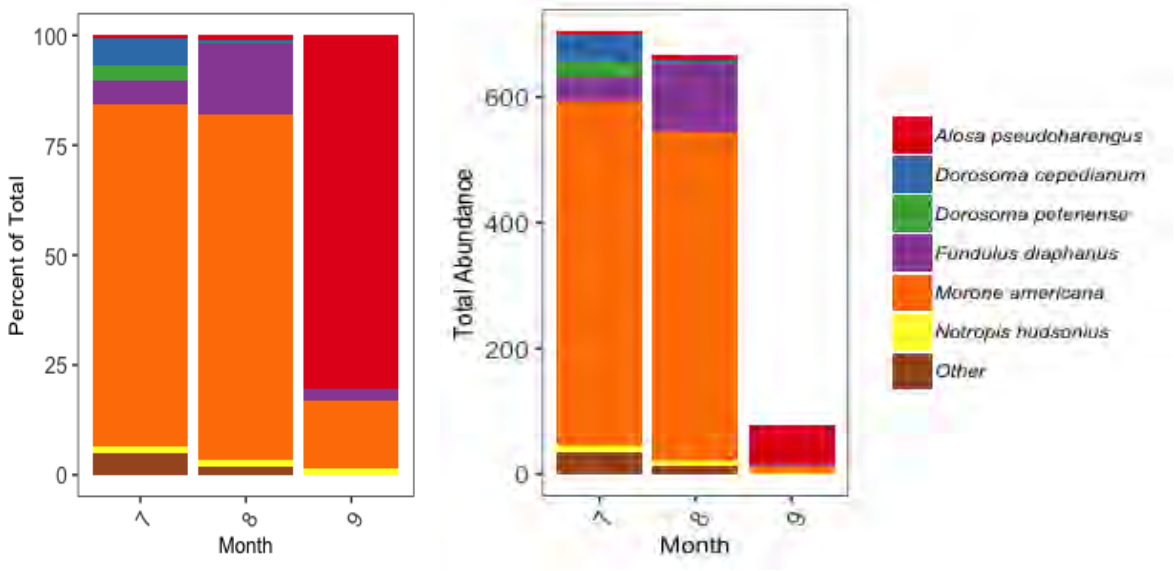

Figure 106A and B. Adult and juvenile fish collected by seining in 2020. Dominant species by month in percentage of total (A) and total abundance (B).

H. Submersed Aquatic Vegetation – 2020

SAV data overflights by VIMS were conducted in 2019 and the aerial imagery is available (Figure 107). This imagery shows very little SAV coverage in 2019 compared with recent typical pre-2018 years. While the VIMS reports are not available yet for 2020, the cruises that we conducted and the transects that were done on August 21 (Table 12) indicate that the 2020 imagery will look very similar.

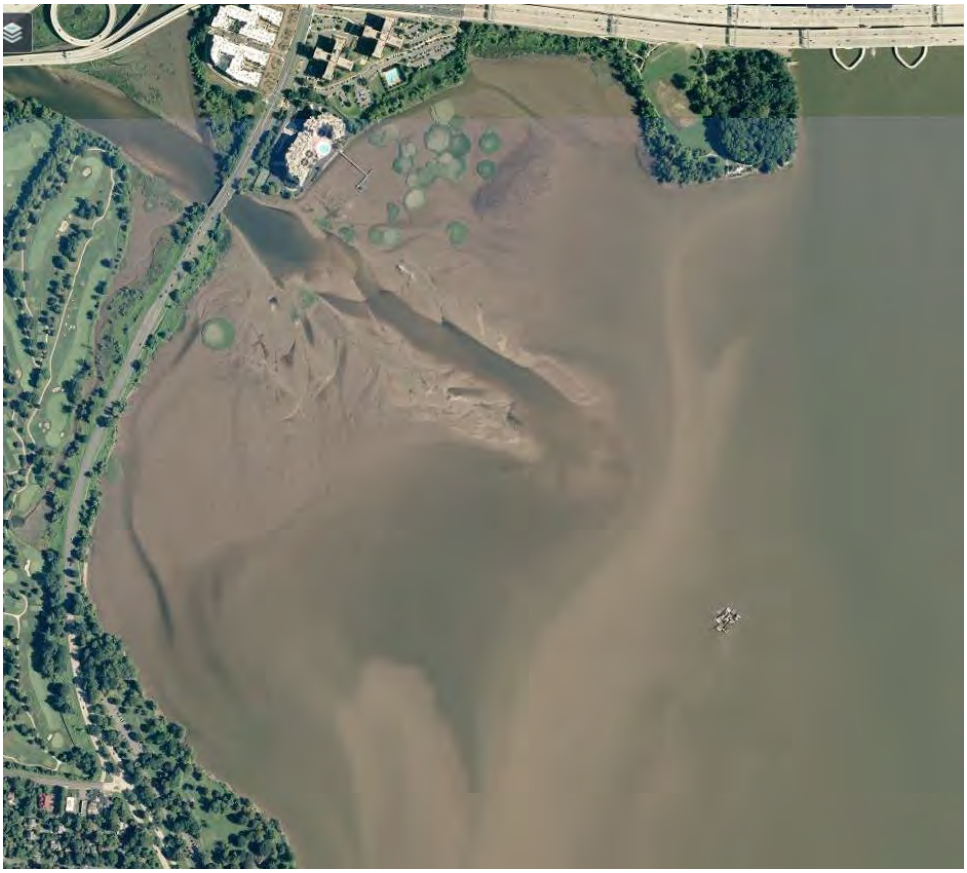

Figure 107. Aerial imagery of Hunting Creek taken in late summer 2019. http://web.vims.edu/bio/sav/savwabmap/ downloaded March 3, 2020.

All SAV taxa were greatly reduced in 2018 and virtually absent in 2019 (Table 12). Coontail, a native species, which was dominant in 2017 was greatly reduced in 2018 and absent in 2019. This decline most certainly started with the very turbid water in 2018 which obstructed light penetration. In 2019, conditions were somewhat better, but at key times in the year light penetration dropped following runoff events and this inhibited SAV recovery. Transects measured in 2020 failed to find any SAV.

Table 12. Average Density of Submersed Aquatic Vegetation Species in Transects. Average included all sites with water depth less than or equal to 2 m. 2017-2020. Density scale: 0 (absent) – 4 (very abundant).

		Average Density per sample by SAV Species - 2020
Taxon Scientific Name	Taxon Common Name	August 21
Ceratophyllum demersum	Coontail	0
Heteranthera dubia	Water Stargrass	0
Hydrilla verticillata	Hydrilla	0
Najas guadalupensis	Southern Naiad	0
Najas minor	Spiny Naiad	0
Various	Filamentous algae	0

		Average Density per sample by SAV Species - 2019	
Taxon Scientific Name	Taxon Common Name	July 16	August 19
Ceratophyllum demersum	Coontail	0	0
Heteranthera dubia	Water Stargrass	0	0
Hydrilla verticillata	Hydrilla	0.04	0
Najas guadalupensis	Southern Naiad	0	0
Najas minor	Spiny Naiad	0	0
Various	Filamentous algae	0	0

		Average Density per sample by SAV Species - 2018	
Taxon Scientific Name	Taxon Common Name	July 16	August 28
Ceratophyllum demersum	Coontail	0.20	0.10
Heteranthera dubia	Water Stargrass	0.07	0
Hydrilla verticillata	Hydrilla	0.43	0.27
Najas guadalupensis	Southern Naiad	0.02	0.07
Najas minor	Spiny Naiad	0.07	0
Various	Filamentous algae	0.09	0

		Average Density per sample by SAV Species - 2017	
Taxon Scientific Name	Taxon Common Name	July 12	August 10
Ceratophyllum demersum	Coontail	1.76	1.74
Heteranthera dubia	Water Stargrass	0.19	1.19
Hydrilla verticillata	Hydrilla	0.78	0.32
Najas guadalupensis	Southern Naiad	0.20	0
Najas minor	Spiny Naiad	0.45	0.21
Various	Filamentous algae	0.03	0.43

I. Benthic Macroinvertebrates - 2020

River and Embayment Samples

Triplicate petite ponar samples were collected from AR2, AR3, and AR4 monthly from July through September.

Taxonomic Groups: Annelid worms (including Oligochaetes and Leeches) were found in high numbers at each site over all dates (Table 13, Figure 108). Overall, they accounted for 84% of all benthic organisms found. Oligochaetes were by far the dominant taxonomic annelid, being found in all samples in substantial number. Leeches were less common and only found at AR2 and AR3 during July. Insects were the second highest group in abundance across sites and dates, accounting for 5.4% of all individuals accounted for and, more importantly, for the greatest number of distinct taxa (three taxa). Chironomids were by far the most numerous and omnipresent insect taxon. Most other insect taxa were present in only a few samples. Crustaceans (including amphipods and isopods) were the third highest group in abundance across sites and dates, accounting for 5.4% of all individuals. Gammarid amphipods (scuds) dominated this group with the isopod *Cyathura polita* being the second most common crustacean. The remainder of the taxonomic groups accounted for minor components of the overall abundance and were generally most common at AR4. These included Bivalvia (1.0% of total abundance), Turbellaria (i.e., flatworms) (5.4%), and Gastropoda (0.2%). The bivalve group was composed of both the invasive Asian clam, *Corbicula fluminea*, and a native fingernail clam from the Sphaeriidae family. The gastropod (i.e., snails) group was only composed of the invasive Japanese mystery snails (*Cipangopaludina japonica*) from the family Viviparidae.

Table 13. Taxa Identified in Hunting Creek Tidal Benthic Samples.

Taxon	Common Name	Average # / ponar		
		AR2	AR3	AR4
Platyhelminthes*	Flatworms	0	11	15.5
Nematoda	Roundworms	1	0	1
Annelida-Oligochaeta*	Oligochaete worms	261.3	75.1	120.7
Annelida-Hirudinea	Leeches	1	1	1
Bivalva-Corbicula*	Asiatic clams	1.7	1	2.5
Bivalvia- Sphaeriidae	Fingernail clams	0	0	2
Gastropoda-Viviparidae	Mystery snails	0	1	0
Crustacea-Isopoda-Cyathura*	Isopods	1	1	4
Crustacea-Amphipoda-Gammarus*	Amphipods	0	23	8.2
Diptera-Chironomidae*	Midges	17.8	5.5	9.3
Trichoptera-Leptoceridae	Long-horned caddisflies	1	0	0
Coleoptera-Elmidae	Riffle beetles	0	1	0
	TOTAL	284.8	119.6	164.2

Taxa identified with an asterisk were found on three or more station-dates and were included in the multivariate analysis.

Spatial trends: The average abundance of organisms per ponar sample was highest at AR2, but

this was entirely attributable to the large number of oligochaetes at that station. All three sites were dominated by Annelida, driven by high abundances of Oligochaeta (Figure 108A). Sites AR3 and AR4 had a higher diversity of taxa (8 and 9 taxa) than the Potomac River site (7 taxa). Due to the high abundance of Annelida across all sites, additional analyses were conducted with non-Annelida taxa. Native fingernail clams were present only at AR4, while gastropods were found only at AR3. Bivalves were the most abundant at AR4. When examining all non-Annelida taxa, Insects were the dominant group in percent contribution at AR2 (84%), while Crustaceans dominated at AR3 (42%), and Turbellarians dominated at AR4 (48%) (Figure 108C). Other taxa varied in their percent contribution by site. For example, Bivalvia were more dominant at AR2, while Gastropoda contributed little to the average abundances found at AR3 only.

Temporal trends: Members of Annelida, composed of oligochaetes and leeches, were the dominant taxa recorded during all months (Figure 108B). There was a seasonal increase in crustaceans driven by Gammarid amphipods, which peaked during July and September most likely due to recruitment and were not found during August. Bivalve average abundances, dominated by the invasive Asian clam *Corbicula fluminea*, increased over the sampling period and were highest during September. Average abundances of Turbellaria were also highest during September. The lowest average abundances of insect larvae across all sites occurred during August, with highest abundances in July, mostly driven by the numbers of midge larvae (Chironomidae) found in the samples. Only one gastropod was found during the sampling period - an invasive mystery snail from the Viviparidae – in AR3 during July. Comparing percent contributions of all non-Annelida taxa across all of the sites, months were dominated by either the Insecta (July – 44%, August – 86%) or the Turbellarians (September – 54%) (Figure 108D). Overall, larger increases in abundances and relative percent contributions over the sampling period for many of the taxa described above are in direct relation to seasonal changes and recruitment.

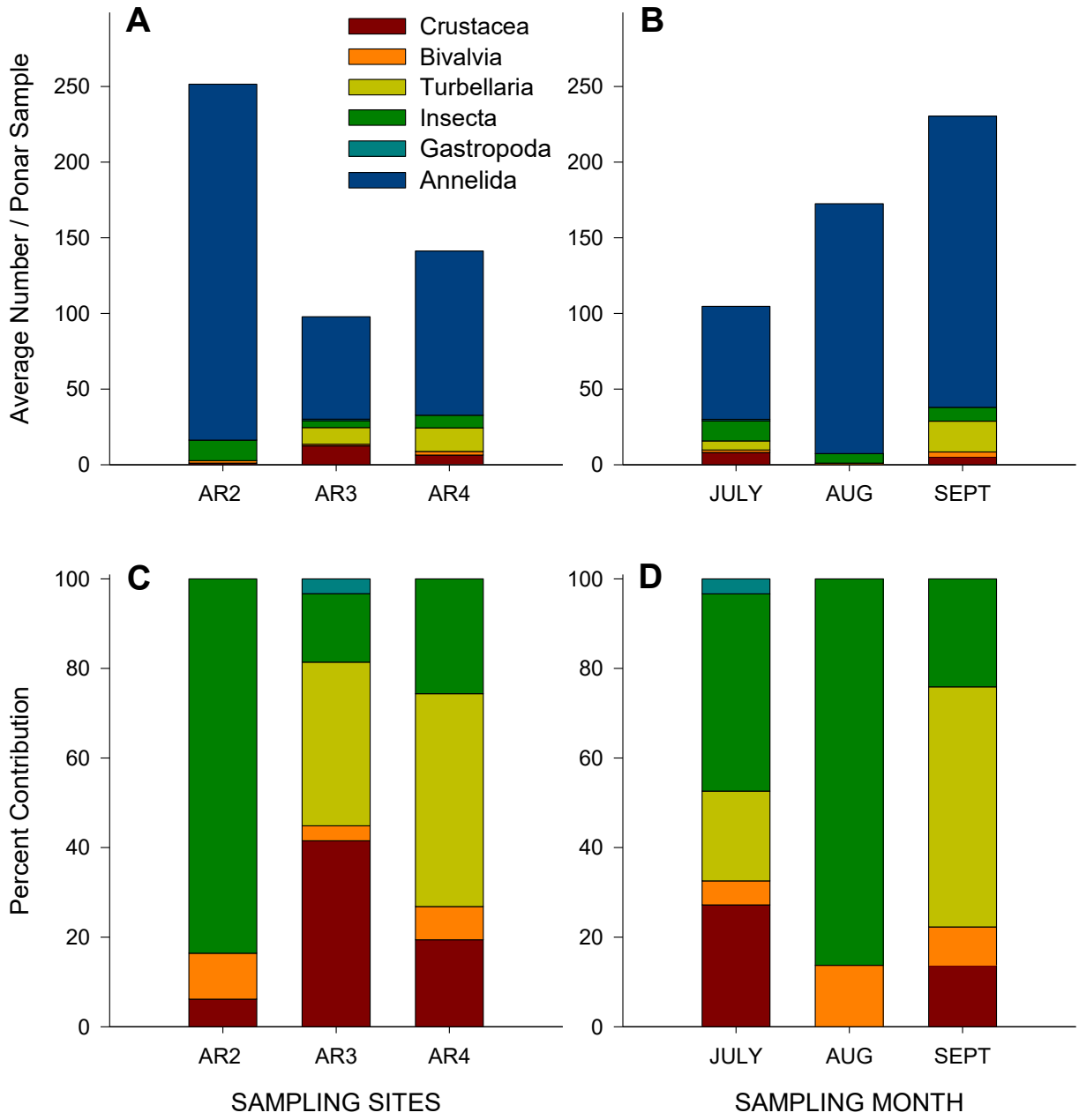

Figure 108. Average number per ponar sample of all benthic macroinvertebrate taxa (A, B) and percent contribution of all non-Annelida benthic macroinvertebrate (C, D) in petite ponar samples separated by site and month.

Multivariate analyses: Due to the multispecies aspect of benthic communities, it is often useful to use multivariate analyses or ordination to examine relationships among samples. This allows multiple taxa to be considered simultaneously when assessing these relationships. In order to get the most meaningful relationships, the full macroinvertebrate sample/taxa matrix was condensed. Taxa that were present in less than three of the original replicate sample matrix were excluded. Then, the remaining, more consistently found taxa were used in the analysis (indicated by asterisks in Table 13, were averaged over the replicates for each date and station combination).

This resulted in one set of taxa values for each station on each date. This reduced matrix (9 samples x 6 taxa) was then subjected to an ordination using a technique called Non-metric Multidimensional Scaling (nMDS). This allows relationships among samples based on their full complement of taxa to be visualized. If successful, relationships among samples can be shown on a two dimensional plot. The taxa differences responsible for the observed relationships can also be examined. The program PRIMER v.6 was used to conduct the ordinations.
The results of an nMDS ordination using the fourth-root transformed data (to decrease the importance of very abundant organisms, like Oligochaetes) is shown in Figure 109. In general, all of the AR2 samples separate from the AR3 and AR4 samples, as noted by the two circles of data points. The AR3 samples in August and September are almost on top of one another in the bottom left-hand corner, indicating that these communities were almost identical in the types and number of organisms present. The AR3 sample from July was very different from the rest of the AR3 samples from other months; this sample had all 6 taxa present while only Chironomidae and Oligochaetes were found at AR3 during the other two months. Overall AR4 had higher taxa richness across all months (average=5, range=3-5) as compared to both AR2 and AR3 (both averages=3). The higher richness at AR4 is probably due to better habitat conditions especially large and more heterogeneous sediment particle size. Also apparent is a slight seasonal change from July to August/September. In July (green diamonds), samples across all sites cluster together in the top right quadrant of the plot, indicating similar communities. By August (blue diamonds), the communities have shifted and group on the left bottom of plot. By September (light blue square), the sites clearly host different communities due to differences in taxa richness (AR2 taxa richness=3; AR3=2; AR4=5).

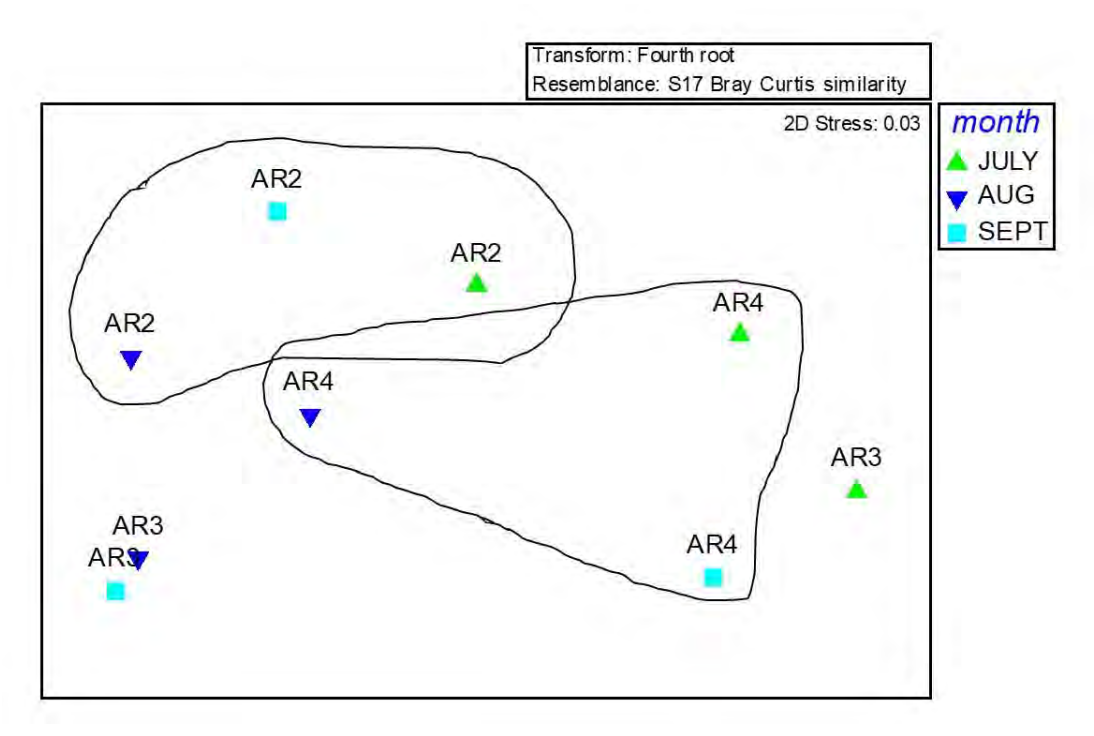

Figure 109. nMDS ordination of benthic samples from tidal stations. The station names are placed above each symbol. Colors represent month. Triplicates were averaged to get a single value for each month-station combination, and then fourth-root transformed. The distance measure was Hellinger.

Summary: Similar to previous years, the macroinvertebrate community was dominated by Annelids (including Oligochaetes, Polychaetes, and Leeches) across sites, with Oligochaetes contributing most to this group. Outside of the Annelids, Crustaceans (dominated by gammarid amphipods) were the most abundant group at AR3, while AR2 was dominated by Insect larvae from the Chironomidae family (midges) and AR4 dominated by flatworms (Turbellarians). Each site had their own unique taxa. Native fingernail clams (family Sphaeriidae) were only found at AR4, while invasive Japanese mystery snails (*Cipangopaludina japonica*) and insect larvae from the family Elimidae were only found at AR3. Insect larvae from the family Leptoceridae were only found at AR2. Comparing percent contributions of all non-Annelida taxa across all of the sites, months were dominated by either the Turbellarians (September) or Insecta (July and August) (Figure 108). Ordination analyses of the community indicated a clear separation between communities sampled at the AR2 site and those sampled from AR3 and AR4 across all months. There was also a change of the community composition throughout the months, as it common for aquatic communities experiencing changes in abiotic conditions and recruitment during the summer months.

Tributary Samples

Duplicate kick net samples were taken in eight tributaries of Hunting Creek on October 31, 2020. The exact locations of the sampling sites are given in Table 14 and Figure 1c. Individuals from each sample were identified to lowest taxonomic unit, usually genus, except for Oligochaetes (aquatic worms) and Chironomidae (midges).

Table 14. Location of Tributary Benthos Sampling Stations

Station ID	Stream	Location on Stream
CR	Cameron Run	Just below Metrorail bridge
BR	Backlick Run	At trail bridge just upstream of the confluence with Holmes Run
TR	Turkeycock Run	In Bren Mar Park just above Edsall Road
IR	Indian Run	Just below Bren Mar Drive crossing
HR1	Holmes Run	First riffle upstream of confluence with Backlick Run
HR2	Holmes Run	Holmes Run Park just below pedestrian bridge at Pickett Street
TA	Taylor Run	In Angel Park, underneath the trail bridge
TB	Timber Branch	Just east of Ivy Hill Cemetry at W Timber Branch Parkway

Water quality variables were measured on the date of benthic sampling (Table 15) and were generally supportive of aquatic life. It is important to note that all streams were at base flow conditions during the sampling period; water quality is expected to be more degraded during high flow.

Table 15. Water Quality Results from Tributary Benthos Sampling

Station	Temp (°C)	SpCond (uS/cm)	DO (mg/L)	DO (%)	pH	Turbidity YSI units
Cameron Run	13.5	235.5	10.72	100	7.52	1.94
Backlick Run	12.4	263.0	10.91	100	7.68	3.32
Turkeycock Run	12.2	236.5	10.47	97.7	7.67	0.11
Indian Run	11.9	239.9	11.08	100	7.67	3.07

Holmes Run 1	13.3	190.3	10.87	100	8.07	0.96
Holmes Run 2	13.3	180.5	10.77	100	7.88	0.96
Taylor Run	12.2	309	10.57	98.8	7.71	2.90
Timber Branch	12.3	392	10.31	94.9	7.72	1.08

Taxonomic Groups: Across all sites, 23 different taxa were found. The four most abundant taxa observed included two groups of Tricoptera insect larvae (caddisflies of the families Hydropsychidae and Philopotamidae), a group of Dipteran insect larvae (midges of the Chironomidae family) and Oligochaeta (Table 16, Figure 110). Of these, the Oligochaeta, Chironomidae, and Hydropsychidae were found at all of the sites. The Philopotamidae were found at all sites except Taylor Run. All other taxa were significantly less abundant and included Nematodes, Platyhelminthes (flatworms), Ephemeroptera (mayflies of the family Baetidae), Crustaceans (Gammarid amphipods and Asellidae isopods), Diptera (families Tipulidae, Simuliidae, Empididae, and Pstchodidae), Coleoptera (family Elmidae), Odonata (family Coenagrionidae), Gastropods (families Ancylidae, Physidae, Pleuroceridae, and Planorbidae), Hydrachnidia (water mites), Collembola (springtails), Trichoptera (family Hydroptilidae), and the invasive Asian clam *Corbicula fluminea*. (Figure 110). Of the less abundant taxa, none of these were present at all sites.

Spatial trends: Holmes Run 2 had the highest abundances of the four dominant taxa (N = 352). Interestingly, dominant taxa differed by site. Hydropsychidae larvae (caddisflies) were the dominant group across the majority of the sites (i.e., Holmes Run 1 and 2, Indian Run, Timber Branch and Turkeycock Run), while Philopotamidae were dominant only at Cameron Run. Backlick Run and Taylor Run were dominated by Chironomidae. There were only four taxa at were only found at a single location. For example, the Hydrachnidia water mites were only found at Timber Branch, the Asellidae isopod only at Turkeycock Run, *Pleurocera virginica* (snail) only at Taylor Run, and the Coenagrionidae damselflies were only found at Holmes Run 2.

Table 16. Taxa Identified in Hunting Creek Stream Benthic Samples.

Taxon	Common Name	Average # / kicknet							
		Backlick Run	Cameron Run	Homes Run 1	Holmes Run 2	Indian Run	Taylor Run	Timber Branch	Turkeycock Run
Platyhelminthes	Flatworms	1	5.5	4.5	2	2.5	0.5	0	2
Nematoda	Round worms	1	3.5	0	0.5	0	0.5	1	2
Annelida-Oligochaeta	Oligochaete worms	34.5	8.5	13.5	17.5	16.5	13.5	11	21
Bivalva-Corbicula	Asiatic clams	0	1	0.5	1.5	0	0	0	0
Gastropoda-Ancylidae-Ferrissia rivularis	Limpet	0	0	2	0	0	0.5	0	0.5
Gastropoda-Physidae-Physa acuta	Physid snail	0.5	1	0	0	0	1	0	4
Gastropoda-Planorbidae-Gyraulus parvus	Planorbid snail	0.5	0	0	0.5	0	1.5	0	0
Gastropoda-Pleuroceridae-Pleurocera virginica	Pleurocerid snail	0	0	0	0	0	0.5	0	0
Hydrachnidia	Water mites	0	0	0	0	0	0	0.5	0
Crustacea-Amphipoda-Gammarus	Amphipods	0	1.5	3.5	8.5	0	0	0	6.5
Crusteacea-Isopoda-Asellidae	Isopods	0	0	0	0	0	0	0	0.5
Collembola	Springtails	7.5	0	1	0.5	0	0	0	0
Ephemeroptera-Baetidae	Small minnow mayflies	0	0	1.5	2.5	0	0	1.5	0
Diptera-Tipulidae	Crane fly	2.5	0	0.5	0.5	3.5	3	2	4.5
Diptera-Chironomidae	Midges	49.5	14.5	30	26	10.5	45	13.5	20
Diptera-Empididae	Dagger fly	1	4	0.5	9.5	0	0	0	8
Diptera-Psychodidae	Drain fly	1.5	0	0	0	0	0.5	0	0
Diptera-Simuliidae	Black fly	0	0	0.5	0.5	1	0.5	0	0.5
Coleoptera-Elmidae	Riffle beetle	0.5	0.5	0	0	0	0	0	3
Odonata-Coenagrionidae	Damselfly	0	0	0	0.5	0	0	0	0
Trichoptera-Hydroptilidae	Microcaddisfly	0	2	5.5	5.5	0.5	1	0	1.5
Trichoptera-Hydropsychidae	Hydropsychid caddisfly	4	37	45.5	98	47	5	16	60
Trichoptera-Philopotamidae	Finger-net caddisfly	6.5	44.5	18	34.5	36	0	1.5	9.5
	TOTAL	110.5	123.5	127	208.5	117.5	73	47	143.5

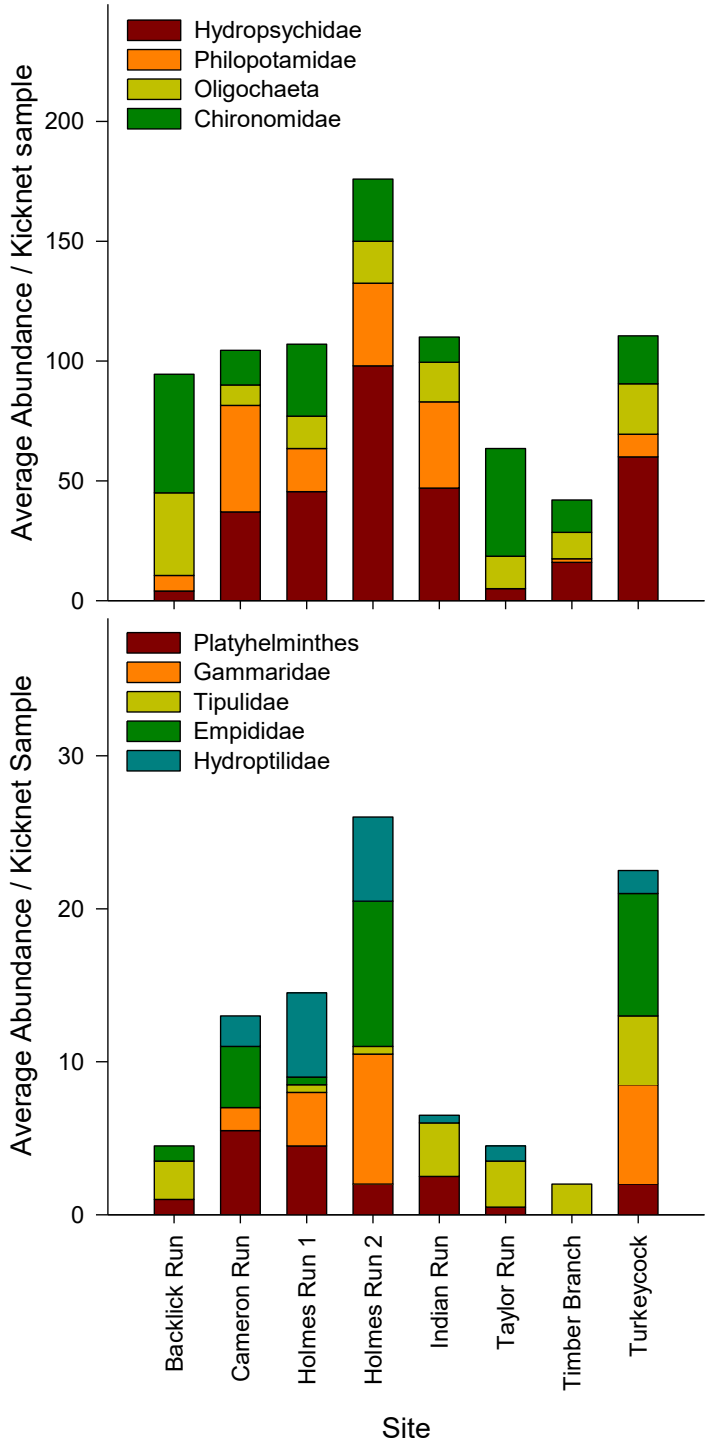

Figure 110 TOP: Average abundance per kicknet sample of the four dominant benthic invertebrate taxa in tributary kick samples. BOTTOM: Average abundance per kicknet sample of five less dominant benthic invertebrate taxa in tributary kick samples. Note the different scales of the y-axes between the two graphs.

Benthic Invertebrate Community Metrics: In general, increasing taxa richness reflects increasing water quality, habitat diversity, or habitat suitability (Table 17). Taxa richness across all eight sites ranged from 8 to 16 taxa, with lowest richness at Indian Run and Timber Branch and highest richness at Holmes Run 2. "Good" sites were classified as having more than 14 taxa, while "moderate" sites had between 7 and 13; "poor" sites had less than 6 taxa present.

A subset of abundance, EPT richness is the number of species from the generally more environmentally sensitive Insecta groups Ephemeroptera, Plecoptera, and Trichoptera. In general, if the EPT richness is ≤ 2, then conditions are poor. If between 3 and 5, then conditions are moderate. If ≥ 5, then conditions are good. EPT richness in five sampled locations ≤ 2, indicating poor conditions at the majority of sites. All sites had at least three species, except for Backlick Run and Taylor Run.

Calculating the percentage of total organisms that are from the Ephemeroptera, Plecoptera, and Trichoptera groups, without including the family Hydropsychidae, provides another metric for stream condition. In this case, if the value is >9.3%, then conditions are good. If the value is between 4.7 and 9.3%, then conditions are moderate. If the value is < 4.7%, then conditions are poor. Both Taylor Run and Timberbranch had values below the threshold of 4.7%. Cameron Run, both Holmes Run sites, and Indian Run had high percent of EPT taxa (>20%), while Backlick Run, Timber Branch, and Turkeycock all had moderate percentage values (5.9-7.7%). Taylor Run had the lowest value at 1.9%.

Examining the Trichopteran family (without Hydropsychidae) closer can provide more detail about the site conditions, as this insect family has a range of tolerance values for abiotic conditions. Here, good conditions are >50, moderate are 25 – 50, and poor are <25. Only Cameron Run and Indian Run had percent Trichopteran values higher than 25%; the rest of the site were considered poor.

Looking at the Coleopteran (beetle) family can also tell us about the stream conditions. In this case, good conditions are values above 1.5, moderate values are 0.75-1.5, and poor conditions are values less than 0.75. Beetles were not found at the majority of sites; only Turkeycock Run had a good percentage of beetles (Elmidae larvae).

The Family Biotic Index (FBI) estimates the overall tolerance of the community in a sampled area toward organic (nutrient) enrichment, weighted by the relative abundance of each taxonomic group (family, genus, etc.). Organisms are assigned a tolerance number from 0 to 10 pertaining to that group's known sensitivity to organic pollutants; 0 is most sensitive, 10 is most tolerant. Low FBI values reflect a higher abundance of sensitive groups, thus a lower level of pollution. Family-level tolerance values from USEPA (Barbour et al. 1999) were used for organisms that could not be identified to the genus level because of size or condition. Taxa with tolerance values ≤3 were considered *intolerant,* whereas those with values ≥7 were considered *tolerant.* Low FBI (≤4.7) values reflect a higher abundance of sensitive groups, indicative of a lower level of pollution. Two locations (Cameron Run and Indian Run) had "good" FBIs. Two other locations (Holmes Run 2 and Turkeycock) fell into the "moderate" category (values 4.7 – 5.4), indicating some organic pollution is probable. Half of the locations were categorized as "poor" (values >5.4), indicating that very substantial pollution was likely (Table 21).

In most cases, as the diversity of a community declines, a select few taxa will dominate the assemblage. Tolerant taxa can replace specialized species, and these communities are indicative of poor stream quality. Percent dominance is calculated as the total number of individuals in the top three most abundant taxa divided by the total number of individuals. A percent dominance above 79% is considered "poor" quality, a value between 57 and 79 is "moderate", and anything below 57% is "good." This year, the top 3 taxa were the Trichopteran families- Hydropsychidae, Oligochaeta and Dipteran Chironomidae larvae. The majority of sites were dominated by these top three taxa, including Backlick Run, Taylor Run, and Timberbranch. Holmes Run 1 and 2, Indian Run, and Turkeycock Run were calculated as moderate, while only Cameron Run was categorized as good.

The percent of organisms that are clingers, which are those that have fixed retreats or adaptations for attachment to surfaces in flowing water, is another indicator of environmental quality. While this metric would normally also include the percent of organisms are from the Plecoptera group (which are one of the first groups to disappear as human disturbance increases), none of the organisms sampled this year were from that group. Increasing metric values indicate increasing substrate stability. In this case, if the value is >14%, then conditions are good. If the value is between 7 and 14%, then conditions are moderate. If the value is <7%, then conditions are poor. All of the locations, except Backlick Run and Taylor Run, had values >14%, indicating good substrate stability.

Shredder taxa are those that tear apart organic material, usually leaves, and dominate low-velocity, high-retention pools. Sites were categorized as "poor" if the percent of shredders was <2, as "moderate" if the percent was between 2 and 4, and as "good" is the percent was higher than 4. As Chironomidae are considered shredder taxa, and that was a dominant group this year, all locations had high percentages of shredders indicating good conditions.

Predator taxa are at the top of the food web and depend on a reliable source of other invertebrate prey items. The percentage of taxa that are obligate predators can provide a measure of how trophically complex a site is. Less distributed sites support a greater abundance and diversity of prey items, thus supporting a greater number and diversity of predators. Sites were categorized as "poor" if the percent of predators was <3.2, as "moderate" if the percent was between 3.2 and 6.5, and as "good" is the percent was higher than 6.5. Only two sites were categorized as "poor" (Holmes Run 1 and Indian Run), Turkeycock Run had the highest percentage of predators indicating good conditions. The rest of the locations had a moderate percentage of predators.

Using these 10 measures of biological health, we can calculate a summary statistic of relative overall health of these streams. In this case, we assign values of high (6), moderate (3), or low (0) health for each metric at each site, sum these values for each site and divide by 60 (i.e., the maximum score achievable). Streams characterized as "excellent" would achieve summary statistics of 80-100% of the maximum summary statistic. "Good" streams would be between 60 and 79%, "fair" streams would come in at between 40 and 59% of the summary statistic, while "poor" streams would be between 20 to 39%. Using the criteria for each metric laid out above, four streams were categorized as "good" (i.e., Cameron Run, Holmes Run 2, Indian Run, Turkeycock Run), two were categorized as "fair" (i.e., Holmes Run 1 and Timberbranch), and

two were categorized as "poor" (i.e., Backlick Run and Taylor Run) (Table 18). Those that are "good" are slightly degraded sites with decreasing numbers of intolerant species. "Fair" sites have a marked decrease in intolerant species, and the community has shifted to be dominated by a few species. Lastly, "poor" sites lack intolerant species and are lower in taxa diversity.

Table 17. Benthic invertebrate community metrics on the sum total of organisms found from both replicate kicknets. EPT include the Insecta from Ephemeroptera, Plecoptera, and Trichoptera. Color shading indicates relatively good (green), moderate (yellow), or poor (red) conditions for each of the metrics and the summary statistic.

	Abundance	Taxa Richness	EPT Richness	% EPT w/o Hydropsychidae	% Trichoptera w/o Hydropsychidae	% Coleoptera	Family Biotic Index	% Dominance	% Clingers + % Plecoptera	% Shredders	% Predators
Backlick Run	221	13	2	5.9	5.9	0.5	7.5	79.6	12.2	47.1	3.2
Cameron Run	247	12	3	37.7	37.7	0.4	4.6	48.6	68.0	13.4	3.2
Holmes Run 1	254	14	4	19.7	18.5	0	5.5	70.1	56.3	28.3	0.8
Holmes Run 2	417	16	4	20.4	19.2	0	4.8	67.9	67.9	15.3	5.0
Indian Run	235	8	3	31.1	31.1	0	4.4	63.0	74.9	12.3	3.0
Taylor Run	146	13	2	1.4	1.4	0	8.0	87.0	13.0	67.1	4.1
Timber Branch	94	8	3	6.4	3.2	0	5.9	86.2	44.7	33.0	5.3
Turkeycock Run	287	15	3	7.7	7.7	2.1	5.2	70.4	55.1	18.1	8.7

Table 18. Index scores of the benthic invertebrate community metrics on the sum total of organisms found from both replicate kicknets. Color shading indicates relatively good (green), moderate (yellow), or poor (red) conditions for each of the metrics and the summary statistic.

	Taxa Richness	EPT Richness	% EPT w/o Hydropsychidae	% Trichoptera w/o Hydropsychidae	% Coleoptera	Family Biotic Index	% Dominance	% Clingers + % Plecoptera	% Shredders	% Predators	**Index Score**
Backlick Run	3	0	3	0	0	0	0	3	6	3	**30%**
Cameron Run	3	3	6	3	0	6	6	6	6	3	**70%**
Holmes Run 1	3	3	6	0	0	0	3	6	6	0	**45%**
Holmes Run 2	6	3	6	0	0	3	3	6	6	3	**60%**
Indian Run	3	3	6	3	0	6	3	6	6	0	**60%**
Taylor Run	3	0	0	0	0	0	0	3	6	3	**25%**
Timber Branch	3	3	3	0	0	0	0	6	6	3	**40%**
Turkeycock Run	6	3	3	0	6	3	3	6	6	6	**70%**

Summary: Twenty-three taxa were identified across all sites in 2020. In general, the top four most abundant taxa observed across all sites stayed the same as in previous years with the exception of an increase in the Insecta family Chironomidae across all sites. In 2020, Holmes Run 2 had the highest abundance of all macroinvertebrates and the four dominant taxa, mostly composed of the Insecta family Hydropsychidae. Similar to previous years, Hydropsychidae larvae (caddisflies) were the dominant group at the majority of the sites. Taxa richness across all sites ranged from 8 to 16 taxa, with lowest richness at Indian Run and Timber Branch and highest richness at Holmes Run 2. Using 10 measures of biological health, we calculated a summary statistic of relative overall health of these streams. Using the criteria for each metric laid out above, four streams were categorized as "good", two were categorized as "fair", and two were categorized as "poor".

DISCUSSION

A. 2020 Synopsis

In 2020 the onset of sampling was delayed until July because of COVID restrictions. Air temperature was above normal for the entire study period of July through September and was particularly warm in July. There were 38 days with maximum temperature above 32.2ºC (90ºF) in 2020 which is well above the median number over the past decade. Precipitation was well above normal in 2020 especially in August when Hurricane Isaias passed through the area.

To better understand relationships between flow events and Hunting Creek ecology, time course graphs were constructed overlaying the sequence of precipitation, stream/river flow, and water quality/plankton sampling dates (Fig. 111). Significant rainfall preceded and coincided with the July 7 sampling date. The July 21 and September 2 sampling dates may also have experienced some lesser rainfall and runoff effects.

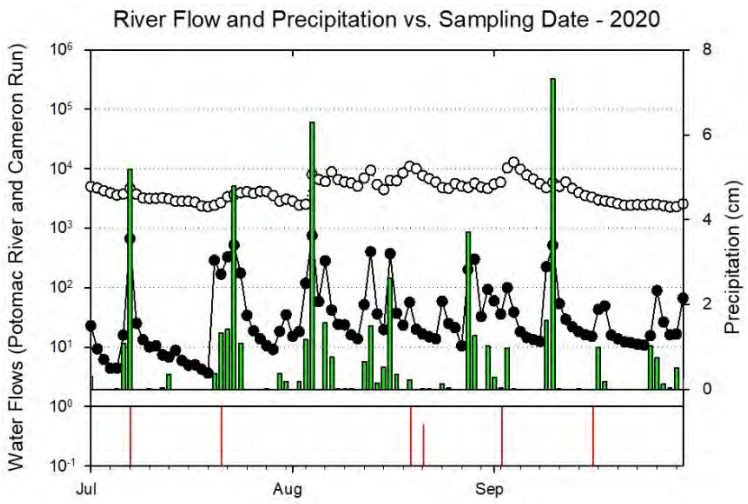

Figures 111. Precipitation (green bars), Cameron Run flows (solid circles), Potomac River flows (open circles) and water quality/plankton sampling events (red lines at bottom).

Water temperature followed a typical seasonal pattern at all stations with peak temperatures of about 30°C. Most of the embayment and river stations exhibited a peak in specific conductance and chloride in late July whereas stations nearer the shore increased steadily from July through September. Dissolved oxygen peaked in late July at values at or slightly above saturation at the time of a chlorophyll peak in the embayment and river stations. Field and lab pH did not increase in late July remaining fairly constant at about 7.0-8.0. Total alkalinity was generally 80-90 mg/L as $CaCO_3$ at most embayment and river stations, but was lower at near shore stations such as AR1, AR24, and AR25.

Secchi disk transparency was generally 0.5-0.7 m and there was little change through the sampling period.. Light attenuation was in the -2 to -3 m^{-1} range through the study period. The values of both Secchi and light attenuation indicate water clarity continues to be a problem for SAV recolonization in Hunting Creek.

Ammonia nitrogen showed a general increase from July through September at most stations and all values were quite low (<0.2 mg/L). Nitrate nitrogen was very low in late July at the time of the phytoplankton bloom as the algae drew down the levels and then increased through September.. Nitrite was very low at all stations and did not show consistent seasonal patterns. Organic nitrogen was mostly in the range 0.2-1.0 mg/L and showed little seasonal pattern. Total phosphorus was generally between 0.5 and 1.0 mg/L but was somewhat higher on occasion at nearshore Hunting Creek stations. N/P ratio remained above 7.2, consistently pointing to P limitation of primary producers. BOD was generally below 4 mg/L. Total suspended solids was typically in the 10-30 mg/L range with some higher spikes at the near shore Hunting Creek stations. VSS values hovered around 5 mg/L in the river mainstem with higher values at the nearshore Hunting Creek embayment stations in late July and early August.

In the tributaries, water temperature also generally followed air temperature although somewhat cooler than the tidal stations. Specific conductance at the tributary stations showed a general rise from 100-200 uS/cm in early July to 300-500 uS/cm in late September. Dissolved oxygen was generally 80-100 percent saturation except at AR34 in Hooffs Run which showed one value of

less than 4 mg/L in late July. pH values were consistently 7.0 to 7.8 range. YSI turbidity was generally low (<30 NTU) except in early July during a period of substantial precipitaton and runoff. Total alkalinity was fairly uniform in all of the tributaries exhibited a gradual increase over the perod. Total phosphorus and ortho-phosphorus were variable with no clear pattern. Organic nitrogen showed a general decline except at AR23 and AR34 which remained high in September. Ammonia nitrogen was uniformly low (<0.15 mg/L) at all stream stations except AR34. Nitrate nitrogen was consistently elevated at AR33, followed by AR13. Other stations were consistently below 1 mg/L. Nitrite nitrogen was consistently below 0.04 mg/L except for an unexplained spike at AR12 in early September. TSS and was generally less than 20 mg/L except at AR30 and AR23 which were sometimes higher.

Phytoplankton biomass as indicated by chlorophyll *a* exhibited a distinct maximum (of over 40 ug/L) at the Hunting Creek embayment stations in late July. This maximum is one of the highest values observed during the eight years of study and was also reflected in high values of total phytoplankton density and biovolume. This was followed by a steady decline for the remainder of the year. Cell density at the late July maximum was dominated by cyanobacteria and green algae with diatoms also making a contribution at both stations. At this time *Oscillatoria* was the most abundant cyanobacterium with *Anabaena* also making a contribution at both stations. *Dictyosphaerium* was the most numerous green alga. When biovolume was considered diatoms were dominant during this July peak and *Melosira* was the dominant at both stations with Pennate 50x15 being subdominant at AR2.

Rotifers were very abundant in early July reaching over 3000/L at both AR2 and AR4. These values were similar to those found in 2019 and among the highest observed to date in the study. Rotifers declined somewhat in late July and then were much reduced in August and September at both stations. *Brachionus* was the strong dominant on every sampling date.

Since spring sampling was missed in 2020 due to COVID 19 and spring is the time when most zooplankton reach their maxima, observed levels of zooplankton were generally quite low in 2020. *Bosmina*, *Diaphanosoma*, *Daphnia*, *Sida, Leptodora,* Chydoridae and *Ceriodaphnia* all showed highest values in July and then declined. Copepods also exhibited this pattern.

B. Correlation Analysis of Hunting Creek Data: 2013-2020

To better understand the ecological relationships in Hunting Creek and the nearby Potomac River, relationships among parameters were assessed using correlation analysis. Since all samples were collected by PEREC personnel at the same time, it was possible to pool the data on all field and lab water quality parameters at the level of depth-averages and/or surface samples. Three tables were constructed: PEREC field and lab parameters correlated against each other, ARE lab parameters correlated against each other, and all water quality parameters correlated against Cameron Run flow. This final set of correlations was added this year to determine the effect of freshwater flow pulses into Hunting Creek on the water quality variables.

Table 19 shows the correlations among PEREC-collected water quality parameters from the regular sampling. These reflect relationships over all eight years of the study. Indicators of photosynthesis (DOPPM, DOSAT, Field pH) were highly intercorrelated. Also, measures of

particles in the water column and resultant water clarity (turbidity, TSS, Secchi disk depth, and extinction coefficient) were also highly intercorrelated. Indicators of phytoplankton abundance (CHLDI, CHLSF, and VSSSF) were highly intercorrelated.

Table 19. Correlations among PEREC collected water quality parameters from regular sampling. Depth-integrated samples unless otherwise indicated. AR2, AR3, and AR4 pooled. 2013-2020. April-September. Strongest correlations (r>0.400) are have **bolded** text. N=177-239.

Pearson Correlation Matrix

	TEMP	SPC	DOPPM	DOSAT	FLDPH	SD	EXTCO	CHLDI	CHLSF	TSSSF	VSSSF	YSITUR
TEMP	1.000											
SPC	**0.435**	1.000										
DOPPM	**-0.434**	-0.271	1.000									
DOSAT	-0.027	-0.105	**0.906**	1.000								
FLDPH	0.115	-0.010	**0.571**	**0.678**	1.000							
SD	0.027	0.310	-0.034	-0.036	0.069	1.000						
EXTCO	0.084	0.328	-0.065	-0.039	0.158	**0.813**	1.000					
CHLDI	**0.450**	0.285	-0.079	0.098	0.104	-0.206	-0.236	1.000				
CHLSF	**0.452**	0.273	-0.108	0.072	0.079	-0.224	-0.256	**0.982**	1.000			
TSSSF	-0.102	-0.242	0.056	0.008	-0.281	**-0.616**	**-0.746**	0.310	0.322	1.000		
VSSSF	0.103	-0.041	0.024	0.068	-0.144	**-0.421**	**-0.561**	0.578	**0.587**	**0.790**	1.000	
YSITUR	-0.098	-0.282	0.042	0.002	-0.218	**-0.533**	**-0.731**	0.082	0.093	**0.754**	**0.465**	1.000

TEMP – water temperature (°C), SPC – specific conductance (µS), DOPPM – dissolved oxygen (mg/L), DOSAT – dissolved oxygen (% saturation), FLDPH – field pH,SD - secchi disk depth (m), EXTCO (light attenuation coefficient (m^{-1}), CHLDI – depth-integrated chlorophyll a (µg/L), CHLSF – surface chlorophyll a (µg/L), , TSSSF - TSS on surface samples (mg/L), VSSSF – VSS on surface samples (mg/L) YSITUR – Turbidity as measured by YSI sonde *in situ*.

The correlation coefficients among AR lab parameters are shown in Table 20. Among the most highly correlated variables in this dataset were TSS and VSS (0.855). Total P was positively correlated with TSS and VSS. Most phosphorus is bound to particles so these correlations make sense. TP was negatively correlated with N to P ratio and this makes sense since it is in the denominator of this ratio. Organic N was highly correlated with VSS Lab pH was negatively correlated with ammonia nitrogen, but this may just reflect that lab pH is highest in summer when ammonia nitrogen is lowest. Other correlations were not strong.

Table 20. Correlation coefficients between AR lab parameters. AR2, AR3, and AR4 pooled. 2013-2020. April-September. Strongest correlations (r>0.400) are **bolded**. N=227-236.

Pearson Correlation Matrix												
	PHLAB	ALK	TP	OP	ON	NO3	NH4	NO2	CLD	TSS	VSS	NTOP
PHLAB	1.000											
ALK	0.278	1.000										
TP	-0.171	-0.066	1.000									
OP	-0.194	-0.309	-0.038	1.000								
ON	-0.049	0.028	0.349	-0.216	1.000							
NO3	-0.210	0.061	0.310	0.098	-0.190	1.000						
NH4	**-0.428**	-0.258	0.316	0.301	-0.002	0.334	1.000					
NO2	-0.170	0.108	0.098	-0.133	0.205	-0.075	0.114	1.000				
CLD	0.087	0.205	-0.088	-0.173	0.069	-0.248	0.016	0.099	1.000			
TSS	-0.106	0.081	**0.610**	-0.035	0.332	0.279	0.183	0.054	-0.172	1.000		
VSS	-0.097	0.104	**0.606**	-0.044	**0.407**	0.197	0.174	0.091	-0.050	**0.855**	1.000	
NTOP	-0.021	0.165	**-0.597**	0.013	-0.182	0.172	-0.061	-0.103	0.109	-0.276	-0.309	1.000

PHLAB – lab pH, ALK – total alkalinity (mg/L as $CaCO_3$), TP – total phosphorus (mg/L), OP – orthophosphorus (mg/L), NO3N – nitrate nitrogen (mg/L), NH4N – ammonia nitrogen (mg/L), NO2N – nitrite nitrogen (mg/L), CLD – chloride (mg/L), TSS – total suspended solids (mg/L), VSS – volatile suspended solids (mg/L), NTOP – nitrogen to phosphorus ratio by mass.

Since the study began in 2013 it has been noted that certain water quality variables appear to be impacted by major rainfall and runoff events. In this year's report we have tested the correlations between recent runoff coming down Cameron Run and a wide array of water quality variables (Table 21). This analysis reveals that many variables are strongly correlated with recent stream flow. Specific conductance, chloride pH, and alkalinity are all significantly reduced by increased streamflow, probably due to the dilution effects of the runoff on the water already in the river. Turbidity, Secchi depth, light attenuation, and TSS are all increased by runoff because solids are either brought in or resuspended by the higher runoff resulting in poorer light penetration. Ammonia nitrogen is increased at all except AR4; the reason for this is unclear.

Table 21. Pearson Correlation Coefficients between Water Quality Parameters and Log_{10}(5 day flow) where 5-day flow is the average stream flow on Hunting Creek as measured at USGS Gaging Station 01653000 for the day of sampling and the 4 previous days. N=64-80.

Water Quality Parameter	AR 1 GW Pkwy Br	AR 2 N. Hunting Cr	AR 3 S. Hunting Cr.	AR 4 River Mainstem
Temperature (°C)	-0.438**	-0.428**	-0.407**	-0.431**
Sp. Conductance (µS/cm)	-0.520**	-0.635**	-0.773**	-0.743**
Dissolved Oxygen (mg/L)	0.081	0.062	-0.036	0.390*
Dissolved Oxygen (%sat)	-0.152	-0.087	-0.178	0.234
Field pH	-0.090	-0.291	-0.296	0.050
Secchi Disk Depth (m)	-----	-0.301*	-0.338*	-0.224
Light Atten. Coef. (m^{-1})	-----	-0.339*	-0.439**	-0.230
YSI Turbidity (NTU)	0.430**	0.451**	0.392*	0.084
YSI Chlorophyll (µg/L)	0.097	-0.084	-0.096	-0.099
Chlorophyll a, DI (µg/L)	-----	-0.162	-0.197	-0.273
Chlorophyll a, Surf (µg/L)	-----	-0.117	-0.179	-0.330
TSS, Surf, GMU (mg/L)	0.146	0.389*	0.279	0.083
VSS, Surf, GMU (mg/L)	-0.082	0.132	0.091	-0.019
pH Lab	-0.445**	-0.400**	-0.449**	-0.346*
Total Alk. (mg/L as $CaCO_3$)	-0.572**	-0.572**	-0.542**	-0.523**
Total Phosphorus (mg/L)	0.084	0.296	0.254	0.040
Ortho Phosphorus (mg/L)	0.206	0.254	0.267	0.386*
Organic Nitrogen (mg/L)	-0.163	-0.080	0.005	-0.182
Nitrate Nitrogen (mg/L)	0.122	0.333	0.284	0.281
Ammonia Nitrogen (mg/L)	0.384*	0.392*	0.475**	0.150
Nitrite Nitrogen (mg/L)	-0.113	-0.032	-0.009	-0.312
Chloride (mg/L)	-0.142	-0.206	-0.352*	-0.472**
TSS, DI, ARE (mg/L)	0.242	0.398*	0.208	0.021
VSS, DI, ARE (mg/L)	0.131	0.233	0.097	-0.016
BOD (mg/L)	0.079	0.179	0.130	0.149
N to P ratio	-0.152	-0.091	-0.123	0.073

C. Water Quality: Comparison among Years

Since eight years of data are now available for the Hunting Creek area, comparisons were made for each parameter among years. In order to assess overall patterns in the data among years and stations, box plots were constructed. In a box plot, the spread of the middle 50% of the data is shown by a box with a line in the middle which is the median. Whiskers extend out to the limits of the data.

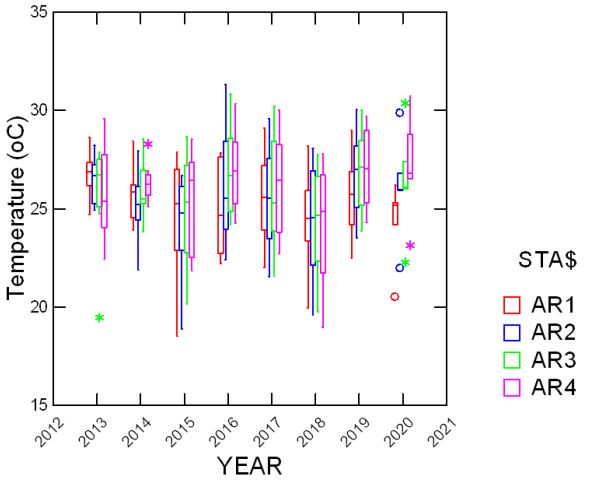

Figure 112. Box plots comparing values of Temperature between years. June through September.

Temperature did not show much difference between the years with the medians in the 24-27ºC range at all sites and years (Figure 112). The 2020 medians were at the higher end of that range and varied very little between stations. Specific conductance showed clear differences among stations in most years with AR 1 consistently higher due to input from AR effluent (Figure 113). In 2020 values at all stations were lower than most years and similar to the wet year 2018.

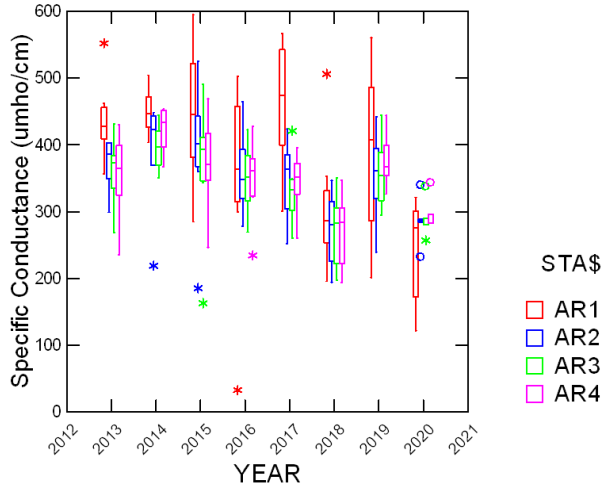

Figure 113. Box plots comparing values of Specific Conductance between years. June through September.

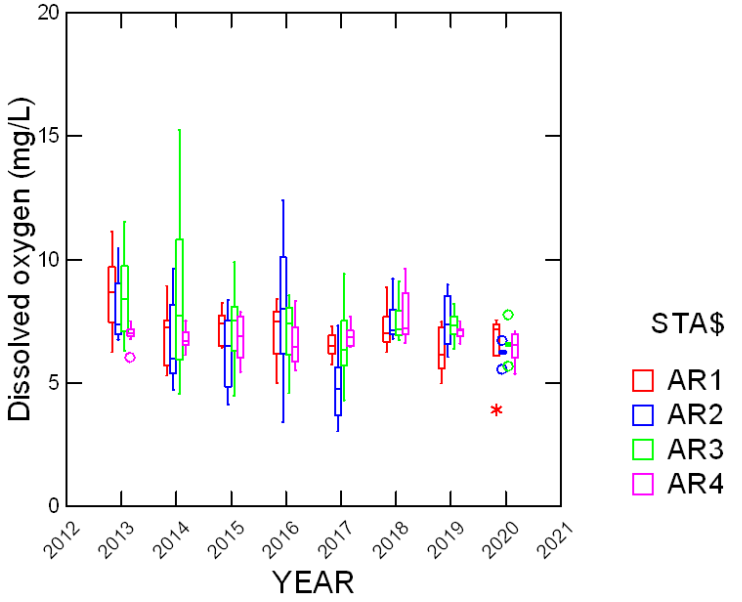

Figure 114. Box plots comparing values of dissolved oxygen as mg/L between years. June through September.

Dissolved oxygen showed little difference among stations in 2020 compared with some more marked differences in previous years (Figure 114). The interquartile range was also quite low at all stations in 2020 as in 2019 A similar pattern was observed in dissolved oxygen (as % saturation) (Figure 115).

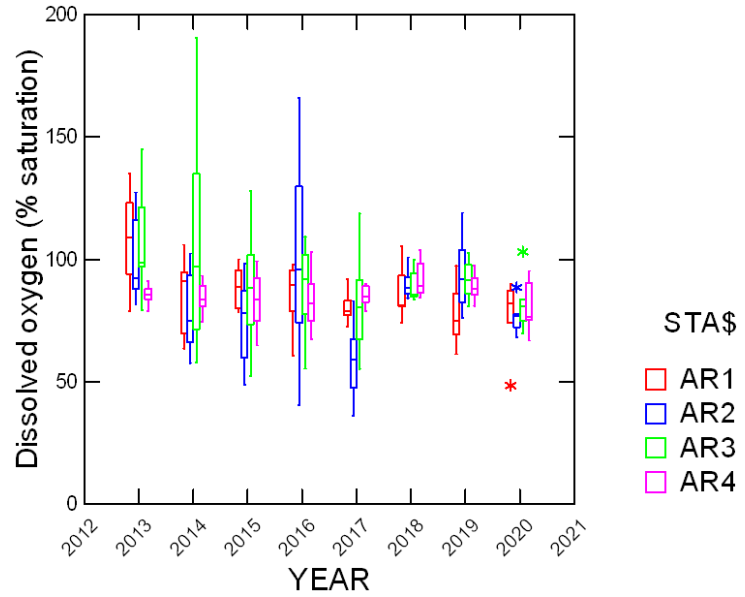

Figure 115. Box plots comparing values of dissolved oxygen as percent saturation between years. June through September.

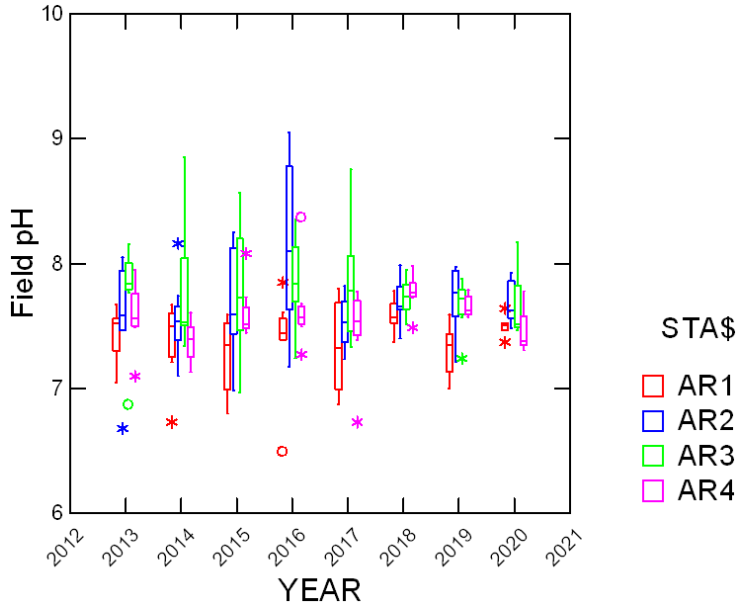

Figure 116. Box plots comparing values of field pH between years. June through September.

Field pH values fell into a relatively narrow range in 2020 as in 2018 and 2019 (Figure 116). In some years median values at AR2 and AR3 were much higher than at the other two stations. This was attributed to photosynthesis by SAV which tends to increase pH since the high values were observed in July and August when SAV was most abundant. In the period 2018 to 2020 SAV was minimal in Hunting Creek.

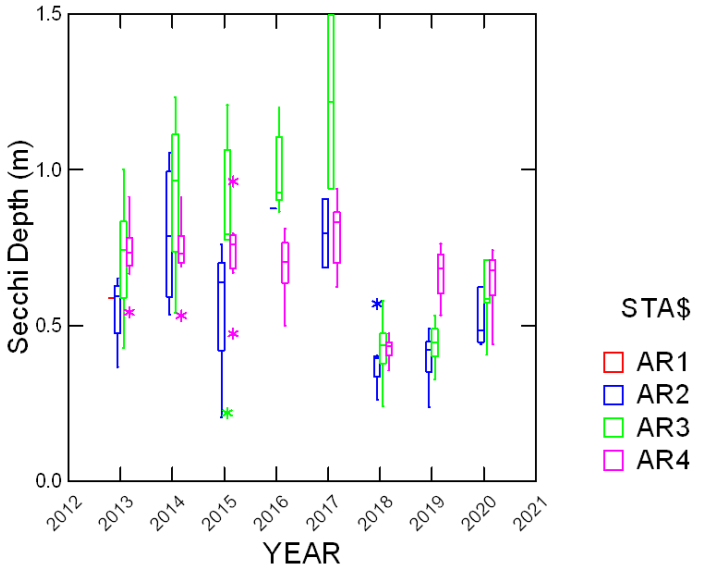

Figure 117. Box plots comparing values of Secchi disk depth between years. June through September.

Secchi disk depth (Figure 117) has generally shown major and consistent differences between stations, attributable to major differences in SAV abundance between the stations. In particular AR3 was often much higher than the other stations. However, starting in 2018 and continuing through 2020, Secchi depths were lower overall and were generally lower at AR2 and AR3 (in the embayment) than at AR4 in the river channel. Light attenuation coefficient is another way of measuring water clarity: less negative values of light attenution coefficient indicate clearer water. Median values in light attenuation coefficient were similar from year to year until 2018 (Figure 118). As with Secchi disk depth, values for light attenuation in 2018 to 2020 showed much reduced water clarity than previous years.

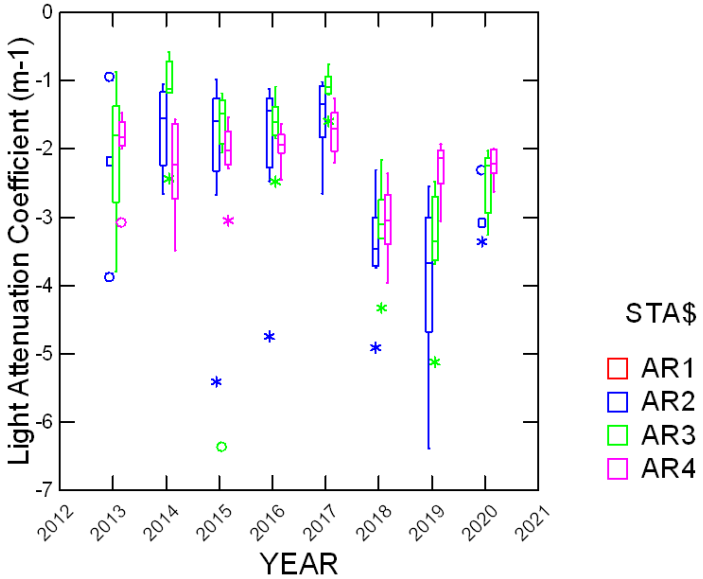

Figure 118. Box plots comparing values of Light Attenuation Coefficient between years. June through September.

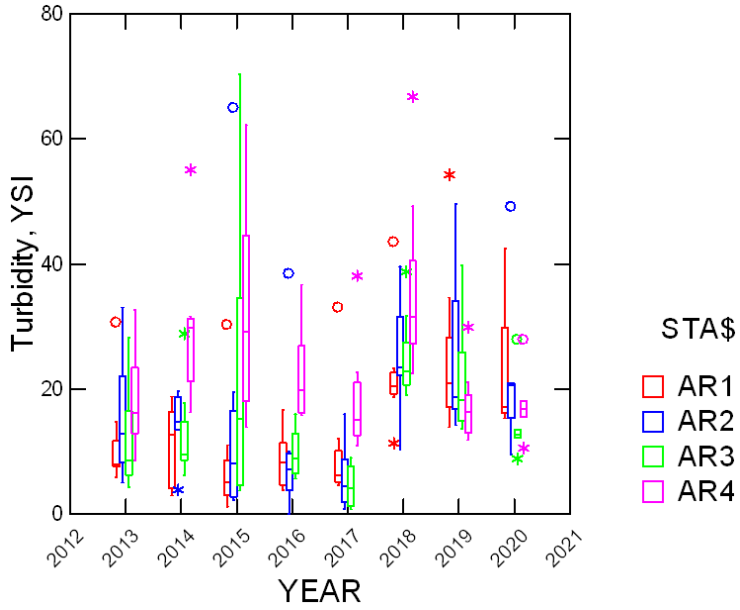

Figure 119. Box plots comparing values of Turbidity between years. June through September.

Turbidity, another measure of water clarity, continued to exhibit much higher values at AR2 and AR3 in 2020 as compared to 2013-2017 (Figure 119). Values at AR4 were not as different as in previous years.

Total phosphorus values were again higher in may samples at AR1 than in previous years. Values at AR2, and AR3 were similar to previous years (Figure 120). In contrast to previous years, AR4 was lower than the other stations, mainly due to their elevated levels.

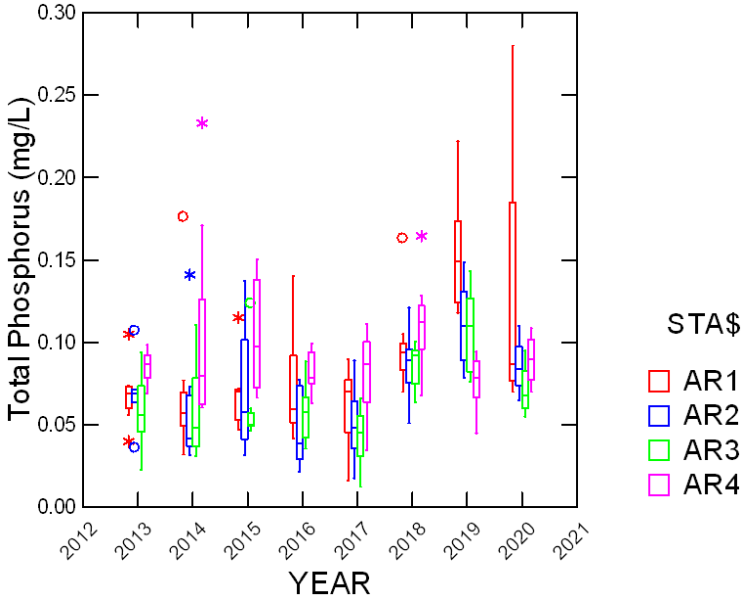

Figure 120. Box plots comparing values of Total Phosphorus between years. June through September.

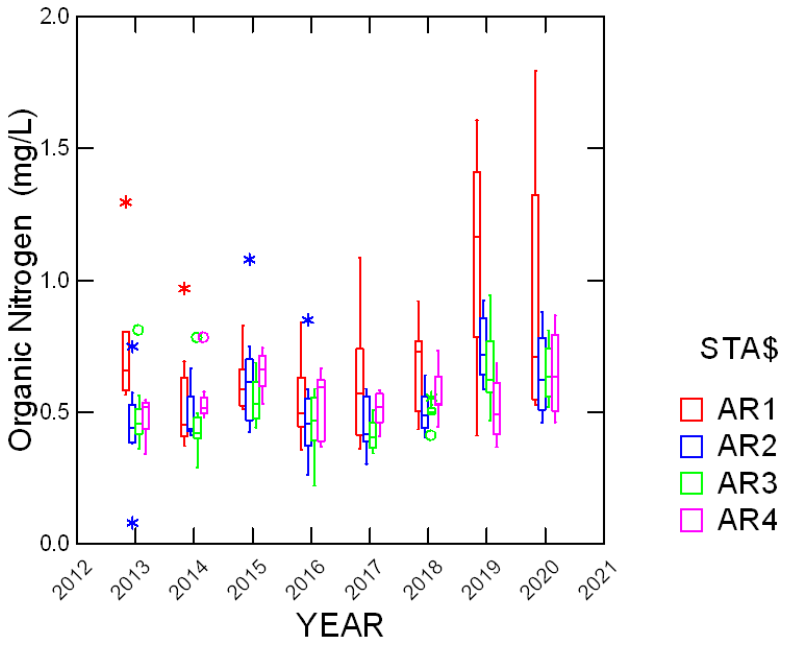

Figure 121. Box plots comparing values of Organic Nitrogen between years. June through September.

Organic nitrogen values in 2020 overlapped extensively with the ranges from previous years (Figure 121). A clear pattern was observed with AR1 highest and greater than normal, while AR4 was little changed compared with previous years. Nitrate nitrogen values in 2020 were consistently lower at all stations than in 2018 and 2019, returning to the ranges found in previous years (Figure 122).

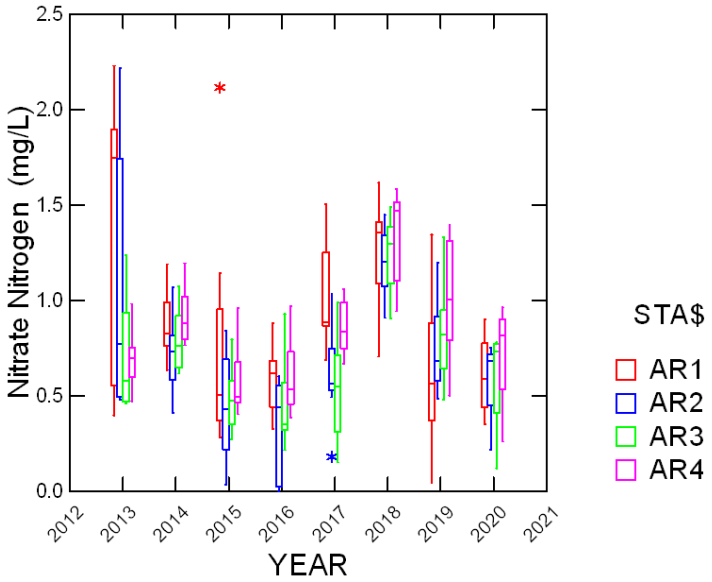

Figure 122. Box plots comparing values of Nitrate Nitrogen between years. June through September.

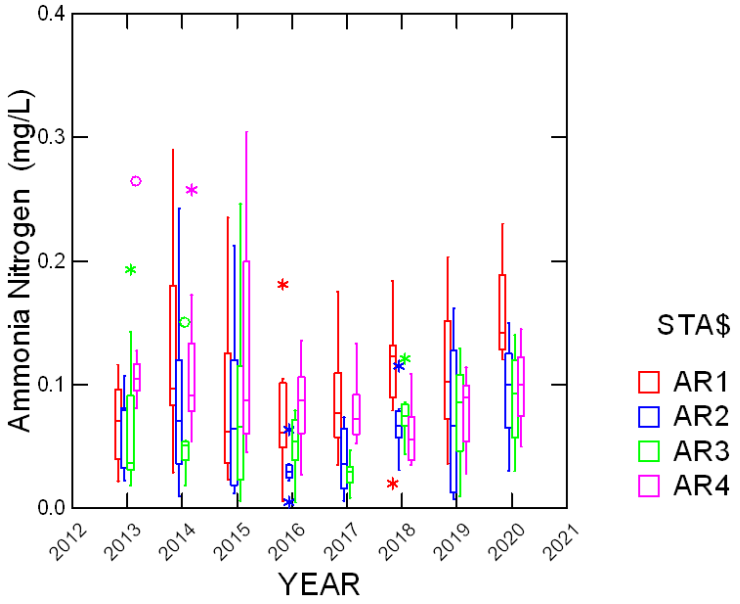

Figure 123. Box plots comparing values of Ammonia Nitrogen between years. June through September.

Ammonia nitrogen values in 2020 were similar to those observed in previous years (Figure 123). The exception is AR1 where valeus have steaily increased since 2016. Nitrite nitrogen values in 2019 were in the middle of the range for previous years and did not vary much among stations (Figure 124).

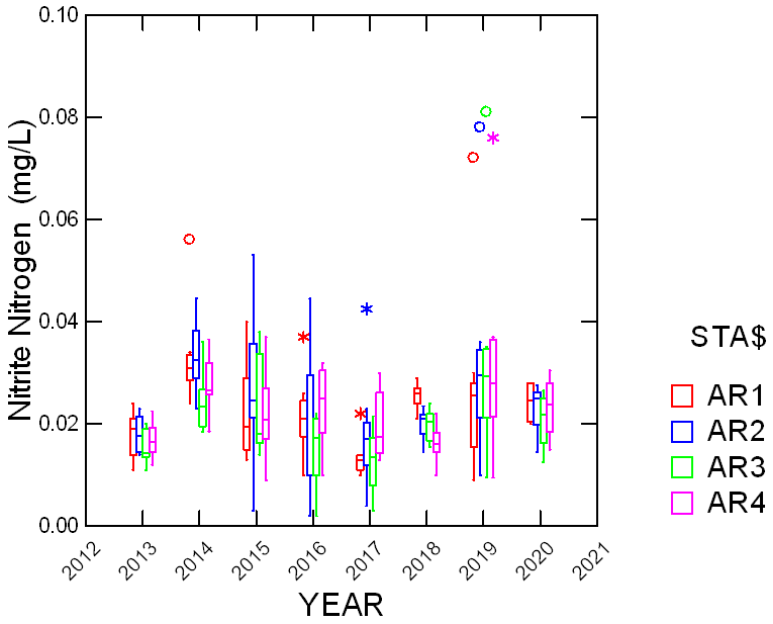

Figure 124. Box plots comparing values of Nitrite Nitrogen between years. June through September.

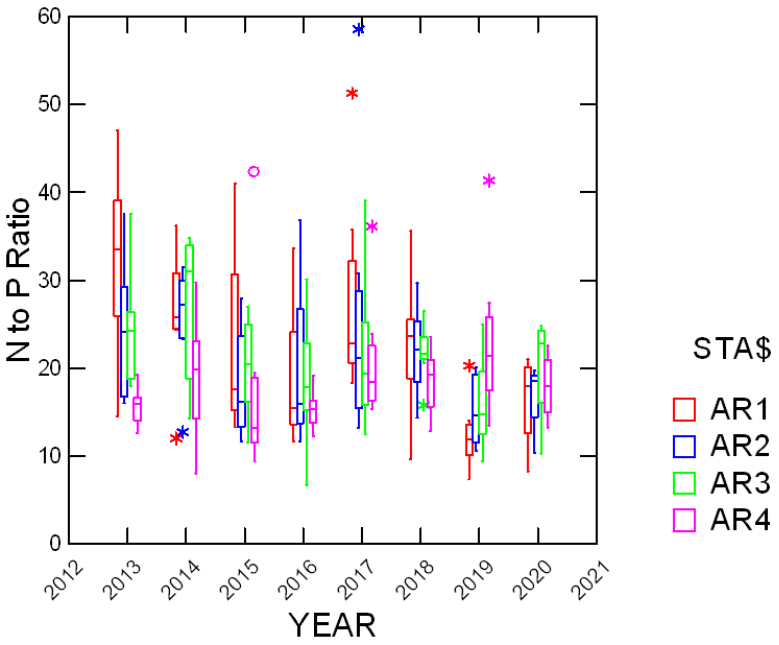

Figure 125. Box plots comparing values of N to P ratio between years. June through September.

N to P ratio for 2020 was in the lower range of values from previous years, but still within the range indicating phosphorus limitation (Figure 125). There is slight downward trend suggested in data from AR1, AR2, and AR3 while AR4 does not exhibit an obvious change over the years.

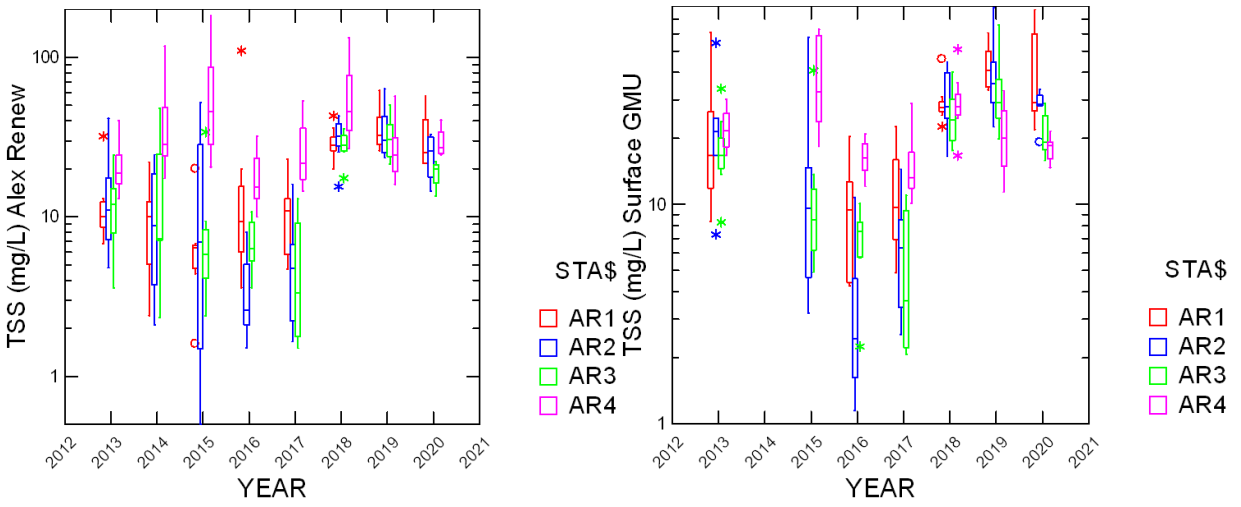

Figure 126. Box plots comparing values of Total Suspended Solids between years. Alex Renew data (a. left) and GMU data (b. right). June through September.

As in 2018 and 2019 total suspended solids (TSS) for AR1, AR2, and AR3 was higher in 2020 than in previous years (Figure 126a,b). The patterns were similar in samples analyzed by both Alex Renew and GMU. Volatile suspended solids (VSS) was in 2020 was similar to 2019 and higher than in many previous years (Figure 127a,b).

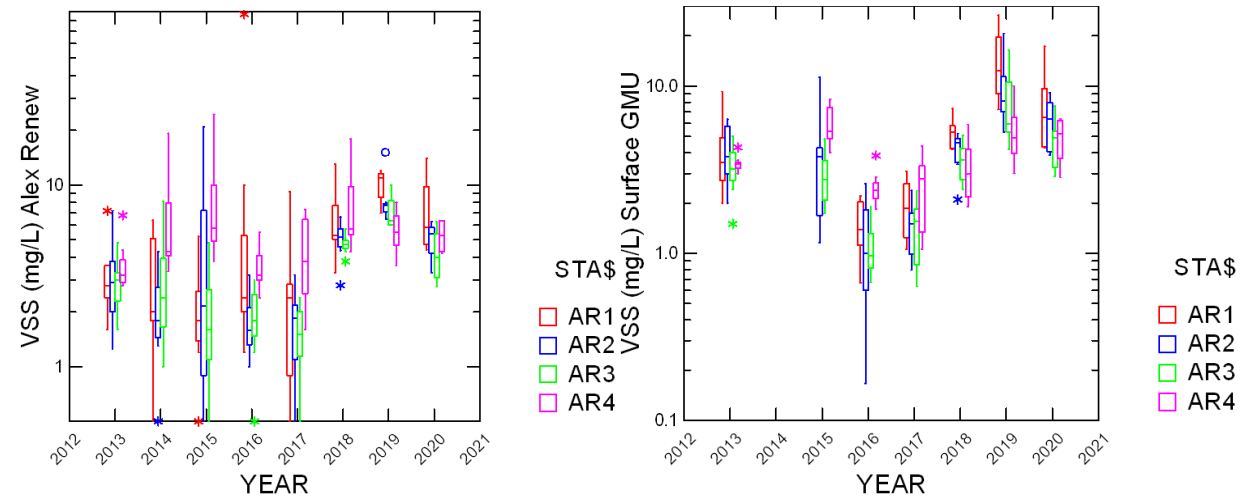

Figure 127. Box plots comparing values of Volatile Suspended Solids between years. Alex Renew Lab data (left) and GMU Lab data (right). June through September.

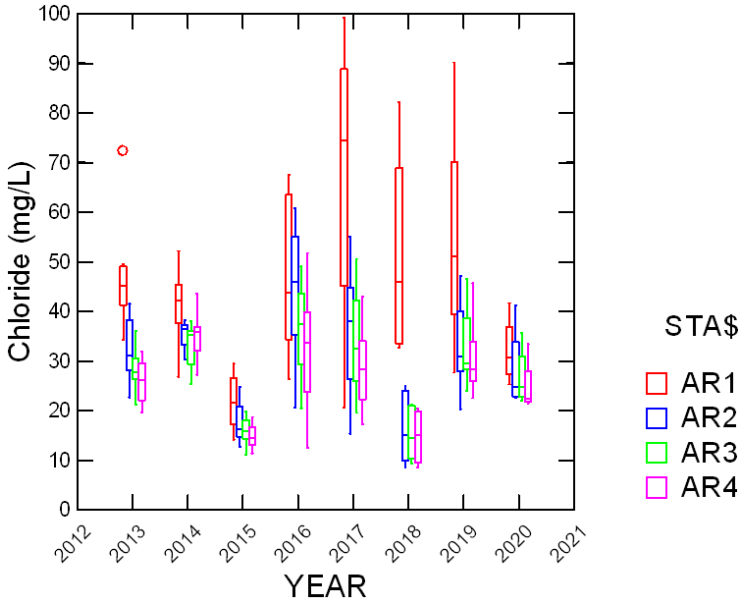

Figure 128. Box plots comparing values of Chloride between years. June through September.

As compared with most recent years chloride levels were tightly grouped over all stations (Figure 128). Total alkalinity was much lower in 2020 than in previous years at all stations ending an upward trend (Figure 129). In contrast to chloride, total alkalinity was generally lower at AR1 than at the other stations.

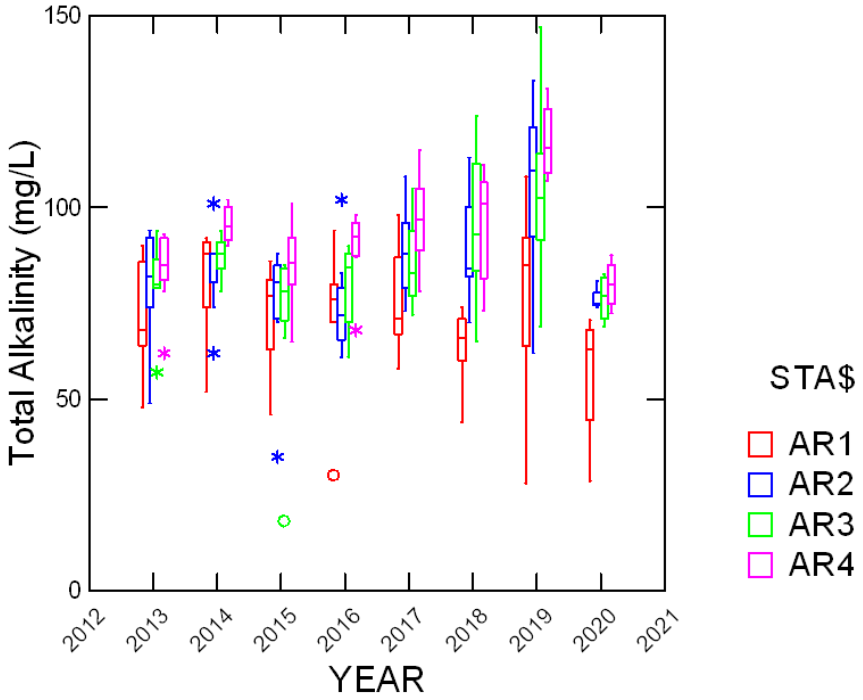

Figure 129. Box plots comparing values of Total Alkalinity between years. June through September.

D. Phytoplankton: Comparison among Years

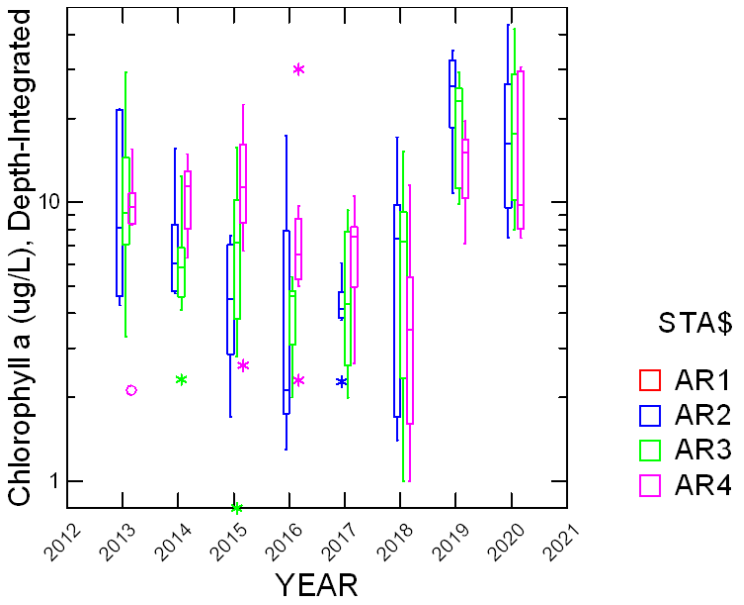

Figure 130. Box plots comparing values of depth-integrated Chlorophyll *a* among years. June through September.

In 2020 chlorophyll *a* levels were similar to 2019, reflecting a strong rebound from the generally low levels found in 2018 and were actually among the highest of all previous years. Also, values at all stations were much less variable than in 2018 (Figure 130, 131). Similar results were observed with surface chlorophyll. Chlorophyll values in the water are a measure of phytoplankton populations which compete with SAV for light and nutrients.

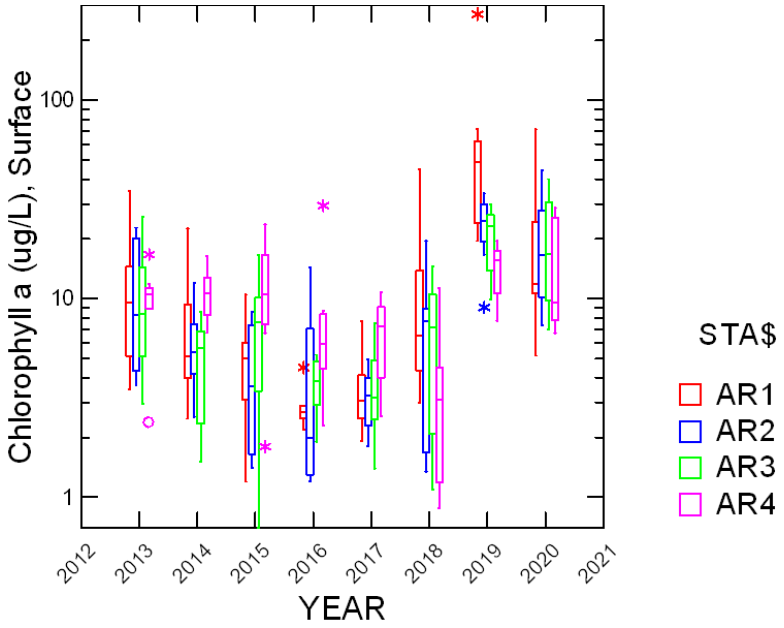

Figure 131. Box plots comparing values of surface Chlorophyll *a* among years. June through September.

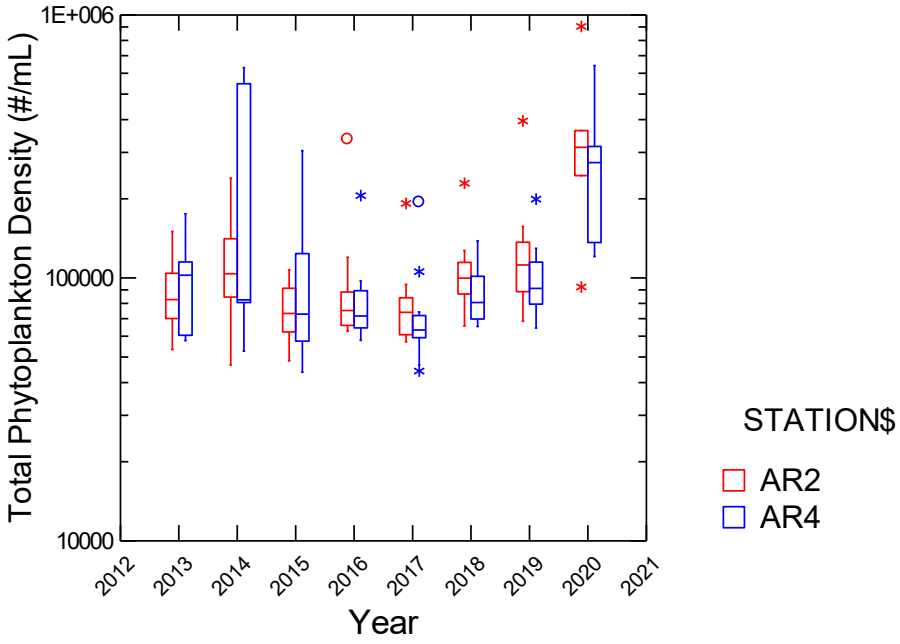

Figure 132. Box plots comparing values of Total Phytoplankton Density.

The median values for total phytoplankton cell density were higher in 2020 than in any previous year at both stations (Figure 132). This may be partially due to the fact that data were only available for the July to September period which often has the highest densities. Total cyanobacterial cell density was clearly higher in 2020 than in any previous year (Figure 133). 2020 values at AR4 were similar to those in several recent years.

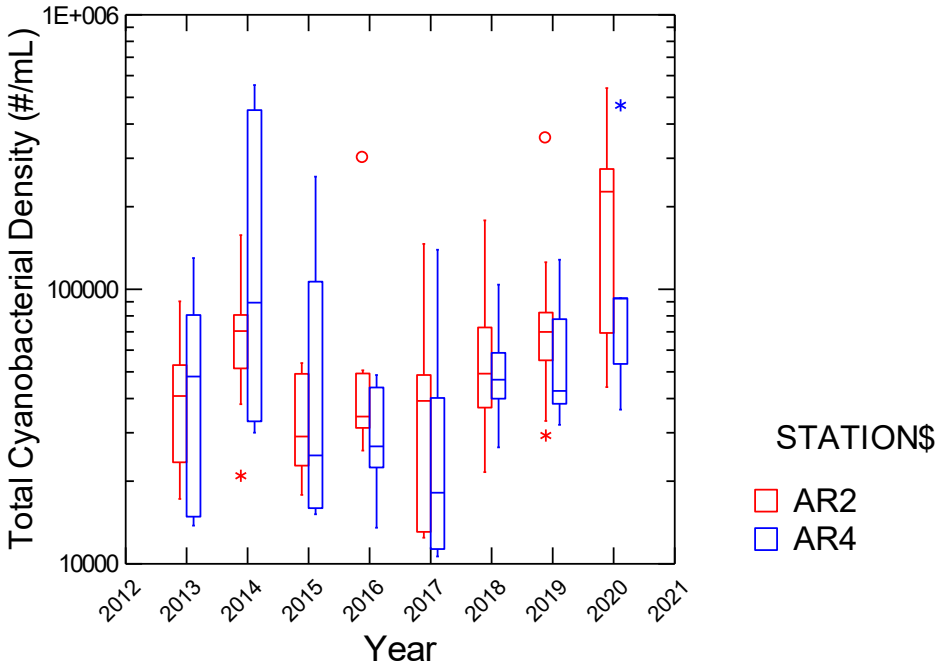

Figure 133. Box plots comparing values of Cyanobacterial Density.

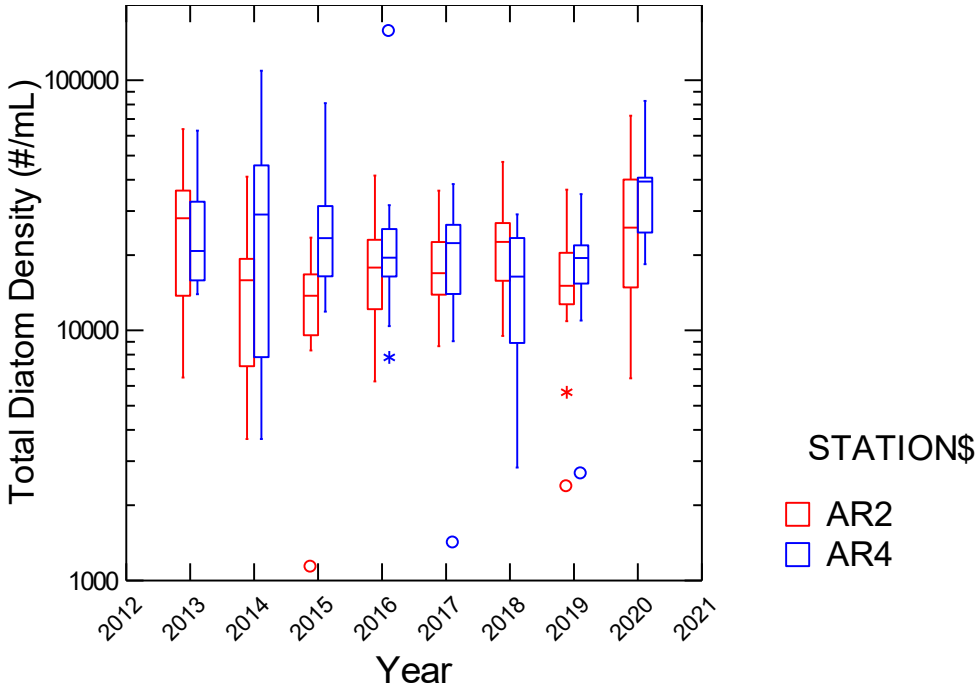

Figure 134. Box plots comparing values of Diatom Density among years.

Median diatom densities in 2020 at AR2 were within the range observed in previous years while the observations at AR4 were among the highest since the study began (Figure 134). Green algal cell densities were clearly much higher in 2020 than in any previous year, but did not vary much between stations (Figure 135).

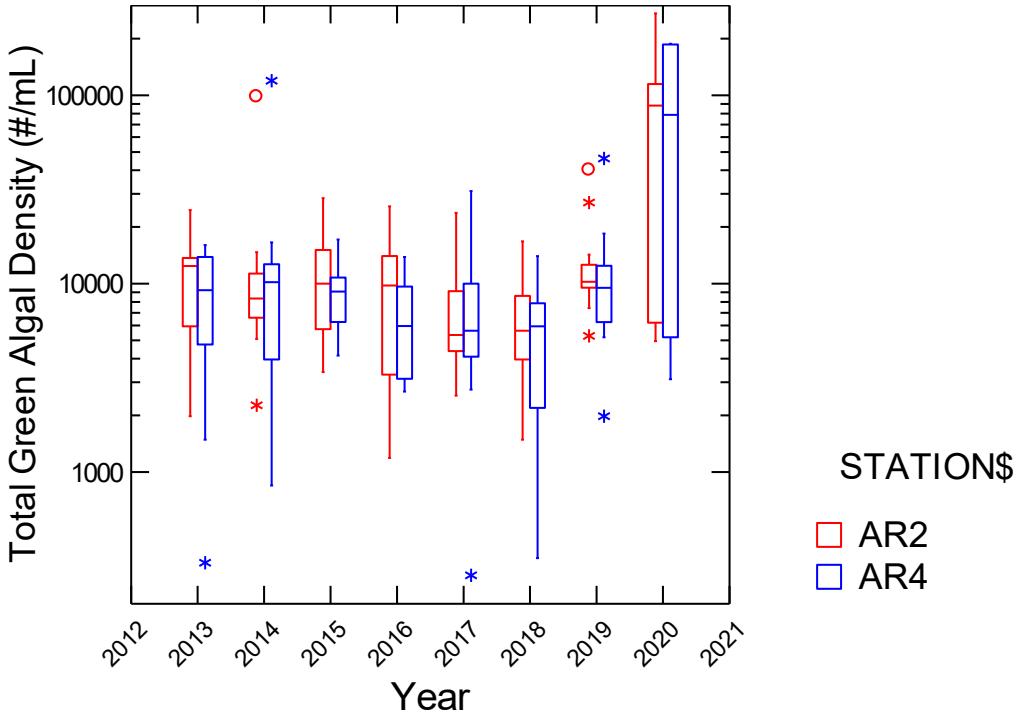

Figure 135. Box plots comparing values of Green Algal Density among years.

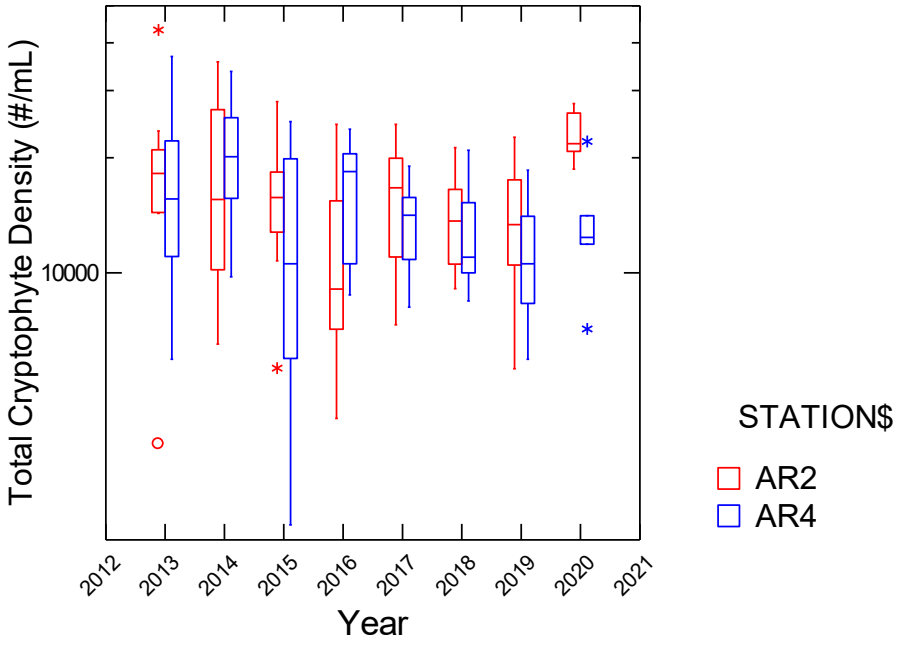

Figure 136. Box plots comparing values of Cryptophyte Density among years.

Median cryptophyte cell densities at AR2 was the highest of the study to date (Figure 136). At AR4 cryptophyte densities were in the middle to lower end of the range of previous years.
Other taxa includes those species of phytoplankton in groups not tallied above. These are mainly dinoflagellates, crysophytes and euglenoids whose abundances are somewhat sporadic in the study area. This is reflected in interannual patterns which show a wide range (Figure 137).

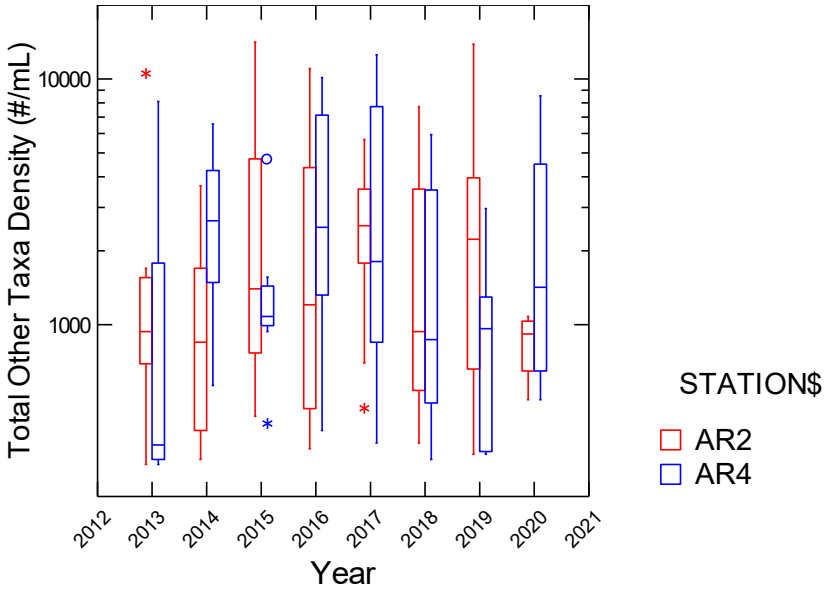

Figure 137. Box plots comparing values of Miscellaneous Taxa Density among years.

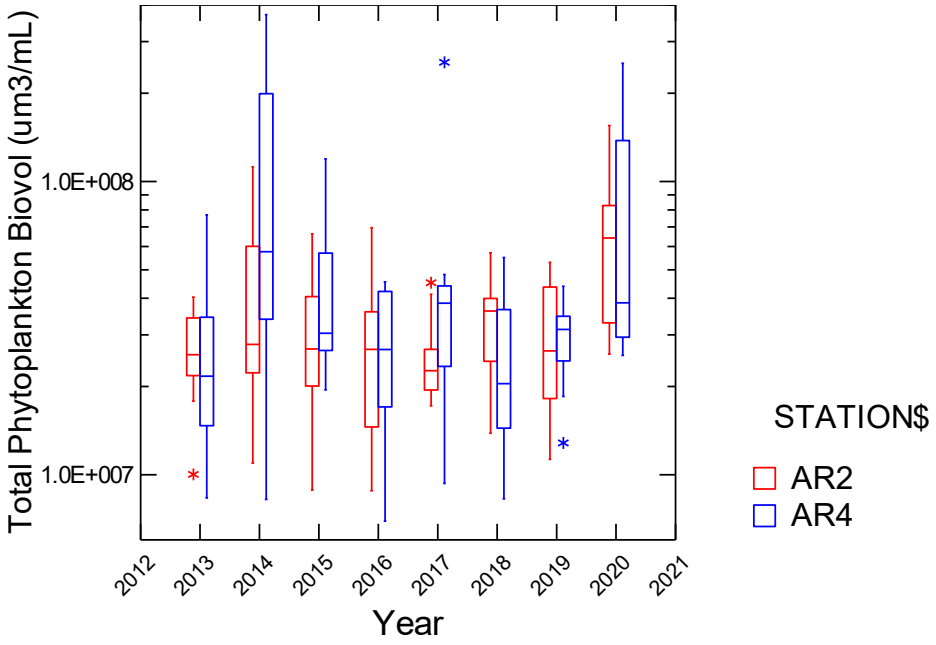

Figure 138. Box plots comparing values of Total Phytoplankton Biovolume among years.

Biovolume takes into account both the number of cells and their relative size. In 2020 total biovolumes were at the higher end of the range of previous years similar to 2014 (Figure 138). Total cyanobacterial biovolume median in 2020 was the highest observed to data at AR2 (Figure 139). At AR4 median value was within the upper range of recent years.

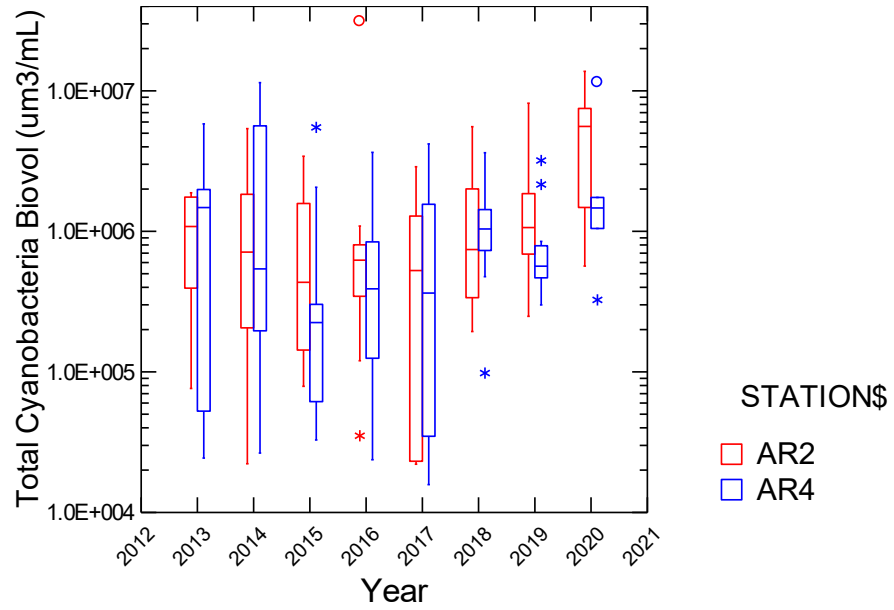

Figure 139. Box plots comparing values of Cyanobacterial Biovolume among years.

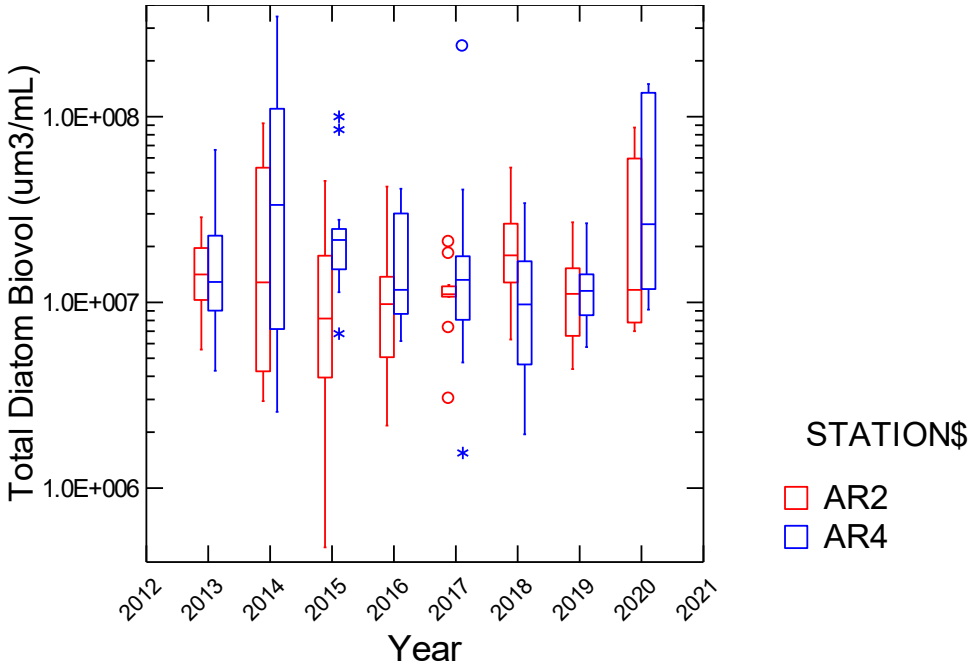

Figure 140. Box plots comparing values of Diatom Biovolume among years.

Median diatom biovolume in 2020 at AR4 was among the highest observed to date (Figure 140). Median diatom biovolume at AR2 was about average for previous years. Median values in green algal biovolume were very different between the two stations (Figure 141). At AR2 median value was the highest observed to date while at AR4 the median was among the lowest.

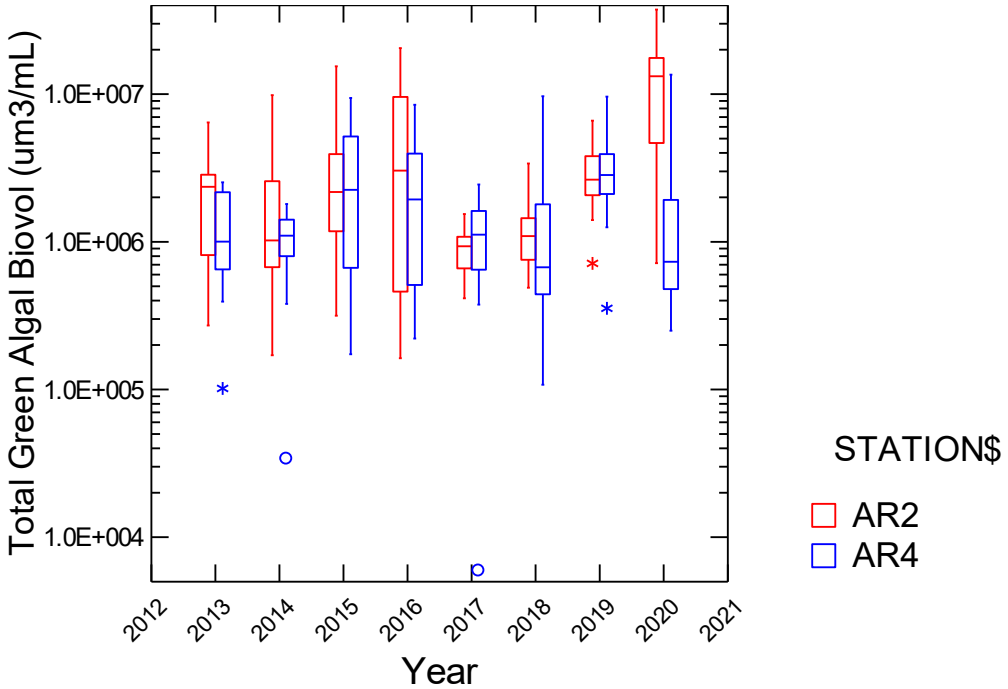

Figure 141. Box plots comparing values of Green Algal Biovolume among years.

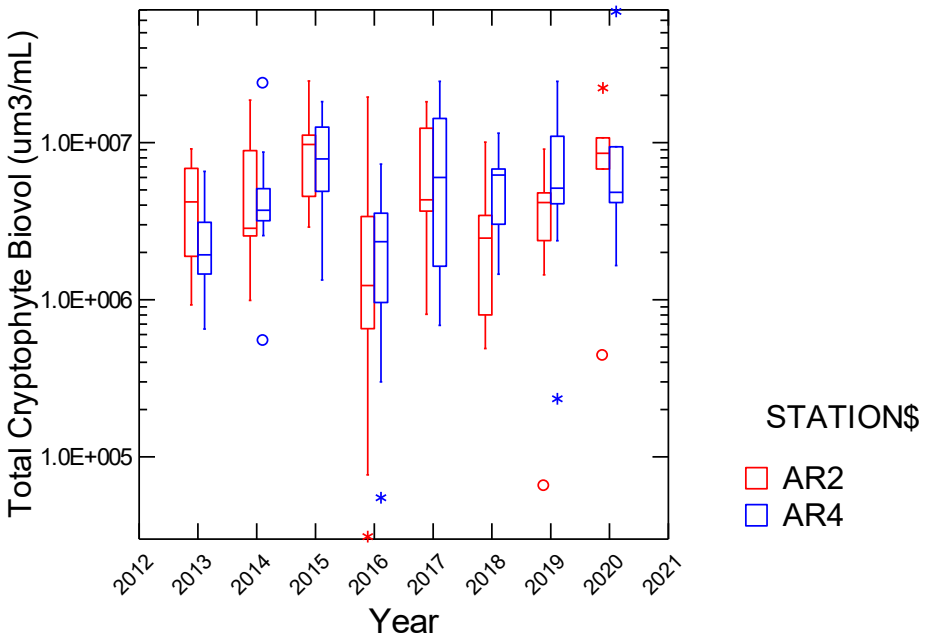

Figure 142. Box plots comparing values of Cryptophyte Biovolume among years.

Cryptophyte biovolume increased at AR2 for the third straight year (Figure 142). Levels at AR4 were somewhat lower and more in line with previous years. The patterns in Miscellaneous Taxa Biovolume were a bit sporadic and quite variable in some years (Figure 143). The median values in 2020 fell within the normal range.

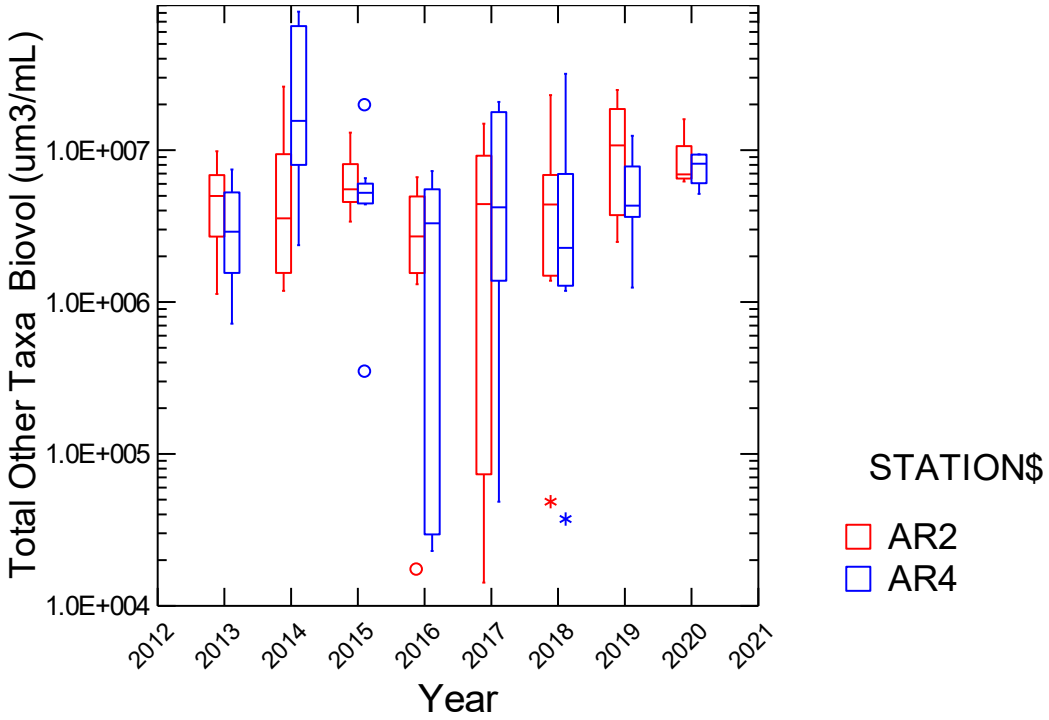

Figure 143. Box plots comparing values of Miscellaneous Biovolume among years.

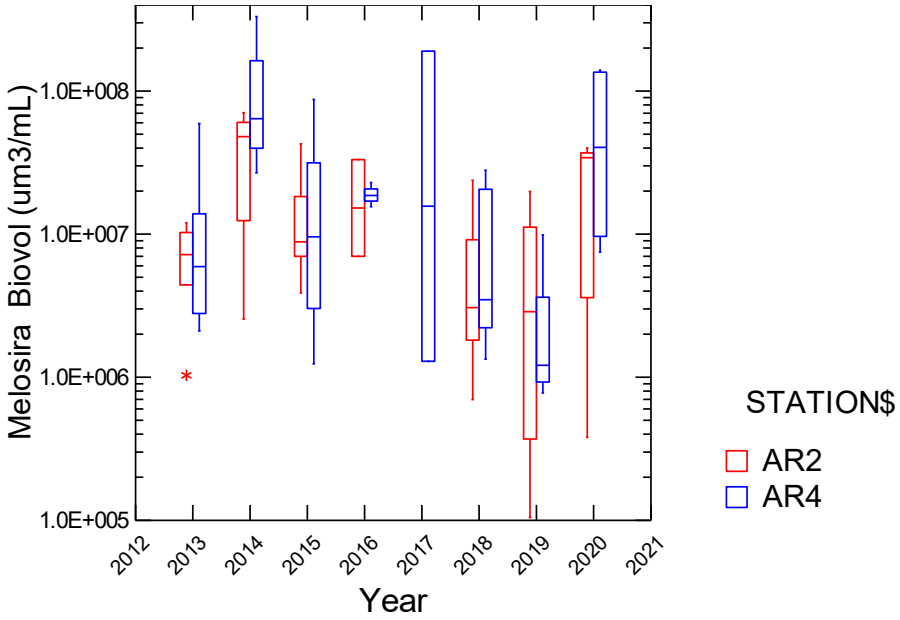

Figure 144. Box plots comparing values of *Melosira* Biovolume among years.

An analysis of interannual and seasonal effects also done for selected individual taxa. Median biovolume values of the filamentous diatom *Melosira* showed a clear peak in 2014 at both stations, then declined steadily through 2019, but cameb back strongly in 2020 (Figure 144). Discoid centric biovolume in 2020 was was similar at the two stations and showed a recovery from low values in 2019 (Figure 145).

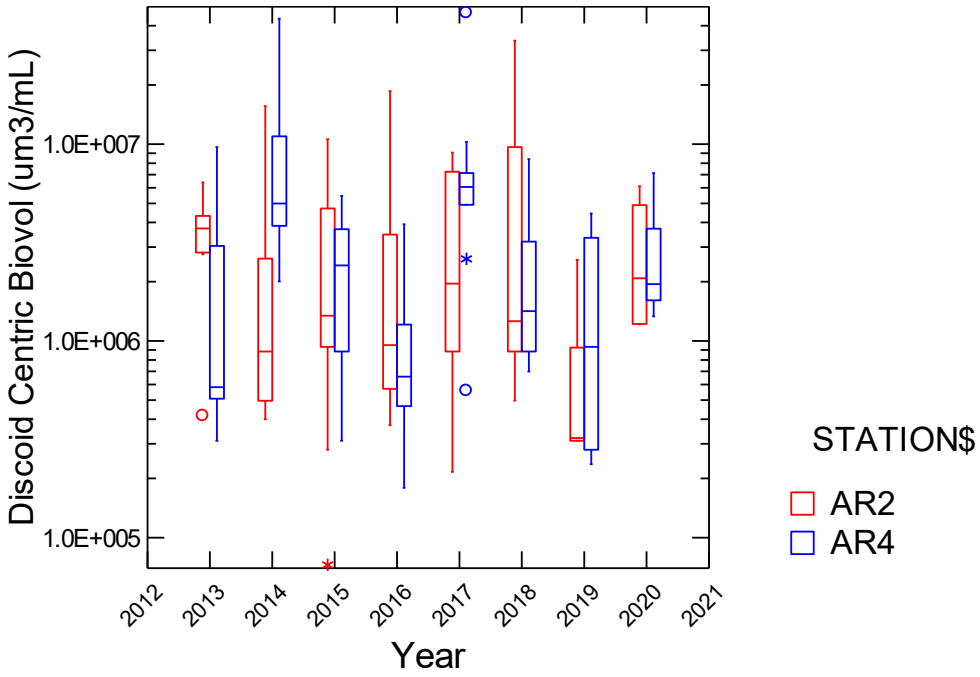

Figure 145. Box plots comparing values of Discoid Centric Diatom Biovolume among years.

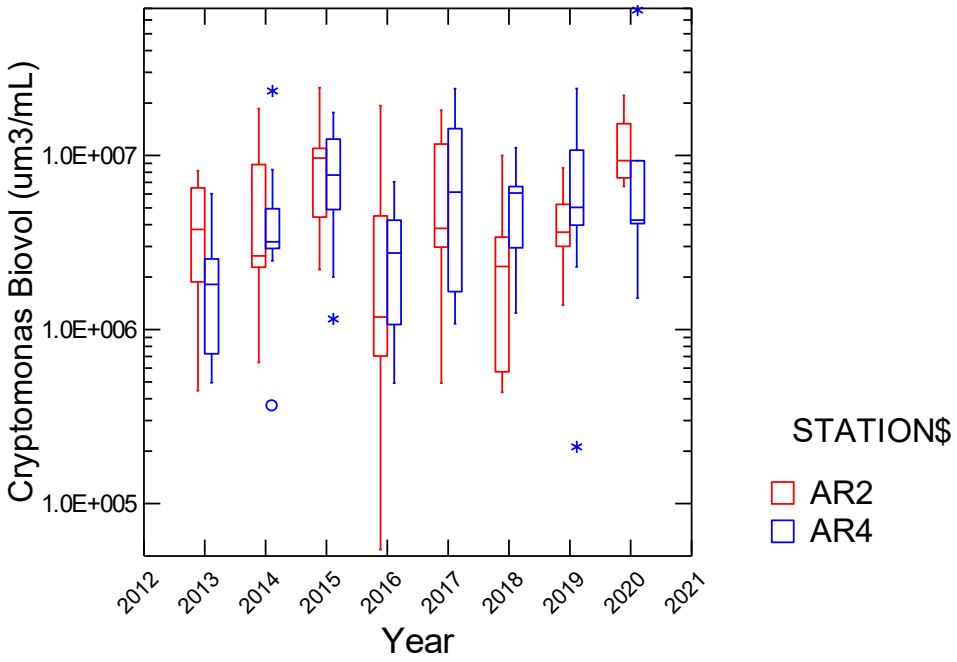

Figure 146. Box plots comparing values of *Cryptomonas* Biovolume among years.

Cryptomonas biovolume increased at AR2 for the third consective year (Figure 146). At AR4 values have remained fairly steady for the past four years. *Oscillatoria* is the most consistently abundant cyanobacterium in the study area. In 2020 levels recovered strongly at AR2, but remained somewhat depressed at AR4 (Figure 147).

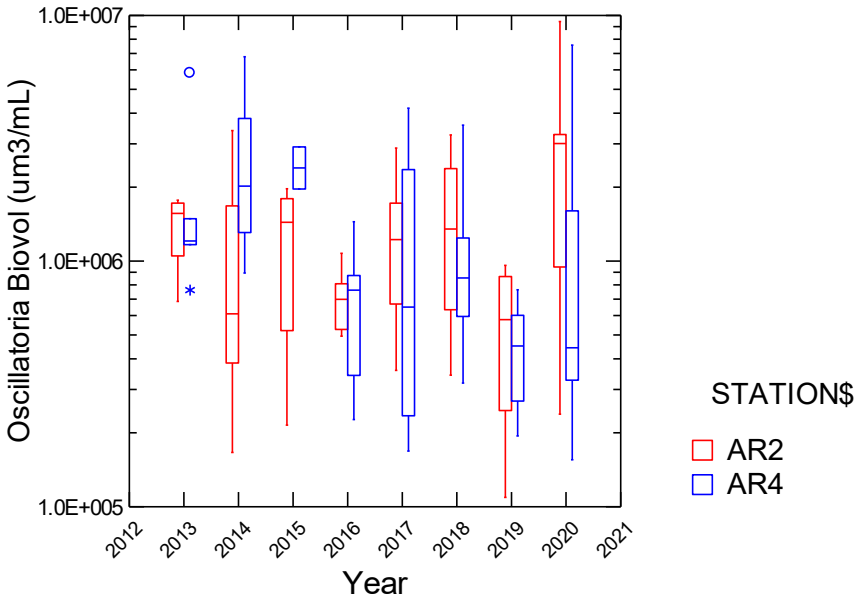

Figure 147. Box plots comparing values of *Oscillatoria* Biovolume among years.

E. Zooplankton: Comparison among Years

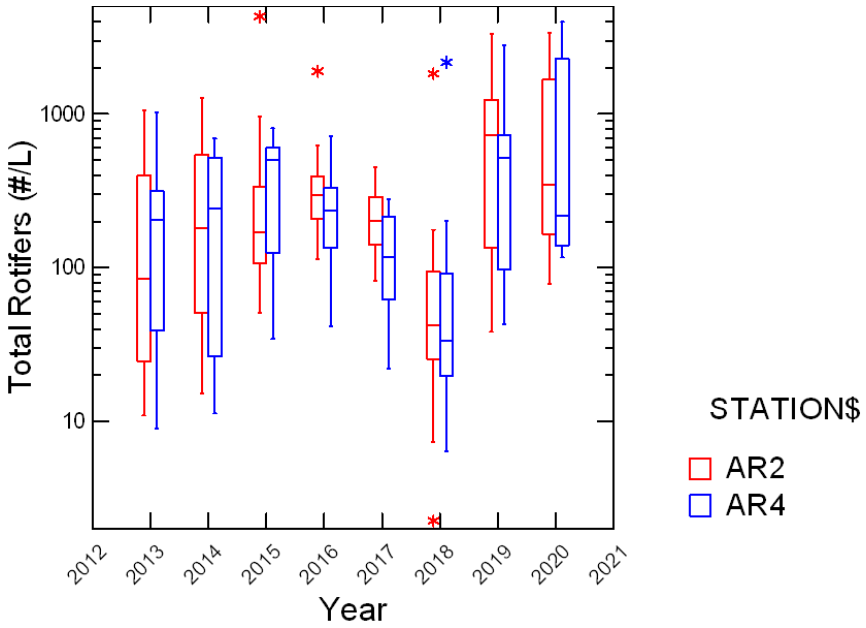

Figure 148. Box plots comparing values of Total Rotifers among years.

Total rotifer densities were very robust in 2020 similar to 2019 (Figure 148). Of particular interest was the strong recovery from the record low values of 2018 which were probably a result of the high rainfall and subsequent flushing of organisms observed that year. Episodic flushing occurred in 2020 as in 2019 and may have actually stimulated the rotifers. The common rotifer *Brachionus* (Figure 149) was the dominant taxon and displayed a similar trend as total rotifers with 2019 and 2020 levels very high and 2018 the lowest year to date. *Brachionus* exhibited similar values at both station sin most years.

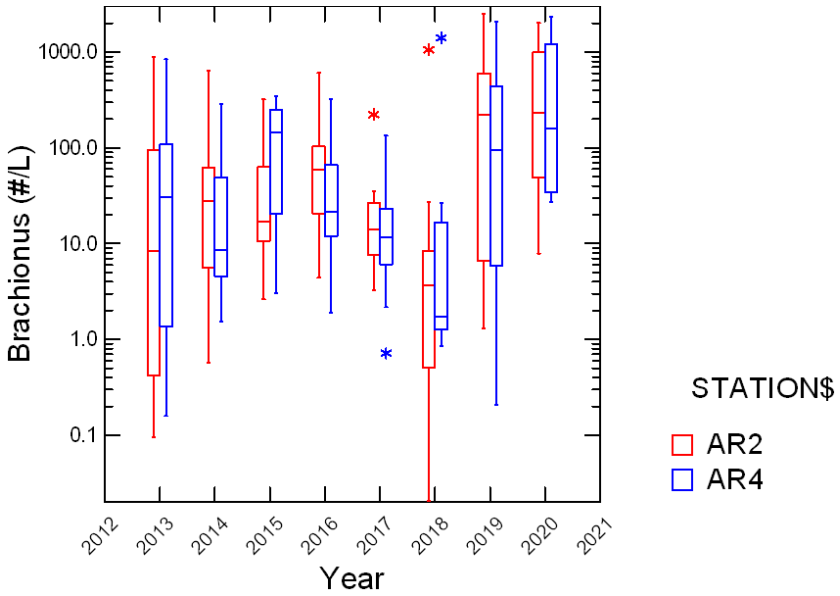

Figure 149. Box plots comparing values of *Brachionus* among years.

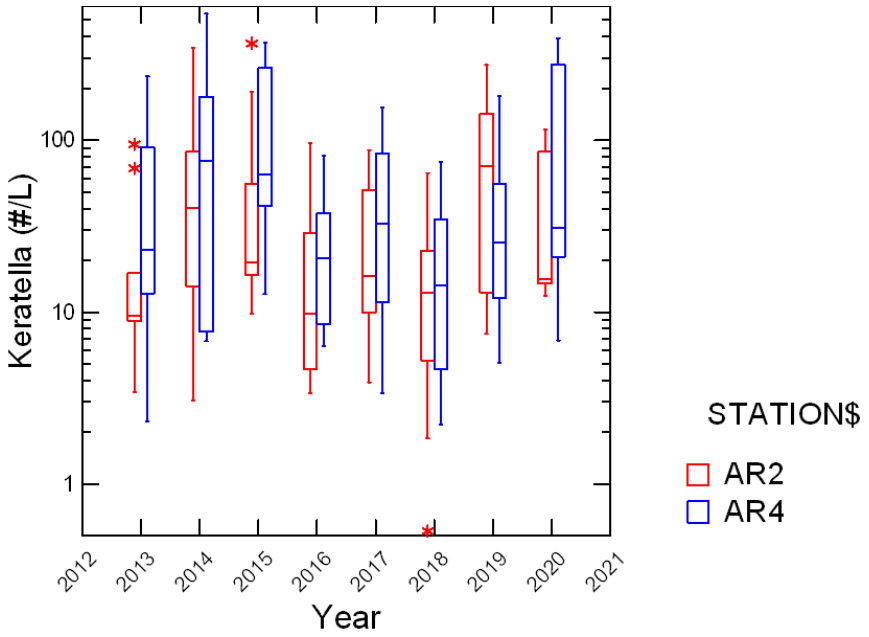

Figure 150. Box plots comparing values of *Keratella* among years.

Another common rotifer *Keratella* exhibited a similar, but less dramatic trend. Values in 2020 were higher in 2018, but 2018 was not as low relative to other years (Figure 150). *Polyarthra*, consistently observed, but less common than *Brachionus* or *Keratella*, also showed a continued rebound from low 2018 levels (Figure 151).

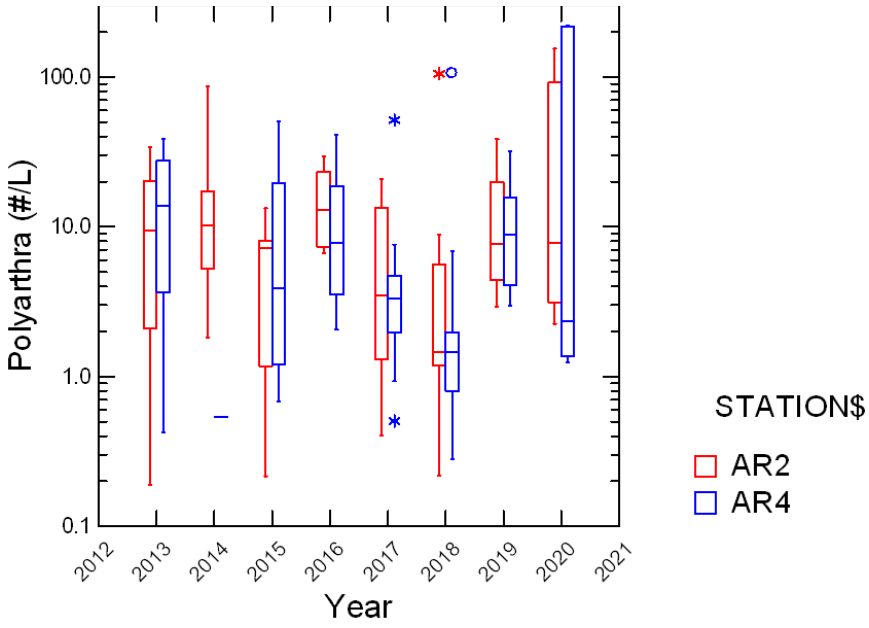

Figure 151. Box plots comparing values of *Polyarthra* among years.

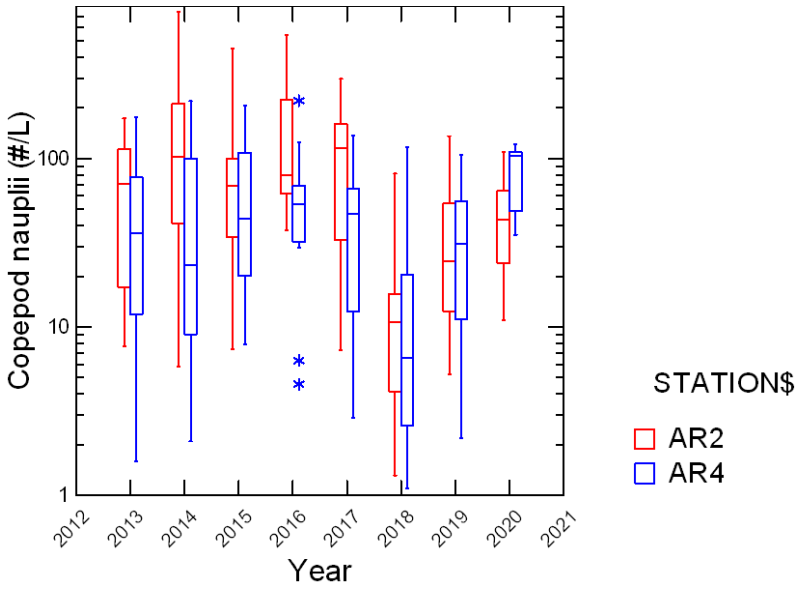

Figure 152. Box plots comparing values of Copepod Nauplii among years.

Nauplii are the juvenile stages of copepods. As such it is hard to identify them to species since they do not have mature characteristics so they have been lumped for all copepod taxa. Nauplii showed a continued recovery in 2020 after the low values of 2018 (Figure 152). Values were similar at the two stations. *Bosmina* is a small cladoceran enumerated in the 44 µm samples, but related to *Daphnia* and *Diaphanosoma* collected in the 202 µm nets. As with copepod nauplii, *Bosmina* continued to recover in 2020 after the sharp decline in 2018 (Figure 153). There was not a consistent difference in *Bosmina* levels between the two stations.

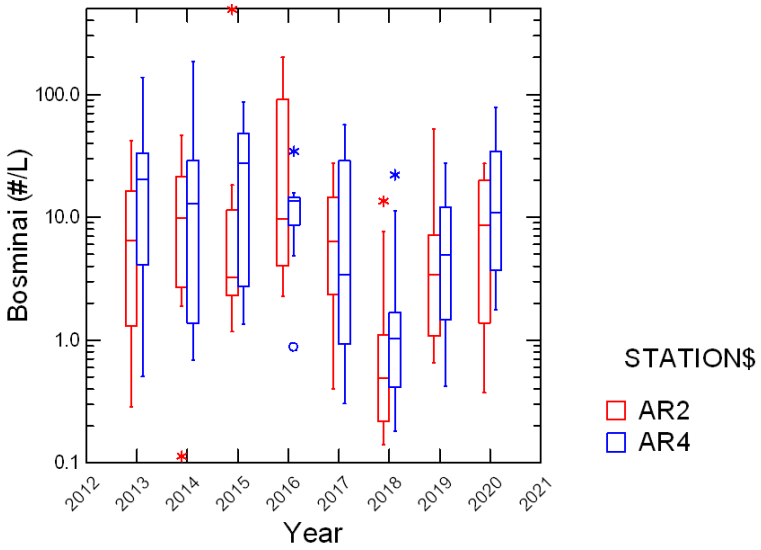

Figure 153. Box plots comparing values of *Bosmina* among years.

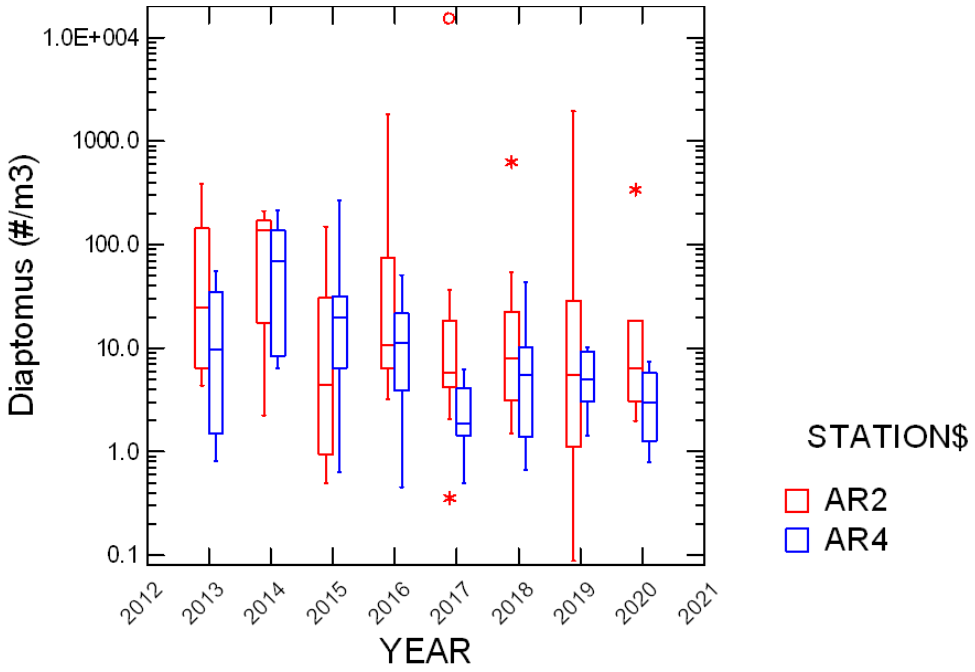

Figure 154. Box plots comparing values of *Diaptomus* among years.

Median *Diaptomus* densities remained at the low end of values observed during the study at both stations (Figure 154). *Eurytemora* is the most common calanoid copepod (Figure 155). It consistently was more abundant at the river station AR4 than at AR2 in Hunting Creek. *Eurytemora* did not exhibit much response to the very different flow regimes of 2018 to 2020 compared to previous year.

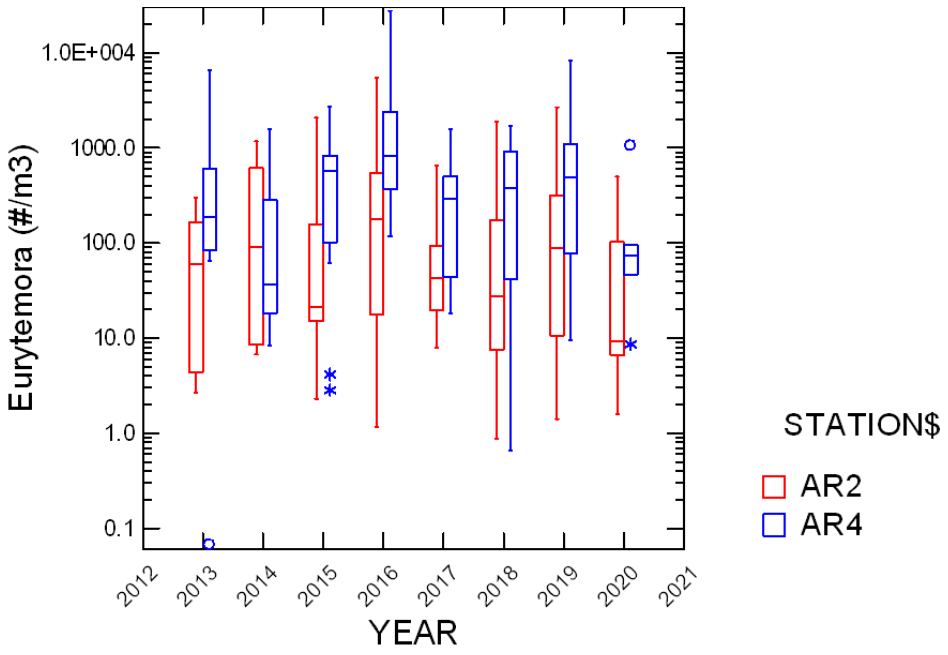

Figure 155. Box plots comparing values of *Eurytemora* among years.

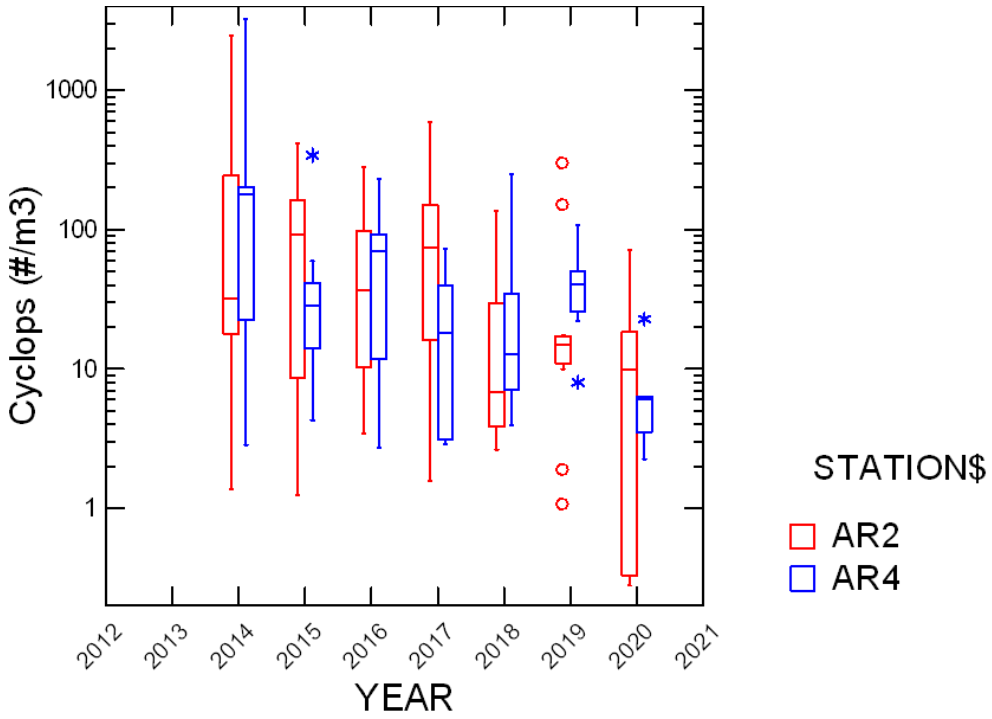

Figure 156. Box plots comparing values of *Cyclops* among years.

The copepod *Cyclops* was present at lower levels in 2020 continuing a downward trend over the study period (Figure 156). *Mesocyclops* is one of the more common cyclopoid copepods. Median values of *Mesocyclops* at AR2 continued to be at the low end of the range of previous years, while AR4 levels showed little change (Figure 157).

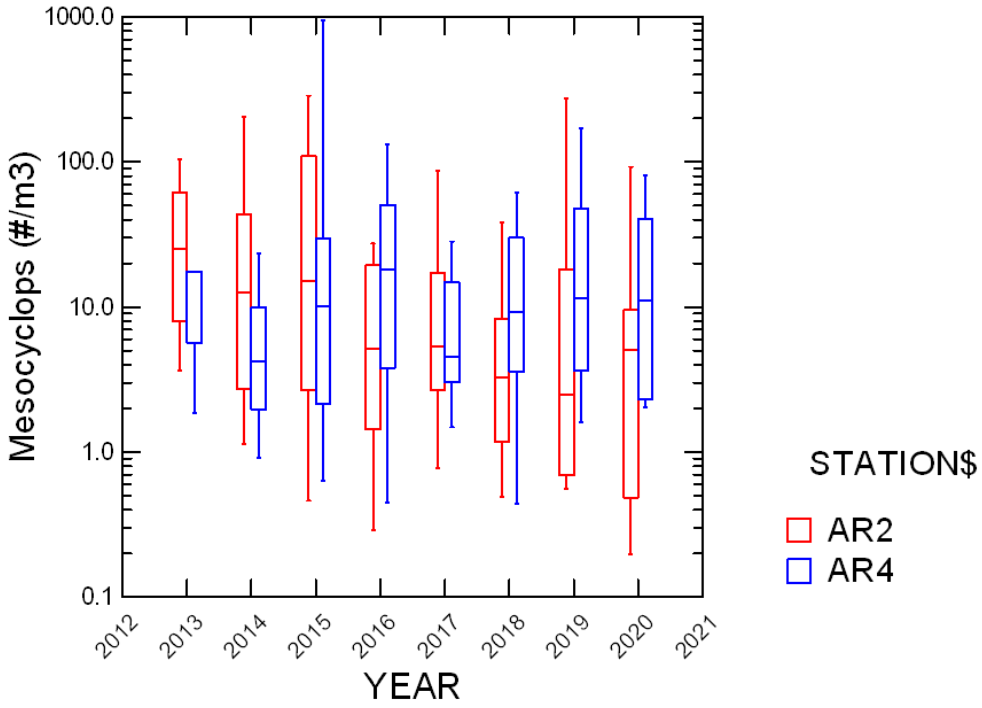

Figure 157. Box plots comparing values of *Mesocyclops* among years.

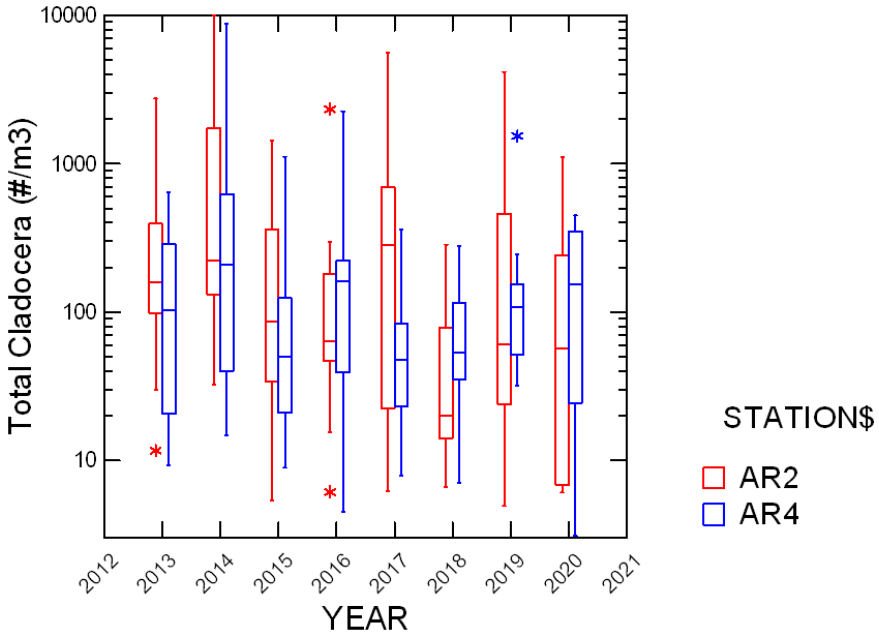

Figure 158. Box plots comparing values of Total Cladocerans among years.

Total cladoceran values (excluding *Bosmina*) at AR2 continued to recover in 2020 after the low levels in 2018 (Figure 158). Values at AR4 remained within the range of previous years. *Daphnia* was found at clearly higher levels in 2014 than in the other years of the study (Figure 159). Values observed in 2020 were among the lowest observed to date, especially at AR4. This was partially due to the lack of data for June, a time of the year when *Daphnia* is generally abundant.

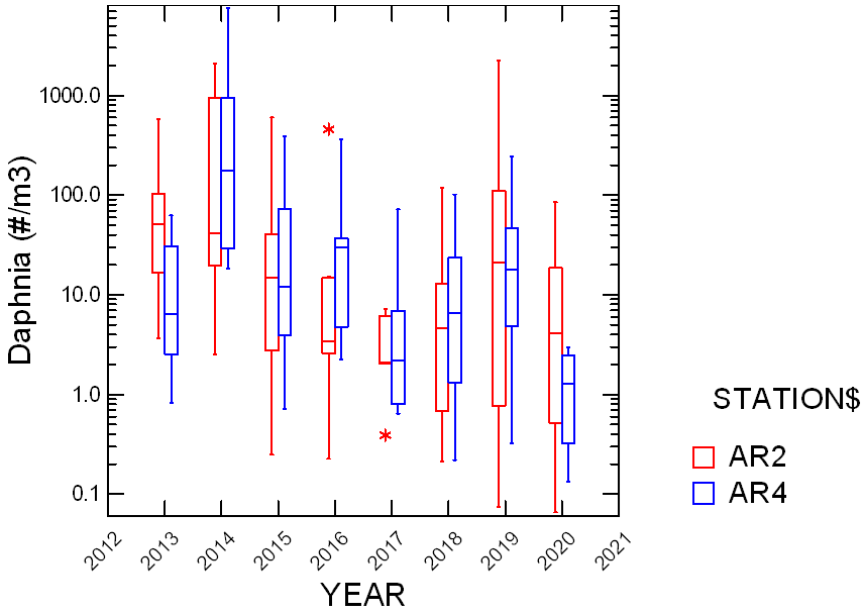

Figure 159. Box plots comparing values of *Daphnia* among years.

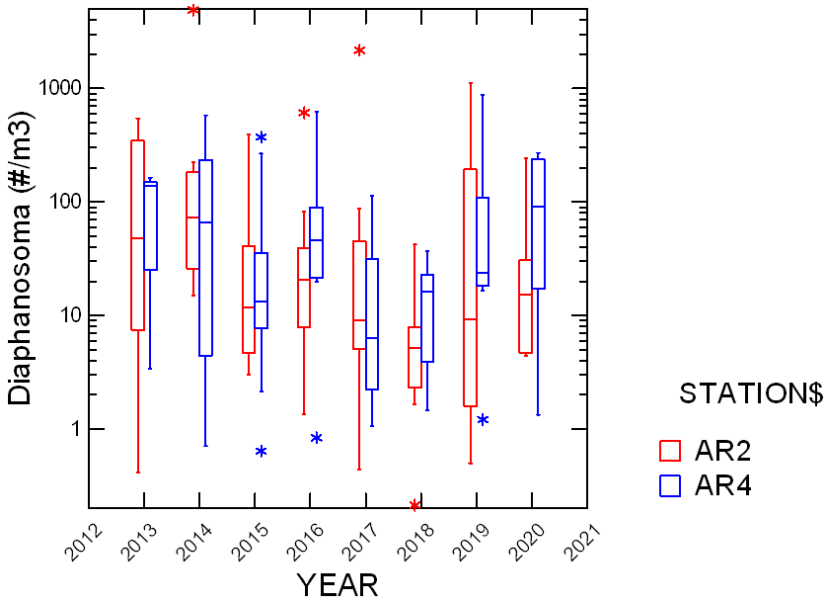

Figure 160. Box plots comparing values of *Diaphanosoma* among years.

Diaphanosoma is a very abundant cladoceran in Gunston Cove, but has proven to be less abundant in the Hunting Creek area, although still important. *Diaphanosoma* levels at AR2 were at record lows in 2018, and showed continued recovery in 2020 (Figure 160). Levels at AR4 were also higher in 2020 than in 2018. *Sida* was generally less abundant than *Diaphanosoma*, but has maintained its levels over time. It was also reduced in 2018 did not recover much in 2019 and 2020 (Figure 161).

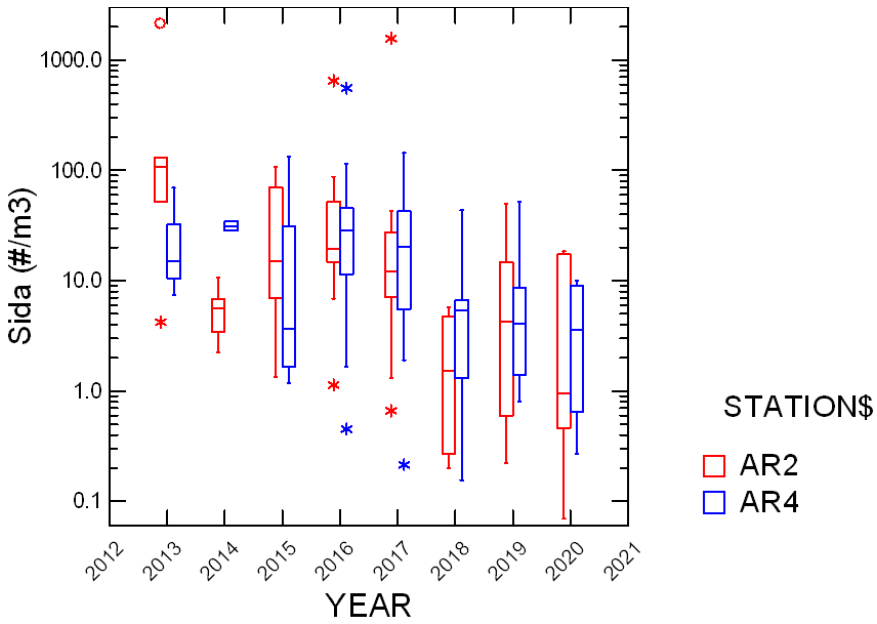

Figure 161. Box plots comparing values of *Sida* among years.

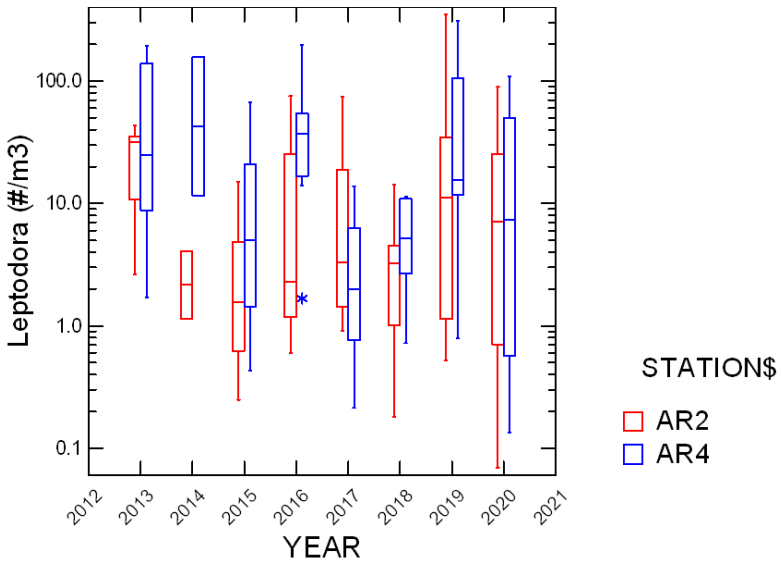

Figure 162. Box plots comparing values of *Leptodora* among years.

Leptodora is a large predacious cladoceran which occurs consistently in the study area (Figure 162). Values in 2020 continued to be robust at both stations and were distinctly higher than in 2017 and 2018. *Leptodora* was generally higher at AR4 as has been usual. Total macrozooplankton, those collected in the 202 µm net, showed a clear interannual pattern with greatest numbers at both stations in 2014 (Figure 163). 2020 values are among the lowest of any year, at least partially due to the lack of June samples.

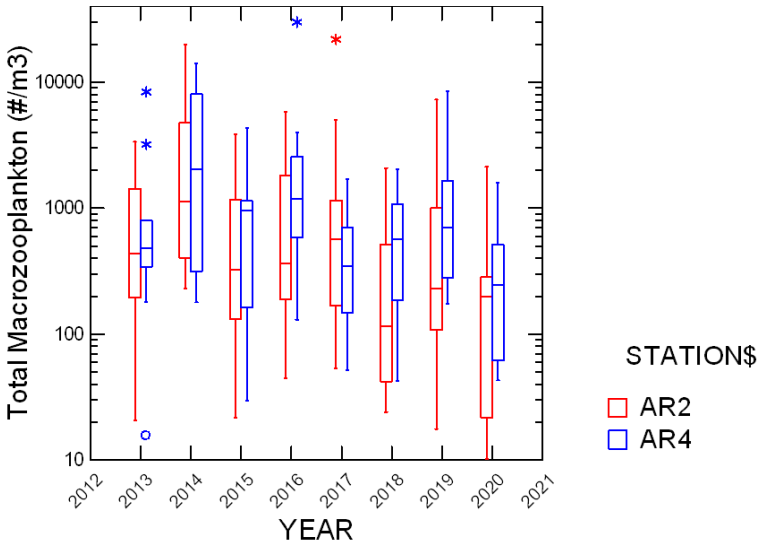

Figure 163. Box plots comparing values of Total Macrozooplankton among years.

F. Ichthyoplankton: Comparison among Years

2020 marks the eighth year of our fish collections in Hunting Creek. Both trends and inter-annual variability become apparent when comparing the years of data. Due to sampling restrictions in response to the COVID 19 pandemic, only two ichthyoplankton sampling events occurred, and only five adult and juvenile fish sampling events. As a result of this, our data on density and abundance of fishes in Hunting Creek in 2020 are not representative of the fish assemblages present. We will still present our 2020 result here as part of the multi-year time series.

The larval data show a much lower density of fish larvae than previous years, likely due to the much lower amount of sampling events (Table 22). Evaluation catch per unit effort does not solve this since the chance of encountering a high density of larvae during a sampling event is very low when only two sampling events have taken place. This should therefore not be interpreted as a sign of a reduction in ichthyoplankton density. Looking at relative abundance the same species as previous years were abundant in the samples, that some are missing (e.g. Hickory Shad) is likely a result of not sampling at a time when they are present, and the low encounter rate due to having two sampling events. Species found in relative higher densities than previous years were sunfishes such as Bluegill and Green Sunfish. The trend of relative high densities of river herring (Alewife and Blueback Herring) continued in 2020.

Table 22. Density of larvae collected all years.

Scientific Name	Common Name	2013	2014	2015	2016	2017	2018	2019	2020
Alosa aestivalis	Blueback Herring	61.69	200.35	382.05	91.54	205.29	56.54	271.72	4.89
Alosa mediocris	Hickory Shad	4.80	4.13	12.11	9.63	4.28	1.58	11.36	0.00
Alosa pseudoharengus	Alewife	139.80	57.71	265.97	78.52	81.75	38.85	214.34	3.65
Alosa sapidissima	American Shad	0.12	1.32	0.61	1.97	2.80	0.15	0.00	0.00
Alosa sp.	unk. *Alosa* species	0.00	18.49	0.00	0.00	0.00	0.00	0.00	0.00
Carassius auratus	Goldfish	56.78	0.89	0.00	0.30	7.02	0.00	0.00	0.00
Carpiodes cyprinus	Quillback	0.00	0.00	0.00	0.78	0.00	0.92	8.14	0.00
Catostomidae	unk. catostom. species	0.00	0.00	0.00	0.00	0.00	0.00	0.17	0.00
Centrarchidae	unk. centrarch. species	0.00	0.00	0.00	0.13	0.00	0.00	0.00	0.00
Clupeidae	unk. clupeid species	422.94	781.67	444.54	175.51	193.31	129.35	169.13	5.55
Cyprinidae	unk. cyprinidae species	1.14	0.00	0.59	0.00	0.00	0.00	0.00	0.00
Cyprinus carpio	Carp	0.00	0.00	0.00	0.00	2.98	0.00	0.00	0.00
Dorosoma cepedianum	Gizzard Shad	438.39	381.85	592.25	221.54	293.50	83.18	1999.48	0.98
Eggs	eggs	0.16	3.09	2.69	17.80	25.66	11.17	62.25	0.00
Enneacanthus gloriosus	Bluespotted Sunfish	0.00	0.24	0.00	0.00	0.00	0.00	0.00	0.00
Etheostoma olmstedi	Tessellated Darter	0.00	0.00	0.00	0.13	0.00	0.00	0.00	0.00
Etheostoma sp.	unk. darter species	0.00	0.00	0.00	0.00	0.00	0.00	0.19	0.00
Fundulus diaphanus	Banded Killifish	0.00	0.00	0.00	0.00	0.50	0.00	0.00	0.00
Hybognathus regius	Eastern Silvery Minnow	0.00	0.00	0.00	0.00	0.50	0.00	0.19	0.00
Lepisosteus osseus	Longnose Gar	0.00	0.00	0.00	0.00	0.25	0.00	0.00	0.00
Lepomis cyanellus	Green Sunfish	0.00	0.00	0.00	0.41	0.50	0.00	0.00	0.37
Lepomis gibbosus	Pumpkinseed	0.00	0.00	0.00	1.62	0.99	0.39	0.35	0.00
Lepomis macrochirus	Bluegill	0.00	0.00	0.00	0.00	0.50	0.00	0.00	2.38
Lepomis sp.	unk. sunfish	0.60	2.83	0.49	0.00	8.23	0.00	0.19	0.31
Menidia beryllina	Inland Silverside	2.48	3.32	1.98	20.36	60.78	0.66	1.21	1.78
Micropterus dolomieu	Smallmouth Bass	0.00	0.00	0.00	0.00	0.25	0.00	0.00	0.00
Morone americana	White Perch	0.00	5.90	15.93	8.60	17.54	15.48	66.30	0.14
Morone saxatilis	Striped Bass	0.00	4.02	0.00	1.10	7.71	0.00	0.00	0.00
Morone sp.	unk. perch/bass species	39.06	43.46	4.32	14.11	3.71	0.00	0.00	0.00
Notemigonus crysoleucas	Golden Shiner	0.00	0.84	0.00	0.00	0.00	0.00	0.00	0.00
Notropis hudsonius	Spottail Shiner	0.00	0.00	0.00	0.39	2.48	4.94	0.23	0.00
Perca flavescens	Yellow Perch	38.22	1.41	0.00	0.65	0.50	0.74	0.73	0.00
Strongylura marina	Atlantic Needlefish	0.00	0.12	0.00	0.00	0.13	0.00	0.00	0.00
Unidentified	unidentified	11.45	84.35	27.42	34.65	84.23	6.43	126.74	1.03
Total		1217.66	1595.98	1750.95	679.72	1005.39	350.38	2932.72	21.08

G. Adult and Juvenile Fish: Comparison among Years

The total number of adult and juvenile fishes collected in 2020 was surprisingly high, due to a higher abundance of White Perch than collected in any of the previous years (Table 23). The relative abundances of other species are pretty similar to previous years. While the shorter sampling season biases any trends in abundance, we may see a continued decrease of Banded Killifish and Mummichog and increase of Alewife, Gizzard Shad, and Blue Catfish. Reasons for these trends are a decline in SAV which favors open water species and reduced abundances of SAV-associated species. The increasing trend in Alewife is likely due to the positive results of a moratorium on catch that has been in effect since 2012. The increase in Blue Catfish abundance is concerning as this is an invasive species that continues to increase. The fyke nets were not deployed in 2020 due to the small crew allowed due to COVID restrictions. This could be another reason SAV-associated species were low in total abundances. New species to these collections in 2020 were Threadfin Shad and Flathead Catfish. Threadfin Shad prefers higher salinities and we have witnessed it migrate this far into the freshwater tidal area for the first time. Flathead Catfish is an invasive species that has been reported in the area, but for us it is the first time we found it in our collections.

The two most dominant species throughout the sampling period, White Perch and Banded Killifish, have opposite trends through the years, with Banded Killifish abundances declining and White Perch abundances increasing. This trend holds true in 2020. The opposite trend is seen in the longer survey record of Gunston Cove (Jones and De Mutsert 2018), which seems mostly due to SAV resurgence since 2005. The decline in SAV cover in Hunting Creek in recent years could be a reason for the decreasing Banded Killifish abundances and increasing White Perch abundances.

In 2020, 22 different species were collected, which is lower than previous years, but most likely a result of less sampling events than a reflection of the true diversity. The Simpson's Index of Diversity (calculated as $1-(\mathbf{\Sigma}\ (n_i/N)^2)$) was calculated for all years based on adult and juvenile abundances (Figure 164). Note that in the 2016 report the Simpson's index (D) was reported, in which communities with higher diversity or evenness approach zero. In the reports since 2016 we calculated the Simpson's Index of Diversity, which is 1-D. In this index the communities with higher diversity have higher values (approaching 1) which is more intuitive to interpret. While evenness was reduced each year of sampling before 2017, 2017 and 2018 showed high Simpson's Index of Diversity values, with 2019 slightly lower but still very close to that (Figure 169). 2020 was the lowest on record with a value of 0.309, which should not be interpreted as a reflection of true diversity. With a full sampling season likely to be possible in 2021, we will continue these time series with better interpretation of the results possible.

Table 23. Abundances of species (adults and juveniles) collected all years.

Scientific Name	Common Name	2013	2014	2015	2016	2016 with Fyke	2017	2017 with Fyke	2018	2018 with Fyke	2019	2019 with Fyke	2020
Alosa aestivalis	Blueback Herring	16	8	12	29	29	0	0	0	0	32	33	0
Alosa mediocris	Hickory Shad	0	0	0	0	0	0	0	0	0	8	8	4
Alosa pseudoharengus	Alewife	6	23	28	12	12	0	0	14	14	67	69	113
Alosa sapidissima	American Shad	208	32	163	19	19	2	2	2	2	12	12	0
Alosa sp.	unk. Alosa species	299	8	55	11	12	3	3	433	433	822	822	18
Ameiurus catus	White Bullhead	0	0	0	1	2	0	0	8	8	1	1	4
Ameiurus natalis	Yellow Bullhead	0	0	0	0	0	0	0	0	0	4	4	0
Ameiurus nebulosus	Brown Bullhead	3	2	3	3	3	2	5	13	13	2	2	1
Anchoa mitchilli	Bay anchovy	69	70	7	0	0	0	0	0	0	86	86	8
Anguilla rostrata	American Eel	1	3	2	0	0	0	0	0	1	2	2	0
Brevoortia tyrannus	Atlantic Menhaden	0	0	0	0	0	0	0	0	0	30	30	0
Carassius auratus	Goldfish	20	39	2	0	9	18	107	1	1	0	0	0
Carpiodes cyprinus	Quillback	9	19	2	0	0	0	0	0	0	72	72	13
Cyprinella spiloptera	Spotfin shiner	0	0	1	0	0	0	0	0	0	0	0	0
Cyprinus carpio	Carp	0	3	1	7	14	3	3	2	2	4	4	0
Dorosoma cepedianum	Gizzard Shad	5	1	3	0	0	0	0	50	50	52	52	71
Dorosoma petenense	Threadfin Shad	0	0	0	0	0	0	0	0	0	0	0	24
Enneacanthus gloriosus	Bluespotted Sunfish	0	0	0	0	0	27	47	0	0	0	0	0
Erimyzon oblongus	Creek Chubsucker	0	0	0	0	0	0	0	1	1	0	0	0
Etheostoma olmstedi	Tessellated Darter	292	49	39	3	8	33	35	212	221	29	30	11
Fundulus diaphanus	Banded Killifish	1798	2382	2723	1387	1547	692	769	777	777	423	424	147
Fundulus heteroclitus	Mummichog	53	152	174	16	16	62	62	20	20	14	14	4
Gambusia holbrooki	Mosquitofish	11	69	19	0	0	1	1	0	0	7	7	6
Hybognathus regius	Eastern Silvery Minnow	0	6	31	2	4	40	40	13	14	6	6	0
Ictalurus furcatus	Blue Catfish	12	4	4	1	1	6	6	57	57	93	93	61
Ictalurus punctatus	Channel Catfish	0	0	2	0	0	0	0	2	2	2	2	3
Lepisosteus osseus	Longnose Gar	0	0	3	1	1	1	1	0	0	0	0	0

Lepomis auritus	Redbreast Sunfish	0	0	1	2	2	0	0	0	0	0	0	0
Lepomis cyanellus	Green Sunfish	0	0	2	0	0	4	7	0	0	0	0	0
Lepomis gibbosus	Pumpkinseed	6	17	11	11	22	39	180	91	100	16	22	6
Lepomis macrochirus	Bluegill	12	52	21	8	20	28	188	75	81	3	5	1
Lepomis megalotis	Longear Sunfish	0	0	0	0	0	1	1	0	0	0	0	0
Lepomis microlophus	Redear Sunfish	6	11	5	2	8	0	0	0	0	0	0	0
Lepomis sp.	unk. sunfish	5	12	5	27	85	50	169	0	2	1	4	1
Menidia beryllina	Inland Silverside	15	6	73	209	210	114	124	107	120	84	86	4
Micropogonias undulatus	Atlantic Croaker	1	0	0	0	0	0	0	0	0	0	0	0
Micropterus dolomieu	Smallmouth Bass	5	5	9	6	6	62	70	20	20	10	10	6
Micropterus punctulatus	Spotted Bass	1	0	0	0	0	0	0	0	0	0	0	0
Micropterus salmoides	Largemouth Bass	3	7	0	5	5	2	2	4	4	2	3	0
Micropterus sp.	unk. bass species	1	0	0	0	0	0	0	0	0	0	0	0
Morone americana	White Perch	574	107	693	19	57	393	439	667	675	1353	1364	2920
Morone saxatilis	Striped Bass	2	0	2	1	5	5	8	2	2	6	6	0
Morone sp.	unk. perch/bass species	0	1	0	0	0	0	0	0	0	0	0	0
Moxostoma erythrurum	Golden Redhorse	0	0	0	0	0	0	0	0	0	3	3	0
Moxostoma macrolepidotum	Shorthead Redhorse	0	0	0	0	0	0	0	1	1	0	0	0
Notemigonus crysoleucas	Golden Shiner	2	3	13	2	2	2	2	5	5	1	1	0
Notropis hudsonius	Spottail Shiner	338	666	87	13	17	11	13	124	125	109	113	96
Perca flavescens	Yellow Perch	22	16	7	7	7	1	2	36	37	6	6	0
Pomoxis nigromaculatus	Black Crappie	0	0	4	0	1	0	0	3	3	3	4	0
Pylodictis olivaris	Flathead Catfish	0	0	0	0	0	0	0	0	0	0	0	1
Sander vitreus	Walleye	0	0	0	0	0	0	0	1	1	0	0	0
Strongylura marina	Atlantic Needlefish	2	4	3	0	0	9	9	1	1	2	2	0
Unidentified	unidentified	2	0	0	0	0	0	0	0	0	0	0	0
Total		3798	3777	4210	1804	2125	1611	2294	2742	2794	3367	3402	3524

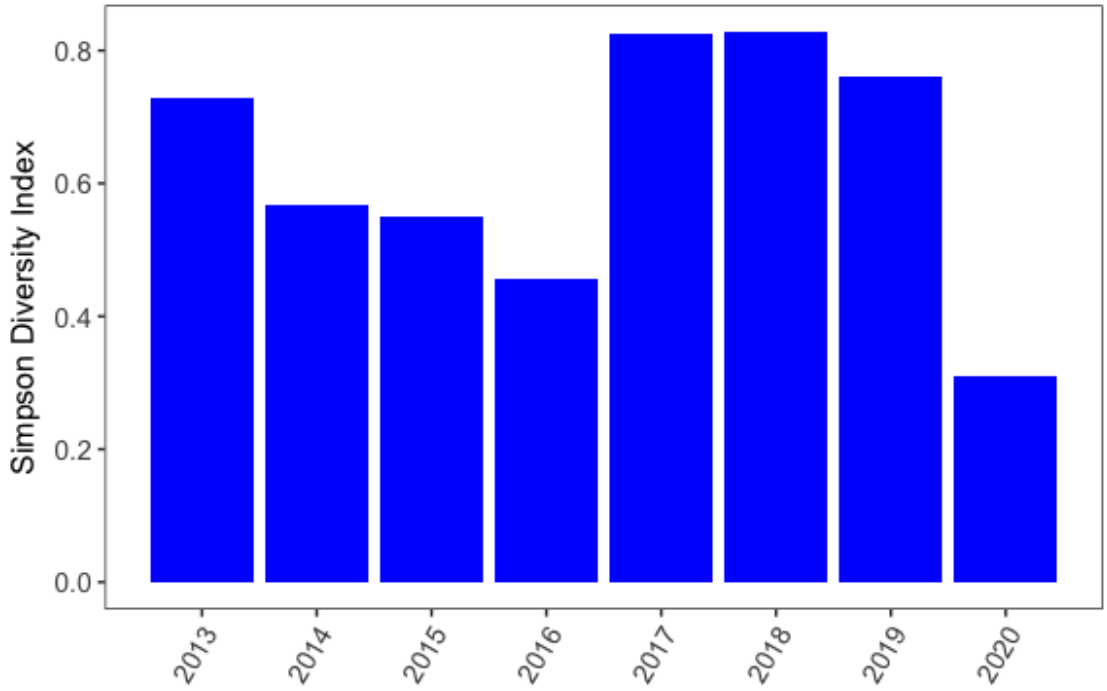

Figure 164. Simpson Diversity Index of fish species collected in Hunting Creek all years.

H. Submersed Aquatic Vegetation: Comparison among Years

According to annual reports of the Virginia Institute of Marine Science (VIMS) SAV Monitoring Program (http://web.vims.edu/bio/sav/maps.html), virtually the entire surface area of the Hunting Creek embayment was covered with submersed aquatic vegetation during the first five years of this study (2013-2017). In 2018 there was a severe decline in SAV coverage. Furthermore, due to the frequent rainfall events and resulting poor water clarity, VIMS was unable to conduct the aircraft remote sensing so we were not able to make direct comparisons of 2018 coverage with 2016 and 2017. In 2019 VIMS was able to obtain aerial imagery which appears to show no SAV growing in Hunting Creek. In 2016 and 2017 mapping of species was done via boat in association with the water quality mapping surveys and the results have been reported in the results section of these reports. In 2017 the native SAV species *Ceratophyllum demersum* was substantially more abundant than the exotic species *Hydrilla verticillata* in contrast to 2016 when they had a similar abundance. The boat transects studies in 2018, 2019, and 2020 confirmed the severe dieback has persisted.

I. Benthic Macroinvertebrates: Comparison among Years

River and Embayment Samples

Comparison among Years: As we expected, the macroinvertebrate community from the embayment of Hunting Creek has been dominated by Oligochaete worms across all sites and years (Figure 165). However, if Annelids are removed and we examine the other dominant taxon groups, we see a few different trends in dominant taxa between the three Hunting Creek sites across years (Figure 166). In general, AR2 is dominated by the insect larvae of Chironomids (midges), AR3 is dominated by Gastropods (mostly composed of the invasive Japanese mystery snails), and AR4 is dominated by Gammarid amphipods. AR2 is the site closest to the outflow from Hunting Creek, and across years, this site is mostly dominated by Chironomids (2013, 2014, 2018, 2019, and 2020), but some years Gammarid amphipods (2016, 2017) and Gastropods (2015) dominate (Figure 166). The AR4 site is the closest to the Potomac River and has been consistently dominated by Gammarid amphipods over the past six years (2014-2019); however, in 2020 this site was dominated by the Turbellarians (flatworms). Only in 2013 were the samples dominated by Chironomid insect larvae (Figure 166). The AR4 site also has the highest relative abundances of Bivalvia (mostly driven by the invasive Asian clam *Corbicula fluminea*) and Isopoda (Crustacean) compared to the other two sites. AR4 receives higher water flow and movement, which many species of Bivalvia require, and may help explain why there are higher abundances of Bivalvia located closer to the Potomac River. The site with the most fluctuations in percent contributions of macroinvertebrate taxa was AR3, which is located in the middle of the embayment. In any given year, dominant macroinvertebrate groups change from Gastropods (2013, 2015, and 2016) to Gammarid amphipods (2014, 2017, 2018, and 2020) or Chironomid insect larvae (2019). AR3 is also the only site where Gastropods dominate the community composition frequently. This site is probably influenced by both the Potomac River, through the daily movement of the tidal freshwater water body, and by the outfall of Hunting Creek, which moves nutrients and sediments from terrestrial sources. Only in a few years do AR2 and AR3 share the same dominant taxa; in 2015, they were both dominated by Gastropods (mostly composed of the invasive Japanese mystery snails), in 2017 by Gammarid amphipods,

and in 2019 by Chironomid insect larvae. In comparison, AR4 seems to show different patterns of dominance than either of the other two sites further in the embayment. The relative importance of both of these waterbodies on determining benthic macroinvertebrate community structure probably varies annually due to climatic events.

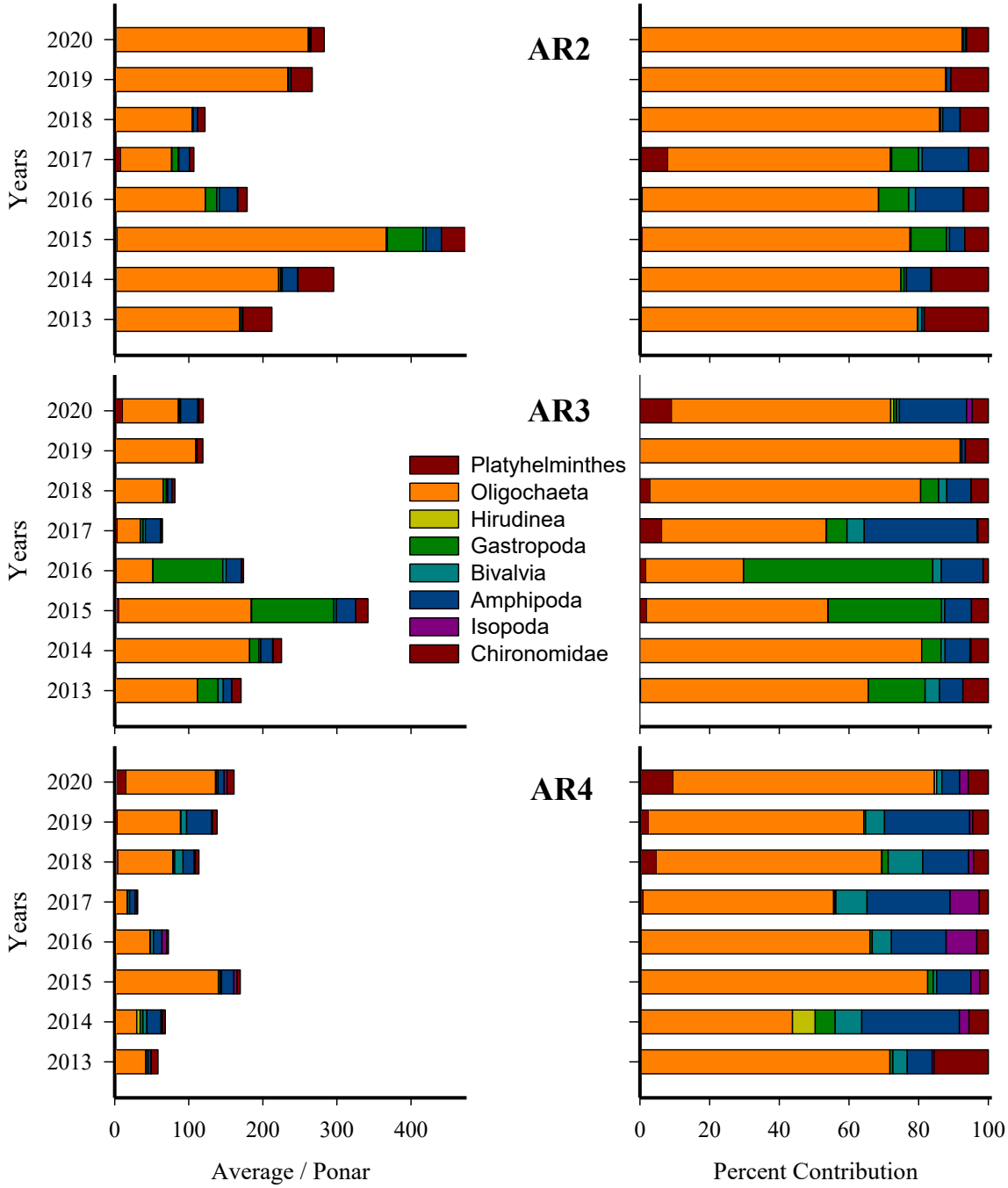

Figure 165. Average number per ponar sample (Left) and percent contribution (Right) of the eight dominant benthic invertebrate taxa in Hunting Creek embayment samples collected between 2013 and 2020 separated by site and year. Note the dominance of the Oligochaeta (worms).

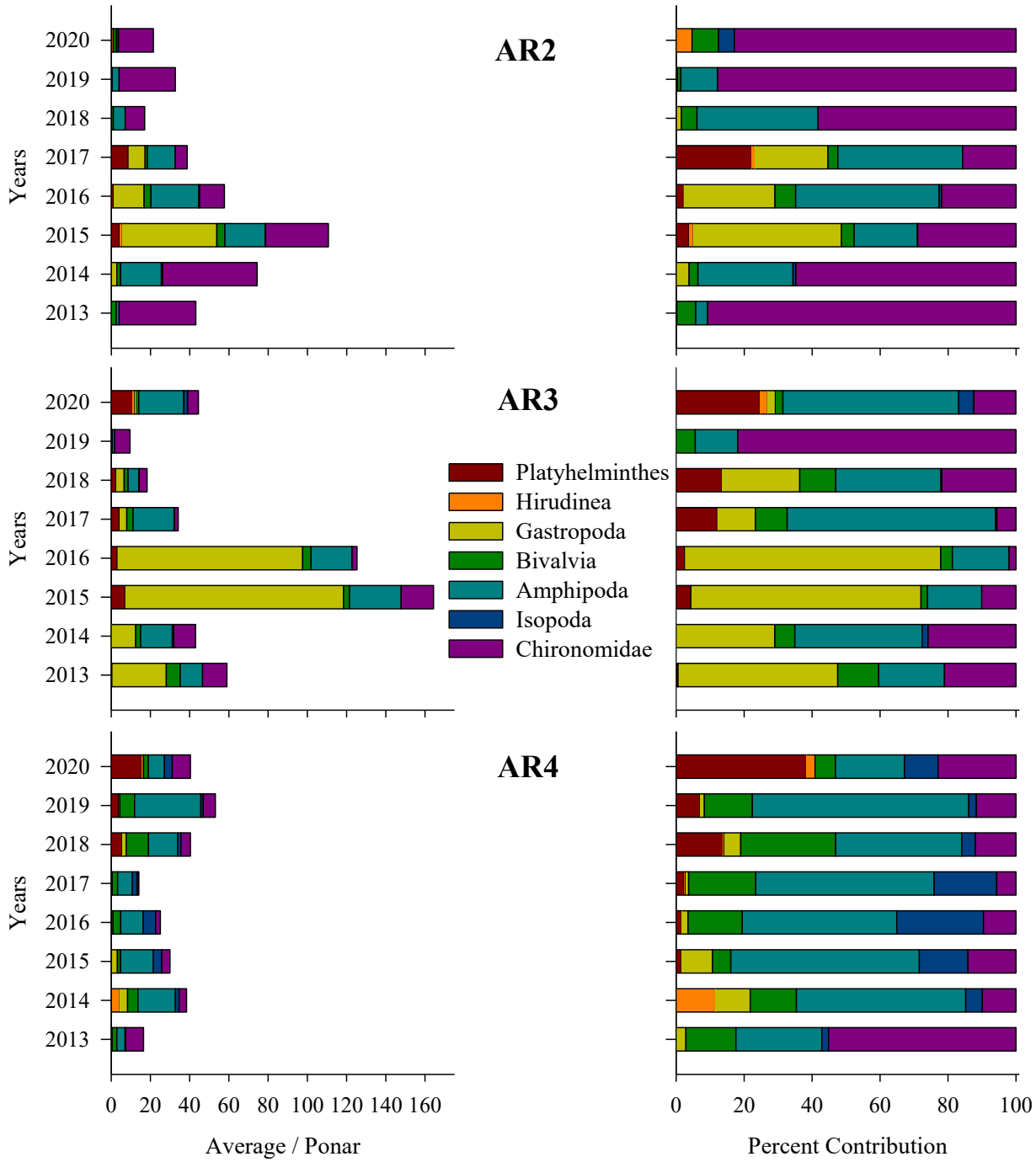

Figure 166. Without Oligochaeta, average number per ponar sample (Left) and percent contribution (Right) of the dominant benthic invertebrate taxa in Hunting Creek embayment samples collected between 2013 and 2020 separated by site and year.

Tributary Samples

Comparison among Years: We have been collecting benthic macroinvertebrate samples from the original six streams emptying into Hunting Creek since 2016 (Figure 167). Taylor Run and Timber Branch are excluded from the analyses here, as they were first sampled in 2018. Looking across all sites and years, the taxa that dominates are members of the Insecta family Hydropsychidae. They are the most dominant group 43% of the time across all years and sites. All sites sampled in 2020, except Backlick Run, Cameron Run and Turkeycock Run, were dominated by the Hydropsychidae. Members within this family are netspinning caddisflies, which live in debris and under stones and spin concave silken nets that face upstream to capture floating or swimming prey. All of these sites have stones and gravel as habitat. The next most dominant group across all sites and years are members of the Insecta family Chironomidae (23% across all years and sites), known as midges. Chironomid larvae are filter-feeders and often live in tubes in the mud. Backlick Run and Turkeycock Run were dominated by Chironomidae in 2020. Other macroinvertebrate groups can dominate a site during particular years. For example, Oligochaetes (worms) have been the most frequently encountered group at Cameron Run during 2017 and at Holmes Run-1 and Turkeycock Run in 2018. Turbellarians (flatworms) have only been the most dominant group at Holmes Run-1 during 2016 and at Turkeycock Run in 2019. Members of the Insecta family Philopotamidae and Baetidae are rarely the most dominant group at a site; although Philopotamidae were the most frequently encountered group at Indian Run in 2019 (accounting for 43% of organisms counted) and Cameron Run in 2020 (41% of organisms counted). In general, across all years, Backlick Run and Cameron Run are dominated by Chironomidae. Holmes Run-2, Indian Run, and Turkeycock Run are dominated by Hydropsychidae, and Holmes Run-1 is dominated by Turbellarians. All of these sites are probably influenced by differences in the types and amounts of nutrients and sediments moving from terrestrial sources, the flow of water, and anthropogenic impacts to the system. The relative importance of a variety of abiotic factors on determining benthic macroinvertebrate community structure probably varies annually, and even monthly, due to climatic events. Therefore, site-level trends may be apparent with continued annual sampling.

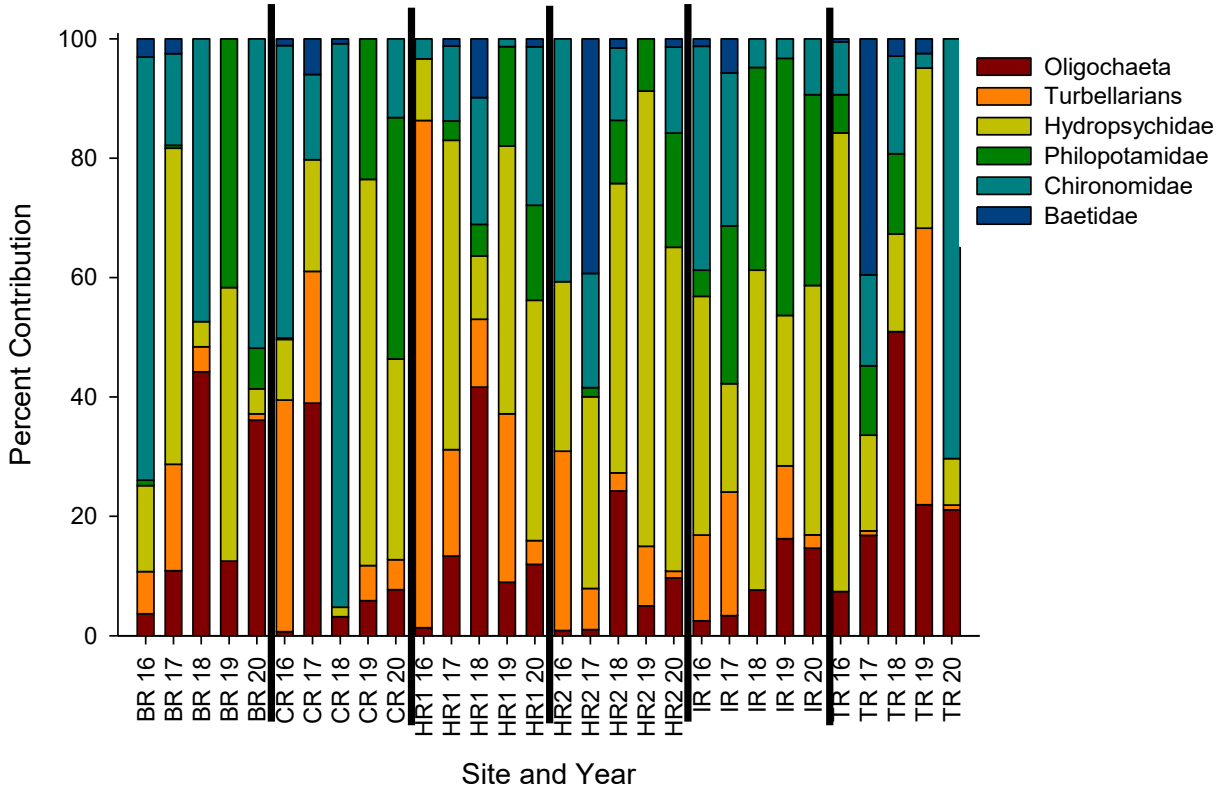

Figure 167. Percent contribution of of the six dominant benthic invertebrate taxa in tributary kick samples collected between 2016 and 2020 separated by site and year. Sites have been separated with black lines for ease of interpretation. Abbreviations for sites are noted in Table 17.

LITERATURE CITED

Bigelow, H.B. and W.C.Schroeder. 1953. Fishes of the Gulf of Maine. Fishery bulletin No. 74, Vol. 53. U.S. Government Printing Office. Washinton, D.C. 577 pp.

Carter, V., P.T. Gammon, and N.C. Bartow. 1983. Submersed Aquatic Plants of the Tidal Potomac River. Geological Survey Bulletin 1543. U.S. Geological Survey. 63 pp.

Chesapeake Bay Program. 2006 Ambient water quality criteria for dissolved oxygen, water clarity, and chlorophyll *a* for the Chesapeake Bay and its tidal tributaries. 2006 Addendum. Downloaded from Bay Program website 10/13/2006.

Cummings, H.S., W.C. Purdy, and H.P. Ritter. 1916. Investigations of the pollution and sanitary conditions of the Potomac watershed. Treasury Department, U.S. Public Health Service Hygienic Laboratory Bulletin 104. 231 pp.

Dahlberg, M.D. 1975. Guide to coastal fishes of Georgia and nearby states. University of Georgia Press. Athens, GA 187 pp.

Douglass, R.R. 1999. A Field Guide to Atlantic Coast Fishes: North America (Peterson Field Guides). Houghton Mifflin Harcourt, Boston. 368 pp.

Eddy, S. and J.C. Underhill. 1978. How to know the freshwater fishes. 3rd Ed. W.C. Brown Co.

Dubuque, IA. 215 pp.
Froese, R. and D. Pauly (Eds.). 2012. Fish Base. World Wide Web electronic publication. www.fishbase.org, version (04/2012).
Hildebrand and Schroeder. 1928. Fishes of the Chesapeake Bay. U.S. Bureau of Fisheries Bulletin 53, Part 1. Reprinted 1972. T.F.H. Publishing, Inc. Neptune, NJ. 388 pp.
Hogue, J.J, Jr., R.Wallus, and L.K. Kay. 1976. Preliminary guide to the identification of larval fishes in the Tennessee River. Technical Note B19. Tennessee Valley Authority. Knoxville, TN.
Islam, S. 2001. Seasonal dynamics of micro-, nanno-, and picoplankton in the tidal freshwater Potomac River in and around Gunston Cove. Ph.Dissertation. George Mason University. 127 pp.
Jenkins, R.E. and N.M. Burkhead. 1994. The freshwater fishes of Virginia. American Fisheries Society. Washington, DC. 1080 pp.
Jones, P.W., F.D. Martin, and J.D. Hardy, Jr. 1978. Development of fishes of the Mid-Atlantic bight. Volumes I-VI. Fish and Wildlife Service, U.S. Department of the Interior. FWS/OBS-78/12.
Kraus, R.T. and R.C. Jones. 2011. Fish abundances in shoreline habitats and submerged aquatic vegetation in a tidal freshwater embayment of the Potomac River. Environmental Monitoring and Assessment. Online: DOI 10.1007/s10661-011-2192-6.
Kelso, D.W., R.C. Jones, and P.L. deFur. 1985. An ecological study of Gunston Cove - 1984-85. 206 pp.
Lippson, A.J. and R.L. Moran. 1974. Manual for identification of early development stages of fishes of the Potomac River estuary. Power Plant Siting Program, Maryland Department of Natural Resources. PPSP-MP-13.
Loos, J.J., W.S. Woolcott, and N.R. Foster. 1972. An ecologist's guide to the minnows of the freshwater drainage systems of the Chesapeake Bay area. Association of Southeastern Biologists Bulletin 19: 126-138.
Lund, J.W.G., C. Kipling, and E.C. LeCren. 1958. The inverted microscope method of estimation algal numbers and the statistical basis of estimations by counting. Hydrobiologia 11: 143-170.
Mansueti, A.J. and J.D. Hardy, Jr. 1967. Development of fishes of the Chesapeake Bay region: an atlas of egg, larvae and juvenile stages: Part 1. Natural Resources Institute. University of Maryland. 202 pp.
Merritt, R.W. and K.W. Cummins. 1984. An introduction to the aquatic insects of North America. 2nd edition. Kendall/Hunt Publishing Co., Dubuque, IA. 722 pp.
Pennack, R.W. 1978. Fresh-water invertebrates of the United States. 2nd ed. Wiley-Interscience. New York, NY.
Schloesser, R.W., M.C. Fabrizio, R.J. Latour, G.C. Garman, G.C., B. Greenlee, M. Groves and J. Gartland. 2011. Ecological role of blue catfish in Chesapeake Bay communities and implications for management. American Fisheries Society Symposium 77:369-382.
Scott, W.B. and E.J. Crossman. 1973. Freshwater fishes of Canada. Bulletin 184. Fisheries Research Board of Canada. Ottawa, Canada. 966 pp.
Standard Methods for the Examination of Water and Wastewater. 1980. American Public Health Association, American Waterworks Association, Water Pollution Control Federation. 15th ed. 1134 pp.
Thorp, J.H. and A.P. Covich, eds. 1991. Ecology and classification of North American

Freshwater Invertebrates. Academic Press. San Diego, CA. 911 pp.
Wetzel, R.G. 1983. Limnology. 2nd ed. Saunders. 767 pp.
Wetzel, R.G. and G.E. Likens. 1991. Limnological analyses. 2nd ed. Springer-Verlag. 391 pp.

ESCHERICHIA COLI ABUNDANCES IN HUNTING CREEK/CAMERON RUN AND ADJACENT POTOMAC RIVER - 2020

Final Report
By

Benoit Van Aken
Associate Professor, Department of Chemistry & Biochemistry
George Mason University

Introduction

During 2020, in connection with examination of ecological and chemical parameters, a study of *Escherichia coli* in waters in the areas of Hunting Creek/Cameron Run and adjacent waters of the Potomac River was continued with samples being collected at 17 sites. These sites included 10 sites sampled in the period 2016 – 2018 (AR-1, AR-2, AR-3, AR-4, AR-10, AR-12, AR-13, AR-21, AR-23, and AR-30). AR-11 (outlet of Lake Cook) was not sampled in 2020 because it was considered redundant with a nearby downstream site in Camron Run: AR-21. Note that AR-22, sampled in 2016 and 2017 was not accessible in 2018, 2019, and 2020 due to existence of large-scale construction projects and earthwork along the stream bank of Huntington Park. Three new sites sampled in 2019 included one off-shore sites: AR-32 (Potomac Mainstem downstream of Outfall 001) and two shore sites: AR-33 (Hooff Run at Linden St) and AR-34 (Hooff Run at Alex Renew). Note that site AR-31 (Potomac Mainstem upstream of Outfall 001), which was sampled in 2019, was not sampled in 2020. In 2020, four new sites were added, including three shore sites: AR-24 and AR-25 by the Hunting Creek Embayment near shore just west and east of Royal St. CSO outfall, respectively, and AR-35 by the Timber Branch of Hoof's Run at downstream end of Ivy Hill Cemetery, and one off-shore site in the Potomac River at Daingerfield Island (marker '6'): AR-38.

This work provides current microbiological water quality information in these aquatic ecosystems adjacent to and receiving water from the wastewater reclamation facility operated by Alexandria Renew Enterprises (hereafter Alex Renew). The research continues to determine if these waters are impaired under the Clean Water Act in terms of their uses as designated by the Commonwealth of Virginia.

The text of the Virginia Water Quality Standards (9 VAC 25-260-10) is as follows:

"All state waters, including wetlands, are designated for the following uses: recreational uses, e.g., swimming and boating; the propagation and growth of a balanced, indigenous population of aquatic life, including game fish, which might reasonably be expected to inhabit them; wildlife; and the production of edible and marketable natural resources, e.g., fish and shellfish" (VSWCB 2011).

Section 9VAC25-260-170 of the Virginia Water Quality Standards (amended as of January 2011) specifies the bacteriological criteria for *E. coli* that apply to primary contact recreational use surface waters:

1. "*E.coli* bacteria shall not exceed a monthly geometric mean of **126 CFU/100 mL** in freshwater […]."

2. "Geometric means shall be calculated using all data collected during any calendar month with a minimum of four weekly samples."

3. "If there are insufficient data to calculate monthly geometric means in freshwater, no more than 10% of the total samples in the assessment period shall exceed **235 *E. coli* CFU/100 mL** […]."

5. "For beach advisories or closures, a single sample maximum of **235 *E. coli* CFU/100 mL** in freshwater […] shall apply." (VSWCB 2011b)

Of all of the conditions in rivers and streams which can lead to a listing of 'impaired water', the one criterion that, more than any other, results in such a listing is coliform bacteria or *E. coli* abundances (USEPA 2014). Both Hunting Creek and Cameron Run were listed as impaired under the Clean Water Act for exceedances of Virginia's water quality criterion for *E. coli* bacteria (VADEQ, 2012), although the earlier impairment listing of Hunting Creek was based on the then applicable fecal coliform criterion (VADEQ 2010). The fecal coliform criterion was subsequently changed to *E. coli* based on the understanding that this subset of fecal coliforms is more specifically associated with fecal material from humans and other warm-blooded animals. The U.S. EPA (USEPA 2012) recommended and the Commonwealth of Virginia accepted *E. coli* as the better indicator of health risk related to recreational water contact. That is the current microbiological water quality criterion.

Due to this impairment, total maximum daily load (TMDL) allocations for *E. coli* were developed for both of these watersheds in late 2010 (VADEQ 2010). The City of Alexandria is working toward achieving the bacteriological criteria for these waters through a variety of programs including a storm water program, minimizing combined storm water sewer system overflows and eventually eliminating those discharges, reductions in pet waste sources, and discovery of illegal discharges. Because the sources of *E. coli* to water systems are many and varied, including wildlife sources which are generally not controlled unless at a nuisance level, continued monitoring of *E. coli* in these waterways is an important aspect of maintaining and improving water quality. The results reported here add to the understanding of the microbiological quality of these systems.

Methods

Sampling Regime & Methods

In the prior years, the approach was to sample on a biweekly basis in May through September with one sampling in April. In 2020, due to the COVID-19 pandemic, samples were collected only on five dates, from July 7, 2020 to September 16, 2020 (**Table EC1**). Water samples were collected at 17 stations on each sampling day. Station identifiers and locations are shown in **Table EC2** (the map of EC sampling stations is provided in Appendix A, **Figure A1**). Samples were collected in clean, steam sterilized (autoclaved), 1-liter, wide-mouth polypropylene bottles. Eleven stations were approached from the shore: AR-1, AR-12, AR-13, AR-21, AR-23, AR-24, AR-25, AR-30, AR-33, AR-34, and 35, and 6 stations were sampled from a small, outboard-powered research vessel: AR-2, AR-3, AR-4, AR-10, AR-32, and AR-38. Among the shore stations, stations AR-21, AR-24, AR-25, AR-30, and AR-35 were sampled from the shore without wading into the stream. At these stations, samples were simply collected as grab samples using the 1-liter bottle. Sampling was operated in the most active flow zone that could be reached from the shore. At station AR-1, AR-23, and AR-34, samples were collected remotely using a sterilized, 1- or 4-liter round, polypropylene wide-mouth bottle fitted with a

harness and nylon line. At station AR-1, the sample bottle was deployed from atop the George Washington Parkway Bridge over Hunting Creek on the downstream side approximately at mid-span. At stations AR-23 and AR-34, the sample bottle was deployed from the shore and thrown to about 5-10 yards into the water. When accumulation of surface debris prevented the collection of grab samples, AR-25 was sampled using a bottle fitted with a harness and nylon line. Collection of three shore-approached samples required wading in the streams; AR-12, AR-13, and AR-33. At station AR-12, we waded into the water downstream of the collection site to approximately midstream, waited for the current to carry away any disturbed sediment and then collected the sample by submerging the 1-liter bottle upstream of the sample collector. At station AR- 13, the bottom of the stream at the approach site is paved with concrete. At this site, we waded to approximately midstream and to the edge of the concrete paved segment. After waiting for any disturbed sediment to be washed away, the sampled was collected by submerging the sterile 1-liter bottle in the stream. At station AR- 33, the bottom of the stream is entirely paved with concrete. At this site, we waded (or simply walked when the water flow was low) to approximately midstream. After waiting for any disturbed sediment to be washed away, the sample was collected again by submerging the sterile 1-liter bottle in the stream. Boat-approached sites, AR- 2, AR-3, AR-4, AR-10, AR- 32, and AR-38, were sampled by submerging the collection bottles over the side of the research vessel as the vessel coasted on final approach to the station.

In all cases, the bottles were rinsed twice with sample water and then the final sample was collected. Immediately after collection, samples were placed in dark, insulated containers packed with ice. Samples were returned to the George Mason University at the Potomac Science Center, where they were processed within about 5 hours of collection.

Table EC1. Sampling Dates

Date	**Date Codes**
7-Jul-2020	20200707
21-Jul-2020	20200721
19-Aug-2020	20200819
2-Sep-2020	20200902
16-Sep-2020	20200916

Table EC2. Station identifiers, locations and access type

Station ID	Access Type	Location Description	Latitude	Longitude
AR-1	Shore	Hunting Cr just above GW Parkway Bridge	38.78992	-77.05126
AR-2	Boat	Northern portion of Hunting Cr.	38.78509	-77.04951
AR-3	Boat	Southern portion of Hunting Cr.	38.78181	-77.04890
AR-4	Boat	Potomac River Channel off Hunting Cr.	38.78124	-77.03529
AR-10	Boat	Potomac River North of Wilson Bridge	38.79816	-77.03907
AR-12	Shore	Last Riffle of Cameron Run near Beltway crossing	38.80218	-77.08467
AR-13	Shore	Hoff's Run upstream of Alex renew outfall	38.80278	-77.05848
AR-21	Shore	South side of Cameron Run downstream from Lake Cook drain	38.80318	-77.09565
AR-23	Shore	South side of Cameron Run across from AlexRenew outfall	38.79372	-77.05966
AR-24	Shore	Hunting Creek Embayment near shore just west of Royal St CSO outfall	38.79156	-77.04680
AR-25	Shore	Hunting Creek Embayment near shore just east of Royal St CSO outfall	38.79205	-77.04538
AR-30	Shore	Cameron Run upstream near metro rail bridge	38.80545	-77.10745
AR-32	Boat	Potomac Mainstem downstream of Outfall 001	38.80940	-77.03727
AR-33	Shore	Hooff Run at Linden St	38.81103	-77.05993
AR-34	Shore	Hooff Run at Alex Renew	38.79918	-77.05997
AR-35	Shore	Timber Branch of Hoof's Run at downstream end of Ivy Hill Cemetery	38.8175	-77.070654
AR-38	Boat	Potomac River at Daingerfield Island; at marker '6'	38.82348	-77.03802

Analytical Method

Determination of the abundance of *E. coli* was performed following the EPA Method 1603 (*Escherichia coli* in Water by Membrane Filtration Using Modified Membrane-Thermotolerant *Escherichia coli* Agar–Modified mTEC). This is an EPA-approved method for determining abundance of *E. coli* in fresh water. It is a one-step modification of the EPA Method 1103.1. It is based on *E. coli* production of β-D-glucuronidase and the consequent metabolism of 5-bromo-6-chloro-3-indolyl-β-D-glucuronide in the medium to glucuronic acid and a red- or magenta-colored product (USEPA 2009).

For this work, mTEC medium (Fisher) was prepared in our laboratory at George Mason University (Potomac Science Center) shortly before each sampling trip. The medium was prepared as per package directions, and ~5 mL of the molten medium was placed aseptically into sterile, 50-mm Petri dishes with tight fitting lids. Prepared medium was stored at 4°C in the dark until use. Phosphate buffered saline (PBS) was prepared as per Method 1603 and autoclave sterilized. PBS was added to smaller samples (1.0 mL and 10 mL) to make volumes up to at least 20 mL before filtration. This aids in distributing bacteria uniformly across the membrane surface. The PBS was also used for blank controls.

Upon return to the laboratory, samples were processed immediately. Sterile, gridded, 0.45 µm membrane filters were aseptically positioned, grid side up, on the base of a sterile, polycarbonate filter holder, and the filter tower was placed in position on a vacuum flask over the filter and base. Samples were shaken vigorously to assure complete mixing and appropriate volumes (1.0 mL, 10.0 mL, and 100.0 mL) of sample were added to each of three replicate filter systems. Before adding the two smaller volume aliquots to the filter funnels, sufficient PBS was added to make the final volume approximately 20 mL. Samples were then filtered with vacuum (approximately 10 in. Hg). Each filter was then removed from the filter holder base aseptically with sterile, blunt-tipped forceps and placed onto the surface of the mTEC agar without trapping any air bubbles beneath the filter. After replacing the Petri dish tops the plates were incubated in a 35°C incubator for 2 ± 0.5 hours. They were then removed, placed in tightly closed double, zipper-locked plastic bags and submerged in a water bath at 44.5°C ± 0.2°C for 22 ± 2 hours. Two blank controls consisting of 3 x 100 mL of PBS were checked each time samples were processed (3 at the beginning and 3 at the end of the sample analysis, except in July 7, where only 2 x 2 controls were used). Generally, no *E. coli* were detected in these blank controls, although occasionally controls had one or two presumptive *E. coli* colonies. The data were not corrected for this low background as it was generally far less than 1 percent of the abundances on countable plates.

After the water bath incubation, samples were retrieved and observed immediately for typical red or magenta *E. coli* colonies. All Petri dishes (3 volumes x 3 replicates = 9 Petri dishes per sample) were observed. Although only dilutions yielding colony counts between 20 and 80 needed to be enumerated, we generally recorded colonies for each countable dilution. Often, however, when *E. coli* were too abundant, the higher volume samples were not countable due to overgrowth. Calculation of final *E. coli* abundances followed the procedures described in Appendix B of the EPA Method 1603 (USEPA 2009). Since there were triplicate analyses of each dilution, the colony count per Petri dish was separately converted to *E. coli* abundance per 100 mL and then the triplicates were averaged. If no dilution gave individual counts between 20 and 80, the nearest count was selected and used for the final calculation as described in appendix B of the EPA Method 1603.

Results & Discussion

In 2020, typical *E. coli* colonies were observed in some dilution(s) in every sample tested. There is then a point estimate of *E. coli* per 100 mL for each sample. *E. coli* abundances grouped by station are shown in **Figure EC1** and *E. coli* abundances grouped by sampling date are shown in **Figure EC3** (tabular data is in Appendix A, **Table A1**). Only one (over the two) controls analyzed in July 7 showed positive counts (i.e., 1 count per 100 mL). Other controls did not show positive counts and were reported as 'less than 1 count/100 mL'.

Since there was no situation in which four weekly samples were collected in a single calendar month, the '235 per 100 mL' (in more than 10% of the samples) criterion is applicable in determining impairment.

Data Grouped by Station

The different stations sampled have been selected with the purpose of capturing the potential contribution of Alex Renew CSOs to receiving waters. These CSOs include the Cameron Run COS across station AR-23 on Cameron Run, the Hooff Run CSO between station AR-13 and AR-34 on Hooff Run, the Royal St. CSO between stations AR-24 and AR-25 on the Potomac River, and the Pendelton St. CSO by station AR-32 on the Potomac River.

In 2020, thermotolerant *E. coli* abundances grouped by station exceed the 235 per 100 mL 'impaired water' criterion at all shore stations and three out of the six off-shore stations (AR-2, AR-3, and AR-38) at some time during the sampling period. Only three off-shore sites (AR-4, AR-10, and AR-32) did not show any exceedance during the sampling period (**Figure EC1**). This is in contrast to observations made in 2015, 2016, 2017, and 2019, where all stations showed exceedance for at least one sampling date -- this could be explained by the fact that only five sampling campaigns were conducted in 2020 versus ~11 in the prior years. Six shore stations showed exceedance of 235 per 100 mL for all sampling dates: AR-1, AR-23, AR-24, AR-33, AR-34, and AR-35. All other stations on shore showed exceedance of 235 per 100 mL for four sampling dates out of five: AR-12, AR-13, AR-21, AR-25, and AR-30.

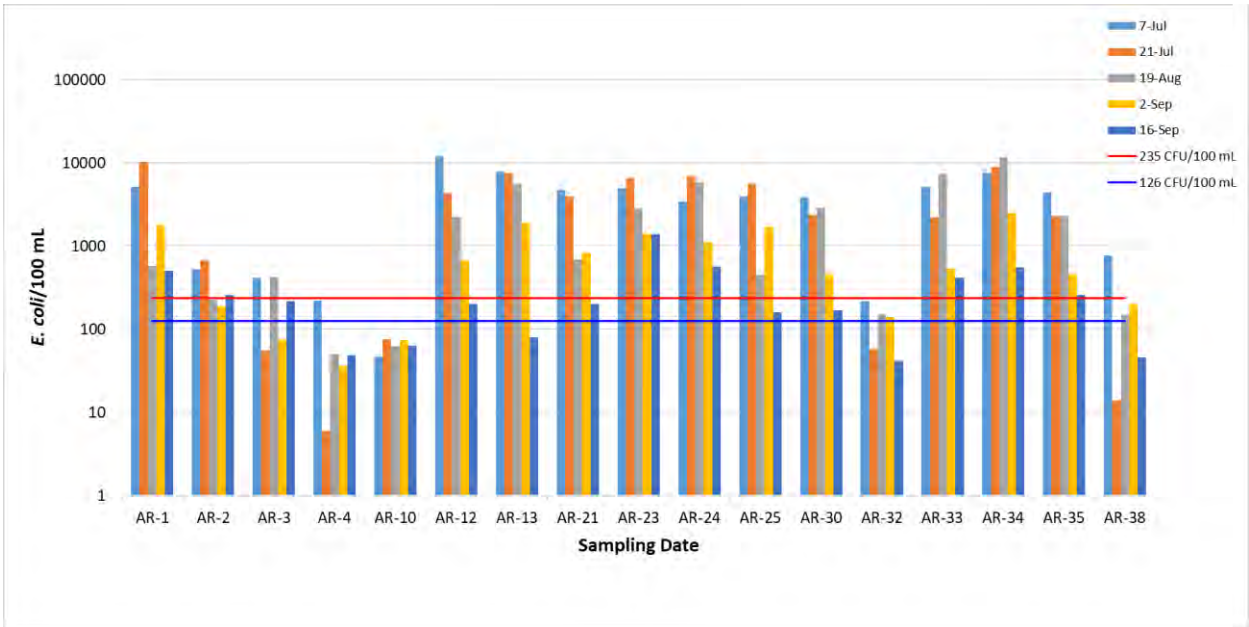

Figure EC1. *E. coli* abundance per 100 mL in Cameron Run, Hunting Creek, and the adjacent Potomac River grouped by stations from July to September 2020. The blue horizontal line represents the *E. coli* criterion for the geometric monthly mean allowable abundance (126 per 100 mL), and the red line represents the criterion for allowable abundance in the absence of four monthly samples (235 per 100 mL).

Figure EC2 shows the box plots of *E. coli* numbers per 100 mL as arrayed by site. In this figure, the stations were grouped by streams, including the shore stations on Cameron Run (orange), the shore stations on Hooff Run (green), the shore stations on the Potomac River near the Royal St. CSO outfall (purple), and the off-shore stations (blue). Five sampling station are located along Cameron Run and include, from upstream to downstream: AR-30, AR-21, AR-12, AR-23, and AR-1. AR-30 and AR-12 are in flowing Cameron Run, AR-21 and AR-23 are in tidal Cameron Run. Four stations are located along Hooff Run (a tributary of Cameron Run) and include, from upstream to downstream: AR-35, AR-33, AR-13, and AR-34. Hooff Run is a tributary of Cameron Run, which is suspected to contribute to *E. coli* contamination observed in Cameron Run. Two shore stations are located on Potomac River near the Royal St. CSO outfall and include AR-24 and AR-25. Off-shore stations include two stations in the Hunting Creek embayment, near the Hunting discharge point, AR-2 and AR3, and four stations in the mainstem Potomac river, from upstream to downstream: AR-38, AR-31, AR-10, and AR-4.

On average, we observed an increase of the detected *E. coli* numbers on Cameron Run when

moving downstream: from 1,946 counts at AR-30 to 3,655 at AR-1. We did not observe a significant increase between AR-12 and AR-23 (we even see a large decrease in July 7), so it is not possible to evaluate the contribution of the Cameron Run CSO to the contamination of Cameron Run (located at almost the same level as AR-23 on Cameron Run). In addition, AR-23 is also downstream from the Hooff Run discharge, which also has high counts.

On average, we also observe an increase of the *E. coli* numbers when going downstream along Hooff Run: from 1,951 counts at AR-35 to 4,498 at AR-34. We did not observe a significant increase of the counts between AR-13 and AR-34, except for the August 19's sampling, so it is difficult from these data to evaluate the contribution of Hoof Run CSO (located between AR-13 and AR-34 on Hooff Run) to Hooff Run contamination.

The shore Potomac stations nearby the Royal St. CSO outfall showed average numbers of 3,601 and 2,375 for AR-24 and AR-25 respectively. These numbers are much higher than the nearby off-shore numbers at stations AR-10 or AR-2, indicating a likely contribution of the Royal St. CSO outfall the water contamination at these.

All off-shore numbers were on average much lower than the shore numbers (72 – 374 versus 1,946 – 4,619 counts per 100 mL). Off-shore stations by the Hunting Creek Embayment, AR-2, AR-3, and AR-4, showed decreasing counts when increasing the distance from Cameron Run discharge, which suggests that Cameron Run is a significant source of *E. coli* to the Potomac River. All off-shore stations in the mainstream Potomac River showed rather similar low numbers. Station AR-32, which is nearby the Pendelton St. CSO in Orinoco Bay shows similar counts as the downstream stations in mainstem Potomac river, AR-38, AR-10, and AR-4.

In summary, the average *E. coli* counts by stations increased from upstream to downstream, along both Cameron Run and Hooff Run. These counts are also the highest that we recorded over all stations. The Potomac River stations near the Royal St. CSO outfall (AR-24 and AR-25) also showed numbers much higher than nearby off-shore numbers at stations AR-10 or AR-2, suggesting a contribution of the Royal St. CSO outfall. The off-shore counts were about one or more orders of magnitude lower that the shore counts, which is easily explained by dilution of the stream water.

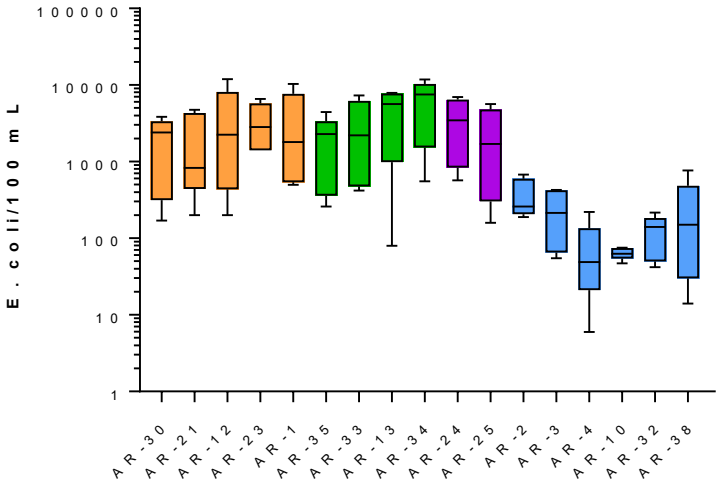

Figure EC2. Box plots of *E. coli* abundance per 100 mL for each site in Cameron Run, Hunting Creek, and the adjacent Potomac River from July to September 2020. The bars show the minimum and maximum counts, the boxes show the 25 and 75-percentile, and the median. Shore stations on Cameron

Run are in orange, shore stations on Hooff Run are in green, shore station on the Potomac River are purple, and off-shore stations are blue.

Data Grouped by Date

E. coli abundance grouped by dates show that environmental and/or climatic conditions may have played an important role in the counts obtained for selected sampling dates, resulting in large *E. coli* numbers and exceedance of the 235 CFUs per 100 mL (**Figure EC3** and **EC4**). The highest average *E. coli* numbers and higher exceedance of 235 CFUs per 100 mL were observed on July 7 and July 21, which were also the dates we observed the highest Cameron flows (667 and 169 cfs). A significant correlation was observed between Cameron Run flows and average *E. coli* abundance: Pearson's correlation coefficient, $r = 0.70$.

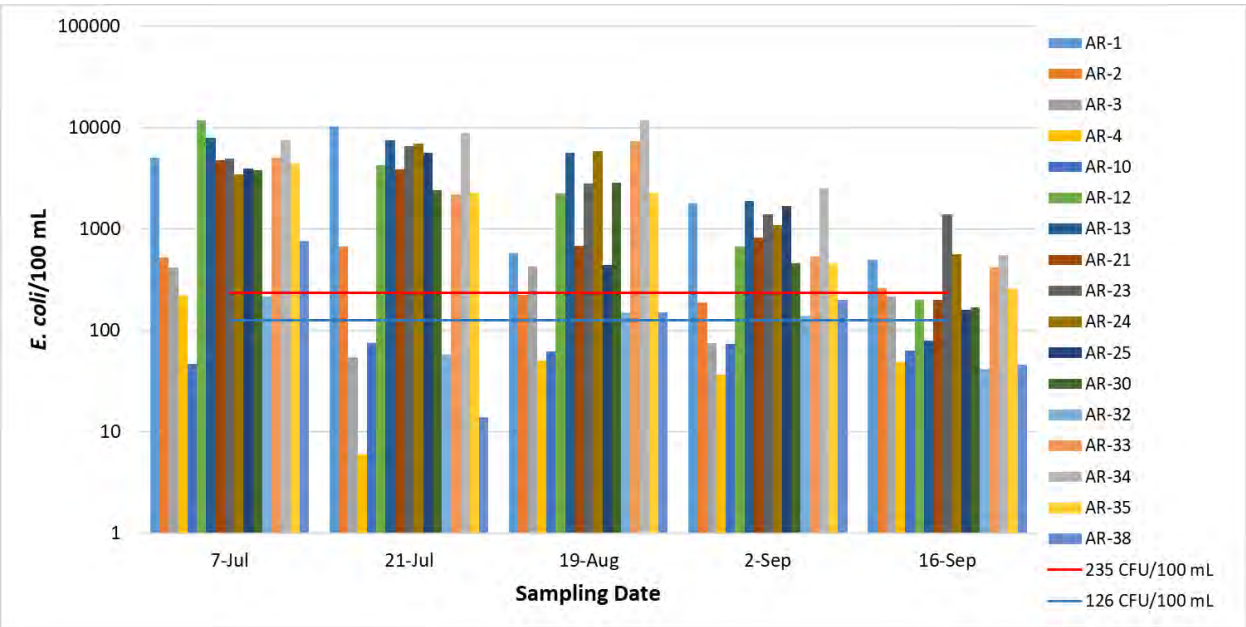

Figure EC3. *E. coli* abundance per 100 mL in Cameron Run, Hunting Creek, and the adjacent Potomac River grouped by sampling dates for all stations. The blue horizontal line represents the *E. coli* criterion for the geometric monthly mean allowable abundance (126 per 100 mL), and the red line represents the criterion for allowable abundance in the absence of four monthly samples (235 per 100 mL).

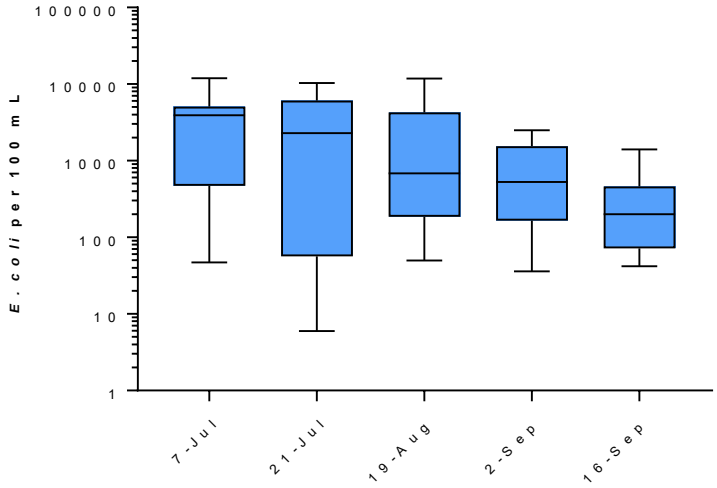

Figure EC4. Box plots of *E. coli* abundance per 100 mL for each sampling dates in Cameron Run, Hunting Creek, and the adjacent Potomac River over all sites. The bars show the minimum and maximum values, the boxes show the 25 and 75-percentile, and the median.

Temporal Trends

The number of stations and sampling events have increased between 2014 and 2019 (8 sites and 6 sampling times in 2014 to 15 sites and 11 sampling times in 2019). However, 2020 was marked by an increase of the sampling stations but a reduction of the sampling campaigns due to COVID-19 (17 stations and 5 sampling times). We present here a timeline of changes in the percentage of samples that exceeded the 235 per 100 mL standard (**Figure EC5**). Even though over the period 2014 – 2017, this trend globally suggested increasing exceedances of the 235 CFUs per 100 mL standard (as mentioned in the 2019 Final Report), examination of the *E. coli* abundances per 100 mL over the period 2017 – 2020 does not indicate any worsening of the conditions (**Figure EC6**). We observe globally higher numbers in 2020 than in 2019, but this seems to be the results of the very high counts recorded on July 7 and July 21, 2020, which are associated with the unusually high flows recorded on these dates. For instance, we recorded counts of 7,900 and 7,550 at AR-13 on July 7 and 21, respectively, while the highest counts observed at AR-13 over the entire 2019 period was only 3,170. The exceptional high flows observed in July 7 and 21 may therefore bias the results, especially because only five sampling campaigns were conducted.

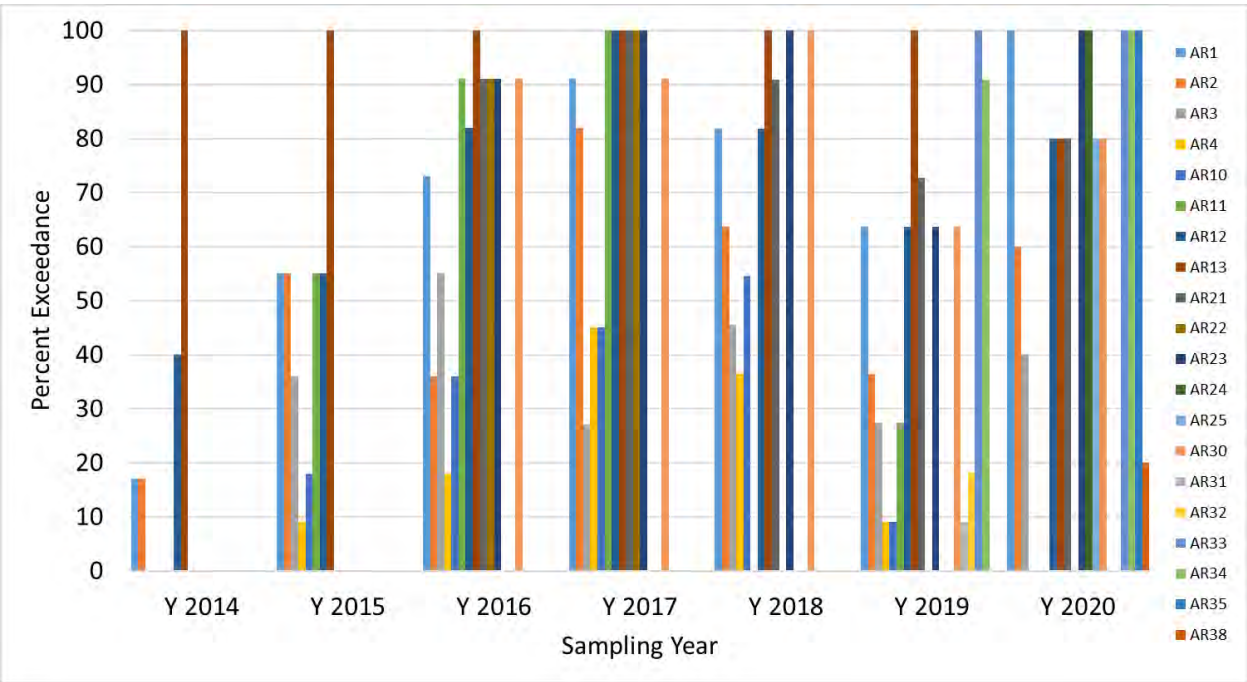

Figure EC5: Percentage of sample events when *E. coli* abundances exceeded 235 per 100 mL in the year 2014, 2015, 2016, 2017, 2018, 2019, and 2020. Samples were collected 6 times during 2014, whereas in each of the subsequent years, samples were collected 11 times.

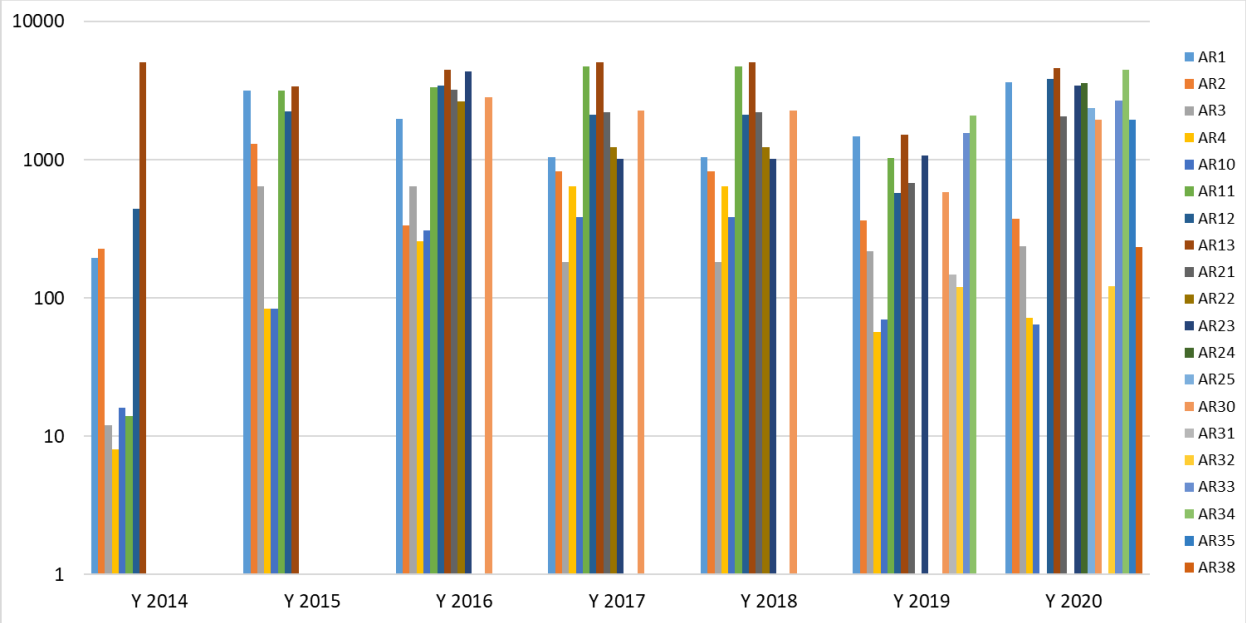

Figure EC6: *E. coli* abundances per 100 mL in year 2014, 2015, 2016, 2017, 2018, and 2019. Samples were collected 6 times during 2014, whereas in each of the subsequent years, samples were collected 11 times.

CONCLUSIONS

The data continue to support a conclusion that the entire area sampled, including the mainstem of the Potomac River (AR-4), is impaired for the bacteriological water quality criterion (*E. coli*) content under Section 9VAC25-260-170 of the Virginia Water Quality Standards that applies to primary contact recreational use surface waters. Although our data showed an increase of the *E. coli* abundance and percent exceedance of the 235 criterion from 2014 to 2016, these numbers seemed to have peaked in 2016 – 2017 and even showed a slight decrease in 2018 and 2019.The higher average counts recorded in 2020 seems to be partially caused by high counts occurring during high-flow conditions in July, 2020.

Sampling additional sites in Hooff Run/Cameron Run seems to indicate that Hooff Run is a significant contributor of the Hunting Creek contamination by *E. coli*. Similarly, sampling additional sites on the Potomac River by the Royal St. CSO seems to indicate a contribution of this CSO to *E. coli* contamination of the receiving water.

Literature Cited

U.S. Environmental Protection Agency (USEPA). 2009. Method 1603: *Escherichia coli* (*E. coli*) in Water by Membrane Filtration Using Modified membrane-Thermotolerant *Escherichia coli* Agar (Modified mTEC). Available at: < http://water.epa.gov/scitech/methods/cwa/bioindicators/> search Method 1603, December 2009.

U.S. Environmental Protection Agency (USEPA). 2012. Water: Monitoring & Assessment: 5.11 Fecal Bacteria. Available at: http://water.epa.gov/type/rsl/monitoring/vms511.cfm

U.S. Environmental Protection Agency (USEPA). 2014. National Water Quality Assessment Report, water Quality Assessment and Total Maximum Daily Loads Information. Available at: <http://ofmpub.epa.gov/waters10/attains_index.control>

Virginia Department of Environmental Quality (VADEQ). 2010. Bacteria TMDLs for the Hunting Creek, Cameron Run, and Holmes Run Watersheds. Available at: <deq.state.va.us>

Virginia Department of Environmental Quality (VADEQ). 2012. 2012 Impaired Waters: Category 4 & 5 by Basin and Stream Name, Potomac and Shenandoah River Basins, Cause Group Code: A13R-03-BAC - Cameron Run/Hunting Creek. Available at: <http://www.deq.virginia.gov/Programs/Water/WaterQualityInformationTMDLs/WaterQualityAssessments.aspx>

Virginia. *State Water Control Board* (VSWCB). 2011. 9 VAC 25-260-10 Designation of uses. Virginia Water Quality Standards. Available at: <http://lis.virginia.gov/cgi-bin/legp604.exe?000+reg+9VAC25-260-10>

Virginia. *State Water Control Board* (VSWCB). 2011b. 9 VAC 25-260-170 Bacteria; other recreational waters. Virginia Water Quality Standards. Available at: <http://lis.virginia.gov/cgi-bin/legp604.exe?000+reg+9VAC25-260-170>

Appendix A

Figure A1. Maps of sampling sites

Table A1. 2020 *E. coli* abundances per 100 mL for all station, all sampling dates

Stations	Sampling Dates				
# CFU Per 100 mL	07/07/20	07/21/20	08/19/20	09/02/20	09/16/20
AR-1	5100	10300	573	1800	500
AR-2	520	677	223	190	260
AR-3	420	55	427	75	215
AR-4	220	6	50	36	49
AR-10	47	75	62	74	63
AR-12	11900	4300	2250	675	200
AR-13	7900	7550	5667	1900	80
AR-21	4733	3900	683	830	200
AR-23	4967	6567	2833	1400	1400
AR-24	3467	7000	5867	1100	570
AR-25	3933	5633	447	1700	160
AR-30	3833	2400	2867	460	170
AR-32	217	58	150	140	42
AR-33	5100	2200	7333	530	420
AR-34	7550	8900	11800	2500	553
AR-35	4433	2300	2300	460	260
AR-38	765	14	150	200	46

Table A2. Mean of *E. coli* abundances per 100 mL, seasonal means and standard deviations and percent exceedances of the 126 and 235 CFUs/100 mL criteria

Station	Seasonal Mean (*E. coli* /100 mL)	Seasonal St. Dev. (*E. coli* /100 mL)	Percent Exceedance 126 CFUs/100 mL	Percent Exceedance 235 CFUs/100 mL
AR1	3655	4157	100	100
AR2	374	214	100	60
AR3	238	180	60	40
AR4	72	84	20	0
AR10	64	11	0	0
AR12	3865	4769	100	80
AR13	4619	3480	80	80
AR21	2069	2086	100	80
AR23	3433	2280	100	100
AR24	3601	2835	100	100
AR25	2375	2352	100	80
AR30	1946	1579	100	80
AR32	121	72	60	0
AR33	2681	3328	100	100
AR34	4498	5040	100	100
AR35	1951	1695	100	100
AR38	235	306	60	20